Inhibition and Enhancement of Respiratory Syncytial Virus Replication by Nucleoside Analogues and Bis(indole) Compounds

by

Lionel Dylan Jensen

A thesis submitted in partial fulfillment of the requirements for the degree of

Doctor of Philosophy

in

Virology

Department of Medical Microbiology and Immunology
University of Alberta

Abstract

Respiratory syncytial virus (RSV) is an *Orthopneumovirus* that infects the epithelium of the airways. Severe RSV infection of the lower respiratory tract in infants is a leading cause of pediatric hospitalizations. RSV also causes substantial morbidity in immunocompromised and elderly populations. Palivizumab, a humanized monoclonal antibody, is available for the prophylactic treatment of high-risk infants. However, this intervention is expensive and has a limited impact on annual hospitalization rates caused by RSV. No vaccine is available to prevent RSV infection and no efficacious antivirals are available to treat active infection. To address the burden of disease imposed by RSV, this project sought to develop and implement a screening assay to identify compounds with antiviral activity against RSV. Different screening protocols were examined as platforms for testing antiviral activity. The first protocol quantified changes to RSV replication complex morphology during antiviral treatment. Through confocal microscopy, changes to replication complex morphology were identified as early as six hours post infection. However, this assay was hindered by the low signal intensity produced by replication complexes. Therefore, alternative RSV-antiviral screening protocols were investigated. Subsequent protocols quantified initial monolayer infection, or quantified RSV progeny production, via colourimetric or immunofluorescence (IF) staining. Automated detection of IF-stained RSV-infected cells was conducted using a high content imaging system. This protocol (referred to as 'the IF protocol') offered the highest throughput screening capacity and most reliable detection of RSV infection versus the other methods that were tested. Using the IF protocol, the chemotherapeutic nucleoside analogue cytarabine was investigated and antiviral activity against RSV was observed. The IF protocol was then used to screen a series of bis(indole) compounds for antiviral activity against RSV. Bis(indole) compounds were hypothesized to have antiviral activity as they were derived from Isatisine A, a naturally occurring compound with modest antiviral activity. Bis(indole)

compounds with antiviral activity against RSV were identified; the IF protocol was then used to guide the synthesis of novel bis(indole) compounds with improved cytotoxicity profiles.

The Toll-like receptor 7 (TLR7) agonist loxoribine was investigated for antiviral activity against RSV, however, enhancement of RSV replication during loxoribine treatment was observed. This observation was unexpected as TLR7 is a pattern recognition receptor which contributes to the identification of pathogens by the innate immune system and TLR7 stimulation typically elicits an antiviral immune response. Furthermore, TLR7 agonists are undergoing clinical investigations to examine their potential as immunomodulatory treatments for airway diseases. As enhancing the severity of RSV infections in this population could be hazardous, it was considered essential to further characterize the relationship of loxoribine with RSV replication. Loxoribine-mediated enhancement of RSV replication in human airway epithelial cells was determined to be concentration-dependent and this effect was reproducible with the distinct TLR7 agonist CL097. Inhibition of TLR7 stimulation by the antagonist IRS-661, or by siRNA knock down of TLR7, prevented enhancement of RSV replication by loxoribine. Finally, TLR7-mediated enhancement of RSV replication was determined to be dependent on extracellular signal-regulated kinase activation. These results support the novel conclusion that exogenous stimulation of TLR7 benefits RSV replication. These results also suggest caution is warranted during the ongoing development of TLR7-based therapeutics, especially for therapeutics being developed for the treatment of airway diseases.

Preface

A portion of research conducted for this thesis forms part of a collaboration with Dr. Rachel Fearns at Boston University Medical Center, Boston, MA. The *in vitro* RSV transcription assay described in chapter 2 was designed by Dr. Rachel Fearns, and guidance with this protocol was provided by Dr. Sarah Noton. All subsequent experimentation and analyses of results using this protocol were completed by myself.

A portion of research conducted for this thesis forms part of collaboration between Dr. Frederick West, Department of Chemistry at the University of Alberta, and Dr. David Marchant, Department of Medical Microbiology and Immunology at the University of Alberta. Resultantly, a portion of chapter four has been previously published as "Dual Catalytic Synthesis of Antiviral Compounds Based on Metallocarbene-Azide Cascade Chemistry" in The Journal of Organic Chemistry (available online April 17, 2018). With respect to this manuscript, B. Atienza was responsible for synthesis of bis(indole) compounds and composure of the manuscript relating to these chemical syntheses. I was responsible for data collection, analysis, and manuscript composition with respect to respiratory syncytial virus. F. West and D. Marchant were supervisory authors responsible for concept formation.

Lastly, experimentation to produce figures 5.5c and 5.5e in chapter five of this thesis was completed by L. Bilawchuk, Department of Medical Microbiology and Immunology at the University of Alberta.

Acknowledgements

This work would not have been possibly without the endless encouragement and input of my project supervisor, Dr. David Marchant. I would also like to thank Cameron Griffiths. This project benefitted immensely from his wealth of knowledge, his undefeatable enthusiasm for science, and the endless thoughtful discussions we held - Cameron Griffiths, I am truly grateful. It is not hyperbole to say that every experiment I conducted benefitted from the input of our laboratory manager Leanne Bilawchuk. I must thank Leanne for her patience and expertise. I would like to thank my committee members Dr. Edan Foley and Dr. Michael Houghton. Throughout my project their guidance and critiques inspired me to attempt new techniques and greatly accelerated my research project. I greatly appreciate the help of the supporting administrative staff of Medical Microbiology and Immunology. They are the unsung heroes of the research conducted our department. In particular, I would like to thank Tabitha Vasquez and Debbie Doudiet. I have many fellow Medical Microbiology and Immunology students to thank for their input on techniques and experimentation. Namely, I would like to thank Farah Elawar, Ninad Mehta, David Fast, Brittany Fraser, Ben Kostiuk, Brittany Umer, Jason Wong, Amanda Scott, Adil Mohamed, Ken Gavina, and Kevin James. I would also like to thank all of those outside of academia who have supported me. This includes my close friends Alanna Poole, Sierra Poole, Laurence Pryer, Heather Nixdorff, Danielle Gregoire and David Strahl, and the good people of the Alpine Club of Canada, Edmonton section. Lastly, the most important contributors to any of my past, present, or future achievements are my parents, Randy and Nomi Jensen.

Table of Contents

List of Tables

List of Figures

List of Abbreviations

1HAEo- cells	Human airway epithelial cells
5-FC	5-fluorocytidine
ADME	Absorption, distribution, metabolism, and excretion
AdV	Adenovirus
AML	Acute myeloid leukemia
ANOVA	Analysis of variance
AP-1	Activator protein-1
ATP	Adenine triphosphate
aUY11	5-(perylen-3-yl)ethynyl-arabino-uridine
BAL	Bronchoalveolar lavage
BEGM	Bronchial epithelial cell growth medium
BI-D	Boehringer Ingelheim compound D
BSA	Bovine serum albumin
CARD	Caspase recruitment domain
CBP	cAMP response element-binding protein binding protein
CC_{50}	Cytotoxicity concentration 50%; the concentration at which cell viability is reduced by 50%
CCL5	Chemokine (C-C motif) ligand 5
CHD	Chronic Heart Disease
CLD	Chronic Lung Disease
CM	Confocal microscopy
CPE	Cytopathic effect
CPSII	Carbamoyl phosphate synthetase II
CT	Clinical trial
CTL	Cytotoxic lymphocyte
CX3CR1	CX3 chemokine receptor 1
DAPI	4′,6-diamidino-2-phenylindole

DC	Dendritic cell
DIP	Defective interfering particle
DMEM	Delbecco's modified eagle medium
DMSO	Dimethyl sulfoxide
dsRNA	Double stranded RNA
EC_{50}	Effective concentration 50%; the concentration at which viral replication is reduced by 50%
EDTA	Ethylenediaminetetraacetic acid
EGTA	Ethylene glycol-bis(2-aminoethylether)-N,N,N',N'-tetraacetic acid
eIF-2α	Eukaryotic initiation factor 2 α
ERD	Enhanced respiratory disease
ERK	Extracellular signal-regulated kinase
ERKi	ERK inhibitor UO126
FBS	Fetal bovine serum
FI-RSV	Formalin-inactivated RSV
GE	Gene end
GFP	Green fluorescent protein
GS	Gene start
HBE cell	Human bronchial epithelial cell
HBV	Hepatitis B virus
HCIS	High content imaging system
HCV	Hepatitis C virus
HEK293 cell	Human embryonic kidney 293 cell
HEK293T cells	Human embryonic kidney 293 transformed with Large-T antigen cells
HeLa	Henrietta Lacks
HEp-2 cells	Human epithelial type 2 cells
HEPES	4-(2-hydroxyethyl)-1-piperazineethanesulfonic acid
HiT	High titre clade
hpi	Hours post infection

HPV	Human papilloma virus
HRP	Horse radish peroxidase
HSP90	Heat shock protein 90
HSPG	Heparan sulfate proteoglycans
HSV1	Herpes simplex virus type 1
HSV2	Herpes simplex virus type 2
IAV	Influenza A virus
IBV	Influenza B virus
IC	Immune complex
ICAM-1	Intercellular adhesion molecule 1
ICU	Intensive care unit
IF	Immunofluorescence
IFN	Interferon
IFNAR	IFN α receptor
IgA	Immunoglobulin A
IgG	Immunoglobulin G
IKKα	IκB kinase α
IKKε	IκB kinase ε
IL-1	Interleukin 1
IL-4	Interleukin 4
IL-6	Interleukin 6
IRAK1	IL-1R-associated kinase 1
IRF3	IFN regulatory factor 3
IRF7	IFN regulatory factor 7
IRF9	IFN regulatory factor 9
IRS	Immunoregulatory sequences
ISG	IFN stimulated gene
ISGF3	IFN-stimulated gene factor 3

IκB	Inhibitor of NF-κB
K_D	Dissociation constant
LM	Light microscopy
Lox.	Loxoribine
Loxoribine	7-allyl-7,8-dihydro-8-oxoguanosine
LRTI	Lower respiratory tract infections
mAb	Monoclonal antibody
MAPK	Mitogen activated protein kinase
MAVS	Mitochondrial antiviral signaling protein
mCMV	Murine cytomegalovirus
MD-2	Myeloid differentiation factor 2
MDA5	Melanoma differentiation-associated gene 5
MEM	Minimum essential medium
MeV	Measles virus
MLKL	Mixed lineage kinase domain-like protein
MOI	Multiplicity of infection
MosLB	Mos lysis buffer
MTT	3-(4,5-dimethylthiazol-2-yl)-2,5-diphenyl tetrazolium bromide
MyD88	Myeloid differentiation primary-response protein 88
NADH	Nicotinamide adenine dinucleotide
NADPH	Nicotinamide adenine dinucleotide phosphate
NET	Neutrophil extracellular trap
NF-κB	Nuclear factor kappa-light-chain-enhancer of activated B cells
NK cell	Natural killer cell
NLR	NOD-like receptor
OASL	2'-5'-oligoadenylate synthetase-like protein
OMe	Methyl group
pAb	Polyclonal antibody

PAGE	Polyacrylamide gel electrophoresis
PBMC	Peripheral blood mononuclear cells
PBS	Phosphate buffered saline
pDC	Plasmacytoid Dendritic Cells
P-ERK	Phosphorylated ERK
PFU	Plaque forming unit
PIV1	Parainfluenza virus type 1
PIV3	Parainfluenza virus type 3
PKR	Protein kinase termed “PKR”
P-MLKL	Phosphorylated MLKL
P-RIP1	Phosphorylated RIP
PRR	Pattern recognition receptors
PVM	Pneumovirus of mice
qRT-PCR	Quantitative reverse transcriptase polymerase chain reaction
RdRp	RNA-dependent RNA polymerase
Ribavirin	1-β-D-ribofuranosyl-1,2,4-triazole-3-carboxamide
RIG-I	Retinoic-acid-inducible gene-I
RIP1	Receptor-interacting protein 1
RIP3	Receptor-interacting protein 3
RLR	RIG-I-like receptor
RNP	Ribonucleoprotein
RSV	Respiratory syncytial virus
RSV3Ab	Novus proprietary 4 monoclonal antibody cocktail
RSV-F	RSV fusion protein
RSV-G	RSV glycoprotein
RSV-L	RSV large protein
RSV-M	RSV matrix protein
RSV-M2-1	RSV M2 protein encoded by open reading frame 1

RSV-M2-2	RSV M2 protein encoded by open reading frame 2
RSV-N	RSV nucleoprotein
RSV-NS1	RSV non-structural 1 protein
RSV-NS2	RSV non-structural 2 protein
RSV-P	RSV phosphoprotein
RSV-SH	RSV small hydrophobic protein
RV	Rhinovirus
SAR	Structure activity relationship
SDS	Sodium dodecyl sulfate
Sf9 cells	*Spodoptera frugiperda* cells
siRNA	Short interfering RNA
SLE	Systemic Lupus Erythematosus
SOD1	Superoxide dismutase 1
ssRNA	Single stranded RNA
STAT1	Signal transducer and activator of transcription 1
STAT2	Signal transducer and activator of transcription 2
TANK	TRAF family member-associated NF-κB activator
TBK-1	TANK-binding kinase 1
T_H1	Type 1 helper
T_H2	Type 2 helper
T_H17	Type 17 helper
TIR	Toll- IL-1 receptor
TLR2	Toll-like receptor 2
TLR3	Toll-like receptor 3
TLR4	Toll-like receptor 4
TLR6	Toll-like receptor 6
TLR7	Toll-like receptor 7
TLR8	Toll-like receptor 8

TLR9	Toll-like receptor 9
TNFα	Tumor necrosis factor α
TRAF3	Tumor necrosis factor receptor-associated factor 3
TX-100	Triton X-100
UNC93B1	Uncoordinated 93 homolog B1
VOPBA	Virus overlay protein binding assay
VSV	Vesicular stomatitis virus
WB	Western blot
X-Gal	5-bromo-4-chloro-3-indolyl-β-D-galactopyranoside
XTT	2,3-bis-(2-methoxy-4-nitro-5-sulfophenyl)-2H-tetrazolium-5-carboxanilide disodium salt

Chapter 1: Introduction

1.1. RSV history

Respiratory Syncytial Virus (RSV) is a member of the *Orthopneumovirus* genus, *Pneumoviridae* family, and *Mononegavirales* order [1]. Originally referred to as Chimpanzee Coryza Agent, RSV was first identified in 1955 in a chimpanzee colony at the Walter Reed Army Institute of Research [2]. RSV was immediately suspected as a human pathogen, as the authors noted RSV neutralizing antibodies were present in a laboratory worker who contracted an upper respiratory tract infection after working closely with infected chimpanzees. The importance of RSV as a human pathogen was also suggested by pre-existing neutralizing antibodies in serum of patients who had no contact with the chimpanzee colony. RSV was successfully isolated from a human patient in 1957 [3], and by 1963 the importance of RSV as a major contributor to bronchiolitis in pediatric populations was recognized [4]. In the 1980s the significance of RSV infection in elderly populations became apparent [5].

Early attempts to develop a vaccine against RSV ended with the deaths of two infants. These deaths were the result of an enhanced respiratory disease (ERD) occurring during subsequent natural RSV infection [6]. The antiviral nucleoside analogue ribavirin was recommended for the treatment of severe RSV infection in 1993 [7], however, clinical trials leading to this recommendation were methodologically flawed and exaggerated efficacy [8,9]. Subsequent studies found that the benefits of ribavirin were limited or non-existent [10,11], and ribavirin is no longer included as a standard of care for RSV infection. Palivizumab, a humanized monoclonal antibody against RSV, was licensed in 1998 for the prophylactic prevention of RSV infections [12]. Due to its significant cost and the necessity of monthly prophylactic injections, palivizumab is only administered to high-risk infants. Palivizumab is not efficacious in the treatment of ongoing RSV infection and has an insignificant effect on overall RSV transmission rates [13].

Despite discovery of RSV dating back over six decades and intense efforts to combat RSV, no vaccine to prevent infection or efficacious antiviral to treat infection is available. As a result, RSV continues to impose a significant global burden of disease.

1.2. RSV burden of disease

1.2.1. Burden of disease in Canada and worldwide

In neonatal intensive care units (ICUs), RSV is well known as a leading cause of pediatric hospitalizations [14,15]. While individuals will be reinfected with RSV throughout life, the primary infection during infancy is typically the most severe. Approximately 40% of primary infections in infancy result in lower respiratory tract infections (LRTI) which manifest as bronchiolitis or pneumonia. In infants without pre-existing conditions, 0.5-2% of all infants will require hospitalization due to RSV LRTI [16]. In Canada and the United States RSV LRTI in infants results in approximately 12 000 and 77 000 annual hospitalizations, respectively [16]. Estimates of the worldwide burden of disease due to RSV are difficult to produce as RSV-related mortality disproportionately affects developing countries where disease reporting infrastructure is lacking. Despite this, in 2010, Nair *et al* estimated that LRTI caused by RSV in children under 5 years old resulted in 3.4 million hospitalizations and 66 000 to 199 000 deaths annually (examining data from 2005) [17]. A decade later, the RSV Global Epidemiology Network observed a comparable worldwide burden of disease in children under 5 years of age, with RSV LRTI responsible for 3.2 million hospital admissions and 94 600 to 149 400 deaths annually [18].

1.2.2. Risk factors and groups associated with severe RSV infection

A variety of risk factors contribute to the likelihood of hospitalization due to RSV infection. Risk factors independently associated with disease severe enough to require hospitalization include young age (less than 24 months) at the time of infection and premature birth (less than 35 weeks gestational age) [19]. Preterm infants infected with RSV have longer hospital stays, increased ICU usage, increased length of stay in ICU, increased supplemental oxygen usage, and increased mortality [20]. Other risk factors are also thought to be associated with disease severity, these include birth month in November, December or January, daycare attendance, more than 5 individuals living in the same home as the infant, familial atopy, reduced breast feeding, low birth weight, male sex, and infant exposure to environmental smoking [21,22].

Aside from these risk factors, certain populations are at a greater risk of hospitalization and morbidity due to RSV infection. Chronic Lung Disease (CLD) is a common complication of preterm birth and preterm infants with CLD who are infected with RSV are at a higher risk of hospitalization [19,23,24]. Other groups who suffer increased RSV infection severity include patients

with neuromuscular disease, trisomy 21, cystic fibrosis, immunodeficiency, and aboriginal children [16].

The impact of RSV on elderly populations is often under-appreciated, remaining in the shadow of other respiratory pathogens such as influenza. However, the significance of disease caused by RSV and influenza is comparable in older adults. In patients over 50 years of age hospitalized with acute respiratory illness, 6.5% and 6.1% tested positive for influenza and RSV, respectively. Rates of hospitalization in this population were 15 per 10 000 for RSV, and 11.8 per 10 000 for influenza [25]. In hospitalized elderly patients, RSV and influenza infections result in comparable lengths of hospitalization, ICU usage, and mortality [26,27]. Mortality rates due to RSV and influenza vary between studies. In community dwelling elderly patients, mortality due to RSV infection exceeded influenza infection with death rates of 10% and 6%, respectively [28]. Thus, while pediatric populations are often the focus of the rationale for RSV drug discovery campaigns elderly patients will also benefit immensely from the development of antivirals against RSV. Older adults also offer a competent population who can offer informed consent towards participating in clinical trials investigating RSV antivirals. This offers a means of investigating the efficacy of RSV antivirals prior to usage in vulnerable patients, namely infants.

1.2.3. RSV clinical presentation

In adults, RSV infection typically constitutes a self-limiting cold. A robust 2009 literature review estimated an average incubation period of 4.4 days for RSV infection (based on symptom onset) [29]. This agrees with a 2010 study in which 36 adult volunteers were experimentally inoculated that found an incubation period of 3.1 and 4.0 days based on qPCR and quantitative culture, respectively [30]. RSV loads peak between 5 and 7 days after infection and throughout infection viral load correlates with symptom severity. By 12 days post infection viral shedding ceases and symptoms resolve [30].

A study which included 5067 children under 5 years of age provides insight towards typical clinical presentation of severe RSV infection in children. Of 564 hospitalized children infected with RSV, 70% were diagnosed with bronchiolitis, 95% required supplemental oxygen due to labored breathing, 78% had wheezing, and 69% had a fever; of 355 outpatients infected with RSV, 98% had a cough, 75% had fever, 73% had labored breathing, and finally 65% had wheezing [19].

Interestingly, only 45% of hospitalized patients and 3% of outpatients were correctly diagnosed with RSV-associated illness.

1.2.4. RSV infection and the development of asthma

Asthma is characterized by bronchial hyper-reactivity, airway remodeling including narrowing, and mucus overproduction resulting in periodic exacerbations. These exacerbations are characterized by chest tightness, wheezing, and shortness of breath [31]. The strong association between severe respiratory viral infection early in life (predominantly with RSV or rhinovirus (RV)), and recurrent wheeze or asthma at a later age, is widely accepted [32-36]. Whether severe infection early in life predisposes one to the later development of asthma in a causal manner has been a point of contention for two decades [37,38]. The development of antiviral interventions limiting the severity of RSV infection early in life could help answer this question. Specifically, does a reduction in disease severity following antiviral treatment result in a reduced incidence of asthma and recurrent wheezing later in life? Insight is available from a retrospective study which found reducing RSV infection via prophylactic palivizumab treatment reduced the later development of recurrent wheeze by 61% [39].

1.3. RSV communicability

1.3.1. RSV seasonality

In temperate climates the RSV season lasts 3-5 months typically beginning in autumn, peaking in winter, and tapering off in the spring; RSV transmission is greatly reduced or not detected during the summer months [40-43]. In contrast, very cold or tropical climates do not obey this pattern and RSV transmission occurs year-round [42,43]. A variety of hypotheses have been proposed to explain the transmission patterns observed across regions, including changes to viral stability in the environment that are dependent on temperature, humidity, and ultraviolent light intensity. Alternatively, changes in human behavior throughout the seasons have been proposed to play a role [40-43]. No animal reservoir is known or suspected for RSV, and the reintroduction of RSV in regions with seasonal transmission cycles is not understood [40,44].

1.3.2. RSV transmission

RSV is primarily transmitted via large nasopharyngeal droplets from infected individuals [16]. Large droplets (>100 μm in size) remain in air for only a matter of seconds, quickly falling onto surfaces due to gravity [45]. Therefore, direct contact with an infected individual, or contact with

contaminated surfaces, is required for transmission via large droplets. In the environment, non-enveloped viruses may remain viable for periods of weeks or months. As an enveloped virus, RSV is not expected to remain viable outside of the body for extended periods [46]. However, infectious RSV can be isolated from hard surfaces 6 hours after transfer and can survive on hands for 25 minutes [47]. As RSV may enter through the eyes or nose [48], and remains viable in the environment for several hours, fomites present an important route for RSV transmission.

In contrast to large droplets, droplets less than 10 μm in diameter remain suspended in the air as an aerosol for a matter of hours [45]. Recently, it was observed that viable RSV is present in aerosols produced by infants with bronchiolitis [49]. The air was sampled at distances of 1 metre, 5 metres and 10 metres from infected infants. Air was also sampled in the presence of infants and 2 hours after discharge. RSV titers from airborne particles were highest at a distance of 1 metre, however, RSV was detected up to a distance of 5 metres from patients. RSV titers were highest when sampling was conducted in the presence of the patient, yet aerosols containing viable RSV remained detectable at 2 hours post discharge. Furthermore, RSV was found in particles less than 4.7 μm in diameter. While large diameter particles are typically caught in the upper respiratory tract, particles less than 5 μm in size may be directly inhaled into the lower airways [50]. Thus, a significant portion of these aerosolized particles were small enough to access the lower airways [49]. This discovery may have implications for public health measures used to prevent nosocomial RSV transmission, suggesting that airborne transmission of RSV may be possible. However, whether an appreciable degree of RSV transmission occurs through this route remains to be confirmed.

1.4. RSV biology: proteins and functions

1.4.1. Genome and Nucleoprotein

RSV has a single stranded negative sense RNA genome of approximately 15.2kb; within this genome are 10 genes which encode 11 proteins [51]. The RNA genome is tightly bound to RSV nucleoprotein (RSV-N) in a helical ribonucleoprotein (RNP) complex. Specifically, the RNA is bound to a basic groove near the external surface a decameric ring of RSV-N [52]. Each RSV-N protein interacts with 7 bases, as a result 70 bases are associated with each turn of the decameric ring. Interestingly, the function of RSV-N during infection by RSV extends beyond genomic organization to antagonism of the host innate immune response.

1.4.1.1. Antagonism of the innate immune response by nucleoprotein

During RSV infection RSV-N colocalizes with retinoic-acid-inducible gene-I (RIG-I), melanoma differentiation-associated gene 5 (MDA5), and mitochondrial antiviral signaling protein [53] (MAVS; also known as IPS-1, CARDIF, or VISA [54]). RIG-I and MDA5 are cytosolic pattern recognition receptors (PRRs) [55,56]. RIG-I detects 5'-triphosphorylated RNA and double stranded RNA (dsRNA), while MDA5 detects only the latter [57]. Following activation by their cognate ligands, both RIG-I and MDA5 signal through the MAVS adaptor protein to stimulate an interferon (IFN)-β response. Transfection of RSV-N into cells infected with Newcastle Virus (which elicits a strong IFN-β response) attenuates the IFN-β response via inhibition of RIG-I and MDA5 signaling through sequestration of MAVS to inclusion bodies [53]. This represents one strategy by which RSV antagonizes the innate immune response (**Figure 1.1**). A protein kinase termed PKR [58] is produced in response to type I IFNs as a means of inducing an antiviral state in cells [59]. PKR is activated by cytosolic dsRNA (reviewed in [60]). Briefly, binding to dsRNA results in activation of PKR via phosphorylation of multiple serine and threonine residues. Phosphorylated PKR inactivates eukaryotic initiation factor 2 α (eIF-2α) via phosphorylation. In the absence of eIF-2α, cellular translation of mRNA into protein ceases. During RSV infection there is an accumulation of phosphorylated PKR, however, eIF-2α is not inactivated. Instead, phosphorylated PKR is bound by RSV-N [61]. Given the localization of RSV-N to inclusion bodies during RSV infection, it is likely that binding of PKR by RSV-N sequesters PKR in inclusion bodies [53]. Thus, inhibition of PKR represents a second mechanism by which RSV-N antagonizes the host innate immune response.

1.4.2. RNA-dependent RNA polymerase

The RSV RNA-dependent RNA polymerase (RdRp) conducts transcription and replication of the RSV genome. At a minimum, RSV RdRp is comprised of large protein (RSV-L) and phosphoprotein (RSV-P). The RSV -L/-P complex is able to initiate transcription or replication and produce short transcripts up to 200 nucleotides in length [62,63]. Expression of RSV-L, -P and -N is sufficient for minigenome replication, indicating that concurrent encapsidation of the growing genome by RSV-N is required for RdRp replicase processivity [64]. Conversely, transcriptase activity by RSV RdRp requires the RSV-M2-1 anti-termination factor [65]. As a result, a full compliment of RSV-L, -P, -M2-1, and -N is required to produce infectious RSV from a cDNA antigenome [66].

RSV-L is the catalytic subunit of RSV RdRp, responsible for polymerizing chain elongation [67], polyadenylation (reviewed by Cowton *et al* [68]), and 5' capping [69]. Studies on the *Mononegavirales* Measles Virus (MeV) have observed that the MeV phosphoprotein mediates interaction between the RdRp and the RNP [70]. Given the similarity amongst RdRp of *Mononegavirales* viruses, it is expected that RSV-P completes this role in a similar fashion. Phosphorylation of RSV-P at serine-232 is required for chain elongation [71], and phosphorylation of RSV-P at threonine-108 enables interaction of the RdRp with RSV-M2-1 [72]. The production of subgenomic mRNA begins with the initiation of RdRp at the +3 nucleotide in the leader promoter region [73]. The RdRp scans the genome until reaching the first Gene Start (GS) site. After identifying a GS site, the RdRp begins synthesis of mRNA until a Gene End (GE) site is reached [74,75]. All genes contain one GS and GE, except for the RSV-M2 gene which contains two open reading frames encoding RSV-M2-1 and RSV-M2-2, respectively.

Known nucleoside analogues with antiviral activity against RSV target the polymerization activity of the RSV-L component of the RdRp [76]. This mechanism of antiviral activity is not universally applicable to all RdRp inhibitors, some of which target regions outside of the polymerization active site [77] or target components of the RdRp other than RSV-L. This is the case for RSV604; one mechanism of action proposed for RSV604 is inhibition of RSV transcription through binding RSV-N [78]. It is not unexpected that interference with a variety of target proteins inhibits RSV RdRp, given the essential nature of multiple viral and cellular proteins. Specifically, cellular proteins including heat shock protein 90 (HSP90) are necessary for optimal RdRp processivity [79]. Antagonism of any RdRp enzymatic process or antagonism of interactions between RdRp constituents offers mechanisms by which antivirals may inhibit RSV replication. (**Table 1.1**).

1.4.2.1. RdRp error rate and quasispecies theory

The fidelity of the RSV RdRp is best estimated using values available for Vesicular Stomatitis Virus (VSV), another *Mononegavirales* virus. The mutation rate per base pair and mutation rate per genome replication for VSV are approximately $1.6 \times 10^{-4} – 2.3 \times 10^{-3}$ and 2.8 – 4.3, respectively [80]. The rate of spontaneous mutation for RdRps overall has been estimated to be 10^{-3} to 10^{-5} errors per base pair [80]. Lack of a proofreading function contributes to this low fidelity [81]. By contrast, the mutation rate in microbial DNA genomes has been observed to range from $7.2 \times 10^{-7} – 7.2 \times 10^{-11}$ errors per base pair [80]. As RSV has a genome size of approximately 15kb, a mutation rate of 10^{-3}

to 10^{-5} errors per base pair would result in 0.15 – 15 mutations per genome replication. The low fidelity of RSV RdRp precludes RSV from existing as a clonal species, instead RSV exists as a quasispecies where the wild type sequence is defined as a weighted average of the multitude of genotypes present during infection [82]. The diversity of the quasispecies is limited by evolutionary fitness, specifically, the ability of a given sequence to reproduce. Quasispecies theory is important to the development of RSV-antivirals, as it explains the notorious rate at which RNA viruses develop resistance to antivirals.

1.4.3. Envelope proteins: fusion protein, glycoprotein, and small hydrophobic protein

The RSV viral envelope proteins include fusion protein (RSV-F), glycoprotein (RSV-G), and small hydrophobic protein (RSV-SH). RSV entry is mediated by a complex interaction of RSV-F and RSV-G envelope proteins and host cell proteins (reviewed by Griffiths *et al* [40]). Briefly, candidate receptors that have been proposed include CX3 chemokine receptor 1 (CX3CR1), epidermal growth factor (EGF), annexin II, calcium dependent lectins, Toll-like receptor 4 (TLR4), intercellular adhesion molecule 1 (ICAM-1), nucleolin, and heparan sulfate proteoglycans (HSPGs). The functions of these proteins include tethering RSV to the surface and triggering fusion [40]. Of these receptors, the interaction between nucleolin and RSV-F has been observed to be of significant importance for entry by RSV. RSF-F is essential for entry; prior to interaction with the host cell it exists as a trimer in a pre-fusion conformation [83]. It is hypothesized that fusion of the viral membrane to the host cell is driven by a conformational shift in multiple spring-loaded RSV-F proteins [40]. Host-cell nucleolin was first identified as a candidate receptor for RSV-F via virus overlay protein binding assay (VOPBA) [84]. The VOPBA incorporated lysates from human airway epithelial (1HAEo-) cells, Chinese hamster ovary cells, Madine-Darby canine kidney cells, and human epithelial type 2 (HEp-2) cells. In the VOPBA, cell lysates were separated by sodium dodecyl sulfate polyacrylamide gel electrophoresis (SDS-PAGE) and transferred to a nitrocellulose membrane. RSV in solution was added to the membrane and RSV bound to a factor in each cell lysate at 100 kDa. The 100 kDa band was excised following the VOPBA and subjected to mass spectrometry analysis. Mass spectrometry revealed nucleolin as a common hit in each excised sample. Nucleolin was observed to co-immunoprecipitate with RSV-F, and colocalize with RSV at the cell surface during infection, suggesting nucleolin and RSV-F may directly interact or interact through a common protein complex. The physiological relevance of this interaction was pursued through neutralization assays. Specifically, pre-treatment of 1HAEo- cells with nucleolin-

specific antibodies significantly reduced RSV infection. Likewise, pre-treatment of virus with soluble nucleolin significantly reduced RSV infection. Cell culture experimentation also supported the role of nucleolin as a receptor for RSV. Expression of nucleolin in *Spodoptera frugiperda* (Sf9) insect cells, which are not permissive to RSV infection, was sufficient to confer susceptibility of RSV infection. Finally, short interfering RNA (siRNA) knockdown of nucleolin expression *in vivo* reduced nucleolin expression on the apical surface of airway epithelial cells of mice and reduced RSV replication in the lung.

Depending on the type of immortalized cell line, RSV-G is dispensable in cell culture [85]. However, interaction between RSV-G and the cellular membrane protein CX3CR1 appears to be of importance in robust models of infection using differentiated primary airway epithelial cells and in mice [86]. Like RSV-G, RSV-SH is not essential for RSV replication in cell culture [85,87], and recombinant RSV strains lacking RSV-SH were only slightly attenuated in mice [87]. In chimpanzees, RSV lacking RSV-SH was not attenuated in the upper respiratory tract, but replication was reduced in the lower respiratory tract [88]. While the role of RSV-SH in RSV replication is not well characterized, these observations have precipitated investigations of RSV-SH-deletion vaccine candidates [89].

1.4.4. Non-structural protein 1 and non-structural protein 2

The RSV non-structural 1 (RSV-NS1) and non-structural 2 (RSV-NS2) proteins demonstrate a remarkable number of immunomodulatory functions centering around antagonism of the host IFN response (reviewed in [90]), delaying apoptosis in an IFN-independent manner [91], and arresting the cell cycle in the G_0/G_1 phase [92].

1.4.4.1. Antagonism of the innate immune response by non-structural protein 1 and non-structural protein 2

Cascades of pathogen recognition receptors, adaptor proteins, and kinases mediate the synthesis of type I IFNs in response to viral infection (reviewed in [93]). Collectively, RSV-NS1 and RSV-NS2 target these pathways by interfering with RIG-I [94], tumor necrosis factor receptor-associated factor 3 (TRAF3) [95], inhibitor of NF-κB (IκB) kinase ε (IKKε; note NF-κB abbreviates nuclear factor kappa-light-chain-enhancer of activated B cells) [95], interferon regulatory factor 3 (IRF3) [96], and interferon regulatory factor 7 (IRF7) [97] (**Figure 1.1**). RSV-NS1 and RSV-NS2 also inhibit the

cellular response to IFN-β by targeting signal transducer and activator of transcription 2 (STAT2) [95,97] and 2'-5'-oligoadenylate synthetase-like protein (OASL) for degradation [98].

As described above, after activation RIG-I interacts with MAVS [55], an interaction mediated by caspase recruitment domains (CARD). Via co-immunoprecipitation in human embryonic kidney 293T (HEK293T) cells overexpressing RSV-NS1, -NS2, and RIG-I, it was observed that RSV-NS2 (but not RSV-NS1) directly binds RIG-I [94]. This interaction was mapped to the N-terminus of RIG-I, the location of the RIG-I CARD. Binding of RIG-I by RSV-NS2 prevented association of RIG-I and MAVS, preventing IFN-β transcription.

TRAF3 is an essential component of the RIG-I pathway downstream of MAVS (**Figure 1.1**). TRAF3 complexes with TRAF family member-associated NF-κB activator (TANK), IKKε, and TANK-binding kinase 1 (TBK-1); this complex then phosphorylates IRF3. Transfection of A549 cells with a plasmid encoding RSV-NS1 resulted in a depletion in TRAF3; infection with wild type RSV, but not RSV-NS1-deficient RSV, also depleted TRAF3 [95]. It is not known if RSV-NS1 directly interacts with TRAF3, as a co-immunoprecipitation experiment was not performed. It is also not known how RSV-NS1 mediates the reduction in TRAF3, although proteasomal degradation was ruled out. Finally, the authors also observed a reduction in IKKε attributable to RSV-NS1 [95].

Synthesis of IFN-β is dependent on IRF3 phosphorylation, translocation into the nucleus, dimerization, association with cAMP response element-binding protein binding protein (CBP), and finally binding of the IRF3/CBP dimer to the IFN-β promoter [93]. In A549 cells overexpressing IRF3, RSV-NS1 did not prevent IRF3 phosphorylation, translocation to the nucleus, or dimerization. However, RSV-NS1 bound IRF3, preventing association with CBP and subsequent binding of IRF3 to the IFN-β promoter [96].

IRF7, a common member of signaling cascades downstream of Toll-like receptor 3 (TLR3), Toll-like receptor 7 (TLR7), Toll-like receptor 9 (TLR9) and RIG-I (reviewed in [99]), is targeted for degradation during by RSV-NS1 [97]. In the absence of IRF7, myeloid differentiation primary-response protein 88 (MyD88) dependent and independent type-1 IFN production is impaired [100]. Following binding of type I IFNs to the IFN α/β receptor (IFNAR), IRF7 expression is induced. *De novo* synthesized IRF7 is then phosphorylated, translocates to the nucleus, and further drives IFNα and IFNβ production in a positive feedback loop (reviewed in [101]). In plasmacytoid dendritic

cells (pDC), which are highly important to the type I IFN response during viral infection, IRF7 is constitutively expressed at a high level [99]. By targeting IRF7 for degradation, RSV-NS1 undermines the IFN response downstream of a series of PRRs [97].

STAT2 is a transcription factor which is important to the autocrine and paracrine responses to type I IFNs [93,102]. Following phosphorylation, STAT2 associates with signal transducer and activator of transcription 1 (STAT1) and interferon regulatory factor 9 (IRF9) to form the IFN-stimulated gene factor 3 (ISGF3) complex; ISGF3 translocates to the nucleus and drives the expression of 2'-5'-oligoadenylate synthetase, PKR, P56, Myxovirus resistance gene A, interferon stimulated gene 15, Viperin, C-X-C motif chemokine 10, inducible nitric oxide synthase, IRF7, STAT1 and various other IFN stimulated genes (ISGs) [102,103]. RSV-NS2 inhibits this pathway by targeting STAT2 for degradation [97,104].

OASL, while related to the family of oligoadenylate synthetases, restricts RSV replication in a manner independent of second messenger 2'-5'-oligoadenylate (2-5A) synthesis. While the antiviral mechanism of OASL is not yet clear, RSV-NS1 targets OASL for proteasomal degradation offering yet another means of interfering with the innate immune response [98].

RSV-NS proteins are not limited to undermining the innate immune response. The RSV-NS proteins also contribute to the ability of RSV to evade the adaptive immune response. When dendritic cells (DC) are infected by RSV, DC maturation is stunted by wild type RSV but not by RSV ΔNS deletion mutants [105]. Inhibition of IFN signaling through antibody-mediated blockade of IFNAR compensates RSV ΔNS deletion mutants, resulting in stunted DC maturation. Greater activation and proliferation of $CD8^+$ T cells and $CD4^+$ T-cells were also observed following coculture with RSV ΔNS-infected DCs compared to wild type RSV-infected DCs [106,107]. *In vivo* experiments in BALB/c mice have shown increased $CD8^+$ T cell proliferation and activation in RSV ΔNS2-infected mice than in wild type RSV-infected mice [108]. These studies illustrate how RSV-NS1 and RSV-NS2 undermine the adaptive immune response to RSV. Thus, RSV-NS1 and RSV-NS2 may contribute to the profound lack of lasting protective immunity to RSV reinfection.

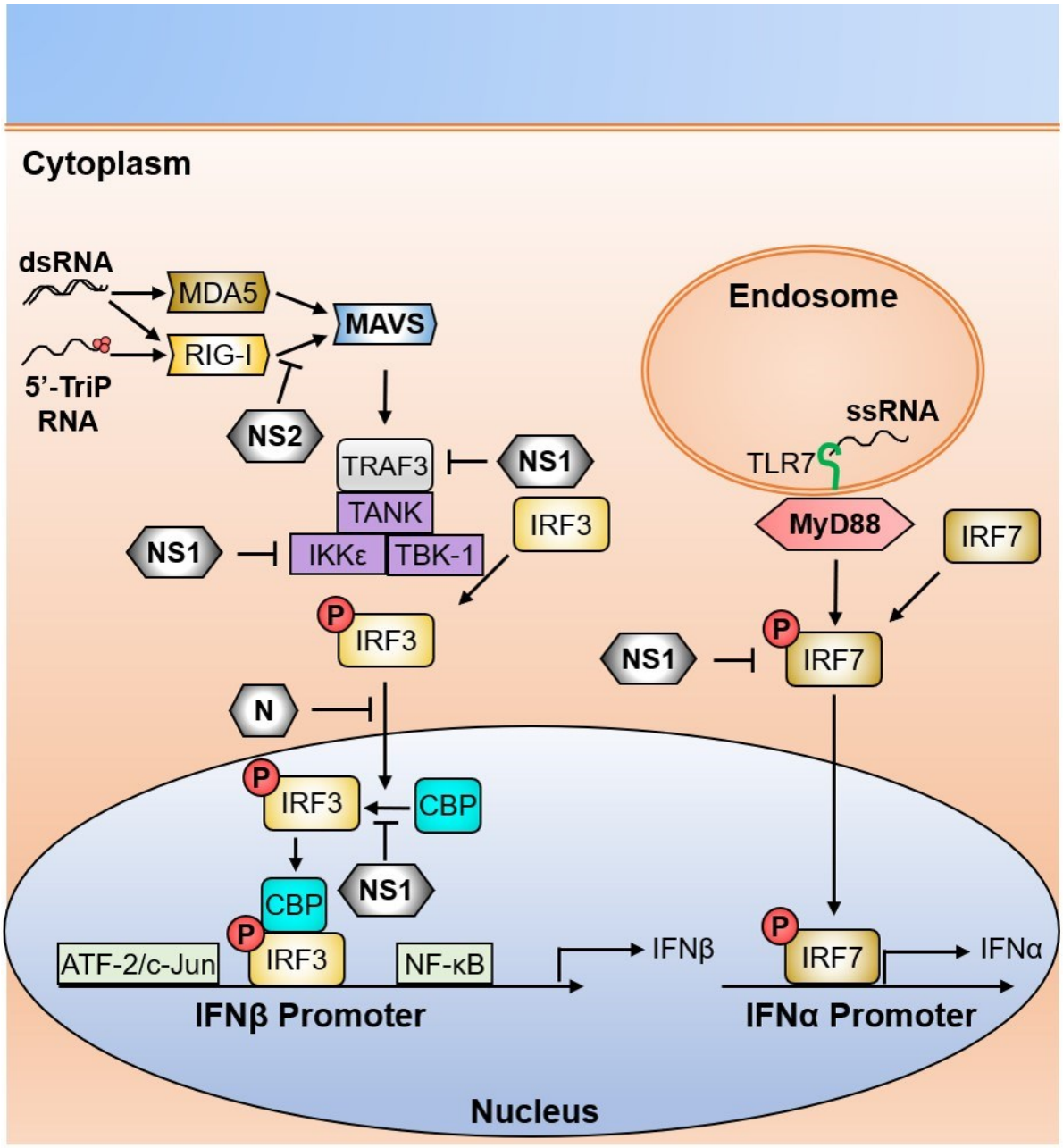

Figure 1.1. RSV-NS1, RSV-NS2, and RSV-N inhibit the host IFN response by targeting multiple components of signaling pathways. Schematic showing cytosolic and endosomal detection pathways for single stranded RNA (ssRNA) and double stranded RNA (dsRNA). The production of Type I IFNs is inhibited by RSV through redundant targeting of signalling cascades by RSV-NS1, RSV-NS2, and RSV-N.

1.4.5. Matrix protein

The matrix protein (RSV-M) is a structural protein which lines the inside of the viral envelope and associates with the RNP via RSV-M2-1 [109].

1.4.6. Serotyping and Genotyping

Convalescence following infection with RSV results in serum containing antibodies that neutralize all other strains of RSV. Thus, RSV cannot be taxonomically distinguished through traditional serology; all RSV strains belong to a single serotype [110]. Using monoclonal antibody panels, RSV was antigenically delineated into two subgroups based on subtype specific binding of RSV-N, -P, -M, -G, and –F [111]. The most extensive sequence divergence between subgroups is found in RSV-G [112]. As a result, RSV-G is used to distinguish between RSV-type A and RSV-type B. Sequence analysis of RSV-G has led to the classification of 11 RSV-type A and 23 RSV-type B clades [113].

When novel clades emerge, they have been observed to displace ancestral clades and spread globally. The RSV-type B BA clade emerged in 1999 and became the dominant global RSV-type B clade in the ensuing decade [114]. Owing to the low fidelity of its RdRp, RSV evolves rapidly. RSV-BA continued to evolve with four genotypes emerging in the ten years following its emergence. The constant population-level evolution of RSV results in the replacement of antigenic epitopes and contributes to the explanation of how RSV successfully reinfects individuals throughout life [115]. This viral evolution occurs within the individual host due to selective pressures imposed by the immune response. In an infant lacking an adaptive immune response RSV genetic diversity was relatively stagnant. Following bone marrow transplant RSV genetic diversity increased rapidly [116].

While novel clades spread rapidly, they are not necessarily more virulent. The association of pathogenesis with RSV subtype has remained a pressing question since RSV was first divided into RSV-type A and RSV-type B in the 1980s. Conflicting evidence suggest that RSV subtype does, [117-119] or does not, [120,121] predict disease severity. The ability to further organize subtypes into genetic clades may help address this question. Recently, a pilot study observed that RSV strains that replicate to high titers in patients and have high replication kinetics in cell culture are genetically similar. These were termed High Titre (HiT) clades [122]. This study did not directly examine the severity of illness; however, an association of RSV viral load and disease severity has been observed previously [123]. Thus, identification of HiT clades may enable forecasting of dominant strains causing severe infections in the subsequent RSV season.

1.5. The immune response to RSV

1.5.1. Detection of RSV infection

Recognition of foreign pathogens begins with PRRs. In 2000, the observation that RSV-F stimulated TLR4 constituted the first discovery of a viral PRR [124]. This study observed that murine macrophages stimulated with RSV-F secreted pro-inflammatory interleukin 6 (IL-6), however, in mice lacking TLR4 IL-6 production was absent. Furthermore, RSV titers from lungs were significantly higher and replication prolonged in mice lacking TLR4. More recently, it has been suggested that TLR4 signalling during RSV infection produces responses which are anti-inflammatory. Specifically, TLR4 is required for the differentiation of anti-inflammatory alternatively activated macrophages [125]. In both cases TLR4 is beneficial to the host, but the mechanism by which TLR4 stimulation benefits the immune response during RSV infection requires further study. The full list of PRRs which may be involved in sensing RSV infection now includes the Toll-like receptor 2 (TLR2)/Toll-like receptor 6 (TLR6) heterodimer (unknown ligand), TLR3 which binds dsRNA, TLR7 which binds single stranded RNA (ssRNA), RIG-I which binds 5' tri-phosphorylated dsRNA, MDA5 which binds dsRNA, Nod-Like Receptors which bind ssRNA, and dsRNA-Binding Protein which binds dsRNA [126]. The importance of each PRR varies. It is likely that those which are most important are those which RSV has evolved to target for inhibition by RSV-N, RSV-NS1, and RSV-NS2 (**section 1.4**).

1.5.2. Immune response in the human host

The immune response to RSV has been studied extensively in patients. Information is gained through examination of cellularity and cytokines present in bronchoalveolar lavage (BAL) fluid, examining post-mortem lung biopsies, and examining circulating cell populations. Studies typically categorize individuals into a mild RSV infection group (upper respiratory tract infection) or severe RSV infection group (lower respiratory tract infection requiring hospitalization). Differences between these groups are used to infer beneficial and harmful immune responses.

The predominant cell type recovered from BAL fluid during RSV infection is neutrophils [127,128]. In biopsies of fatal RSV infections originating from the years 1925 through 1959, neutrophils were observed in the bronchiolar epithelium and to a lesser extent in the peribronchiolar tissue [129]. IL-8 is responsible for neutrophil recruitment; increased IL-8 secretion and resultant neutrophilia are associated with disease severity [130]. Furthermore, symptom severity correlates with increasing

neutrophilia early in disease, and symptoms resolve as neutrophil counts decline [131]. As neutrophils drive inflammation without producing antiviral benefits, neutrophils are thought to be harmful (reviewed in [132]). During RSV infection neutrophils also release neutrophil extracellular traps (NETs). While these NETs have beneficial roles (trapping virions and proinflammatory cytokines), they are typically though to be harmful due to the airway occlusion which results [133]. Neutrophils can be categorized as a component of the type 17 helper (T_H17) $CD4^+$ T-cell response (discussed below).

Recruitment of the adaptive immune response to fight viral infection is dependent on a robust response by pDCs. These professional antigen presenting cells are located throughout the body, including in the lungs. In response to viral infection pDCs are the primary source of type I IFNs [134]. Selective depletion of pDC in mouse models of RSV infection results in enhanced airway disease and increased lung RSV titers [135]. Complementing RSV-infected mice with IFN-α offset the depletion of pDCs, and RSV lung titers did not increase, indicating pDC-conferred protection from RSV is mediated by their characteristic production of IFNα. After Type I IFNs are released in the lung environment, pDCs subsequently migrate to the draining lymph nodes [136]. In the lymph nodes pDCs present antigen and costimulatory molecules to lymphocytes recruiting the adaptive immune response to help counter infection [reviewed in [137]]. To limit the antiviral effect of pDCs, RSV inhibits pDC IFN production [138]. Inadequate pDC activation can have devastating repercussions; lack of pDC activation was a major contributor to the tragic failure of the formalin-inactivated RSV (FI-RSV) vaccination attempt [139].

CD8+ cytotoxic T lymphocytes (CTLs) are an essential component of the antiviral immune response, inducing lysis in virally infected cells [51]. Chemokine (C-C motif) ligand 5 (CCL5) is responsible for recruiting lymphocytes to locations of inflammation; severe RSV infection is associated with overall low plasma CCL5 chemokine levels. In line with this observation, severe RSV infections were associated with low $CD4^+$ T-cell, $CD8^+$ T-cell, and natural killer (NK) cell blood counts [130]. As opposed to neutrophils, increasing $CD8^+$ T-cell counts are associated with convalescence and a decrease in symptom severity [131]. This data contributes to the conclusion that T-cells, especially CTLs, are beneficial during RSV infection [132].

The harmful versus beneficial responses to RSV infection can be thought of in the paradigm of type 1 helper (T_H1) versus type 2 helper (T_H2) responses. T_H1 responses are associated with the

resolution of viral infection. During a T_H1 response, IL-12 drives the differentiation of T_H1 $CD4^+$ T-cells which subsequently produce IFN-γ and support $CD8^+$ CTL proliferation [140]. T_H2 responses are required for controlling parasitic infections; IL-4 production drives the differentiation of T_H2 $CD4^+$ T-cells which subsequently produce IL-4, IL-5, and IL-13 [140]. The T_H2 response antagonizes the T_H1 response. It is hypothesized that during RSV infection a T_H1 response is beneficial, while skewing towards a T_H2 response is harmful. Supporting this hypothesis is that the IL-4/ IFN-γ ratio in nasal lavage fluid was greater (indicating a T_H2 response) in infants with bronchiolitis versus upper respiratory tract infection [141]. Reduced IFN-γ expression was also observed in peripheral blood mononuclear cells (PBMCs) collected from infants with severe RSV [142]. These results obtained during natural RSV infection in humans support the paradigm that a T_H2 cytokine response is detrimental and drives severe RSV infection. Interestingly, the T_H2 response is a hallmark of eosinophilic asthma providing a hypothesis for a mechanism by which severe RSV infection early in life predisposes individuals to asthma development in later life [31].

While helpful in categorizing helpful versus harmful immune responses during RSV infection, this paradigm oversimplifies the immune response to RSV by failing to account for T_H17 $CD4^+$ T-cells, which recruit neutrophils through the production of IL-17 [143]. IL-6 contributes to the polarization of naïve $CD4^+$ T-cells into T_H17 CD4+ T-cells. Increased IL-6 and IL-17 was observed in tracheal aspirates from infants with severe RSV LRTI versus healthy infants [144]. In the murine RSV infection model, neutralization of IL-17 by antibody or gene knockout is beneficial. Anti-IL-17 antibody treatment during RSV infection reduced the migration of neutrophils to the lungs and reduced RSV lung titers. This anti-IL-17 treatment was associated with an increase in RSV-specific $CD8^+$ T cells [144]. Finally, B cells and the humoral immune response are also important to the resolution of infection. While they do not confer lasting protection, immunoglobulin G (IgG) and mucosal immunoglobulin A (IgA) responses are protective [132].

1.5.3. Immune response fails to confer lifelong protection

Ultimately, RSV is highly successful at subverting the host immune response. This begins with how well RSV counteracts the IFN response. Like RSV, Parainfluenza Virus Type 3 (PIV3) is a member of the *Mononegavirales* order that infects the human airway epithelium. PIV3 is second only to RSV with respect to causing LRTI in children [145]. Exogenous addition of type I IFNs in cell culture reduces PIV3 replication by 1000 to 10 000-fold, in contrast, the same addition of type

I IFNs only reduces RSV replication by 10 to 20-fold [146]. Thus, RSV efficiently antagonizes the IFN response (**Figure 1.1**).

The ability of RSV to re-infect individuals throughout life illustrates how poorly the adaptive immune response controls RSV. Following infection neutralizing antibodies against RSV-F and RSV-G are present in serum. However, the limited ability of these neutralizing antibodies to confer protection from reinfection and the rapidity with which serum levels decrease is striking. Healthy adult volunteers were infected with RSV, and subsequently re-challenged with the same RSV strain at 2, 4, 8, 14, 20 and 26 months post infection [147]. Upon reinfection in subsequent months with the same RSV A-2 strain, 73% of volunteers were infected at least once, with 47% re-infected upon the first challenge at 2 months after the initial infection.

1.6. RSV therapeutic landscape

1.6.1. Failed vaccine attempts

Shortly after the discovery of RSV, Kim *et al* attempted to develop a vaccine through formalin inactivation of RSV [6]. This approach had been successful for Jonas Salk, who had recently developed the world's first vaccine against poliovirus [148]. A clinical trial was completed with a group of 31 infants less than one year of age. These infants were primarily from African American low socioeconomic status families [6]. The increase in neutralizing antibodies following immunization was limited to a 4-fold increase in 43% of immunized infants and this rise in neutralizing antibodies afforded no protection from natural infection during the subsequent RSV season. Instead, ERD was observed upon natural infection. 80% of RSV-infected vaccinated infants required hospitalization while only 5% of the control group required hospitalization. In the vaccinated group the duration of hospitalization was significantly increased, the rate of serious complications increased, and two infants died. Understandably, this tragedy stunted RSV vaccine development campaigns.

Over the ensuing decades, mechanisms of ERD have been proposed. One explanation for ERD is based on the pathogenic deposition of antibody-antigen immune complexes (IC) in the lungs. While IC formation can be beneficial towards virus neutralization during viremia, the deposition of ICs into tissue drives the pathogenesis of a variety of infectious and autoimmune diseases [149]. In mice vaccinated with FI-RSV, ERD (measured as an increase in airway hyperresponse) and IC formation in the lungs was observed. ERD was absent in complement-deficient mice and in B cell-

deficient mice (which lack antibodies required for IC formation) [150]. The authors concluded that IC deposition in the lungs and subsequent complement activation drives ERD following vaccination with FI-RSV. This study relies on airway hyperresponse acting as an appropriate measure of ERD, which is only modestly appropriate. However, the authors bolster their conclusions by noting extensive complement activation in lung biopsies obtained from the two infants who succumbed to ERD in the vaccine trial by Kim *et al* [6].

Building on these results, Delgado *et al* observed that FI-RSV elicited non-protective low-avidity antibodies [139]. Insufficient TLR stimulation in pDCs resulted in reduced $CD4^+$ T lymphocyte proliferation and activation. Resultantly, B cells failed to form germinal centers and undergo the affinity maturation process necessary for increasing antibody avidity. In this study, complementing FI-RSV vaccination with UV-inactivated RSV was sufficient to induce a protective antibody response.

In the wake of the failed vaccine attempt by Kim *et al*, candidate vaccines are now carefully monitored for ERD in animal models prior to clinical trials. While no vaccine has been developed to treat RSV, neither has any vaccine which elicits ERD entered clinical trials in infants. Modern RSV vaccination attempts have included the production of immunogenic nanoparticles [151] or generation of live-attenuated RSV virus vaccines through random mutagenesis, guided attenuation through recombinant RSV generation, or generation of recombinant bovine RSV or PIV expressing human RSV-F and RSV-G (reviewed [152]). Owing to the difficult challenge of generating an immune response in the first months of life when protection against RSV is most important, maternal vaccination strategies are also currently being explored in a phase 3 clinical trial (NCT02624947).

*cpts*248/404 was the last live attenuated vaccine candidate to enter clinical trials prior to the utilization of recombinant genetic engineering technologies to introduce specific mutations. “cp” and “ts” refer to mutations generated through cold passaging or chemical mutagenesis-induced temperature sensitive mutations, respectively [152]. In phase I clinical trials *cpts*248/404 was tested in steadily younger age cohorts, culminating in administration to infants less than two months of age [153]. In seropositive children between 15 and 59 months of age *cpts*248/404 live virus was not shed and antibody responses were nearly non-existent. In seronegative children less than 24 months of age *cpts*248/404 live virus was shed and neutralizing antibodies against RSV were

observed in serum, however, this study was not powered to determine the efficacy of protection against natural RSV infection. In the youngest cohort of 1 to 2-month old infants, neutralizing antibody development was rare – as is the case for natural infection in this age group. As expected, maternal antibody levels antagonized the development of most infant antibody responses, including IgG antibodies against RSV-F and RSV -G, and IgA antibodies against RSV-F. Finally, congestion associated with peak *cpts*248/404 shedding precluded the vaccine candidate from further study in the 1 to 2-month old cohort [153].

MEDI-559 was created via reverse genetics wherein *cpts*248/404 was further attenuated by way of deletion of RSV-SH and introduction of a temperature sensitive Y1321K mutation in RSV-L [154]. In RSV-seronegative children aged 5 to 24 months of age, MEDI-559 produced neutralizing antibody responses in 59% of infants versus 9% for the placebo group. Protection from natural RSV infection was not measured. Lower respiratory tract illness was higher in the MEDI-559 arm than placebo yet was comparable to the rate observed in placebo groups in other studies making the safety of MEDI-559 difficult to interpret [154]. To date, subsequent clinical trials on MEDI-559 have not been initiated. Results are not available for other live attenuated vaccine virus candidates including MEDI-ΔM2-2 which lacks the RSV-*M2-2* gene (NCT01459198) or a genetically stabilized version of MEDI-599 (NCT01852266). Lastly, results are not available for RSV ΔNS2 Δ1313 I1314L which lacks RSV-NS2, has a deletion of the 1313 codon in the RSV-L protein, and a temperature sensitive mutation introduced through an I1314L mutation in the RSV-L protein (NCT01893554).

Novavax has led the development of nanoparticle-based RSV vaccines. Nanoparticles were created through infection of Sf9 insect cells with a recombinant baculovirus containing a modified RSV-F gene. RSV-F nanoparticles consist of multiple peptide homotrimers joined via a micelle core [151]. A phase 3 clinical trial in adults over 60 years of age observed no protection against lower respiratory tract infection (0.47% in the vaccinated group versus 0.44% in the placebo arm) (NCT02608502). A separate phase 3 clinical trial is ongoing to investigate whether immunization of pregnant women in their third trimester with the RSV-F nanoparticle confers protection to infants via maternal antibodies (NCT02624947). It is estimated that this study will be completed in June of 2020.

A fundamental challenge to the development of RSV vaccines is that natural infection with RSV in immunocompetent adults offers very little protection [147]. Any vaccine will need to elicit a stronger immune response than natural infection and do so in the absence of deleterious side effects. This hurdle will have to be surmounted for an RSV vaccine to be realized.

1.6.2. The humanized monoclonal antibody, palivizumab

1.6.2.1. Efficacy and cost-effectiveness of palivizumab

Palivizumab is a humanized monoclonal antibody containing murine-origin complementarity-determining regions specific for the pre-fusion conformation of RSV-F [155]. Palivizumab was licensed for prophylactic treatment against RSV infection in high-risk infants following the IMpact clinical trial. This clinical trial included 1502 infants born at less than 35 weeks gestational age [12]. Monthly administration of palivizumab in premature infants without bronchopulmonary dysplasia, a type of CLD, reduced the rate of hospitalization in this cohort from 8.1 % in the placebo arm to 1.8% in the palivizumab arm ($P < 0.001$). For infants with bronchopulmonary dysplasia the rate of hospitalization was reduced from 12.8% to 7.9% between placebo and treated groups, respectively ($P = 0.038$). Shortly thereafter, another large clinical trial was focussed specifically on 1287 infants with hemodynamically significant chronic heart disease (CHD). This study observed a reduction in hospitalization from 9.7% to 5.3% ($P = 0.003$) [156]. Subsequent population-based studies typically confirmed that palivizumab effectively reduced the rate of hospitalization due to RSV infection [157]. Owing to these successes in clinical trials, palivizumab is widely prescribed to high-risk infants.

Many limitations reduce the impact of palivizumab on the annual RSV burden of disease. These include prohibitive cost, the time burden on families and physicians associated with monthly injections throughout the RSV season, the lack of efficacy against ongoing infection, and the development of resistant RSV strains. Cost-benefit analyses vary widely between studies and study populations. Hampp *et al* found that for premature infants in Florida, 30 must be treated to avoid a single hospitalization; the cost per hospitalization avoided in this population was approximately $302103. This is dramatically more expensive than the cost of hospitalization in this region, approximately $8910 per infant in this population [158]. In contrast, for inhabitants of Baffin Island in Nunavut where medical evacuation to the Children's Hospital of Eastern Ontario drastically increases the cost of hospitalization, administering palivizumab to all infants less than 6 months

of age (as opposed to only high-risk infants) may be a cost-effective strategy [159]. The Canadian Pediatric Society notes that palivizumab treatment in Canada costs approximately $5600 per infant, and the number needed to treat to prevent hospitalization ranges from 16-23 for various high-risk groups [13]. As such, outside of Baffin Island palivizumab is not a cost-effective treatment. Currently, the Canadian Pediatric Society recommends prophylactic palivizumab treatment for preterm infants, infants with CHD, and infants with CLD [13].

Palivizumab has been examined as an intervention to treat serious RSV infection, and a significant reduction in tracheal RSV concentration was observed. However, treatment with palivizumab did not produce clinically relevant benefits as there was no reduction in the duration of hospitalization, duration of mechanical ventilation, or duration of supplemental oxygen therapy [160]. Similarly, other studies have found no clinically relevant benefits of treatment of RSV infection with palivizumab [161]. Motavizumab, another humanized monoclonal antibody, was developed through affinity maturation of palivizumab with the goal of improving the efficacy of anti-RSV immunoglobulin therapy [162]. Motavizumab was explored as a potential treatment for active RSV infection. Unfortunately, motavizumab did not influence viral load or clinical outcomes and has not been approved for clinical use [162].

The necessity of monthly injections is detrimental on two fronts, the most obvious is that it creates a time burden for families and physicians. The less apparent downside of monthly injections is that regular trips to physician's offices increase the chance of RSV exposure for high-risk infants. This explanation has been offered as a hypothesis to explain why the use of palivizumab does not reduce the overall rate of infant hospitalization.

1.6.2.2. RSV resistance to palivizumab

As an RNA virus with an error-prone RdRp, RSV exists as a quasispecies [82]. Therefore, RSV is expected to have the capacity to rapidly develop mutations which confer resistance to antiviral interventions. The clinical implications of these resistant mutants depend on the fitness cost associated with each mutation. Prior to the licensure of palivizumab, RSV mutations in the antigenic A site of the RSV-F protein had already been observed to confer resistance to antibody peptide fragments [163]. Resistance to palivizumab was first noted via the K272M mutation in RSV-F which develops readily in cell culture during serial passaging in increasing palivizumab concentrations [164]. This mutation was not associated with a reduction in fitness as growth kinetics

in cell culture were not affected. Resistance to palivizumab via the K272M mutation was confirmed *in vivo* in the Cotton Rat model. The known list of RSV-F mutations which confer resistance to palivizumab has grown to include N262S, N268I, K272N, K272T, K272Q, S275F, and S275L [165]. An RSV strain with an RSV-F K272E mutation was the first clinic isolate with suspected resistance to palivizumab [166]. A much larger study of 6600 patients treated with palivizumab or motavizumab offered insight towards the prevalence of resistance in treated patient populations. Among 178 breakthrough infections approximately 5% were associated with RSV strains possessing putative resistance point mutations in the antigenic A site of RSV-F. The authors confirmed resistance to palivizumab in cell culture experiments; from these clinical isolates resistance was associated with RSV-F K272N/M/T/Q or E mutations [167]. In untreated populations mutations associated with resistance are less common yet remain present. Of 145 untreated infants infected with RSV, palivizumab-resistant isolates RSV-F N262D and S275F were identified with a frequency of 0.7% each [165]. Some studies have found that wild type RSV strains outcompete palivizumab-resistant RSV strains in direct competition assays [167]. This has likely limited the spread of palivizumab-resistant strains in the general population. Studies specifically examining whether palivizumab efficacy has been reduced since licensure, due to the circulation of resistant strains, have not been conducted.

1.6.3. Ribavirin mechanism of action and viral resistance

1.6.3.1. Discovery of ribavirin

Synthesis of 1,2,4-triazole nucleosides in the pursuit of antiviral compounds led to the discovery of ribavirin (1-β-D-ribofuranosyl-1,2,4-triazole-3-carboxamide) in 1972. In this initial study *in vitro* antiviral activity was described for VSV, PIV-3, RV, herpes simplex virus type 1 (HSV1), herpes simplex virus type 2 (HSV2), pseudorabies virus, murine cytomegalovirus (mCMV), vaccinia virus, myxoma virus, adenovirus (AdV), parainfluenza virus type 1 (PIV-1), influenza A virus (IAV), influenza B virus (IBV), coxsackievirus, and poliovirus [168]. Ribavirin was later found to also have antiviral activity against RSV, hepatitis C virus (HCV), human immunodeficiency virus (HIV), Sendai virus, MeV, and Newcastle virus [77,169-175]. In the clinic, ribavirin plus pegylated IFN was a cornerstone standard of care for HCV infection for many years until this treatment was surpassed by curative direct-acting antivirals [176,177].

Clinical treatment of severe RSV infection in infants with ribavirin was at one time recommended, however, its usage and efficacy were controversial and usage is no longer recommended.

1.6.3.2. Antiviral mechanism of action

A variety of non-mutually exclusive mechanisms have been proposed for the broad antiviral activity of ribavirin. Convincing results show that ribavirin interferes with flavivirus replication through inhibition of IMP dehydrogenase [178]. This inhibition reduces the concentration of cytosolic guanosine monophosphate. As a result, pools of deoxyguanosine triphosphate and guanosine triphosphate, required for viral replication by DNA and RNA genome viruses are reduced [179]. Targeting of a host cell enzyme required by a wide array of viruses for replication helps explain the broad spectrum of antiviral activity possessed by ribavirin. Conversely, this does not fully explain the antiviral mechanism of action for ribavirin. For example, the antiviral activity of ribavirin is not counteracted through replenishing the GTP pool via guanosine treatment during PIV-3 infection [180]. This suggests that ribavirin inhibits PIV-3 replication in a manner independent of IMP dehydrogenase inhibition. Other antiviral mechanisms of action include direct RdRp inhibition, catastrophic mutagenesis through unbiased base pairing to cytidine or uridine (noted for poliovirus and HCV) [176,181,182], and immunomodulation [171]. The error catastrophe mechanism of action of ribavirin against Poliovirus is supported by the observation that a single G64S point mutation, which increases Poliovirus RdRp fidelity, confers resistance to ribavirin [183]. A recent study using high resolution RNA sequencing of RSV transcripts found that treatment with Ribavirin produced a 1.5-fold increase in the frequency of transition mutations [184]. Therefore, it is likely that mutagenesis contributes to the antiviral activity of ribavirin against RSV. However, serial passaging of RSV in the presence of ribavirin fails to elicit resistant escape mutants suggesting ribavirin may also inhibit RSV replication via IMP dehydrogenase inhibition [175].

Ribavirin is effective against RSV in cell culture, with reported effective concentration 50% (EC_{50}) values of 6.3 to 28.38 μM [77,169,170,185,186]. Given the efficacy of ribavirin in cell culture, it has been widely used to validate screening assays, provide a point of reference for compounds identified in these screens, and offers a standard through which different screening assays can be compared.

1.6.3.3. Use of ribavirin to validate RSV-antiviral screening assays

Screening protocols have been established previously to identify compounds with antiviral activity against RSV. As ribavirin effectively inhibits RSV replication in cell culture, ribavirin is typically used to validate RSV-antiviral assays.

One successful RSV-antiviral screening campaign employed the use of a subgenomic replicon assay. This subgenomic replicon was developed through substitution of RSV envelope proteins with a blasticidin resistance selection marker and the addition of GFP and renilla luciferase reporters [185,187]. To determine whether this protocol had the capacity to identify compounds with antiviral activity against RSV, three previously described RSV-antivirals were tested. This assay identified the RSV-antiviral activity of ribavirin, YM-53403, and BI-D, which inhibited the production of the reporter signal with EC_{50} values of 6.28 μM, 0.63 μM, and 0.78 μM, respectively. Thus, the subgenomic replicon assay reliably identified known RSV-antivirals, supporting the conclusion that this assay could identify novel compounds with antiviral activity against RSV.

Cytopathic effect (CPE)-based antiviral screening campaigns have also included ribavirin to validate the capacity of their respective antiviral screening assays. A CPE-based screen developed with primary airway epithelial cells included ribavirin, RSV604, and YM-53403 to validate assay results [188]. Ribavirin was also used to validate a similar CPE-based screening assay [189]; this assay was successfully utilized to discovery of the RSV fusion inhibitor JNJ 2408068. A third CPE-based assay was developed by Noah *et al*, this assay was used to screen a 300 000 compound library and led to the discovery of the fusion inhibitor ML232 [186]. This group also validated the capacity of their assay to identify RSV-antivirals by including ribavirin. In this assay, an EC_{50} value of 28.38 μM was observed for ribavirin against RSV. In addition to validating this assay, this result demonstrated that the EC_{50} value of ribavirin varies between assays.

1.6.3.4. The clinical efficacy of ribavirin against RSV

Ribavirin was recommended for the treatment of severe RSV infections following clinical trials which demonstrated that treatment resulted in a reduction in duration of mechanical ventilation, length of supplemental oxygen treatment, and duration of hospitalization [7,8]. However, this clinical trial was methodologically flawed. Nebulized sterile water was used in the treatment of control groups instead of nebulized saline, and aerosolized water is known to be detrimental to the airways [9]. Thus, it is likely that treatment administered to the control group exacerbated disease.

Subsequent studies found that ribavirin was ineffective for the treatment of severe RSV infection. A randomized, double-blinded placebo-controlled trial found that ribavirin treatment did not reduce the duration of oxygen therapy, mechanical ventilation, or hospitalization [10]. Importantly, this study used isotonic saline as a control. A prospective study of 1425 children with community-acquired RSV LRTI stratified patients by risk groups including pre-existing congenital heart disease, premature birth, chronic lung disease, or hypoxia within 48 hours of hospital admission. These groups were further stratified into those which received or did not receive mechanical ventilation. In all groups treatment with ribavirin offered no benefit with respect to duration of hospitalization, hypoxia, intensive care unit stay, or mechanical ventilation [11]. Ribavirin is also a teratogen; therefore, aerosolized therapeutic delivery is cumbersome as healthcare worker exposure must be prevented. As a result, ribavirin is not included as a standard of care for the treatment of RSV infection. In practice, ribavirin use is restricted to cases of persistent RSV infection in immunocompromised individuals such as allogeneic haematopoietic stem cell transplant recipients [190-192]. Ribavirin may offer some benefit in these populations, however, large scale double-blinded placebo-controlled trials have not been conducted.

The discrepancy between the antiviral activity of ribavirin in cell culture experiments and in the clinic may be due to the absorption, distribution, metabolism, and excretion (ADME) properties of ribavirin. Specifically, it is likely the ribavirin simply does not accumulate to a high enough concentration in the airway epithelial cells where RSV replicates for an antiviral effect to be observed.

1.6.4. Strategies for RSV antiviral development

1.6.4.1. Subgenomic replicon systems

A non-cytotoxic stable subgenomic replicon system was developed for RSV through replacement of RSV-F, -G, and -SH with blasticidin S deaminase (which enables selection via blasticidin resistance). This replicon included all genes required for RSV genome replication, including RSV-N, -P, -L, and -M2-1. Also remaining were RSV-NS1, -NS2, and -M. Lastly, this replicon included GFP to enable identification of cells expressing the replicon. The authors were able to introduce this replicon into seven immortalized cell lines, including A549, HEp-2, HeLa, human hepatocarcinoma Huh-7 cells, HEK-293 cells, and Vero cells [187]. This replicon was adapted for use in high-throughput screening to identify small molecule inhibitors of RSV RdRp [185]. GFP was

complemented with renilla luciferase to provide a more robust and stable signal. Replicon activity was measured by renilla luciferase-driven luminescence following a 48-hour incubation with compounds at 10 μM. Subsequently, cytotoxicity was measured in the same well as antiviral activity via quantification of adenine triphosphate (ATP) concentration. This replicon-based system reliably detected known RSV RdRp inhibitors, including YM53403 and BI-D (**Table 1.1**), but was unaffected by the IAV RdRp inhibitor Oseltamivir [185]. This high throughput screen identified three novel inhibitors, cpd 1, 2 and 3, which targeted RSV-L, host cell machinery, and RSV-P, respectively [193]. This replicon assay was further refined and expanded to screen an AstraZeneca library of one million compounds. 379 compounds with an EC_{50} below 10 μM and a therapeutic index greater than 10 were identified. These compounds were examined in HEp-2 cells via CPE assay and four families of lead compounds were selected for further optimization [194]. From these compounds AZ-27 was identified [185,195] (**Table 1.1**). A derivative of AZ-27, PC786, is currently in phase 2 clinical trials NCT03382431; [196]. Separately, this replicon system was used to test a Broad Institute library of 100 000 compounds, resulting in the identification of three series of compounds with an EC_{50} below 10 μM and a therapeutic index greater than 10 [197]. Interestingly, efficacy against RSV-type A and RSV-type B was highly varied within these compounds.

There are advantages to replicon-based systems over cell culture-based systems. A lower biocontainment level is required as live virus is not present. The assay is also efficient, requiring only 48 hours for detection of antiviral activity, as opposed for 6-7 days for detection of CPE. This assay was also made efficient through detection of cytotoxicity and inhibition of viral replication in the same well. The major limitation of subgenomic replicon systems is that they preclude the identification of inhibitors which target viral proteins absent from the assay. A further limitation is that a considerable portion of compounds identified by replicon assays do not have an inhibitory effect during live RSV infection [194].

1.6.4.2. *Cell culture based systems*

Cell culture-based systems examine the effect of compounds on the natural RSV replication cycle in primary or immortalized cell monolayers. Cell culture-based high throughput screening assays indirectly measure CPE by measuring cell viability 6 to 7 days post infection. Briefly, following infection cell viability stains such as CellTiter-Glo [188], 3-(4,5-dimethylthiazol-2-yl)-2,5-diphenyl tetrazolium bromide (MTT) [189], ATP luminescence assay [186], or 2,3-bis-(2-methoxy-4-nitro-5-

sulfophenyl)-2H-tetrazolium-5-carboxanilide disodium salt (XTT) [170] are utilized to measure the reduction in living cells following infection. This reduction in living cells results from CPE caused by RSV infection.

Major pharmaceutical companies have developed cell culture-based high throughput screening protocols with the capacity to examine libraries on the order of millions of compounds. Novartis screened 1.7 million compounds for antiviral activity against RSV in HEp-2 cells [198]; GlaxoSmithKline screened 1.98 million compounds for antiviral activity against RSV in primary cells grown in 384 well plates [188].

CPE-based assays have the advantage of being capable of identifying inhibitors which target any RSV protein or host cell machinery necessary for viral replication. Identification of an inhibitor which targets host cell machinery necessary for viral replication would be valuable for two reasons. The first is that a broad array of viruses often rely on similar host cell processes for replication, such as nucleoside synthesis. A screen of 1.7 million compounds by Bonavia *et al* discovered a novel *de novo* pyrimidine synthesis pathway inhibitor which inhibited the replication of RSV [198]. While this screen sought to identify compounds with antiviral activity against RSV, these compounds also inhibited the replication of IAV, IBV, HCV, Dengue Virus, Yellow Fever Virus, and HIV. The second advantage of inhibitors which target host cell machinery is that the virus is unable to develop resistance to the antiviral through mutation as no viral protein is being targeted. An immediate concern with compounds which target host cell processes, however, is cytotoxicity. For example, health care workers must exercise caution when providing ribavirin therapy as ribavirin is teratogenic. This teratogenicity is likely due to inhibition of cellular IMP dehydrogenase by ribavirin.

A drawback of previously described cell culture-based system is the requirement of a lengthy infection to elapse before CPE may be observed. CPE-based protocols require an infection of 6 [170,188], or 7 days [189]. CPE-based assays also rely on the assumption that CPE accurately represents RSV replication. As CPE produced by RSV is limited and slow to develop this assumption may be tenuous.

1.6.4.3. Alternative screening assays

Prior to the development of subgenomic replicon systems, an alternative non-cell culture-based assay was developed which utilized *in vitro* RSV RdRp transcription (similar to the method described in Section 2.18) and subsequent poly(A) tail capture. Through poly(A) tail capture, the production of RSV mRNA transcripts was measured following a cell extract-based viral transcription assay [199]. Using this assay, Liuzzi *et al* described a series of non-nucleotide inhibitors of RSV replication which targeted the RSV RdRp. Specifically, these inhibitors prevented co-transcriptional guanylylation, the mechanism by which the RSV polymerase complex subunit L applies a 5' cap to mRNA transcripts [200]. The most efficacious of these compounds was BI-D. Unfortunately, BI-D did not progress to investigations in clinical trials as *in vivo* efficacy was limited. xxx

1.6.5. Development of RSV antivirals

Antivirals only offer therapeutic potential if viral replication drives disease; if viral load has already been controlled by the immune response at the time of symptom onset then an antiviral will be of little benefit. This important consideration is exemplified by IAV, where peak viral shedding precedes peak symptom severity [201]. Neuraminidase inhibitors such as zanamivir (Relenza) and oseltamivir (Tamiflu) effectively inhibit IAV replication *in vitro* and have been stockpiled to address the threat posed by pandemic influenza outbreaks. However, the clinical benefits of these antivirals are limited. Zanamivir and oseltamivir have no effect on hospitalization rates or serious complications, and only a minor decrease in the time to symptom alleviation [202]. A larger therapeutic window exists with respect to RSV infection. In experimentally inoculated adult volunteers, RSV replication and titers mirrored symptom severity [30]. Likewise, in hospitalized children, RSV load paralleled disease severity [203]. Therefore, development of antivirals against RSV works under the hypothesis that reducing viral load early during infection will decrease disease severity.

A wide range of strategies have been employed in the search for RSV antivirals, and numerous compounds have undergone clinical trials. These include nucleoside analogues and non-nucleoside analogues which target the RSV polymerase complex, an siRNA which targets RSV N, and small molecules which interfere with viral fusion (**Table 1.1**) [204]. Alternatively, therapeutics such as Danirixin seek to mitigate the damage due to inflammation which occurs during RSV infection [204].

Examples for each of these antiviral strategies will be explored with a focus on compounds which have progressed the furthest in clinical trials.

GS-5806 is an RSV-F inhibitor [205]. In cotton rats the concentration at which viral replication was reduced by 50% was 0.43 nM. In healthy adult volunteers inoculated with RSV, GS-5806 reduced symptom scores and viral replication [206,207]. In a direct comparison, GS-5806 offered a greater therapeutic index than VP-14637, TMC-353121, BMS-433771, BI-D, YM-53403, RSV604, and ribavirin [205]. In April of 2017 GS-5806 completed phase 2b clinical trials in adults hospitalized with RSV, however, results have not been released (NCT02135614). Another fusion inhibitor, JNJ-53718678 (known also as JNJ-678), is being investigated in phase 2 clinical trials (NCT03379675; NCT02387606). As was observed for GS-5806, treatment with JNS-53718678 reduced viral load and symptom scores in healthy adult volunteers experimentally infected with RSV [208].

A creative approach was taken in an attempt to discover efficacious RSV antivirals that employed siRNA. siRNA harnesses host cell machinery to target specific mRNA transcripts for degradation [209]. ALN-RSV01, the first antiviral siRNA approved for testing in clinical trials, targets RSV-N transcripts. In a phase 2 clinical trial using healthy adult volunteers inoculated with RSV, ALN-RSV01 given prophylactically reduced the number of volunteers infected [210]. In a separate phase 2 clinical trial, ALN-RSV01 was administered to adult lung transplant recipients with RSV infections. While ALN-RSV01 reduced progression of bronchiolitis obliterans syndrome, no reduction was observed in symptom severity, viral shedding, or viral load [211].

ALS-008176 (lumicitabine) is a nucleoside analogue which inhibits the polymerase activity of RSV-L. Lumicitabine is currently in multiple phase 2 clinical trials. The results of clinical trials are not available. However, results in adult volunteers challenged with RSV are promising. Volunteers were inoculated with RSV and began treatment with lumicitabine after infection was confirmed by RT-PCR. Treatment with lumicitabine reduced viral load and duration of infection [212]. BI-D and PC786 represent non-nucleoside analogue inhibitors of RSV-L [196,213]. PC786 is currently in Phase 2 clinical trials NCT03382431. PC786 bears structural similarity to AZ-27, which was identified from an AstraZeneca library of one million small molecules [194,195]. Little other information is available for PC786.

Antibody and antibody-like biologicals have been extensively investigated for potential therapeutic use against RSV infection. Palivizumab was originally licensed for prophylactic treatment against RSV in high-risk infants and failed to demonstrate efficacy as a therapeutic intervention during ongoing infection [12,214]. Motavizumab is a humanized monoclonal antibody which was derived from palivizumab. Motavizumab failed to gain regulatory approval for prophylactic or therapeutic treatment against RSV infection after hypersensitivity reactions were observed and no improved efficacy versus palivizumab was observed. The most recent attempt at producing a biologic intervention is ALX-0171; heavy chain antibody fragments generated in llama were genetically linked via glycine-serine segments to form trimeric nanobodies [215,216]. Results in cotton rats were promising, with 2-log reductions in viral titers observed. A phase 1 clinical trial is ongoing (NCT02979431).

Table 1.1 Recent RSV antivirals in development or in clinical trials.

Compound Name	Development Stage	Mechanism of action	Citation
JNJ-53718678 (JNJ-678)	Phase 2 CT completed	Small molecule RSV-F inhibitor	[208] NCT02387606 NCT03379675
GS-5806 (Presatovir)	Phase 2b CT completed	Small molecule RSV-F inhibitor	[205,207] NCT02135614
BTA-C585	Phase 2 CT completed	Small molecule RSV-F inhibitor	[217] NCT02718937
ALX-0171	Phase 1 and 2 CT ongoing	Antibody-like RSV-F inhibitor	[215] NCT02979431 NCT03418571
AK-0529	Phase 1b and 2 CT ongoing	Small molecule RSV-F inhibitor	NCT02654171 NCT02460016
MDT 637 (VP-14637)	Phase 1 CT completed; results not released	Small molecule RSV-F inhibitor	[218] NCT01355016
BMS-433771	No investigation in CT	Small molecule RSV-F inhibitor	[219]
TMC-353121	No investigation in CT	Small molecule RSV-F inhibitor	[220]
ALN-RSV01	Phase 2b CT; partial success	siRNA targeting RSV mRNA encoding RSV-N	[211] NCT01065935

RSV604	Phase 1 CT completed; results not released	Binds RSV-N protein; blocks RNA synthesis	[78] NCT00416442
ALS-008176 (lumicitabine)	Phase 2 CT completed; results not released	Targets RSV-L; causes chain termination	[76,212] NCT02673476
PC786	Phase 2 CT ongoing	Targets RSV-L	[196] NCT03382431
AZ-27	No investigation in CT	Inhibits *de novo* RNA synthesis initiation by RSV	[195]
BI-D	No investigation in CT	Inhibits RSV mRNA elongation and capping producing IFN response	[213]
YM-53403	No investigation in CT	Targets RSV L	[77]
GS-5734	Phase 2 CT ongoing*	Inhibits polymerization by RSV-L *in vitro*	[221] NCT02818582
BCX-4430	Phase 1 CT*	Inhibits polymerization by RSV-L *in vitro*	[222] NCT02319772

Abbreviations: Boehringer Ingelheim compound D (BI-D); Clinical Trial (CT); Fusion (RSF-F); Interferon (IFN); Nucleoprotein (RSV-N); Large protein (RSV-L). * CT to examine activity against Ebola virus, activity against RSV observed in pre-clinical experimentation. Alternative drug names are shown in brackets.

1.7. Toll-like Receptor 7

The intersection of TLR7 biology and RSV replication has not been studied in detail. In this thesis the novel discovery of TLR7-mediated enhancement of RSV replication is explored in chapter five. Given the importance of TLR7 to this thesis, an introduction is provided.

TLR7 binds uridine-containing single stranded RNA and variety of synthetic purine nucleoside analogues [136,223-228]. Separate binding sites within TLR7 are responsible for binding ssRNA or small synthetic ligands [229]. In the clinic, TLR7 agonists are licensed for the treatment of anogenital warts [230], actinic keratosis, and minor basal cell carcinoma [231]. As stimulation of TLR7 results in smooth muscle relaxation and priming of a T_H1 immune response, TLR7 agonists have been investigated as possible asthma therapeutics [232].

1.7.1. TLR7 biology

TLR7 was identified in 2002 shortly after the first discovery of mammalian TLRs [233]. Following its discovery, a great deal has been elucidated with respect to TLR7 cleavage, regulation, and localization within the cell.

Multiple checks are in place to minimize inappropriate detection of self ssRNA by TLR7. Sub-cellular localization of TLR7 to endosomes represents one important check [234]. Cellular ssRNA is rapidly digested by RNases in the extracellular environment, thus it is not expected that self ssRNA would gain access to endosomes via the endocytic pathway. Delivery of TLR7 to endosomes is mediated by uncoordinated 93 homolog B1 (UNC93B1) [235,236]. Prior to TLR7 being functional it must be properly cleaved. Kanno *et al* observed that TLR7 mutants lacking a proteolytic cleavage site are non-functional, furthermore, both the N- and C- fragments of TLR7 must be present in the endosome following cleavage for TLR7 to be functional [237]. It was previously thought that cleavage occurred via proteolytic cleavage by cathepsins and asparagine endopeptidases during acidification in the maturing endosome [238]. This would ensure that TLR7 is not functional prior to localization in mature endosomes. However, during experimental blockage of endosomal acidification, TLR7 is proteolytically cleaved by furin-like proprotein convertases [239]. As such, cleaved and functional TLR7 may be present as early as the endoplasmic reticulum. Thus, the timing of TLR7 cleavage may not be as important to regulation as initially suggested. However, acidification of endosomes is still required for TLR7 activation preventing inappropriate signaling by TLR7 prior to arrival in endosomes [224,238]. Finally, depending on cell type TLR7 expression may be constitutively expressed or inducible via tumor necrosis factor α (TNF-α) and interleukin 1 (IL-1) [238].

As is the case for all TLRs, except for TLR3, TLR7 signaling is dependent on interaction with MyD88 [233]. TLR7 and MyD88 interact via Toll- IL-1 receptor (TIR) domains. Ultimately, three

transcription factors are activated following TLR7 stimulation, IRF7, NF-κB and Activator Protein-1 (AP-1) [240]. The IRF7 pathway is essential for type I IFN production. MyD88 complexes with IRF7 and TNF-associated factor 6, with each component of this complex necessary for IFN production [241]. TRAF3 associates with the MyD88/IL-1 receptor-associated kinase 1 (IRAK1)/IRF7 complex and is required for IFNα production [240,242,243]. The next step in this cascade is phosphorylation of IRF7. Numerous kinases are capable of phosphorylating IRF7, including IκB kinase α (IKKα), IKKε, TBK-1, and IRAK1 [99]. Experimental evidence suggests that, with respect to TLR7 stimulation, IRAK1 [244] or IKKα [245] are responsible for IRF7 phosphorylation. Following phosphorylation IRF7 translocates to the nucleus, binds type I IFN promoters, and IFN is produced [99,100,246].

TLR7 stimulation also results in IκB degradation resulting in the translocation of NF-κB to the nucleus, and phosphorylation of mitogen activated protein kinases (MAPKs) which result in AP-1 phosphorylation and subsequent phospho-AP-1 translocation to the nucleus [247]. Combined, these transcription factors result in the expression of proinflammatory cytokines [reviewed in [240]].

1.7.2. TLR7 ligands

TLR7 was first identified as the receptor for the immune response modifier Imiquimod [233] which was already licensed for the treatment of anogenital warts caused by Human Papilloma Virus (HPV) [230]. Subsequently, two seminal studies on TLR7 using murine models observed that murine TLR7 is stimulated by viral ssRNA from influenza [225] and HIV [226]. TLR7 is also required for pDC-mediated production of IFNα in response to infection by VSV and IAV [136]. Human TLR7 activation by ssRNA was first demonstrated using synthesized ssRNA in activated macrophage (THP-1) cells and PBMCs collected from healthy donors; siRNA knockdown of TLR7 inhibited the response of activated THP-1 macrophage-like cells to ssRNA [223]. Interestingly, the authors noted that ssRNA sequence could determine a bias towards an IFNα or TNFα response. Due to the potential for applications as anti-tumor or airway inflammatory disease therapeutics, a multitude of synthetic TLR7 agonists have been generated [reviewed in [232,248]].

1.7.2.1. Stimulation of TLR7 by the guanosine analogue loxoribine

Loxoribine and structurally similar guanosine analogues were first identified as immunomodulators which stimulated type I interferon production by lymphocytes [249-251]. An NF-κB luciferase reporter assay was used to elucidate the mechanism of action for this

immunomodulatory response. Human embryonic kidney 293 (HEK293) cells were transfected with human TLR2, TLR3, TLR7, Toll-like receptor 8 (TLR8), or TLR9. Only cells transfected with TLR7 responded to stimulation by loxoribine [252]. Results in TLR7-deficient lymphocytes were consistent with this observation. TLR7-deficient lymphocytes failed to respond to loxoribine, however, transfection of TLR7 back into TLR7-deficient lymphocytes rescued responsiveness to loxoribine [224]. Crystal structure analyses have defined the molecular docking site for loxoribine within TLR7 and revealed that TLR7 has two distinct ligand-binding sites. The first ligand-binding site binds small guanosine analogues, including loxoribine, and the second ligand-binding site binds poly-uridine ssRNA sequences [229]. This binding of TLR7 by loxoribine at the first ligand-binding site induces TLR7 dimerization and signalling.

The dissociation constant (K_D) for TLR7 and loxoribine is relatively high. Whereas the K_D of the canonical TLR-ligand interaction between myeloid differentiation factor 2 (MD-2; of the TLR4-MD-2 receptor complex) and lipopolysaccharide is 65 nM [253], the K_D of TLR7 and loxoribine is 5.6 µM [229]. The biological rate of uptake of loxoribine by cells, which is not defined, and this relatively high K_D value, determine the concentrations at which loxoribine is biologically active. In the literature, loxoribine is used at concentrations up to 2 mM. In TLR7-transfected HEK293 cells no increase in NF-κB luciferase reporter activity was observed at 125 µM loxoribine, at 500 µM loxoribine a 2-fold increase was observed, at 1 mM a 3-fold increase was observed, and at 2 mM a 5-fold increase was observed [224]. Relatively high concentrations of loxoribine are also used in non-transfected cells which naturally express a high level of TLR7. In peripheral blood leukocytes stimulation with 100 µM loxoribine is required to induce IFNα production, and peak proliferation of splenocytes was observed during stimulation with 500 µM loxoribine [224].

1.7.2.2. Antagonism of TLR7 by IRS-661

Immunoregulatory sequences (IRSs), known also as inhibitory oligonucleotides, were first isolated from the DNA genome of type 2 AdV in the context of their antagonistic effect on TLR9 stimulation [254]. Owing to this initial characterization as TLR9-antagonists, early research into IRSs focussed on the relationship of IRSs and TLR9.

With respect to their mechanism of action, IRSs do not block the uptake of the TLR9 ligand unmethylated CpG DNA. Instead, IRSs and CpG DNA are taken up at the same rate [255-257]. The oligodeoxynucleotide sequence of each IRS is of paramount importance, as slight changes affect

inhibitory activity. In particular, the inclusion of a "GGGG" motif was found to confer the strongest antagonistic effect [257]. It was hypothesized that this 4-guanine motif enabled the formation of G-tetrads, a nucleic acid secondary structure formed through Hoogsteen hydrogen bonding [258]. Interruption of Hoogsteen hydrogen bonding through the incorporation of a guanosine analogue into the GGGG motif, which prevented G-tetrad formation, resulted in a loss of the inhibitory effect of IRSs [259]. These results suggest that the inhibitory effects of IRSs are mediated through the formation of nucleic acid secondary structures formed by IRSs. IRSs also benefit from the inclusion of a phosphorothioate backbone, which delays degradation by DNases [257,260]. While many initial studies utilized cells of murine origin, the TLR9-antagonistic activity of IRSs against human cells was also confirmed [260]. Finally, the therapeutic application of IRSs as selective immunosuppressive therapies was quickly realized and pursued through *in vivo* experimentation [261]. In mice treatment with IRSs prevented CpG-induced arthritis [262] and prevented death in a TLR9-mediated murine sepsis model [260].

Of importance to experimentation conducted in this thesis, IRSs which antagonize TLR7 signaling have also been described. The most potent antagonist of TLR7 was IRS-661. In cell culture IRS-661 inhibited murine splenocyte activation by the TLR7/8 agonist R-848 [263], or by the TLR7 agonist imiquimod [264]. IRS-661 also significantly reduced IL-6 production by human B cells treated with R-848 and significantly reduced the production of IFNα by human pDC following TLR7 stimulation by RNP-ICs [263]. IRS-954 was subsequently derived from IRS-661 and was pursued as a dual TLR7/9 antagonist. *In vivo,* treatment of mice with IRS-954 reduced IL-12 production in response to treatment with R-848 [263]. A separate group investigated IRS-661 in the context of a murine Systemic Lupus Erythematosus (SLE) model driven by imiquimod. A substantial abatement of disease was observed through treatment with IRS-661 [264].

Collectively, these studies demonstrate that IRSs are a well-defined means of preventing stimulation of TLR7 or TLR9 by their cognate ligands.

1.7.3. Cell types which express TLR7

With respect to PBMCs, TLR7 is expressed in pDCs and B cells [265]. In lung biopsies, TLR7 expression has been observed in neurons, glial cells, airway epithelial cells, macrophages, T lymphocytes, mast cells and eosinophils [266]. TLR7 expression has also been observed in hepatocytes and keratinocytes [238]. As expected, TLR7 expression is observed in airway epithelial

cell lines. In BEAS-2B cells, an immortalized cell line derived from bronchial epithelial cells, TLR7 expression has been observed via quantitative reverse transcriptase polymerase chain reaction (qRT-PCR) [267] and flow cytometry [268]. TLR7 expression has been observed via qRT-PCR in *ex vitro* cultured primary human airway epithelial cells [267]. Reports on the distribution of TLR7 in the airway epithelium vary. In human tracheal sections, and primary airway epithelial cells polarized via air-liquid interface culturing, TLR7 was observed at the apical cell surface [268]. While the authors suggest TLR7 is present on the cell surface, as opposed to typical endosomal distribution, the resolution and staining techniques utilized do not robustly support this conclusion. Conversely, in biopsies collected from healthy and asthmatic patients, TLR7 was localized to the peri-nuclear region [266].

1.7.3.1. Response to TLR7 stimulation varies by cell type

Most knowledge related to TLR7 biology is derived from studies on pDC. In murine models, TLR7 stimulation results in substantial IFNα production by pDC [136,225-227]. Human pDC have the highest expression of TLR7 [265] and secrete substantial amounts of IFNα in response to TLR7 stimulation [228,269]. To a lesser extent, human monocytes produce IFNα in response to TLR7 stimulation [269].

Some studies in mice have observed the release of the proinflammatory cytokines TNFα , IL-6 and IL-12p40 by pDC in response to TLR7 stimulation. However, in humans release of proinflammatory cytokines is associated with TLR8 stimulation in monocytes and monocyte-derived DCs [269], or TLR7 stimulation in human THP-1 macrophage-like cells and peripheral macrophage cells [223,227,233]. TLR8 is thought to be non-functional in mice; TLR7 and TLR8 are closely genetically related, thus it is possible that TLR7 in mice compensates for the absence of TLR8 signalling. This provides one example of why caution must be exercised when drawing conclusions about human immunology from murine models.

Overall, the response to TLR7 agonists is a T_H1 immune response characterized predominantly by pDC production of IFNα, with proinflammatory tumor necrosis factor α, IL-6 and IL-12 production by macrophage cells [232].

Comparatively less is known about the response of other cell types to TLR7 stimulation. B cells express a moderate amount of TLR7 mRNA and expression of the CD69 activation marker increases on B cells following TLR7 stimulation [265]. When supported by IL-12 secretion from

monocytes, NK cells can respond to TLR7 stimulation resulting in the production of IFN-γ [270]. Similarly, $CD8^+$ T cells produce IFN-γ in response to TLR7 stimulation in the context of co-culture with PBMCs [271]. Conversely, in $CD4^+$ T cells an unexpected anergic state is induced in response to TLR7 stimulation. This anergic state benefits the replication of HIV in $CD4^+$ T cells [272]. In response to TLR7 agonists airway nerve cells release nitric oxide which results in smooth muscle relaxation and bronchodilation [273,274]. Human fibroblasts transfected with TLR7 fail to respond to ssRNA, suggesting TLR7 signalling in fibroblasts is restricted [226]. Primary human airway epithelial cells also failed to produce IFN-α or IFN-β in response to the TLR7/8 agonist CL075 [268].

1.7.4. Intersection of TLR7 and viral infection

In reviewing the influence of TLR7 on viral infections, it is important to distinguish between studies in which TLR7 is stimulated via exogenous TLR7 agonists and those which examine the role of TLR7 during natural infection. With respect to the former, the study of the effect of the TLR7 agonist imiquimod on viral infection was underway prior to the discovery of TLR7. Imiquimod, an imidazoquinoline family antiviral nucleoside analogue, has been investigated as an antiviral against HPV [275,276], HSV2 [277] and CMV [278]. The relevance of TLR7 to natural infection by DNA viruses such as HPV, HSV2, and CMV is likely minimal, as the cognate ligand of TLR7 is ssRNA [225,226]. In these infections imiquimod is utilized as an immune response modifier. Another TLR7 agonist, ANA773, was investigated for the treatment of chronic HCV infection in 2011 [279]. ANA773 resulted in reduced serum HCV RNA levels, however, ANA773 has not been pursued further. Similarly, the TLR7 agonist GS-9620 was explored for the treatment of chronic Hepatitis B virus (HBV) infection in a phase 1 clinical trial [280]. GS-9620 was well tolerated, however, efficacy data is not available. Treatment of respiratory viral infections through TLR7 stimulation has been explored in animal models. Respiratory viral infections in rats by IAV are limited by 3M-011, an imidazoquinoline-family agonist which stimulates TLR7 and TLR8 [281]; prophylactic treatment with 3M-011 resulted in decreased lung and nasal IAV titers.

The importance of TLR7 in the natural response to viral infection has been investigated through TLR7 knockout mice. Interestingly, while the immune response is altered in the absence of TLR7, studies have typically not reported an increase in the severity of infection in TLR7 knockout groups. For example, while TLR7 is necessary for IFNα production and splenic B cell activation

during IAV and VSV infections, the authors do not report lung pathology, mouse body weight, mouse mortality, or viral titers in lungs. Therefore, it is difficult to interpret whether TLR7 deficiency resulted in an increase in disease burden following VSV or IAV infection. In mice infected with Japanese Encephalitis Virus, TLR7-deficiency resulted in increased viral load in the lungs, yet no increase in mortality or decrease in body weight was observed [282]. Only two studies have observed that TLR7 deficiency increases the severity of viral infections. In TLR7- deficient mice, infection by the *alphavirus* Ross River Virus resulted in increased viral load, increased clinical severity, and increased weight loss [283]. Like RSV, Pneumovirus of Mice (PVM) has a negative sense ssRNA genome and has a similar genomic arrangement to RSV [284]. PVM is a natural pathogen in mice and is utilized to model acute respiratory viral infection. PVM-infected mice lacking TLR7 had increased viral lung titers and reduced $CD8^+$ T cell responses. PVM infection in wild type and TLR7-deficient mice resulted in weight loss, but this weight loss was delayed in TLR7-deficient mice [285]. Despite many studies examining the contribution of TLR7 to the antiviral responses to IAV, there are no reports of increased viral titers or increased clinical severity due to TLR7 deficiency.

Non-mutually exclusive hypotheses may explain the absence of an increase in symptom scores during infection in TLR7 knockout animals. The absence of an increase in infection severity may be due to redundant pathogen recognition pathways that maintain protection from infection in TLR7 knockout animals, that TLR7 is not important to the antiviral immune response, or that viruses have evolved counter measures against TLR7 which prevent the presence of TLR7 from conferring a benefit to the host.

1.7.4.1. Relationship of TLR7 and RSV infection in the clinic

Few clinical studies have explored the relationship between TLR7 and RSV in the human host. TLR7 gene expression is increased by 2.76-fold in cells collected from nasopharyngeal swabs of infants with severe RSV infection [286]. In contrast, the effect of RSV infection on the expression of other PRRs is more pronounced with 406-fold and 126-fold increases in the expression of RIG-I and MDA-5, respectively. This study found no correlation between PRR expression and clinical outcomes. Thus, the question of whether an increase in TLR7 expression is beneficial or detrimental to the host remains unanswered.

1.7.4.2. Relationship of TLR7 and RSV infection in cell culture experimentation

Cell culture work offers insight into how TLR7 signalling is antagonized by RSV and how this signalling influences disease severity. pDCs produce substantial amounts of IFNα in response to viral infection [134,135,137]. Specifically, TLR7 stimulation in pDCs results in robust IFNα production [136]. However, RSV can inhibit this response; during RSV infection of pDCs IFNα production is substantially decreased [138]. Treatment of pDCs with the TLR7/8 agonist R-848 resulted in the production of nanogram/mL concentrations of IFN-α in culture media, however, RSV infection of pDCs abrogated this response to R-848. Inhibition of TLR7 signalling during RSV infection is likely due to the targeting of IRF7 for degradation by RSV-NS1 [97], as IRF7 is essential for TLR7-mediated IFN production [241].

Interestingly, TLR7 may contribute to antiapoptotic signalling during RSV infection. RSV infection of human neutrophils, or co-culture with heat-inactivated RSV, delayed apoptosis. This was dependent on endosomal acidification and was reproduced through treatment with ssRNA, suggesting that inhibition of apoptosis was mediated by TLR7 [287]. The antiapoptotic effect of RSV was dependent on NF-κB signalling and subsequent IL-6 production which resulted in an increase in cellular levels of the antiapoptotic Bcl-2 family member Mcl-1. Combined with the antiapoptotic functions of RSV-NS1 and -NS2 [91], RSV is capable of interfering with apoptosis through more than one mechanism.

1.7.4.3. Relationship of TLR7 and RSV infection in animal models

In murine models, the absence of pDCs results in increased RSV titers in lung tissue [135]. However, RSV does not replicate to higher titers in TLR7-deficient mice [288]. This suggests that TLR7 is not essential to the protection conferred by pDCs during RSV infection.

Indirect evidence from the study of ERD due to FI-RSV vaccination demonstrate how TLR signalling, including TLR7 signalling, shapes disease outcomes. In comparison to infection with wild type RSV, Delgado *et al* observed FI-RSV immunization in mice resulted in decreased DC activation, decreased $CD4^+$ T cell proliferation and activation, and produced a T_H2 bias (measured by the interleukin 4 (IL-4) to IFN-γ ratio) in lymph node mononuclear cells. Furthermore, B cells did not undergo affinity maturation and produced neutralizing antibodies of low avidity to RSV-F [139]. Finally, ERD was observed in mice immunized with FI-RSV but not in mice immunized with wild type RSV; in FI-RSV immunized mice airway hyperresponse and lung viral titers were

increased. Supplementation of FI-RSV with TLR3, TLR4, and TLR7 agonists resulted in an immune response nearing parity with the response to wild type RSV immunization. Specifically, the addition of TLR agonists increased neutralizing antibody avidity, reduced viral lung titers, and reduced airway hyperresponse. Contrasting results were obtained by another group who found that addition of a TLR7/8 agonist to FI-RSV immunization did not improve protection to subsequent challenge [289]. Interestingly, Johnson *et al* observed increased disease severity when naïve BALB/c, A/J, and FVB mice were treated with TLR7/8 agonists following RSV infection [289]. The authors hypothesized that this disease enhancement was due to increased immunopathology, however, trends towards increased viral lung titers and a reduction in lung eosinophilia were observed. The most prominent difference between the work by Delgado *et al* and Johnson *et al* is that the former simultaneously stimulated TLR3, 4 and 7 during FI-RSV immunization, while the latter utilized R-848 and 3M-012. R-848 and 3M-012 stimulate TLR7 and 8. These results suggest that stimulation of TLR3 and TLR4 is beneficial and offsets the detrimental influence of TLR7 stimulation.

Collectively, these studies demonstrate that TLR7 signalling does not have a net beneficial or detrimental effect during RSV infection [288], yet stimulation of TLR7 by exogenous agonists during RSV infection is detrimental [139,289]. It has been hypothesized that immunopathology underlies these detrimental outcomes, however, the mechanism underlying these results has not been investigated.

1.7.5. TLR7 agonists in development to treat airway diseases

Recently, an interest has arisen to use TLR7 agonists to treat allergic airway diseases, such as asthma and allergic rhinitis, which are associated with a detrimental T_H2 response [31]. Stimulation of TLR7 primes a T_H1 response and antagonizes the T_H2 response [225-227,232,233,290-293]. Therefore, it was hypothesized that treatment of the airways with TLR7 agonists may benefit these patients by reducing the severity of asthma or allergic rhinitis.

GSK2245035 is a TLR7 agonist delivered via intranasal spray which was explored as a therapeutic for mild asthma and allergic rhinitis in phase I clinical trials. GSK2245035 was well tolerated in adult volunteers, however, efficacy data is not available (NCT01480271 and NCT01607372; [294]). Another TLR7 agonist, AZD8848, progressed to a phase IIa clinical trial for the treatment of

seasonal allergic rhinitis. Treatment with AZD8848 modestly reduced symptom severity following allergen challenge [295].

1.7.6. Cautionary notes on the development of TLR7 agonist therapeutics

TLR7 is implicated in the development of the autoimmune disease SLE [227,247,264,296]. In SLE small ribonucleoprotein forms immune complexes with autoantibodies and complement proteins. These complexes are taken up via Fc or CD21 receptors gaining access to TLR7 in endosomes of pDCs [227] and follicular DCs [296] precipitating an autoimmune response. Other autoimmune diseases that are characterized by inappropriate release of IFNα by DCs include Sjögren's syndrome, type 1 diabetes, Hashimoto's disease, and dermatomyositis [247]. As stimulation of TLR7 results in IFNα release by DCs, these autoimmune diseases may also involve inappropriate TLR7 signalling.

To adhere to the principle of non-maleficence, with respect to patient care, it is essential to understand the potential harms of therapeutics. Autoimmunity related to TLR7 signalling exemplifies how stimulation of TLR7 may have unintended and detrimental consequences. In chapter three, treatment of cells with a TLR7 agonist increased the production of RSV progeny. To further characterize how TLR7 stimulation may be detrimental during RSV infection, chapter five characterized TLR7-mediated enhancement of RSV replication.

1.8. Aims of research project and main hypotheses tested

Severe RSV infection is a leading cause of neonatal hospitalizations [14-16] and RSV imposes a substantial burden of disease in elderly and immunocompromised populations [25,190-192]. No efficacious antivirals are available to treat RSV infection and no vaccine is available to prevent RSV infection. The primary goal of this thesis was to help address the paucity of RSV antivirals through an antiviral discovery campaign. This led to a second important goal, specifically, to understand factors which may enhance RSV replication.

1.8.1. Chapter three aims

The primary aim of chapter three was to establish a robust antiviral screening assay with the capacity to identify compounds that inhibit the replication of RSV. The secondary aim of chapter three was to test the hypothesis that nucleoside analogues or the small molecule aUY11 would have antiviral activity against RSV.

1.8.2. Chapter four aims

Bis(indole) compounds were derived from Isatisine A, a naturally occurring compound with modest antiviral activity [297]. The primary aim of chapter four was to test the hypothesis that bis(indole) compounds would have antiviral activity against RSV. After discovering bis(indole) compounds with antiviral activity against RSV, a second aim of chapter four became the improvement of these compounds through investigating structure activity relationships. The final aim of chapter four was to elucidate the RSV antiviral mechanism of action for bis(indole) compounds.

1.8.3. Chapter five aims

In chapter three I observed an increase in RSV progeny production when cell culture media was supplemented with the TLR7 agonist loxoribine. The aim of chapter five was to test the hypothesis that TLR7 stimulation benefits RSV replication.

Chapter 2: Materials and Methods

2.1. Buffers and solutions

Table 2.1. Buffers and solutions.

Buffer	Composition
Laemmli sample buffer (6x)	375 mM Tris pH 6.8, 12% SDS, 60% glycerol, 0.06% bromophenol blue
Mos lysis buffer (MosLB)	10 mM HEPES, 50 mM sodium pyrophosphate tetrabasic decahydrate, 50 mM sodium fluoride, 50 mM sodium chloride, 5 mM EDTA, 5 mM EGTA, 1 mM sodium orthovanadate, 0.5% triton x-100, pH 7.4
SDS-PAGE Tris-glycine running buffer	25 mM Tris, 192 mM glycine, 0.1% SDS
TBS-T	25 mM Tris, 2 mM potassium chloride, 150 mM sodium chloride, 0.1% Tween
Tris-glycine transfer buffer	25 mM Tris, 192 mM glycine, 10% methanol, pH 8.1-8.4
X-Gal (100x)	5-bromo-4-chloro-3-indolyl-β-D-galactopyranoside (X-Gal; Fisher #BP1615-1), 50 mg/mL in DMSO
Yellow substrate solution	3 mM potassium ferricyanide III (Sigma #702587-50G), 3 mM potassium ferrocyanide trihydrate (Fisher #p125-500), 1 mM magnesium chloride hexahydrate (Fisher #m33-500), in PBS

Abbreviations: dimethyl sulfoxide (DMSO); ethylenediaminetetraacetic acid (EDTA); ethylene glycol-bis(2-aminoethylether)-*N,N,N',N'*-tetraacetic acid (EGTA); 4-(2-hydroxyethyl)-1-piperazineethanesulfonic acid (HEPES); sodium dodecyl sulfate (SDS).

2.2. Eukaryotic cell culture

Table 2.2. Eukaryotic cell lines and respective origins.

Cell line	Origin	Citation
1HAEo-	SV-40 T antigen transformed human airway epithelial cell	[299]
293T	SV-40 T antigen transformed human embryonic kidney (HEK 293) fibroblasts	[300]
A549	Human lung epithelial carcinoma	[301]
HBE	Primary human bronchial epithelial cells	[302]
HeLa	Human cervical epithelial adenocarcinoma	[303]
HEp-2 (presumed to be HeLa cells)	Human cervical epithelial adenocarcinoma (Incorrect putative origin: larynx carcinoma cells)	[304,305]
Ramos	Human B lymphocyte lymphoma	[306]
Vero	Adult African green monkey kidney cells	[307]

Abbreviations: Human airway epithelial (1HAEo-) cells; human bronchial epithelial (HBE) cells; Henrietta Lacks (HeLa).

2.3. Thawing cells

Frozen aliquots of cells were stored in liquid nitrogen in a solution of medium plus 10% dimethyl sulfoxide (DMSO) (Fisher Chemical). To thaw cells, aliquots were rapidly warmed via 37°C water bath. After thawing cells were immediately transferred into a tissue culture flask containing 12mL of media. Resuspended cells were incubated overnight; the following day media was replaced to minimize the time cells were cultured in the presence of DMSO. After thawing, cells were passaged at least 3 times prior to experimentation.

2.4. Passaging cells

1HAEo- cells were cultured in Minimum Essential Medium (MEM) with Earle's Balanced Salts and 2.00 mM L-glutamine (HyClone, GE Healthcare Life Sciences) supplemented with 10% heat-

inactivated fetal bovine serum (FBS; Gibco, Thermofisher). 293T, A549, HeLa, and Vero cells were cultured in Delbecco's Modified Eagle Medium (DMEM) with 4.00 mM L-glutamine, 4500mg/L glucose, and sodium pyruvate (HyClone, GE Healthcare Life Sciences) supplemented with 10% FBS. HEp-2 cells were cultured in Opti-MEM media with L-Glutamate (Gibco, Thermofisher), supplemented with 2% FBS. 1HAEo-, 293T, A549, HeLa, HEp-2, and Vero cells were passaged approximately twice per week prior to reaching confluence. These adherent cells were detached using 0.5% Trypsin with 1 mM ethylenediaminetetraacetic acid (EDTA; Thermofisher) and diluted between 1:5 and 1:12 in fresh media.

Ramos cells were cultured in Roswell Park Memorial Institute 1640 medium (Gibco, Thermofisher) containing 2 mM glutatmate, pyruvate, and 50 μM beta-2-mercaptoethanol, supplemented with 10% FBS. As Ramos cells were non-adhereant, Ramos cells were split via 1:4 dilution with fresh media, approximately every two days.

All cells were incubated at 37°C in 5% CO2.

2.5. Primary human bronchial epithelial (HBE) cell culture

HBE cells were provided by Dr. David Proud (University of Calgary). HBE cells were isolated as descibed previously [308] from deceased lung donors lacking inflammatory lung disease. To thaw, $5x10^5$ cells were diluted into 37mL of bronchial epithelial cell growth medium (BEGM; Lonza), supplemented with 5% FBS; 1mL was added per well in 6 well plates, or 0.5mL added per well in 12 well plates. HBE cells were cultured in BEGM for approximately 10 days prior to experimentation. 24 hours prior to experimentation HBE cells were cultured in BEGM lacking hydrocortizone; BEGM lacking hydrocortizone was used throughout experimentation with HBE cells.

2.6. Viruses

Human RSV strain A2 was used for *in vitro* viral transcription assays. RSV-GFP is a lab adapted recombinant A2 RSV strain which incorporates green fluorescent protein (GFP) as a reporter [309]. RSV-GFP was used for all other experiments requiring infection by RSV. RSV-GFP was purified through sucrose gradient ultracentrifugation to remove contaminating cellular debris, as described previously [310].

2.7. MTT cytotoxicity assay

In parallel, 1HAEo- cells were cultured and treated with compounds for antiviral screening and cytotoxicity assays. As described previously [311], 0.3mg/mL of MTT (Sigma-Aldrich) was dissolved in sterile phosphate buffered saline (PBS; Gibco, Thermofisher). A fresh preparation of MTT solution was prepared for each experiment – a stock solution was not used. Media from wells was removed via aspiration and replaced with MTT solution. The plates were then incubated for 1 hour at 37°C. Following this incubation, the MTT solution was carefully removed via aspiration. The remaining purple precipitate was dissolved in DMSO for 10 minutes on a plate shaker. Absorbance was measured at 560 nm using the GloMax Plate Reader (Promega).

2.8. Small molecules and nucleoside analogues screened for antiviral activity

A group of commercially available nucleoside analogues was selected and ordered from Sigma-Aldrich; this collection included 1-β-D-ribofuranosyl-1,2,4-triazole-3-carboxamide (known as ribavirin), 2-iodoadenosine, 5-bromouridine, N4-benzoylcitidine, 5-fluorocytidine (5-FC), and 7-allyl-7,8-dihydro-8-oxoguanosine (known as loxoribine). The chemotherapeutic nucleoside analogues cytarabine (Sigma-Aldrich) and gemcitabine (Sigma-Aldrich) were provided by Dr. Matthius Götte (University of Alberta). The nucleoside analogues ZW2-51 and ZW2-125 were provided by Dr. Lorne Tyrrell (University of Alberta). The small molecule amphipathic fusion inhibitor aUY11 [312] was provided by Dr. Luis Schang.

2.9. Bis(indole) compounds screened for antiviral activity

Bis(indole) compounds were synthesized via a novel dual catalytic cascade pioneered by Dr. Bren Atienza (University of Alberta), under the supervision of Dr. Fred West (University of Alberta) [as described in [313]]. These Istatisine-A inspired compounds were highly amenable to structural modification enabling the production of libraries of related compounds. The synthesis of iterative libraries of compounds was guided by the results of RSV antiviral screening assays. Bis(indole) compounds were provided in DMSO. Mock infected wells were complemented with DMSO to ensure DMSO did not confound results. DMSO concentrations in cell culture did not exceed 0.1%.

2.10. Antiviral screening and concentration-response assays

$1.3x10^4$ 1HAEo- cells were seeded in 96-well plates and incubated overnight. As specified, the following day 1HAEo- cells were immediately infected or pre-treated for 2 hours with a 2x concentration of the compound being tested. 1HAEo- cells were infected with RSV-A2-GFP at a multiplicity of infection (MOI) of 1.0, unless othewise stated, and incubated for 2 hours. Subsequently, wells were washed once with PBS to remove inoculum virus that had not entered cells to prevent carry over into progeny virus. Following this wash media from 0 hour control wells was collected and stored in liquid nitrogen to monitor for carry over of inocolum virus. Fresh media (containing the compound being screened) was added to wells and incubated for 48 hours. The following day $0.7x10^4$ HeLa cells were seeded into 96 well plates (black polystyrene wells with μ-Clear bottom; Greiner) and incubated overnight. At 48 hours post infection (hpi) progeny RSV was collected; neat progeny RSV was transferred onto HeLa monolayers. The MTT cytotoxicity assay (descibed above) was completed in 1HAEo- cells in parallel to the collection of progeny RSV. I made the assumption that compounds that did not cause cytotoxicity during the 48-hour incubation in 1HAEo- cells would not cause cytotoxicity in HeLa cells during a 2 hour infection. Conversely, if cytotoxicity was observed in 1HAEo- cells then compounds would not be pursued further and cytotoxicity caused during the 2-hour incubation in HeLa cells would not be relevant. Therefore, the affect of compounds on HeLa cell viability was not assayed by MTT assay. At 2 hpi the media on HeLa cells was replaced to prevent inhibition of RSV replication by compounds being tested. The HeLa cells were then incubated overnight. Following overnight incubation HeLa cells were fixed and stained (as described below), allowing for quantification of RSV progeny virus.

As opposed to assaying for progeny RSV production, foci of RSV infection in 1HAEo- cells was measured as the dependent variable during examination of antiviral activity of aUY11. $3x10^4$ 1HAEo- cells were seeded per well in 48 well plates and incubated overnight. aUY11 serial dilutions were prepared in glass test tubes at 50°C and pre-mixed with RSV for 10min. The RSV/aUY11 mixture was transferred onto 1HAEo- cells. After 1 hour this mixture was replaced with fresh media and plates were incubated for 48 hours. Following the 48-hour infection, RSV foci of infection were identified and quantified via the colourimetric immunoassay described below.

To quantify the antiviral activity of tested compounds, the EC50 value was determined. This was defined as an absolute EC50 value lying between 100% RSV replication (no compound added) and 0% RSV replication (no detectable amount of RSV replication). For an accurate EC50 value to be obtained, two concentrations above and below a 50% response must be obtained [314]. This requirement was met except in experiments where cytotoxicity precluded testing high enough concentrations to obtain two values with a greater-than 50% reduction.

2.11. Immunostaining for RSV in fixed cells

At 24 hpi with RSV progeny, HeLa cells were fixed with (1:1) methanol (high performance liquid chromatography Grade, Fisher Chemical):acetone (ACS, Fisher Chemical) for 10 minutes at room temperature. Non-specific antibody binding was blocked via 30 minute incubation with PBS supplemented with 5% FBS at room temperature. A polyclonal goat anti-RSV antibody (Cedarlane; **Table 2.3**), diluted 1:1000 in PBS supplemented with 1% FBS, was selected as the primary antibody used to detect RSV infected cells. To detect RSV via fluorescence microscopy, AlexaFluor 647 conjugated chicken anti-goat IgG (Life Tech; **Table 2.4**), also diluted 1:1000 in PBS supplemented with 1% FBS, was used as the secondary antibody. Cell nuclei were counterstained with the DNA intercalating agent 4′,6-Diamidino-2-phenylindole (DAPI), diluted 1:15000 in PBS, via 4 minute incubation at room temperature.

To detect RSV via colourimetric staining cells were fixed and incubated with a polyclonal goat anti-RSV antibody, as described above. As described previously, a β-galactosidase conjugated rabbit anti-goat IgG (Abcam) antibody, diluted 1:1000 in PBS supplemented with 1% FBS, was utilized as the secondary antibody [310,315]. 100x X-Gal (**Table 2.1**) was diluted 1:100 in yellow substrate solution (**Table 2.1**). This mixture was incubated in wells overnight at room temperature or at 37°C for 3-7 hours. Substrate development was ceased after blue RSV foci of infection appeared.

All antibodies were incubated with cells for one hour at room temperature; following cell fixation with methanol:acetone, antibody incubations, and DAPI staining, cells were washed three times with PBS using the 405 Select TS Washer (BioTek).

2.12. RSV quantification using the Elispot plate reader

The Elispot plate reader was utilized to quantify colourimetrically stained RSV-infected cells. PBS was removed from wells and empty wells were imaged. CTL software was calibrated to Greiner 96 well plates and images were captured for all wells. Count parameters were set as follows: low sensitivity threshhold (166 arbitrary units), background set to 50 arbitrary units, with spot separation of 1 and minimum spot size of $0.003mm^2$. In the Quality Control step, errant counts of cellular debris were removed and missed RSV foci of infection were added.

2.13. RSV quantification via the Operetta high content imaging system (HCIS)

Fluorescently stained cells were imaged utilizing the Operetta High Content Imaging System (HCIS; Perkin Elmer) coupled with Harmony4.1 High Content Imaging Analysis Software (Perkin Elmer). The lamp utilized was the Cermax Xenon Fibre Optic Light Source (Perkin Elmer). The HOECHST 33342 channel was used to image DAPI-stained nuclei (excitation 360-400 nm, emmission 410-480 nm). The Alexa 647 channel was used to image RSV infected cells (excitation 620-640 nm, emmission 650-700 nm). A stack of images (20 µm height at 4 µm increments) was captured to focus each channel; subsequently only one plane was imaged. Images were captured using a 10x or 20x objective lense. During analysis, non-infected wells were used to determine the background signal strength of the Alexa 647 channel. The threshhold for RSV-infected cells was set at least 4-fold above this background level. Harmony4.1 software was used to count the number of cell nuclei, the number RSV infected cells, and the percentage of RSV infected cells was determined.

2.14. Light microscopy imaging

An EVOS FL Auto (Life Technologies) microscope was used for light microscopy to image siRNA transfected wells. Images were captured at 4x, 10x, and 20x objective magnification using phase-contrast imaging.

2.15. Identification of RSV via confocal microscopy

1HAEo- cells were seeded in 8 well glass slides at a density of $2x10^4$ cells per well and incubated for 48-72 hours prior to experimentation. 5 µg/mL Deep Red CellMask (Life Tech) in media was added to wells and incubated for 10 minutes at 37°C to stain cell membranes. To fix cells, cells were incubated for 15 minutes at 37°C in 4% paraformaldehyde (EMS Diasum). Non-specific

antibody binding was blocked, and cells permeabilized, via 30 minute room temperature incubation with PBS supplemented with 1%FBS and 0.3%Triton X-100 (TX-100; Fisher). Wells were washed twice with PBS plus 0.3% TX-100. RSV-F, -P, and -N were detected by a proprietary 4 monoclonal antibody cocktail (RSV3Ab; Novus). RSV3Ab was dissolved in PBS plus 0.3%TX-100 and incubated on cells for 1 hour at room temperature or overnight at 4°C. Cells were then washed three times with PBS plus 0.3%TX-100. Primary antibody was bound by an Alexafluor 568 conjugated goat anti-mouse secondary antibody (Thermofisher), dissolved in PBS plus 0.3%TX-100. The secondary antibody was incubated on cells for one hour at room temperature. Cells were then washed twice with PBS plus 0.3%TX-100, and then twice with Milli-Q water (Millipore). DAPI dissolved in Milli-Q water was added to wells for 2 minutes at room temperature to stain cell nuclei. Finally, the fluroescent signal was preserved by dropwise addition of Vectashield mounting medium (Cedarlane) to wells.

Confocal microscopy was completed with the Quorum Wave FX spinning disc confocal microscope, configued with an Olympus IX-81 motorized base and CSU X1 spinning disk confocal scan-head (Yokagawa). To image DAPI a 405 nm pumped diode laser was used with a 465/50 emission filter. To image GFP a 491 nm pumped diode laser was used with a 525/50 emission filter. To image AlexaFluor 568, 561 nm pumped diode laser was used with a Texas Red 624/20 emission filter. Finally, Deep Red CellMask was imaged via 642 nm pumped diode laser coupled with a 700/75 emission filter. Lasers were merged via LMM5 (Spectral Applied Research). Images were captured using the 20x, 40x, 60x, or 100x oil immersion objective lenses. Image acquisition and analysis was performed through Volocity.

2.16. *In vitro* RSV transcription assay

In vitro RSV transcription was measured as described previously [195], following adaptation from a VSV *in vitro* viral transcription assay [316]. Briefly, HEp-2 cells grown in 6 well plates to approximately 80% confluence were infected with RSV A2 at an MOI of 5 for 1 hour before incubating overnight in fresh media. HEp-2 cells were incubated in 2 μg/mL actinomycin D immediately prior to lysis to inhibit cellular transcription. On ice, HEp-2 cells were treated with lysolecithin for 1 minute; lysed cell extract was subsequently collected in transcription buffer containing 50 mM Tris-acetate at pH 8, 8 mM Mg acetate, 300 mM K acetate, 2 mM DTT, 1 mM spermidine, 10 mM creatine phosphatase, 1 μg/mL aprotinin, 16 U creatine phosphokinase, 1 mM

each of ATP, GTP, and CTP, 50 μM UTP, and 2 μg/mL actinomycin D. Cell debris was removed via refrigerated centrifugation. The *in vitro* transcription reaction was performed by combining soluble cell extract, transcription buffer, RNase inhibitor, 10 μCi [α 32-P] UTP, and compounds to be tested were combined and incubated for 3 hours at 30°C. Total RNA was extracted using the Qiagen RNeasy kit as per manufacturer protocol. mRNA transcript poly(A) tails were digested via hybridization with oligo(dT) and incubation with RNaseH. Denaturing electrophoresis of samples was performed using 4% acrylamide containing 7 M urea gels. Gels were dried and autoradiography captured during 4-day exposure. RNA products were quantified by densitometry analysis following phosphorimaging.

2.17. RSV resistant mutant escape assay

1HAEo- cells were infected with RSV-GFP-A2 at an MOI of 0.1 and serial passaged in ribavirin, Cl02, or Br02 OMe at concentrations of 20 μM or 50 μM. Following a 48-72 hour incubation progeny RSV was transferred onto a fresh 1HAEo- cell monolayer. At 2 hpi fresh media was replaced onto cells. During each passage aliquots of media containing progeny RSV were collected and stored in liquid nitrogen. Following thirteen passages aliquots were thawed; progeny RSV in each aliquot was quantified via 24 hour infection on HeLa cells followed by immunostaining and quantification via the Operetta as described above.

2.18. Stimulation by Toll-like receptor 7 agonists and antagonist

1HAEo- cells were seeded in 48 well plates at a density of $5x10^4$ cells per well and incubated overnight. Primary HBE cells were cultured as described above; HBE cells were utilized upon reaching 80% confluency (approximately 10 days post seeding). Prior to infection 1HAEo- or HBE cells were treated with TLR7 agonists loxoribine or CL097 (Sigma) for 1 hour at 2x concentration. Cells were infected with RSV-GFP-A2 at an MOI of 0.6. At 48 hpi progeny virus was collected and transferred onto HeLa cells grown in μ-Clear bottom 96 well plates. At 2 hpi fresh media was replaced onto HeLa cells. At 24 hpi HeLa cells were fixed, immunostained, and RSV infected cells quantified via Operetta as described above.

The synthetic oligonucleotide IRS-661 (5'-TGCTTGCAAGCTTGCAAGCA-3' with phosphorothioate backbone; Integrated DNA Technologies), was described previously to antagonize TLR7 stimulation [263]. IRS-661 was added to culture media at the time of RSV infection. In treatments combining IRS-661 and loxoribine, loxoribine was combined with IRS-661 and both

were added to culture media at the time of infection. Cells were infected with RSV at an MOI of 2; at 2 hpi fresh media was replaced onto cells to prevent carry over of inoculum RSV into progeny RSV. This fresh media contained IRS-661 with or without loxoribine, respective to treatment group, which was present throughout the 48 hour infection until progeny virus was collected.

2.19. Transfection with short interfering RNA

1HAEo- cells were seeded in 12 well plates at a density of $4x10^4$ cells per well and incubated for 48 hours prior to transfection. Immediately prior to transfection, 1HAEo- cells were washed with PBS and exactly 1mL of fresh media was replaced onto cells. Following the manufacturer's protocol, 1HAEo- cells were transfected at a confluency of approximately 50% with siRNA at a final concentration of 15 nM. Briefly, AllStars Negative Control siRNA (proprietary target sequence; Qiagen), AllStars Hs Cell Death siRNA (proprietary mixture of oligonucleotides; Qiagen), or TLR7 (Hs_TLR7_6 target sequence: 5'-CAGACCTTGGATCTAAGTAAA-3'; Hs_TLR7_12 target sequence: 5'-CAGCTGGGTATAAATTCATGA-3' Qiagen) was added to 100 µL of jetPRIME buffer (Polyplus) and vortexed briefly. 3 µL of jetPRIME reagent was added to each reaction mix; transfection mixes were vortexed briefly and incubated at room temperature for 10 minutes. Transfection mixtures were added to respective wells in a dropwise manner. Following transfection, 1HAEo- cells were incubated for 48 hours prior to experimentation to enable knockdown of target protein and recovery of cells from transfection protocol. Transfection efficency was estimated by examing cell rounding and overall monolayer damage in wells transfected with AllStars Cell Death siRNA. Cell rounding and monolayer damage was imaged via light microscopy with a 10x objective lense using the EVOS FL Auto (Life Technologies) microscope.

2.20. Cell lysate collection and western blot

Mos LB, containing Mini EDTA-free Protease Inhibitor cocktail (Roche), was added to cells and incubated on ice for 20 minutes. Protein concentration in cell lysates were measured by Qubit (Life Tech) according to the manufacturer's protocol, and lysates were stored at -80°C.

Protein lysates were thawed on ice while 4-15% pre-cast polyacrylamide gels (Biorad) warmed to room temperature. The reducing agent β-mercaptoethanol (Sigma-Aldrich) was added to Laemmli Sample Buffer to a final conentration of 5%. Five parts lysate was added to 1 part 6x Laemmli Sample Buffer, and samples were boiled for 10 minutes at 100°C on a heating block. Polyacrylamide gels were assembled in the electrophoresis chamber and SDS-Tris-Glycine running buffer was added to chamber. The comb was carefully removed from wells, and wells were rinsed with running buffer. 7 µL of ladder (PageRuler Plus Prestained Protein Ladder 10-250kDa; ThermoFisher) was loaded into respective wells. Lysate plus buffer was loaded into wells, with the total volume not exceeding 35 µL to prevent spillover into neighboring wells (maximum well volume was 50 µL). Polyacrylamide gels were run at 150 V for 45-55 minutes. Four pieces of whatman filter paper (General Electric) and one piece of nitrocellulose membrane (PALL Life Science) were cut per gel for transfering. Transfer buffer was prepared by combining Milli-Q water, 10x Tris-Glycine transfer buffer, and methanol (to a final concentration of 10%; Fisher). Bubbles between the polyacrylamide gel and nitrocellulose membrane were carefully removed by roller. Protein was transferred from the polyacrylamide gel to the nitrocellulose membrane at 110V for 60 minutes at 4°C. After transfer, nitrocellulose membranes were washed three times with TBS-T for 5 minutes on a rocker platform, and subsequently blocked through a one hour incubation in TBS-T plus 5% bovine serum albumin (BSA; Sigma). Nitrocellulose membranes were next incubated with primary antibody (**Table 2.3**) for 1 hour at room temperature or overnight at 4°C.

After incubation with the primary antibody, nitrocellulose membranes were washed three times with TBS-T for 5 minutes on a rocking platform. Secondary antibodies were diluted as described in **Table 2.4**, and incubated for 1 hour at room temperature on a rocking platform. After incubation with the secondary antibody nitrocellulose membranses were washed in TBS-T as described above. 1mL of chemiluminescent Pierce ECL substrate (Fisher) was prepared per nitrocellulose membrane. ECL substrate was added to blots and incubated at room temperature on a rocking platform for 10 minutes or until bands appeared. ECL substrate was washed off with TBS-T and blots were imaged on an ImageQuant LAS4010 imager (GE Healthcare Life Sciences).

2.21. Toll-like receptor 7 agonist time of addition assay

1HAEo- cells were treated with loxoribine at indicated time points and cells were infected with RSV at an MOI of 1. At 2 hpi fresh media was replaced onto cells to prevent carryover of inoculum RSV. For -2 hpi, 0 hpi, and 2 hpi treatments this fresh media contained loxoribine. Loxoribine was maintained on cells throughout the 24-hour infection. At 24 hpi, RSV progeny was collected and transferred onto HeLa cells for quantification via the Operetta HCIS.

2.22. Antibodies

Table 2.3. Primary antibodies.

Specificity	Source	Assay	Dilution	Distributor	Catalogue number.
β-Actin	Rabbit pAb	WB	1/5000 in TBS-T plus 1% BSA	Abcam	Ab8227
Cleaved Caspase-3	Rabbit mAb	WB	1/1000 in TBS-T plus 1% BSA	Cell Signaling	9664
P-ERK1/2	Rabbit mAb	WB	1/2000 in TBS-T plus 1% BSA	New England Biolabs	4370S
P-MLKL	Rabbit mAb	WB	1/1000 in TBS-T plus 1% BSA	Cell Signaling	91689
P-RIP1	Rabbit mAb	WB	1/1000 in TBS-T plus 1% BSA	Cell Signaling	65746
RSV	Goat pAb	LM/IF	1/1000 in PBS plus 1% FBS	Cedarlane	B65860G-1
RSV -F, -N, -P	4x mouse mAb cocktail	CM	1/400 in PBS plus 0.3%TX-100	Novus	NB100-65217
SOD1	Rabbit pAb	WB	1/1000 in TBS-T plus 1% BSA	Santa Cruz	sc-11407
TLR7	Rabbit mAb	WB	1/500 in TBS-T plus 1% BSA	Cell Signaling	5632

Abbreviations: confocal microscopy (CM); immunofluorescence (IF); immunoglobulin G (IgG); light microscopy (LM); monoclonal antibody (mAb); polyclonal antibody (pAb); phosphorylated extracellular signal-regulated kinase 1/2 (P-ERK 1/2); phosphorylated Mixed Lineage Kinase domain-like protein (P-MLKL); phosphyrlated Receptor-interacting Protein 1 (P-RIP1) mitogen-activated protein kinase (MAPK); Respiratory Syncytial Virus

(RSV); RSV fusion protein (RSV-F), RSV nucleoprotein (RSV-N), and RSV phosphoprotein (RSV-P); superoxide dismutase 1 (SOD1); Toll-like Receptor 7 (TLR7); Western blot (WB).

Table 2.4. Secondary antibodies.

Specificity	Conjugation	Source	Assay	Dilution	Distributor	Catalogue number.
Goat IgG	AlexaFluor 647	Chicken	IF	1/1000 in PBS plus 1% FBS	Life Tech	A21469
Goat IgG	β-galactosidase	Rabbit pAb	LM	1/1000 in PBS plus 1% FBS	Abcam	ab136712
Mouse IgG	AlexaFluor 568	Goat pAb	CM	1/800 in PBS plus 0.3%TX-100	Life Tech	A11004
Rabbit IgG	HRP	Goat mAb	WB	1/1000 TBS-T plus 5% BSA	Cell Signaling	7074

Abbreviations: confocal microscopy (CM); fetal bovine serum (FBS) immunofluorescence (IF); immunoglobulin G (IgG); light microscopy (LM); monoclonal antibody (mAb); polyclonal antibody (pAb); phosphate buffered saline (PBS); horse radish peroxidase (HRP); Western blot (WB).

2.23. Statistical analyses

Statistical analyses were performed using Graphpad Prism 6.0. Concentration-response curves were fit after log transformation of the x-axis. Best fit lines were fit to data using linear or nonlinear regression as indicated in figure legends. EC_{50} and CC_{50} values were determined through nonlinear regression. A significant difference between treatment groups was definied as a P value equal to or less than 0.05. Statistical analyses included t-tests to compare means between two data sets, or a Whelch's t-test to compare means between two data sets if the assumption of equal variance between groups was violated. When three or more means were compared an analysis of variance (ANOVA) test with Bonferroni's post-test was used to compare pre-defined treatment groups. Following linear regression, an F-test was performed to test the null hypothesis that the slope of the line equalled zero. To determine if CC_{50} values differed between treatment groups a sum-of-squares F test was completed.

Chapter 3: Inhibition and enhancement of RSV replication by nucleoside analogues

3.1. Introduction

RSV imposes a significant burden of disease on infants, the elderly, and immunocompromised individuals [5,17,18,25-28]. However, following diagnosis treatment is limited to supportive care due to the current absence of efficacious RSV antivirals. The goals of RSV antiviral development are to reduce the duration of hospitalization during severe RSV infections, offer treatment to immunocomprimised individuals with persistent RSV infections, and to provide a treatment to reduce the duration of non-severe infections. To identify RSV antivirals a robust screening protocol is required.

Several attributes are desirable for an antiviral screening assay. An ideal assay would (i) minimize user input to avoid errors or bias, (ii) minimize start-to-finish time to increase the volume of compounds that can be screened, (iii) reliably identify previously established antivirals and produce comparable EC_{50} values, (iv) incorporate measurement of cytotoxicity, (v) have the capacity to identify compounds which inhibit any component of the viral life cycle, (vi) directly quantify viral replication to avoid artifacts associated with using proxies for viral replication such as CPE, and (vii) be scalable for high throughput screening.

No ideal assay has been described, or is likely to be discovered, as different methods have inherent assumptions and limitations. A subgenomic RSV replicon assay was previously established and scaled to enable screening libraries of millions of compounds [185,187,193,194,197]. This assay was highly successful in identifying antiviral compounds and led to the development of PC786, an RdRp inhibitor in a phase 2 clinical trial [185,195,196] (NCT03382431). However, subgenomic replicon assays cannot identify inhibitors of all steps of the viral replication life cycle. Therefore, it is possible that RSV-antiviral compounds examined through this assay were incorrectly determined to lack antiviral activity. CPE-based assays have also been scaled to screen large libraries of compounds [188,198], and the application of CPE-based assays has led to the discovery of antiviral compounds that have entered clinical trials, such as GS-5806 [206,207] (NCT02135614). The primary limitation of CPE-based assays is that they make the assumption that CPE in cell culture accurately represents RSV replication. As RSV does not egress via a lytic replication cycle, and CPE is slow to develop, this assumption may not always be valid.

As no ideal RSV-antiviral screening assay has been described, this research project set out to investigate the potential of screening strategies that have not been explored previously. The primary aim of chapter three was to establish a robust RSV-antiviral screening assay. To achieve this goal, a number of novel screening strategies were explored. Over the course of this research project five iterations of screening protocols were examined before a suitable strategy was developed. The first protocol quantified changes to RSV replication complex size to identify antiviral activity against RSV. This process identified antiviral effects as early as 6 hpi, yet sensitivity was low and this assay was not amenable to screening large collections of compounds. The next screening protocol that was developed utilized blue spot immunostaining to identify RSV foci of infection in cell culture monolayers. The third assay was an extension of the second that incorporated automated quantification of these foci of infection. The fourth screening assay represented a shift from quantifying RSV infection in the initially infected monolayer to measuring the production of viable progeny RSV. The fifth screening assay, and the protocol which was selected for all subsequent experimentation, also measured the production of progeny RSV. However, this assay utilized immunofluoresce (IF)-based detection of RSV-infected cells instead of colourimetric immunostaining. This protocol is referred to as the IF protocol. This enabled the incorporation of a high content imaging system which substantially improved the reliability of automated RSV quantification. The advantages and disadvantages of each iteration of screening assay, with respect to the attributes of an ideal screening assay listed above, are discussed in the results section.

As this antiviral screening campaign evolved, the second aim of chapter three was pursued. Specifically, compounds were screened for antiviral activity. Nucleoside analogues have long been a cornerstone of antiviral research. In 1963 the deoxyuridine analogue idoxuridine, used to treat HSV eye infections, became the first licensed antiviral. In 1985 azidothymidine became the first nucleoside reverse transcriptase inhibitor and antiretroviral licensed to treat HIV infection. Most recently, the HCV-antiviral nucleotide analogue Sofosbuvir was licensed. HCV is one of three cannonical blood borne pathogens in which chronic infection constitutes a lifelong disease. Sofosbuvir offers the first curative treatment for a previously lifelong chronic viral infection [317]. Given the success of nucleoside analogues in the history of antiviral research, a panel of nucleoside analogues was selected to be screened for antiviral activity against RSV. This selection included commercially available nonphosphorylated pyrimidines and purines. Nonphosphorylated

nucleoside analogues were selected to enable uptake by the host cell. Of the nucleoside analogues tested modest antiviral activity against RSV was noted for cytarabine, a chemotherapeutic cytosine analogue [318]. Interestingly, enhancement of RSV replication was noted during treatment with the nucleoside analogue loxoribine, a TLR7 agonist [252]. This observation was further characterized in chapter five.

3.2. Results

3.2.1. Developing an RSV-antiviral screen utilizing recombinant RSV-GFP

3.2.1.1. Identifying GFP production and RSV replication complexes using RSV-GFP

Identifying RSV-infected cells using a fluorescent reporter protein has been described previously using a recombinant RSV-GFP virus. Following infection with RSV-GFP diffuse cytosolic fluorescence from GFP was used to identify infection at 24 hpi [309]. However, RSV transcripts and protein can be detected as early as 4 to 6 hpi [40,319]. Spinning disc confocal microscopy offers a sensitive method of detecting fluorescent signals. I hypothesized that by employing spinning disc confocal microscopy, GFP production indicative of RSV-GFP infection could be detected at timepoints much earlier than 24 hpi. Furthermore, I hypothesized that if RSV-GFP infected cells were treated with antiviral compounds then a reduction in GFP production would be observed at these early time points. If successful, this protocol could offer a rapid means of identifying compounds with antiviral activity against RSV. To test this hypothesis 1HAEo- human airway epithelial cells were infected with RSV-GFP and fixed at time points from 1.5 to 8 hpi. After fixation GFP was detected via spinning disc confocal microscopy. GFP fluorescence was detected at 1.5 hpi, the first time point observed (**Figure 3.1a**). This was unexpected as *de novo* RSV protein production was not expected until approximately 4 to 6 hpi [40,319]. A plausible explanation was that this early fluorescent signal was contamination with GFP aggregates from previous infectious cycles in the RSV-GFP inoculum used to infect 1HAEo- cells. These GFP aggregates would be expected to be present on the surface of 1HAEo- cells and not in the cell cytoplasm. To determine the location of this early GFP fluorescent signal relative to 1HAEo- cells a membrane stain was utilized. A vertical cross section of 1HAEo- cells was then obtained by capturing a z-stack of images and vertical cross sections of GFP-associated 1HAEo- cells were visualized (**Figure 3.1b**). These cross sections revealed that GFP aggregates were located on the outer surface of the cell membrane. This supported the explanation that GFP aggregates had been transferred during

infection with RSV-GFP. This also indicated that the fluorescence observed at early time points was not synthesized *de novo* and was not representative of RSV infection. As such, GFP fluorescence was not sufficient to identify RSV infection. However, at 6 hpi RSV-GFP infected cells with larger regions of GFP fluorescence were observed (**Figure 3.1c**). Cell membrane staining confirmed that this signal was originating inside cells and was not caused by GFP aggregates adhering to the cell surface. During RSV infection, viral transcription and protein translation occur in lipid raft-associated replication complexes (also known as inclusion bodies) which appear as punctate foci within the cytoplasm [320]. RSV3Ab immunostaining was used to detect RSV-F, -P, and -N, and determine whether the GFP signal observed at 6hpi was representative of RSV replication complexes. Colocalization of intracellular GFP with RSV-F, -P and -N was observed, supporting the conclusion that GFP signals were representative of replication complexes (**Figure 3.1c**). I concluded that RSV replication complexes could be identified as early as 6 hours post infection. This offered a rapid means of identifying RSV infection. To determine whether this could translate into a means of screening for RSV antiviral compounds the effect of ribavirin on the number and size of RSV replication complexes was examined. Ribavirin inhibits a broad spectrum of viruses through mechanisms including inhibition of cellular IMP dehydrogenase, inducing catastrophic mutagenesis, and direct inhibition of viral RdRp [176,178-184]. Due to the reliable RSV-antiviral effects of ribavirin in cell culture experimentation, it is widely used to validate RSV-antiviral screening assays [185-189]. Ribavirin is not a viral entry inhibitor, therefore, I hypothesised that ribavirin would reduce the size of RSV replication complexes. To test this hypothesis 1HAEo- cells were treated with 25 μM ribavirin and infected with RSV-GFP (**Figure 3.1c**). A decline in the number of replication complexes per cell was not observed. While treatment with 25 μM ribavirin produced a reduction in the size of replication complexes ($P = 0.05$) (**Figure 3.1d**), several limitations to this protocol were identified. When identifying RSV replication complexes a much lower number of infected cells was observed than expected based on the MOI used. This may be due to the inherent genetic instability of RNA viruses such as RSV. It is possible that the GFP reporter gene was lost from a portion of the RSV-GFP stock during routine passaging. This would reduce the sensitivity of the assay to detect compounds with antiviral activity against RSV. This approach is also restricted experimentation to only use RSV-GFP. Testing the efficacy of antiviral compounds against other laboratory-adapted RSV strains or clinically isolated RSV strains, which do not encode for a fluorescent reporter protein, would

require an alternate protocol. As this assay only captured events in the first 6 hours of RSV replication, this assay was also precluded from identifying inhibitors of later steps of the RSV replication cycle. The most significant limitation of this protocol was that it required significant user input to identify replication complexes via confocal microscopy. The necessity of this labor-intensive process increased the possibility of user error or bias and reduced the scale-ability of this assay to screen large collections of compounds. For these reasons, this assay was not pursed further and alternative screening strategies were investigated.

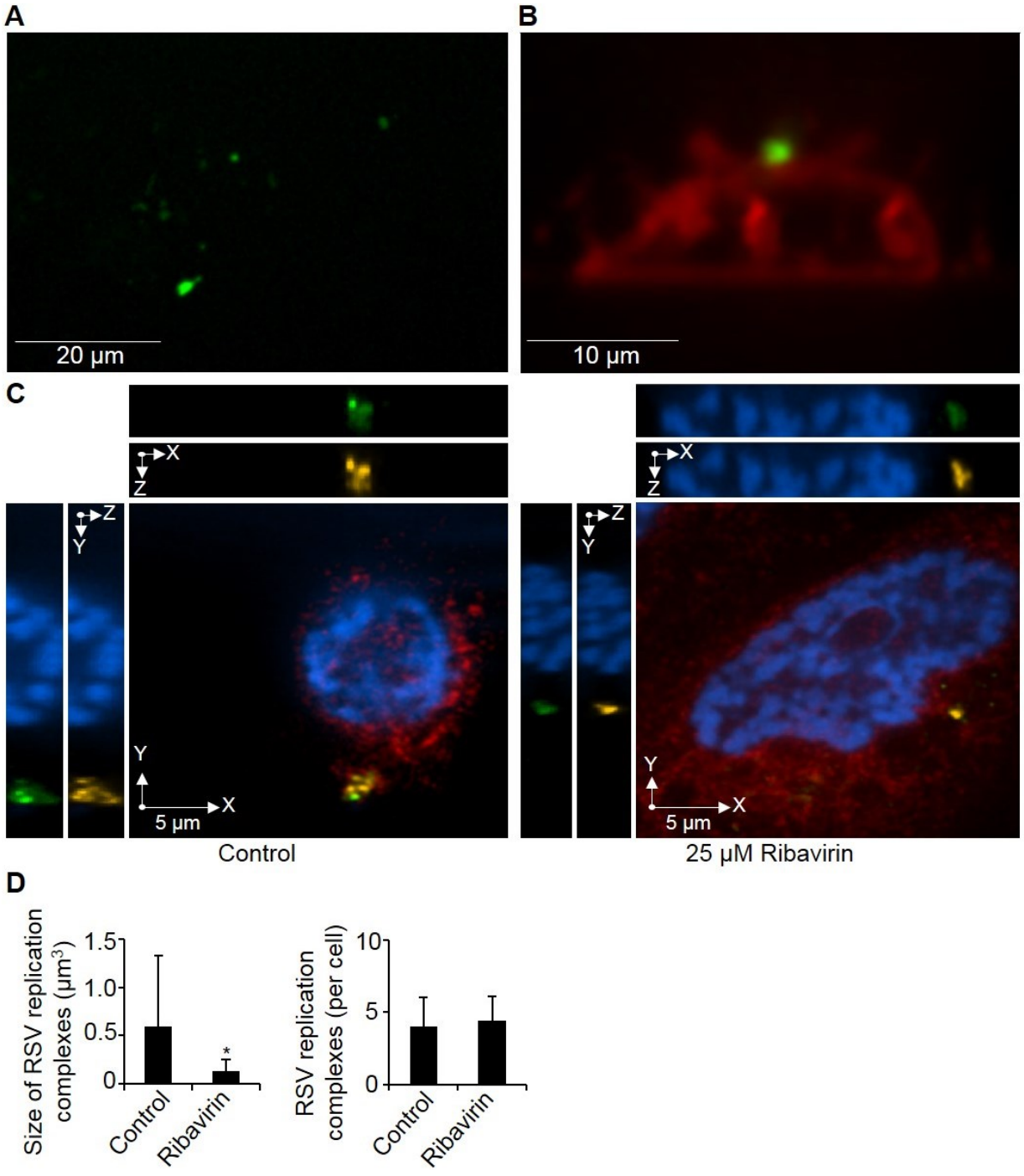

Figure 3.1. Identification of RSV replication complexes in ribavirin-treated 1HAEo- cells via confocal microscopy. (A) Infection of human bronchial epithelial 1HAEo- cells with RSV-GFP results in GFP aggregates attaching to the cell surface. GFP aggregates (green) were observed in the x-y plane at 1.5 hpi. (B) A side profile of a 1HAEo- cell generated through assembly of a z-stack. A cell membrane stain (red) was used to visualize plasma membranes throughout cell. A GFP aggregate is observed on the surface of the plasma membrane at 45 minutes post infection with RSV-GFP. (C) 1HAEo- cells were infected with RSV-GFP and treated with PBS or 25 µM ribavirin. Cells were fixed at 6 hpi. Cell membranes (red), GFP (green) nuclei (blue) and RSV-F,

-P, and -N (gold) were imaged. Figures represent the x-y plane at the location on the z-axis corresponding with the center of the replication complex. x-z and y-z planes were created through compilation of z-stacks. (D) The number of RSV replication complexes per cell and the size of RSV replication complexes were measured using Volocity. Replication complexes were examined in five untreated and five ribavirin-treated cells. In a single experimental replicate, twenty replication complexes were identified in untreated cells and twenty-two replication complexes were identified in ribavirin-treated cells. The size of replication complexes was found to be approximately normally distributed, however, the variances were significantly different between untreated and ribavirin-treated cells. Therefore, a Whelch's t-test was used to test the null hypothesis that the sizes of replication complexes were not reduced by ribavirin. The P value was found to equal 0.05, therefore, the null hypothesis was rejected.

3.2.2. Screening nucleoside analogues via blue spot immunostaining

3.2.2.1. Validation of the blue spot immunostaining protocol for identifying RSV antiviral compounds

Subgenomic replicon systems and other non-cell culture-based systems have been developed previously to identify compounds with antiviral activity against RSV [185,193-195,197,199]. However, these systems are limited to only identifying compounds which inhibit RSV RdRp. Conversely, cell culture-based systems identify compounds which inhibit any component of the viral life cycle. As the RSV replication cycle is not lytic, the main limitation of cell culture-based screening systems is their assumption that CPE accurately reflects RSV replication. CPE-based screening assays are also limited by the 6 to 7-day period required for CPE to become detectable [170,188,189].

Coupling cell culture-based screening with immunostaining has not been explored previously to identify RSV-antiviral compounds. To establish this protocol a colourimetric immunostaining assay (referred to as blue spot immunostaining) was used to detect RSV foci of infection. To confirm that blue spot immunostaining was a viable method to detect RSV infection in 1HAEo- cells, cells were infected with RSV and incubated for 48 hours. At 48 hpi 1HAEo- cells were fixed, permeabilized and immunostained. For immunostaining a polyclonal goat anti-RSV antibody was used as the primary antibody. A β-galactosidase-conjugated monoclonal rabbit anti-goat IgG antibody was used to detect the primary antibody. Following sequential incubations with the primary and secondary antibodies the X-gal substrate was added and incubated overnight at room temperature or for 4 to 6 hours at 37 °C. Cleavage of X-gal by β-galactosidase releases indoxyl from galactose; indoxyl is then oxidized into an insoluble blue indole [321]. This insoluble blue indole was used to identify RSV foci of infection. A robust blue staining appeared which identified RSV infected cells; this staining was absent in mock-infected wells (**Figure 3.2a**). Densely grouped

collections of RSV-infected cells were defined as a single focus of infection and presumed to be the result of infection by a single RSV virion. During infection progeny virus is released beginning at 12 hpi and peaking at 24 hpi [319,322]. Smaller punctate foci represent satellite infections resulting from diffusion and reinfection by progeny RSV during the 48-hour infection. I hypothesized that if ribavirin was added to culture media following RSV infection then the formation of RSV foci of infection would be inhibited. To test this hypothesis 1HAEo- cells were infected with RSV and treated with three concentrations of ribavirin. At 48 hpi, cells were fixed, blue spot immunostained, and the RSV foci of infection were manually counted. Foci counts for ribavirin-treated cells were then normalized to untreated RSV-infected control wells. Increasing concentrations of ribavirin reduced RSV foci of infection in a concentration-dependent manner (**Figure 3.2b**). These results provided proof-of-principle that this assay had the capacity to identify compounds with antiviral activity against RSV. These results support the conclusion that ribavirin has antiviral activity against RSV in cell culture. This conclusion is consistent with previous RSV antiviral screening campaigns described in the literature that have utilized ribavirin to validate the ability of assays to detect RSV antivirals [77,170,185-189]; these results are also consistent with later validation experiments utilizing ribavirin (**Figure 3.4** and **Figure 3.7**). To complement ribavirin and further characterize the capacity of this assay to identify antiviral compounds against RSV, aUY11 was investigated. aUY11 is an amphipathic compound which physically stabilizes viral envelopes to inhibit fusion with the host cell membrane. As such, aUY11 is an entry inhibitor. Accordingly, aUY11 has been observed to inhibit entry and replication of enveloped viruses including IAV, HCV, VSV, HSV-1, HSV-2, and mCMV, but not non-enveloped viruses including poliovirus, RV and AdV [312]. As RSV is an enveloped virus, I hypothesized that the addition of aUY11 to RSV inoculum would inhibit RSV infection of 1HAEo- cells. To test this hypothesis aUY11 was added to RSV and this mixture was added to 1HAEo- cells. After a 48-hour infection 1HAEo- cells were fixed, and foci of infection were identified via blue spot immunostaining. At all concentrations tested aUY11 reduced the formation of RSV foci of infection. The reduction in foci formation was concentration-dependent as increasing concentrations of aUY11 resulted in reduced RSV foci of infection. (**Figure 3.2c**). Similar results were obtained in two independent experiments and supported the conclusion that aUY11 blocks RSV infection. This is the first evidence of aUY11 RSV-antiviral activity. However, the fusion-inhibition antiviral mechanism of action of aUY11 has been

characterized previously [312]. Therefore, this result was expected and further investigations into aUY11 and RSV were not pursued.

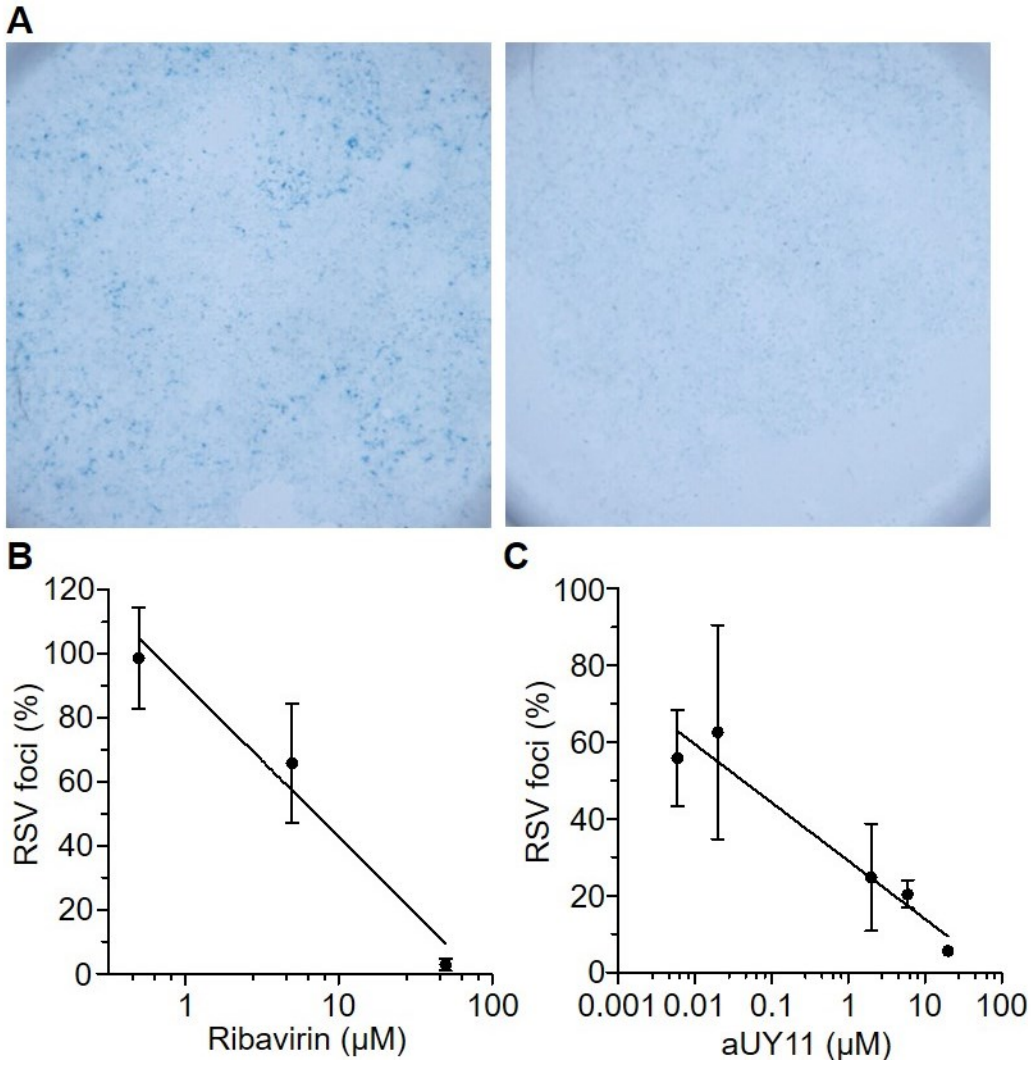

Figure 3.2. Inhibition of RSV replication by ribavirin and aUY11 identified via blue spot immunostaining. (A) 1HAEo- cells were infected with RSV (left), or mock infected (right), and fixed at 48 hpi. For blue spot immunostaining, X-gal substrate was developed for 4 hours at 37°C. A dense grouping of RSV-infected cells constitutes a single focus of infection. (B) RSV foci in ribavirin-treated wells are presented as a percentage after normalizing to untreated wells, wherein the mean of the latter was set as 100% RSV foci production. 1HAEo- cells were infected with RSV at an MOI of 1; at 48 hpi cells were fixed and blue spot immunostained. Foci of infection were then manually counted. Each point represents three biological replicates and error bars represent standard deviation. (C) RSV foci in aUY11-treated wells are presented as a percentage after normalizing to untreated wells, wherein the mean of the latter was set as 100% RSV foci production. RSV was pretreated with aUY11 and then added to 1HAEo- cells at an MOI of 1. At 48 hpi cells were fixed and blue spot immunostained. Foci of infection were manually counted. Each point represents two biological replicates and error bars represent standard deviation. (B and

C) Best-fit lines were produced via linear regression and F-tests were performed to test the null hypothesis that the slope of the lines equalled zero. This null hypothesis was rejected for ribavirin ($P < 0.001$) and aUY11 ($P < 0.01$). Two independent experiments were completed and provided similar results, data from one of two experiments is shown.

The inhibition of RSV foci of infection formation observed during treatment with ribavirin and aUY11 support the conclusion that this assay has the capacity to identify compounds with antiviral activity against RSV. The proposed mechanisms of action for ribavirin include inhibiting cellular IMP dehydrogenase, inhibiting viral RdRp, or inducing error catastrophe [176,178-182]. The proposed mechanism of action for aUY11 is inhibition of virus entry into the host cell. Therefore, these results suggest this assay has the capacity to identify compounds that inhibit RSV entry and post-entry processes necessary for RSV replication [312].

3.2.2.2. Optimizing blue spot immunostaining for quantification by the EliSpot plate reader

Blue spot immunostaining successfully identified the antiviral activity of ribavirin and aUY11 against RSV infection. However, the manual counting of foci of infection was highly time-consuming, as each well of a 96-well plate had to be individually counted on a phase-contrast tissue culture microscope. Automation of quantifying RSV foci of infection was necessary to increase the screening capacity of this protocol. The EliSpot plate reader is capable of automated detection and quantification of colourimetric staining. As such, the blue spot immunostaining protocol was optimized for this instrument. During infection RSV is able to spread through budding from the cell surface and diffusing to neighboring cells, or by directly entering neighboring cells via fusion [322]. This results in the formation of large foci of infection and punctate satellite infections that do not represent drug treated infection. As progeny RSV begin to be released at 12 hpi, and peak release occurs at 24hpi [319,322], I expected to detect foci of infection at 24 hpi and expected foci to increase in size over time. To determine which size of foci were most reliably detected by the EliSpot plate reader, 1HAEo- cells were infected with RSV and incubated for 24, 48, 72 or 96 hours. As the duration of infection increased the size of foci increased (**Figure 3.3a-d**). Interestingly, while larger foci of infection were easier to manually count by eye, smaller punctate foci of infection were more reliably detected by the EliSpot plate reader. At 24 hpi punctate foci were identified correctly, yet at later time points the EliSpot quantification software erroneously divided large foci of infection into multiple foci resulting in an overestimation of the

number of foci (**Figure 3.3e** versus **Figure 3.3f**). In accordance with these results, future experiments were performed using a 24-hour infection.

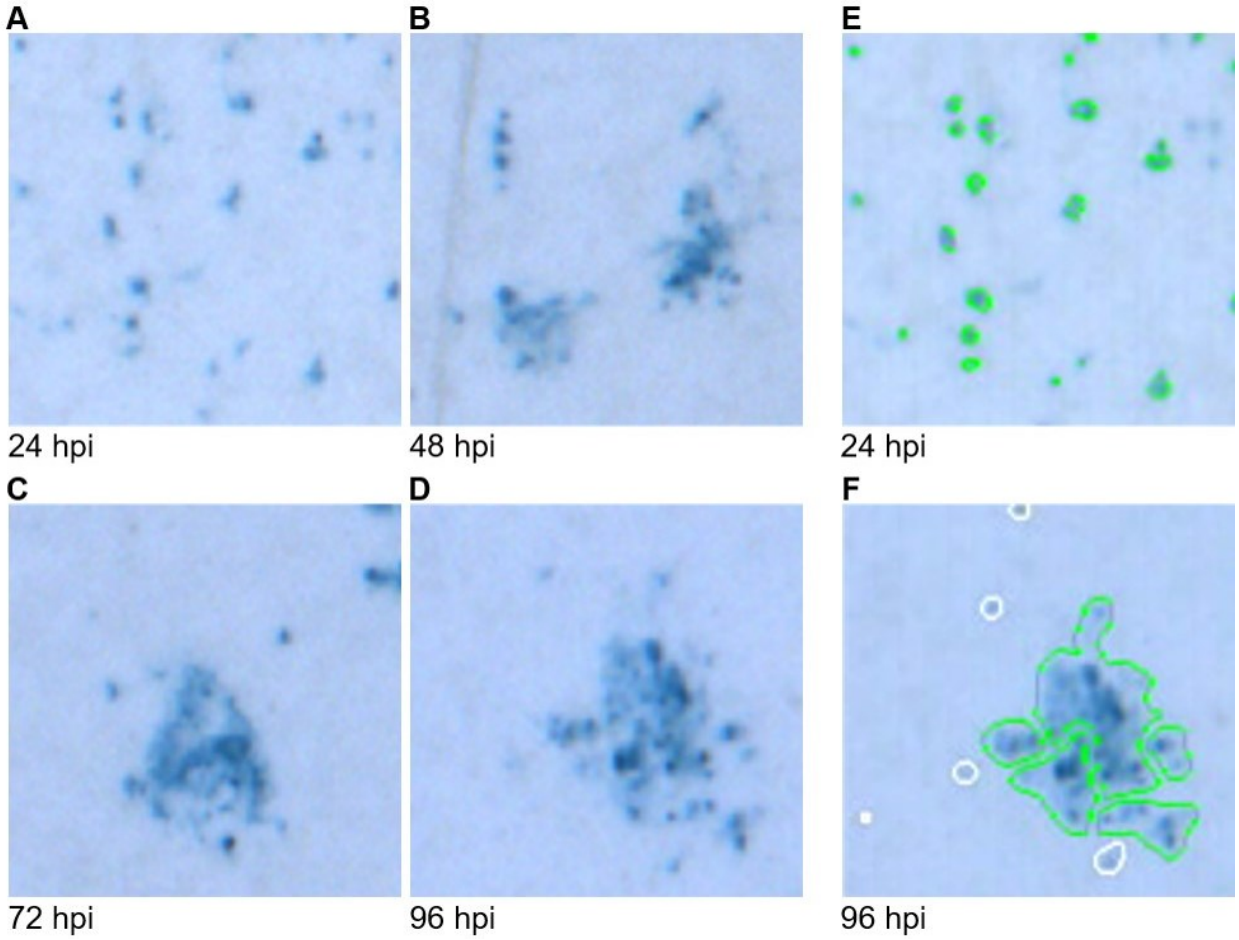

Figure 3.3. Optimization of the blue spot immunostaining protocol for quantification by the EliSpot plate reader. 1HAEo- cells were infected with RSV for 24, 48, 72 or 96 hours before fixation and blue spot immunostaining (A-D). Foci of infection (green perimeter) were then automatically identified by the EliSpot plate reader (E-F). Foci which failed to meet the threshold used to define RSV infection are identified by a white perimeter.

3.2.2.3. Screening nucleoside analogues for antiviral activity via blue spot immunostaining

Nucleoside analogues are a cornerstone of clinical antiviral regimens against HIV, HBV, HCV, HSV, VZV, HCMV, and IAV [317]. To date, 32 compounds derived from nucleosides have been approved for clinical use [317]. Nucleoside analogues typically take advantage of the reliance of viruses on viral polymerase complexes for replication. Interfering with these polymerase complexes can result in chain termination or catastrophic mutagenesis through non-complementary base pairing [317]. Nucleoside analogues have previously been investigated for

antiviral activity against RSV. Two nucleoside analogues which inhibit RSV replication, ribavirin and lumicitabine, have been described [212]. Ribavirin is a potent inhibitor of RSV replication in cell culture; lumicitabine has demonstrated efficacy in adult human volunteers and is currently in multiple phase 2 clinical trials (**Table 1.1**) [212]. Therefore, a selection of nucleoside analogues were screened for antiviral activity against RSV. These nucleoside analogues had not been investigated for antiviral activity against RSV previously. I hypothesized that if a nucleoside analogue was added to culture media then RSV replication would be inhibited. To test this hypothesis 1HAEo- cells were infected with RSV and nucleoside analogues were added to culture media. At 24 hpi 1HAEo- monolayers were fixed and stained for RSV foci of infection. I observed inhibition of the formation of RSV foci of infection when ribavirin was added to culture media. The EC_{50} value of ribavirin against RSV was 7.2 μM (**Figure 3.4**), which agreed with literature values that range from 6.3 μM to 28.38 μM [77,169,170,185,186]. This result suggested this protocol was a valid means of detecting compounds with antiviral activity against RSV. The EC_{50} values of 5-bromouridine, N-4-benzoylcytidine, 2-iodoadenosine, ZW2-51, and ZW2-151 were above 100 μM (**Figure 3.4**). Compounds with an EC_{50} of 10 μM or less are desirable, therefore, these compounds were not pursued further. 5-FC reduced RSV foci of infection formation with an EC_{50} of 94.9 μM. Due to cytotoxicity, higher concentrations of 5-FC could not be reliably included with respect to antiviral activity. For this reason, only one concentration is available elicits a greater-than-50% reduction in RSV replication. Therefore, the EC50 value of 94.9 μM must be interpreted with caution [314]. While this EC_{50} value was considered high, characterization of 5-FC continued.

Determining the effect of compounds on the host cell is of equal importance to determining antiviral effects; while cytotoxic compounds may prevent viral replication, they do not have therapeutic potential as antiviral compounds. Therefore, uninfected 1HAEo- cells were incubated with each nucleoside analogue in parallel duration and concentrations to RSV-infected 1HAEo- cells. Following this incubation cytotoxicity was quantified via the MTT assay. This assay uses nicotinamide adenine dinucleotide (NADH)- and nicotinamide adenine dinucleotide phosphate (NADPH)-dependent oxidoreductase enzymatic activity as a proxy for cell viability. Oxidoreductase reduces the MTT tetrazolium salt into a blue formazan product [323,324]. In this manner the MTT assay indirectly measures NADH and NADPH concentrations in the cell and cell death immediately prevents the reduction of MTT. Therefore, reduction of MTT is proportional to the number of living cells present and cellular metabolic activity [311]. In the literature, ribavirin is

reported to reduce cell viability by 50% (the cytotoxic concentration 50% or CC_{50}) at concentrations greater than 100 μM [77]. In this assay the CC_{50} of ribavirin was consistent with literature values, as it was observed to be greater than 100 μM (**Figure 3.4**). The CC_{50} value of 5-FC was also greater than 100 μM (**Figure 3.4**). As the EC_{50} value of 5-FC was less than the CC_{50} value, 5-FC was investigated further.

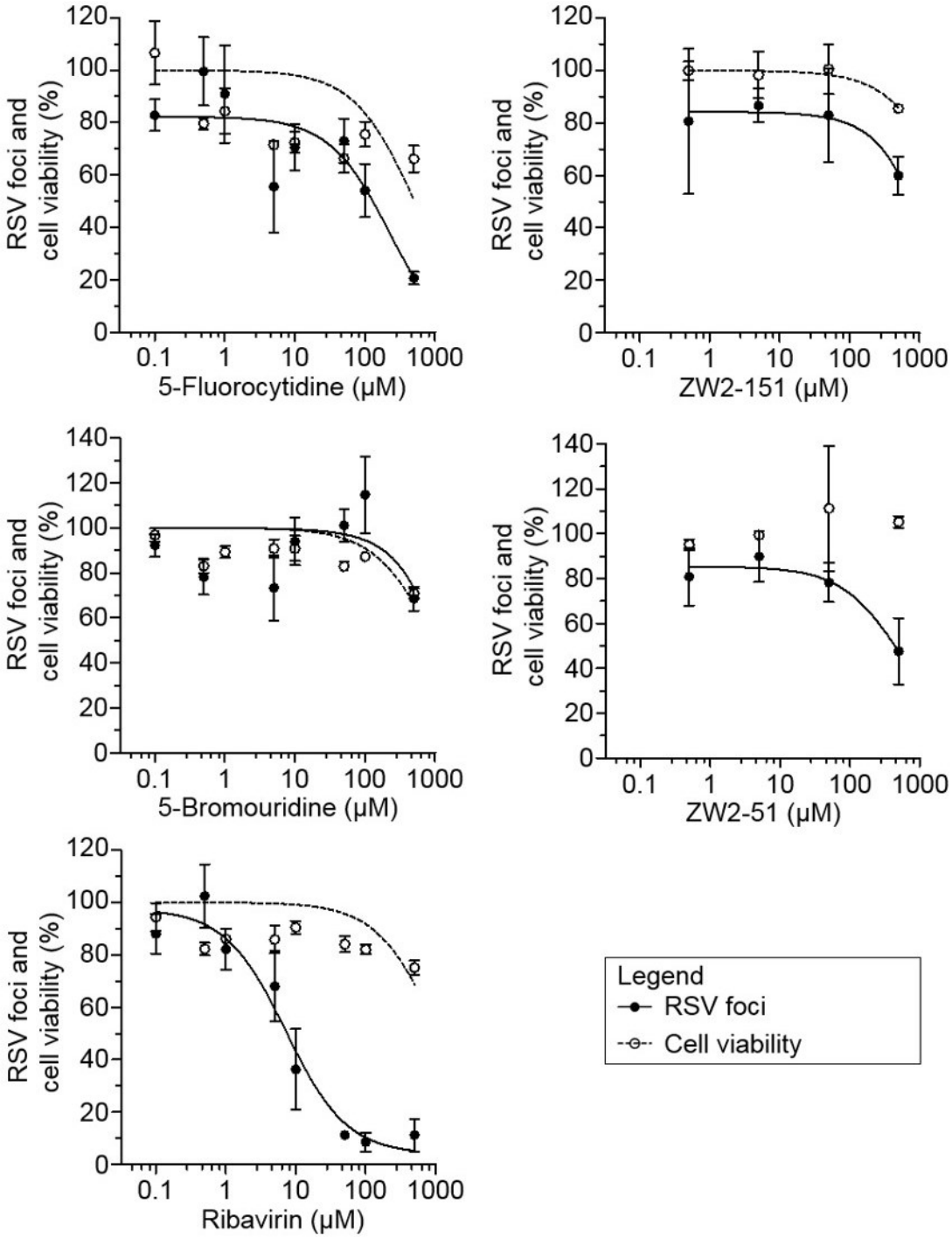

Figure 3.4. Concentration-dependent screening of the effect of ribavirin and nucleoside analogues on the formation of RSV foci of infection and cytotoxicity. RSV foci (filled circles) in nucleoside analogue-treated wells are presented as a percentage after normalizing to untreated wells, wherein the mean of the latter was set as 100% RSV foci production. Likewise, cell viability values (open circles) of nucleoside analogue-treated wells were normalized to the mean of untreated wells (set as 100% cell viability). 1HAEo- cells were pretreated with nucleoside analogues for 2 hours and then infected with RSV at an MOI of 1; cells were treated with

nucleoside analogues throughout infection. At 24 hpi cells were fixed and blue spot immunostained. Foci of infection were then quantified using the EliSpot plate reader. Cell viability was measured by MTT assay. Points represents four biological replicates in a single experimental replicated and error bars represent standard deviation. Two independent experiments were completed and provided similar results; data from one of two experiments is shown. Nonlinear regression was used to fit concentration-response curves to the data and to determine EC_{50} and CC_{50} values.

3.2.2.4. Screening for inhibition of RSV progeny production by nucleoside analuges via blue spot immunostaining

The blue spot immunostaining protocol described above identified antiviral activity of ribavirin, aUY11, and 5-FC against RSV. However, in these experiments it was noted that RSV foci of infection were not only reduced in absolute number but also reduced in size. This introduced the challenge of setting thresholds in the EliSpot plate reader that could distinguish between weakly infected cells and background staining. Furthermore, quantifying RSV replication by counting the number of foci of infection did not fully capture the inhibition of RSV replication. Finally, this protocol did not quantify changes to the infectivity of RSV progeny. Compounds that reduce the infectivity of progeny RSV have been described previously [78]. Therefore, to ensure the assay had the capacity to identify compounds that interfered with any component of the viral life cycle, or reduced progeny infectivity, the protocol was adapted to quantify the production of infectious RSV progeny.

To measure the inhibition of RSV progeny production, 1HAEo- cells were pre-treated with compounds for 2 hours prior to infection and then infected with RSV. At 2 hpi fresh media (containing compounds being tested) was replaced onto cells to prevent carry over of RSV from inoculum into the collected progeny virus. At 48 hpi progeny RSV was collected and transferred onto HeLa cells which are highly susceptible to RSV infection. The media containing progeny RSV was transferred onto HeLa cells without dilution. To mitigate antiviral effects of compounds during replication in HeLa cells fresh media was replaced onto HeLa cells at 2 hpi. At 24 hpi HeLa cells were fixed, immunostained and RSV foci of infection enumerated. Fixing HeLa cells at 24 hpi was necessary to prevent a secondary round of infection which would result in an overestimation of RSV progeny production. As a proof-of-principle, this protocol was used to screen compounds for RSV-antiviral activity at a single concentration of 50 μg/mL (**Figure 3.5**).

As 5-FC inhibited RSV foci of infection formation, I hypothesized that 5-FC would inhibit RSV progeny production. Additional nucleoside analogues were also screened for antiviral activity against RSV. These included 2-iodoadenosine, N4-benzoylcitidine, and loxoribine. As a positive control ribavirin was also included. As expected, RSV progeny production was significantly reduced following the addition of 205 µM ribavirin to cell culture media (**Figure 3.5**). 5-FC at a concentration of 191 µM also reduced RSV progeny production, while the addition of 2-iodoadenosine or N4-benzoylcitidine to culture media did not affect RSV progeny production. Interestingly, the addition of the nucleoside analogue loxoribine at a concentration of 147 µM significantly increased the production of RSV progeny virus. This observation was later pursued extensively in chapter five. As 5-FC reduced the production of RSV progeny, the antiviral activity of 5-FC and the cytotoxicity profile of 5-FC were characterized in subsequent concentration-response experiments.

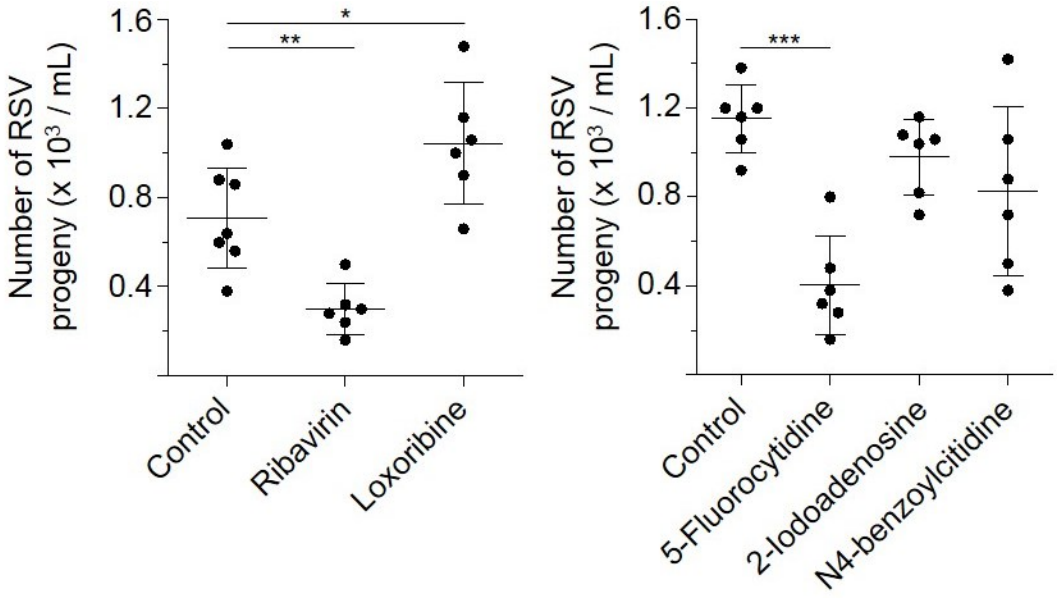

Figure 3.5. The effect of nucleoside analogues on the production of RSV progeny virus. For 2 hours prior to infection 1HAEo- cells were pre-treated with nucleoside analogues at a concentration of 50 µg/mL (205 µM ribavirin, 147 µM loxoribine, 191 µM 5-fluorocytidine, 127 µM 2-iodoadenosine, and 232 µM N4-benzyolcyitidine). 5-fluorocytidine, 2-iodoadenosine, and N4-benzoylcytidine were dissolved in DMSO; therefore, DMSO was added to the untreated RSV-infected control group to an equivalent concentration of 1% DMSO. 1HAEo- cells were then infected with RSV at an MOI of 1. Progeny RSV was collected at 48 hpi and transferred onto HeLa cell monolayers without dilution. At 2 hpi fresh media was replaced onto HeLa cells. Foci of infection in HeLa cells were detected via blue spot immunoassay. Three independent experiments were completed and provided similar results; data from one experiment is shown. Results were analyzed via one-way ANOVA, followed by Bonferroni's multiple comparison test to measure

differences between treatment groups and their respective control group. (*), (**), and (***) indicate $P < 0.05$, $P < 0.01$, and $P < 0.001$, respectively. Error bars represent standard deviation.

3.2.3. Concentration-response screening of 5-fluorocytidine, cytarabine and gemcitabine for inhibition of RSV progeny production

3.2.3.1. Adapting the progeny-based screening protocol to utilize the Operetta high content imaging system (HCIS)

Automated detection of RSV foci of infection increased the screening capacity of the blue spot immunoassay protocol versus manual counting. However, the overall potential of this protocol for high throughput screening was limited by a labor-intensive manual quality control step. This quality control step was necessary as the automated foci-counting software was unable to distinguish between blue foci and dark cellular debris or well contaminants (**Figure 3.6a**); monolayer damage could result in an underestimation of the number of foci of infection (**Figure 3.6b**); and a tendency for staining to develop at different rates between wells of the same plate was observed (**Figure 3.6c** versus **Figure 3.6d**).

I speculated that these issues could be resolved through adapting the protocol to utilize immunofluorescence (IF) to detect RSV-infected cells. To investigate the potential of an IF-based system, HeLa cells infected with progeny RSV were fixed and immunostained using a fluorescently labelled secondary antibody. Cell nuclei were counterstained with DAPI. The Operetta HCIS was utilized to rapidly quantify IF-stained RSV-infected cells (**Figure 3.6e**).

The IF-based method of quantifying RSV-infected cells offered many advantages over the blue spot immunostaining assay. Cellular debris were counted by the EliSpot plate reader following blue spot staining, however, well contaminants and cellular debris did not fluoresce and thus were not erroneously counted by the Operetta HCIS. DAPI staining included in the IF approach enabled the enumeration of the total number of cells. Therefore, the percentage of infected cells could be determined as the dependent variable. This prevented instances of monolayer damage from causing the quantification of RSV progeny to be underestimated. Finally, as fluorescent staining does not rely on enzymatic substrate development there was no tendency for background staining to vary between wells. Thus, the background signal intensity of negative control wells could be reliably quantified and the threshold for infected cells was set 4-fold above background staining levels. Infected cells produced a fluorescent signal substantially greater than background (**Figure 3.6e**). This satisfactory signal-to-noise ratio made automated quantification of IF by the Operetta HCIS

reliable. These advantages of the Operetta HCIS removed the necessity for a labor-intensive quality control step at the end of each experiment. This greatly increased the screening capacity of the protocol.

Inhibition of RSV progeny production by ribavirin was examined using the IF protocol. As expected, ribavirin reduced RSV progeny production in a concentration-dependent manner (**Figure 3.7**). Specifically, ribavirin inhibited RSV progeny production with an EC_{50} concentration of 12.2 μM. This result suggested that the IF-based screening assay had the capacity to identify compounds with antiviral activity against RSV.

The EC_{50} value of 12.2 μM observed in **Figure 3.7** was similar to the EC_{50} value of 7.2 μM determined previously (**Figure 3.4**). Importantly, both of these values fall within the published range of EC_{50} values of ribavirin against RSV that range from 6.3 μM to 28.38 μM [77,169,170,185,186]. The spread of values reported in the literature is likely attributable to the use of different experimental protocols and a distribution of values around a population mean. Similarly, the difference in EC_{50} values from **Figure 3.4** and **Figure 3.7** is likely the product of different experimental protocols and expected natural variation.

The IF-based assay fulfilled many of the criteria of an ideal screening assay outlined in the introduction of chapter 3 **(Table 3.1)**. In particular, reliable automated quantification of RSV-infected cells by the Operetta HCIS minimized user input reducing the opportunity for user errors or bias. The start-to-finish time of this assay only required 72 hours of incubation time, versus the 6 to 7 days required in CPE-based assays [170,188,189]. The IF-based assay identified the antiviral activity of ribavirin against RSV and produced an EC_{50} value that agreed with literature values. As the IF assay measured the production of viable RSV progeny, it was expected to have the capacity to identify inhibitors that target any component of the viral life cycle. Finally, the IF assay directly identified RSV-infected cells, and therefore did not assume that CPE was representative of viral replication. This assumption is inherent to the CPE-based screening assays published previously [170,186,188,189].

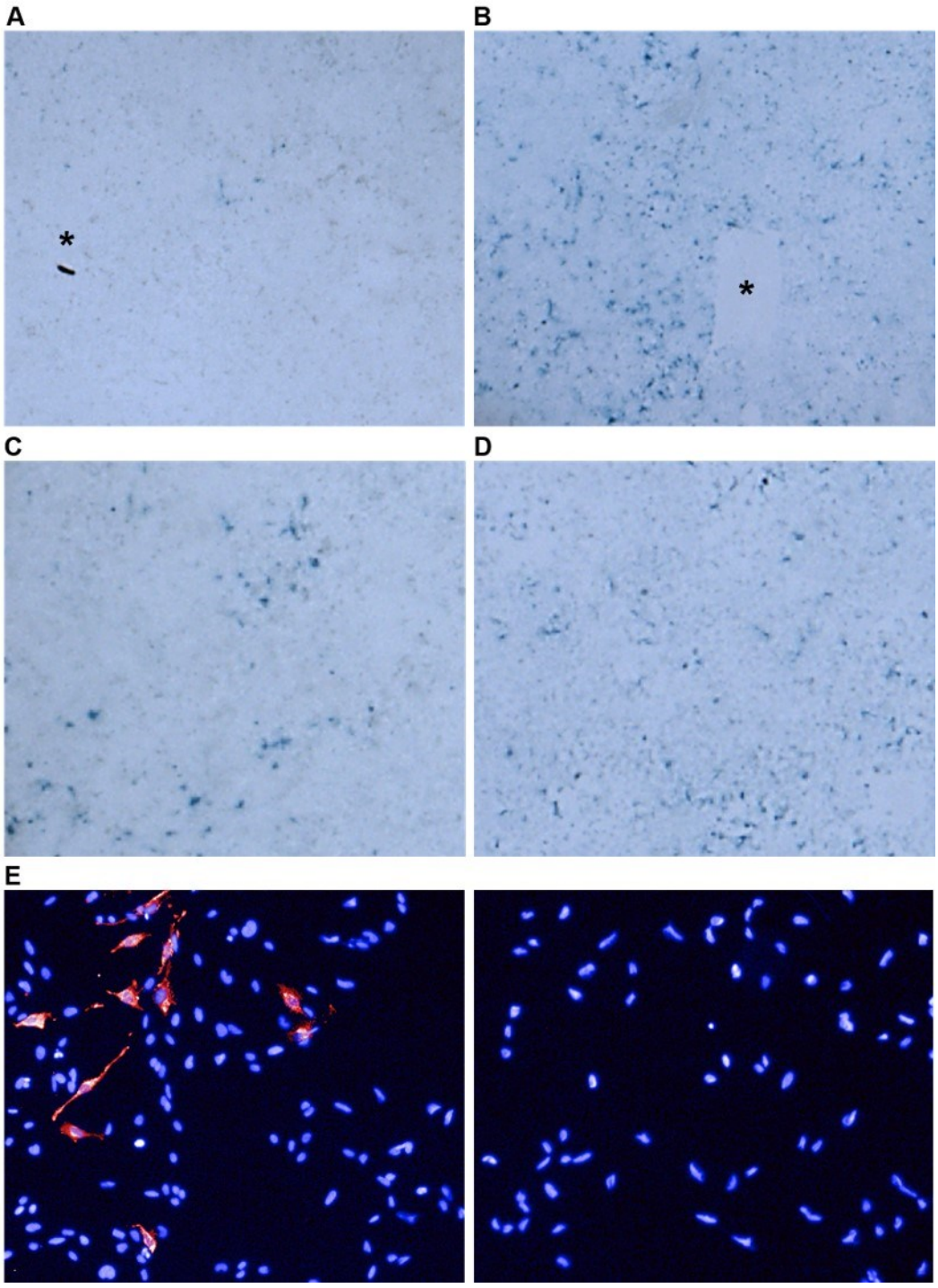

Figure 3.6. Detection of RSV infected cells by IF is superior to detection by blue spot immunostaining. 1HAEo- cells were infected with RSV for 48 hours and blue spot immunostained (A-D) or stained via IF (E). Issues with blue spot immunostaining included debris (directly below * in panel (A)), monolayer damage (highlighted by * in panel B), and a tendency for blue staining to develop at a different rate between wells (panel C versus panel D). When RSV-infected HeLa cells were identified via IF a strong signal from RSV-infected cells (red) was

observed (E – left panel) and minimal background signal was observed in mock infected cells (E – right panel). Cell nuclei are counterstained with DAPI (blue).

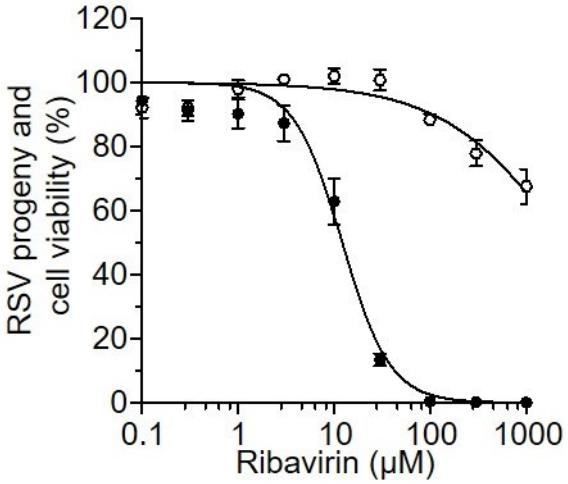

Figure 3.7. Concentration-dependent inhibition of RSV progeny production by ribavirin. RSV progeny production (filled circles) in ribavirin-treated wells are presented as a percentage after normalizing to untreated wells, wherein the mean of the latter was set as 100% progeny production. Likewise, cell viability values (open circles) of ribavirin-treated wells were normalized to the mean of untreated wells (set as 100% cell viability). 1HAEo- cells were infected with RSV at an MOI of 1 and treated with ribavirin. At 48 hpi progeny virus was collected and transferred to HeLa cells. Fresh media was replaced onto HeLa cells at 2 hpi. At 24 hpi RSV-infected HeLa cells were quantified via the IF-assay. An MTT assay was completed in parallel to measure cytotoxicity. Data represent three biological replicates from one experiment; error bars represent standard deviation. Three independent experiments were completed and provided similar results; data from one of the three experiments is shown.

Table 3.1. Comparison of protocols for detecting RSV-antiviral compounds.

Method	Requirement for user input	Rapid (assay duration)	Identify known antivirals	Cytotoxicity measured	All viral replication steps	Directly assay viral replication	Scaled for HTS
Previously published methods							
Subgenomic replicon-based assay	Intermediate	3 days	Y	Y	RdRp inhibitors only	No; relies on signal from replicon	Y
Cell culture-based assays	Low	6-7 days	Y	Y	Y	No; relies on CPE	Y
Methods investigated in thesis							
Replication complex analysis	Very high	6 h	Y	N	Entry and RdRp inhibitors only	No; relies on reporter expression	N
Blue spot assay (manual)	Very high	24 h	Y	N	All steps except egress and progeny viability	Y	N
Blue spot assay (automated)	High	24 h	Y	Y	All steps except egress and progeny viability	Y	N
Progeny detection (blue spot assay)	High	72 h	Y	Y	Y0	Y	N
Progeny detection (operetta HCIS)	Low	72 h	Y	Y	Y	Y	N

Abbreviations: Cytopathic effect (CPE); High content imaging system (HCIS); High throughput screen (HTS); No (N); RNA dependent RNA polymerase (RdRp); Yes (Y)

3.2.3.2. Concentration-dependent effect of 5-fluorocytidine on RSV progeny production and cytotoxicity

5-FC inhibited the formation of RSV foci of infection in a 1HAEo- monolayer during a 24-hour infection in a concentration-dependent manner and inhibited RSV progeny production during a 48-hour infection at a single concentration (**Figure 3.5**). However, cytotoxicity was not assayed when the affect of 5-FC on RSV progeny production was measured during this 48-hour incubation. As I had previously observed 5-FC to inhibit RSV foci in a concentration-dependent manner, I expected that 5-FC would also inhibit RSV progeny production in a concentration-dependent

manner. The cytotoxicity of 5-FC was also measured during this 48-hour incubation. 5-FC inhibited RSV progeny production with an EC_{50} of 62.9 μM, however, cytotoxicity was substantial with a CC_{50} of 1.6 μM. The resultant CC_{50} to EC_{50} ratio (known as the therapeutic index) was less than 1 (**Figure 3.8**). These results suggested that the antiviral effects of 5-FC were mediated by cytotoxicity against the host cell and 5-FC was not pursued further.

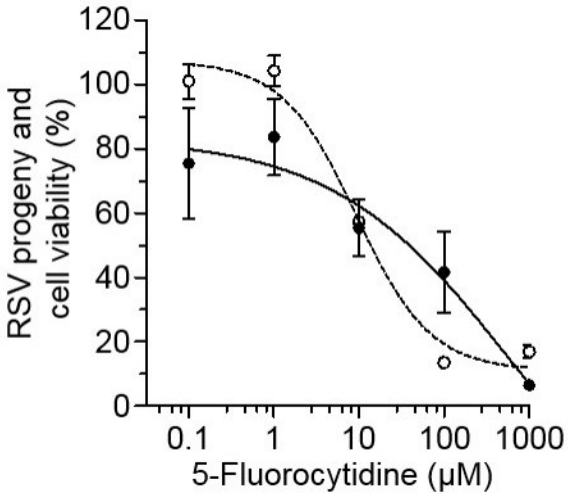

Figure 3.8. Cytotoxicity mirrors antiviral activity of 5-FC during 48-hour infection. RSV progeny production (filled circles) in 5-FC-treated wells are presented as a percentage after normalizing to untreated wells, wherein the mean of the latter was set as 100% progeny production. Likewise, cell viability values (open circles) of 5-FC-treated wells were normalized to the mean of untreated wells (set as 100% cell viability). 1HAEo- cells were infected with RSV at an MOI of 1 and treated with 5-FC. At 2 hpi the culture media was refreshed to prevent carry-over of inoculum virus into progeny virus. 5-FC was maintained on 1HAEo- cells throughout infection. Progeny RSV was collected at 48 hpi and transferred onto HeLa cells. At 2hpi the media on HeLa cells was refreshed. An MTT assay was completed in parallel on cells incubated with 5-FC for 48 hours. At 24 hpi RSV-infected HeLa cells were quantified via the IF-assay. Results represent four biological replicates; error bars represent standard deviation. Two independent experiments were completed and provided similar results; data from one of two experiments is shown.

3.2.3.3. Inhibition of RSV replication by cytarabine

With the IF-based RSV-antiviral discovery protocol established, candidate nucleoside analogues for screening were sought out. Nucleoside analogues having both anti-tumor and antiviral properties have been described previously. For example, cidofovir is approved for the treatment of CMV retinitis and reports have found cidofovir induces apoptosis in glioblastoma cells in tissue culture [325], is beneficial as an augment to therapy for recurrent respiratory papillomatosis [326], and may clear basal cell carcinoma lesions [327]. Cytarabine and gemcitabine are two anti-metabolite chemotherapeutic nucleoside analogues that have been in clinical use for decades [318,328]. As such

the pharmacokinetics, bioavailability, and side effects of these compounds are well characterized [318,328,329]. Thus, these compounds provide good candidates for screening for antiviral activity against RSV. Cytarabine and gemcitabine have also previously been observed to inhibit RSV RdRp *in vitro* [330]. Given the *in vitro* inhibition of RSV RdRp observed previously, I hypothesized that the addition of cytarabine or gemcitabine to culture media would inhibit the production of RSV progeny in infected 1HAEo- cells. To test this hypothesis 1HAEo- cells were infected with RSV and treated with cytarabine or gemcitabine. Following a 48-hour infection progeny RSV was collected and transferred to HeLa cells. Media containing progeny RSV and gemcitabine or cytarabine was transferred onto HeLa cells without dilution. The assumption was made that compounds that did not cause cytotoxicity during the 48-hour incubation in 1HAEo- cells would not adversely alter HeLa cell viability during a 2-hour incubation. Conversely, if cytotoxicity was observed in 1HAEo- cells then compounds would not be pursued further and cytotoxicity caused during the 2-hour incubation in HeLa cells would not be relevant. Therefore, the affect of cytarabine or gemcitabine on HeLa cell viability was not assayed by MTT assay. No evidence of gross cytotoxicity was observed in HeLa cell monolayers during imaging with the Operetta HCIS. Fresh media was replaced onto HeLa cells at 2 hpi to mitigate antiviral affects and enable RSV progeny to replicate unencumbered in HeLa cells. At 24 hpi HeLa cells were fixed and RSV-infected cells were counted via the Operetta HCIS. To assay cytotoxicity in 1HAEo- cells, 1HAEo- cells were incubated with cytarabine or gemcitabine for 48 hours and cell viability was measured via MTT assay.

Following treatment of RSV-infected 1HAEo- cells with cytarabine, EC_{50} and CC_{50} values of 5.9 μM and 127.3 μM were obtained, respectively (**Figure 3.9**). This yielded a therapeutic index of 21.6, supporting the hypothesis that cytarabine inhibits RSV progeny production in cell culture. These results are consistent with *in vitro* experimentation that found cytarabine inhibits RSV RdRp. The large therapeutic index suggests cytarabine inhibits RSV RdRp at concentrations below those at which host cellular processes are inhibited. As a general rule, compounds with a therapeutic index greater than 10 are considered hits which may be further developed into lead compounds. Therefore, these results suggest cytarabine offers a starting point for RSV antiviral development. Given the possible severe side effects of cytarabine treatment, structural modifications which reduce toxicity and increase antiviral activity will be required for cytarabine to realize clinical potential as an RSV antiviral.

Gemcitabine is used for the treatment of ovarian cancer, colon cancer, bladder cancer, non-small cell lung cancer, pancreatic cancer, and breast cancer [reviewed in [328]]. Following phosphorylation by host kinases, gemcitabine inhibits ribonucleotide reductase, DNA polymerase, and DNA synthesis. Significant cytotoxicity was observed with gemcitabine at concentrations where RSV progeny production was only moderately reduced (**Figure 3.9**). These results suggest that gemcitabine does not hold potential as an antiviral against RSV. At a gemcitabine concentration of 0.03 μM, the lowest concentration tested, gemcitabine reduced 1HAEo- cell viability to 46.5% of untreated control wells. At this concentration of gemcitabine RSV progeny production was only reduced to 80.2% of untreated RSV-infected control wells. This result suggests that inducing moderate cytotoxicity does not necessarily halt RSV progeny production. This suggests that compounds that reduce RSV progeny production in the absence of cytotoxicity must target a viral process or host cell process important to the viral life cycle. By extension, this suggests that antiviral compounds identified through this protocol, such as ribavirin and cytarabine, produce an antiviral effect through interfering with the RSV life cycle and not by reducing the viability of the host cell.

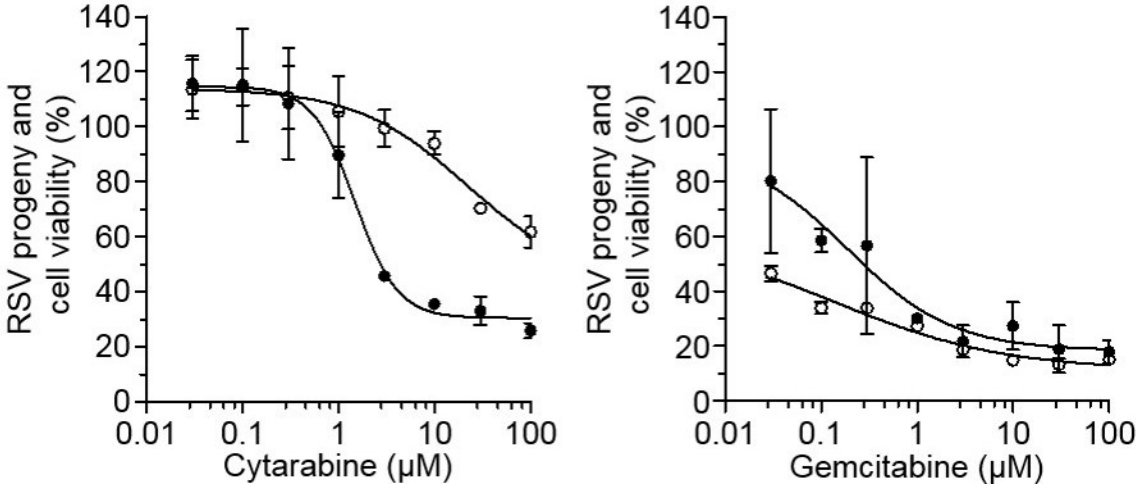

Figure 3.9. Cytarabine, but not gemcitabine, inhibits RSV replication at non-cytotoxic concentrations. 1HAEo- cells were infected with RSV at an MOI of 1 and treated with cytarabine or gemcitabine. RSV progeny production (filled circles) in respective nucleoside analogue-treated wells are presented as a percentage after normalizing to untreated wells, wherein the mean of the latter was set as 100% progeny production. Likewise, cell viability values (open circles) of nucleoside analogue-treated wells were normalized to the mean of untreated wells (set as 100% cell viability). At 2 hpi the culture media was refreshed to prevent carry-over of inoculum virus into progeny virus. Nucleoside analogues were maintained on 1HAEo- cells throughout the infection. Progeny RSV was collected at 48 hpi and transferred onto HeLa cells. The media on

HeLa cells was replaced at 2 hpi; at 24 hpi RSV-infected HeLa cells were quantified via the IF-assay. Cell viability was measured in parallel via MTT assay. Results represent three biological replicates from one independent experiment. Two independent experiments were completed and provided similar results, data from one of two experiments is shown error bars represent standard deviation.

3.3. Discussion

Despite a decades long search, an efficacious antiviral drug for the treatment of RSV infection has not been discovered. To address the substantial burden of disease imposed by RSV, I set out to develop a protocol which could rapidly identify compounds with antiviral activity against RSV. As this protocol advanced through successive strategies a collection of nucleoside analogues were tested for antiviral activity against RSV. A total of ten nucleoside analogues were screened for antiviral activity against RSV. Screening a larger collection of nucleoside analogues would have been preferred. While such libraries exist, none were able to be accessed. Owing to the challenging and costly process necessary to synthesize these compounds, libraries of nucleoside analogues are held tightly and not widely shared.

The first protocol utilized confocal microscopy, immunofluorescence, and a recombinant RSV-GFP strain to rapidly identify RSV replication complexes. RSV replication complexes were identified as early as 6 hpi and a reduction in the size of RSV replication complexes in cells treated with ribavirin was observed. However, technical limitations reduced the practicality of this approach. Specifically, the fluorescent signal produced by replication complexes at 6 hpi was weak and required careful analysis to detect. This limitation would severely hamper the scalability of this protocol for high throughput screening, therefore, this protocol was not pursued further.

The next protocol developed to identify RSV antiviral compounds incorporated blue spot immunostaining to identify RSV foci of infection. This protocol was optimized to incorporate automated RSV-foci detection by the EliSpot plate reader. This novel approach to RSV-antiviral screening had not been explored previously. RSV foci of infection could be detected and quantified as early as 24 hpi. This protocol initially focussed on infection in the initially infected 1HAEo- cell monolayer. Therefore, this assay would not be able to identify compounds that inhibited egress or reduced the infectivity of progeny virus. It is important to consider inhibitors that target processes occurring late in the RSV life cycle or reduce progeny infectivity as RSV-antiviral compounds have already been described which function through this mechanism. Namely, RSV-604 reduces the infectivity of progeny RSV [78]. Therefore, the production of infectious RSV

progeny was measured as this offered an unbiased examination of compounds that could target any step of the viral replication cycle. To measure infectious RSV progeny production, the blue spot immunoassay protocol was adapted so that after a 48-hour infection in 1HAEo- cells, progeny RSV were collected and inoculated onto HeLa cells which are highly susceptible to RSV infection.

In the final iteration of establishing a robust RSV-antiviral screening campaign, the protocol was adapted to utilize IF and the Operetta HCIS. The IF protocol had many advantages (**Table 3.1**); variability in staining was reduced as enzymatic development of a colourimetric substrate was not required, cellular debris was not erroneously added to the count of infected cells, and the greater signal-to-noise ratio of infected cells over background staining allowed for reliable automated foci detection. Given these advantages, this protocol offered adequate capacity to screen compounds for RSV-antiviral activity. The IF-based screening protocol was subsequently utilized to screen bis(indole) compounds for RSV-antiviral activity (chapter four).

The IF-based screening assay also had advantages in contrast to previously established subgenomic replicon-based assays or CPE-based assays (**Table 3.1**). The IF-based screening assay had the capacity to identify compounds that inhibited any step in the RSV life cycle. This provided an advantage versus subgenomic replicon-based assays, which could only identify RSV RdRp inhibitors. The IF-assay did not rely on the assumption that CPE is representative of RSV replication, which offered an advantage over CPE-based screening assays that make this assumption. An important caveat to these advantages, however, is that a subgenomic replicon-based screening assay and various CPE-based screening assays have been successfully scaled to enable screening of libraries containing millions of small molecule compounds. An important future direction for the IF-based screening assay described in this chapter will be determining if this assay can be scaled to screen libraries of this size, if such libraries become available.

The study of nucleoside analogues in the context of antiviral drug research has led to many therapeutic discoveries. Given this history, in this chapter a panel of nucleoside analogues was selected for screening against RSV. This panel included 2-iodoadenosine, 5-bromouridine, N4-benzoylcitidine, 5-FC, loxoribine, cytarabine, and gemcitabine. These compounds had not previously been tested for antiviral activity against RSV. EC_{50} and CC_{50} values were established for nucleoside analogues to describe their respective RSV-antiviral activity and cytotoxicity. The therapeutic index was then derived by division of the CC_{50} by the EC_{50}. Results obtained with the

chemotherapeutic nucleoside analogue gemcitabine offer a baseline point of reference for interpreting therapeutic indices obtained through this protocol. Gemcitabine drastically reduced cell viability in 1HAEo- cells, however, progeny RSV was still produced resulting in a therapeutic index of less than 1. This result suggests that inducing cytotoxicity is not sufficient for preventing RSV progeny production and compounds with a therapeutic index of 1 or greater are producing an antiviral effect. This point of reference is useful towards interpreting the antiviral activity of compounds identified by the IF screening assay. Another point of reference is that screening campaigns typically define a "hit" worthy of lead optimization as having a therapeutic index of 10 or greater [194,197].

The nucleoside analogue 5-FC initially showed promise; at 24 hpi 5-FC reduced RSV replication in 1HAEo- cells and at 48 hpi RSV progeny production was reduced. However, when cells were incubated with 5-FC for 48 hours considerable cytotoxicity was observed and a therapeutic index of less than 1 was observed. Considering these results 5-FC was not pursued further.

In this chapter, one nucleoside analogue with antiviral activity against RSV was identified. The chemotherapeutic nucleoside analogue cytarabine inhibited RSV progeny production with an EC_{50} of 5.9 μM and CC_{50} of 127.3 μM yielding a therapeutic index of 21.6. Cytarabine was originally isolated from the sponge *Cryptotethia crypta* in 1955 and went on to become essential to the treatment of acute myeloid leukemia (AML) [318]. The inclusion of cytarabine for the treatment regimen of AML has remained largely unchanged for forty years. Cytarabine is also used in the treatment of acute lymphoblastic leukemia and non-Hodgkin's lymphoma [329]. The antineoplastic mechanism of action of cytarabine is well defined; cytarabine is incorporated into DNA resulting in DNA damage that inhibits DNA synthesis [318]. The side effects of cytarabine are also well understood. At high chemotherapeutic doses used to treat cancer side effects may be severe or even life threatening [331]. As RSV infection is typically self-limiting it is unlikely treatment with cytarabine would be clinically worthwhile. Nonetheless, the therapeutic index of cytarabine was well above the threshold of 10 used to define hits. As such, it would be worthwhile to produce and screen cytarabine analogues in a campaign towards developing novel RSV antivirals.

The TLR7 agonist and nucleoside analogue loxoribine was screened for antiviral activity against RSV. I hypothesized that loxoribine may interfere with RSV replication through stimulation of the host immune response or through nucleoside analogue-associated mechanisms of action such as

mutagenesis or chain termination. In preliminary experiments treatment of cells with loxoribine resulted in darker staining foci of infection suggesting increased RSV replication. Measuring RSV progeny production following treatment with loxoribine enabled quantification of this observation and treatment with loxoribine increased RSV progeny production. This unexpected result is pursued in chapter five.

Having established this screening protocol, I began seeking other libraries of compounds to screen for antiviral activity against RSV. In the following chapter I will describe the discovery of antiviral activity of bis(indole) compounds against RSV, synthesis of novel bis(indole) compounds with improved therapeutic indices, and the antiviral mechanism of action for these compounds.

Chapter 4: Inhibition of RSV replication by bis(indole) compounds

4.1. Introduction

Millions of compounds have been screened for antiviral activity against RSV in high throughput screens and a small handful of these compounds have entered clinical trials (**Table 1.1**). Despite these RSV antiviral drug discovery campaigns spanning decades, no efficacious antivirals have entered the market. The absence of efficacious RSV antivirals in the clinic highlights the need for creative efforts to identify novel chemical entities with antiviral activity against RSV. Bis(indole) compounds present an exciting avenue for antiviral research. These compounds were inspired by *Isatis indigotica* Fort. (Cruciferae), the roots and leaves of which have been used in Chinese herbal remedies to treat viral pneumonia, influenza, mumps, and hepatitis [297]. Isatisine A was previously isolated from *I. indigotica* and modest antiviral activity was observed. Bis(indole) adducts were synthesized to share a high degree of structural similarity with Isatisine A (**Figure 4.1**).

Compounds being developed as potential therapeutics should obey the Lipinski Rule of Five criteria. The Lipinski criteria originate from the field of medicinal chemistry and recommend that molecular weight not exceed 500 g/mol, hydrogen-bond donors not exceed 5, hydrogen-bond acceptors not exceed 10, and partition coefficient (a measure of lipophilicity referred to as Log P) not exceed 5 [332]. If a compound violates two rules of the Lipinski criteria it will likely be too large, too polar, or too lipophilic to be well absorbed orally reducing clinical potential. It is also unlikely such a compound will be able to permeate the cell membrane. In the absence of diffusion across the cell membrane compounds must rely on transporter proteins for uptake. The likelihood of uptake by transporter proteins for randomly synthesized small molecules is low. Therefore, obeying the Lipinski criteria increases the chances that small molecules will be biologically available and have favourable ADME qualities. Underpinning of the Lipinski rules is the observation that compounds violating two of these rules have a high attrition rates during clinical trials. Conversely, clinically approved compounds typically obey these criteria [332]. Bis(indole) compounds obey at least three of these four requirements; bis(indole) compounds have a molecular weight of 300-400 g/mol, have only 2 hydrogen bond donors and have only 4-5 hydrogen bond acceptors (**Figure 4.1**). The Log P of bis(indole) compounds has not yet been established.

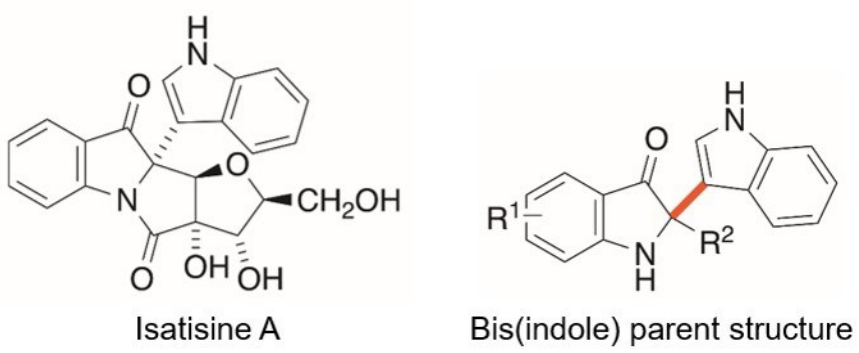

Figure 4.1. Chemical structure of Isatisine A and bis(indole) parent structure. Adapted from B. Atienza and L. Jensen *et al*, [313].

Another advantage of pursuing bis(indole) compounds is they are readily amenable to structural modification via dual catalytic metallocarbene-azide cascade chemistry [313]. This synthesis strategy produced high yields of bis(indole) adducts under ambient conditions. Access to libraries of related bis(indole) compounds offers the opportunity to investigate Structure Activity Relationships (SAR) so that compounds with improved therapeutic profiles may be engineered.

The aim of chapter four was to investigate bis(indole) compounds for RSV-antiviral activity. Bis(indole) compounds were investigated using the IF-based screening assay established in chapter three and bis(indole) compounds with antiviral activity against RSV were identified. These results were used to guide the synthesis of new bis(indole) adducts yielding compounds with improved therapeutic indices. The goal of this screening effort was to identify "hit" compounds with a therapeutic index of 10 or greater. This opens the door to collaborations with medicinial chemists to translate hits into lead compounds. This research program identified one hit against RSV, Br02 OMe, which reduced RSV replication with an EC_{50} below 10 μM and a therapeutic index greater than 10.

4.2. Results

4.2.1. Identifying the antiviral activity of bis(indole) compounds against RSV

Bis(indole) compounds were attractive candidates for antiviral development as they are amenable to structural modification and obey the medicinal chemistry Lipinski criteria. Furthermore, bis(indole) compounds are structurally similar to Isatisine A, a naturally available compound with modest antiviral activities. I hypothesized that if bis(indole) compounds were added to culture media during infection then RSV progeny production would be inhibited. The IF screening

protocol developed in chapter three was utilized to test this hypothesis. A novel series of bis(indole) compounds was screened at 10 μM using the protocol described above. Phe01 reduced the production of RSV progeny virus, however, considerable cytotoxicity was observed. Bis-10 and Me02 were not biologically active, having little affect on cell viability or RSV progeny production. A variety of compounds, including Bis-0, -2, -5, -8, -9, -11, and Cl02, offered support to the hypothesis that bis(indole) compounds could inhibit RSV replication (**Figure 4.2**). These compounds significantly reduced RSV progeny production with limited or no impact on cell viability. Cl02 was the most promising of these compounds as the reduction in progeny production was comparable to ribavirin treatment. I hypothesized that Cl02 would inhibit RSV progeny production in a concentration-dependent manner. Cl01 is structurally similar to Cl02 yet did not reduce RSV progeny production in the initial screen at 10 μM. To gain insight into the consequences of subtle differences to the molecular structure of bis(indole) compounds Cl01 was also investigated in a concentration-response assay. Cl01 did not have an antiviral effect as the cytotoxic effect of Cl01 closely mirrored the reduction in RSV progeny production. Conversely, Cl02 reduced RSV progeny production with an EC_{50} of 9.0 μM (**Figure 4.3**). Treatment with Cl02 also produced a modest reduction in cell viability with a CC_{50} value of 37.4 μM. These results yielded a therapeutic index of 4.1. These results supported the hypothesis that bis(indole) compounds could exert antiviral activity against RSV. This success with Cl02 was used to guide the synthesis of a related series of compounds with structural similarity to Cl02.

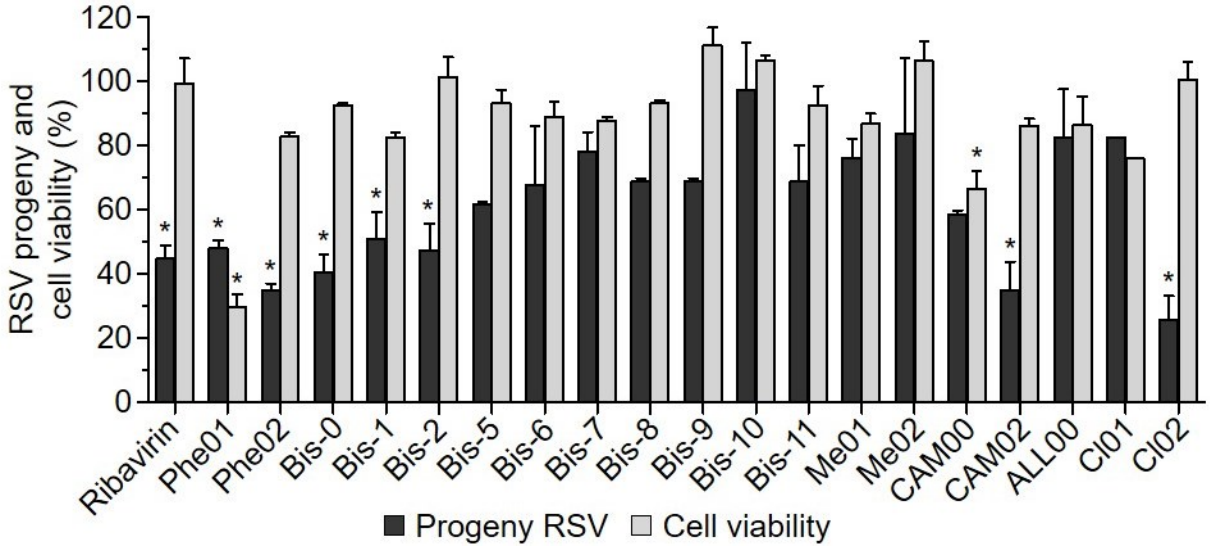

Figure 4.2. Bis(indole) compounds, notably Cl02, reduce RSV progeny production in the absence of cytotoxicity at 10 µM. RSV progeny production in bis(indole)-treated wells are presented as a percentage after normalizing to untreated wells, wherein the mean of the latter was set as 100% progeny production. Likewise, cell viability values of bis(indole)-treated wells were normalized to the mean of untreated wells (set as 100% cell viability). 1HAEo- cells were infected with RSV at an MOI of 1. At 2 hpi media was refreshed to prevent carry-over of inoculum virus. Progeny RSV was collected and transferred to HeLa cells at 48 hpi. At 24 hpi RSV-infected HeLa cells were quantified using the IF-assay. Cell viability was measured by MTT assay. Results represent two biological replicates in a single experiment. A total of three independent experiments were performed and provided similar results. Error bars represent standard deviation. Prior to normalization results were analyzed by one way ANOVA with Bonferroni's post-test to compare treatment groups to respective untreated control groups; $P < 0.05$ (*).

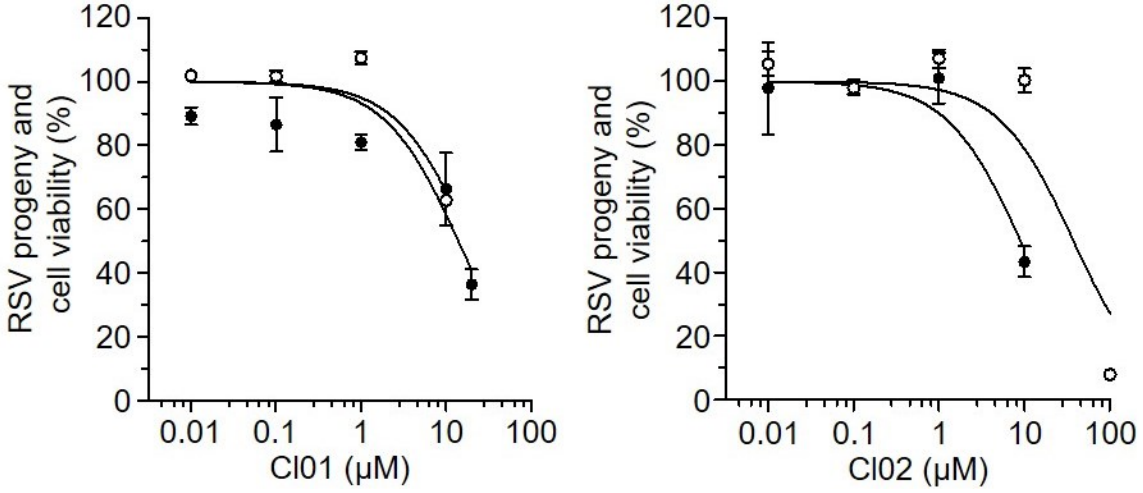

Figure 4.3. Cl02 reduces RSV progeny production in a concentration-dependent manner. RSV progeny production (filled circles) in bis(indole)-treated wells are presented as a percentage after normalizing to untreated wells, wherein the mean of the latter was set as 100% progeny production. Likewise, cell viability values (open circles) of bis(indole)-treated wells were

normalized to the mean of untreated wells (set as 100% cell viability). 1HAEo- cells were infected with RSV at an MOI of 1. At 2 hpi media was refreshed to prevent carry-over of inoculum virus and Cl01 or Cl02 were added to cell culture media. RSV progeny was collected and transferred to HeLa cells at 48 hpi. At 24 hpi RSV-infected HeLa cells were quantified via the IF-assay. Cell viability was measured by MTT assay. Data represent three biological replicates from one experiment. Three independent experiments were completed and provided similar results, data from one experiment is shown. Error bars represent standard deviation.

4.2.1.1. Investigation of Structure-Activity Relationship (SAR) of bis(indole) compounds

Bis(indole) compounds are highly amenable to structural modification. This trait was exploited following the confirmation of the antiviral activity of Cl02 against RSV. To explore the activity of related bis(indole) compounds the chlorine halogen group of Cl02 was replaced with bromine to yield Br02. Cl02 and Br02 were also synthesized with the addition of a methyl group (OMe) (**Figure 4.4**). Small structural changes can substantially alter the activity of antiviral compounds. Lumicitabine is a nucleoside analogue that causes chain termination of RSV transcripts yet has no activity against HCV [76]. However, the removal of a 2'F or 4'ClCH2 group from lumicitabine confers activity against HCV. A reduction in Cl02 cytotoxicity was desirable given the relatively modest therapeutic window observed with Cl02. I hypothesized that small structural modifications to Cl02 would alter its cytotoxic profile. To test this hypothesis Cl02-derived compounds were incubated on 1HAEo- cell monolayers for 48 hours and cytotoxicity was measured by MTT assay. The halogen substitution of bromine for chlorine had a modest non-significant effect on CC_{50} values. A statistically significant increase in CC_{50} values was observed with the addition of the methyl groups to Cl02 or Br02. Cl02 was observed to have a CC_{50} value of 40.2 μM. Cl02 OMe, produced through the addition of a methyl group to Cl02, had a statistically significant increase in its CC_{50} value to 56.4μM ($P < 0.001$) (**Figure 4.5**). Likewise, the addition of a methyl group to Br02 to produce Br02 OMe resulted in a statistically significant increase in the CC_{50} value from 42.6 μM to 70.1 μM ($P < 0.001$). These results support the conclusion that the addition of a methyl group to Cl02, or the Cl02-inspired compound Br02, improved how well the host cell tolerates bis(indole) compounds. These results also supported the conclusion that small structural changes to bis(indole) compounds could have significant effects on their biological activity. Cl02 and Br02 were further modified to incorporate the addition of fluorine or chlorine groups (**Figure 4.4**). An important question remained, how did structural modification alter the antiviral activity of Cl02-inspired bis(indole) compounds? To address this question Cl02-inspired bis(indole) compounds were screened for antiviral activity at 10 μM. An unrelated novel collection of bis(indole)

compounds were additionally included in this screen. The results of this IF screen were encouraging as Cl02-derived compounds consistently significantly reduced RSV progeny production (**Figure 4.6**). Br02 OMe demonstrated the largest reduction in RSV progeny production. None of the Cl02-inspired bis(indole) compounds produced a statistically significant reduction in cell viability.

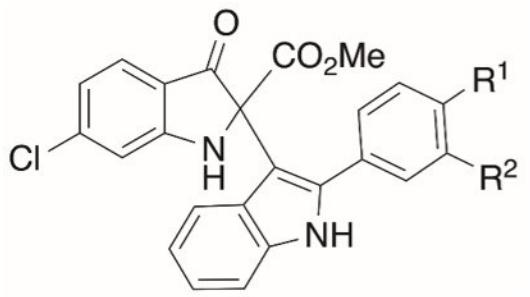

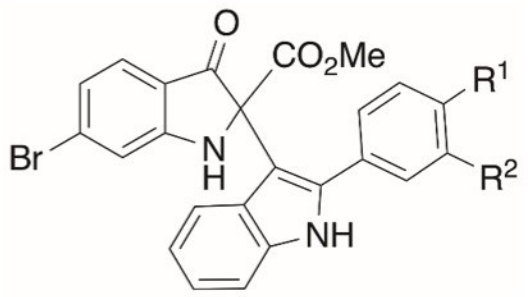

Cl02	R^1, R^2 = H	Br02	R^1, R^2 = H
Cl02 OMe	R^1 = OMe, R^2 = H	Br02 OMe	R^1 = OMe, R^2 = H
Cl02 F	R^1 = F, R^2 = H	Br02 F	R^1 = F, R^2 = H
Cl02 FCl	R^1 = F, R^2 = Cl	Br02 FCl	R^1 = F, R^2 = Cl

Figure 4.4. The chemical structure of Cl02 and Cl02-derived compounds. Halogen atoms and methyl (OMe) groups were substituted at the indicated side chain (R^1 or R^2) positions.

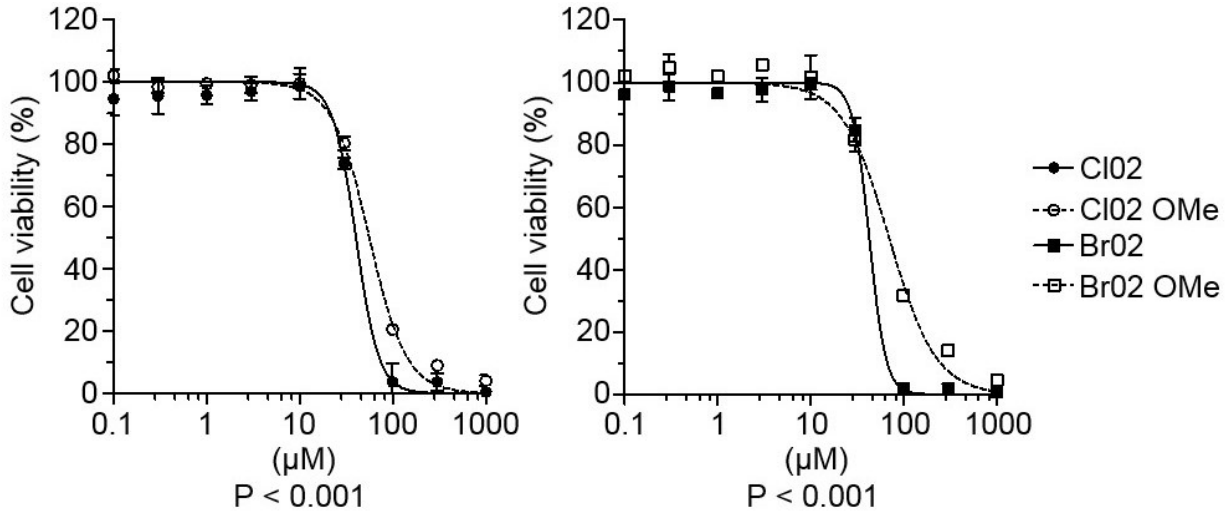

Figure 4.5. The addition of a methyl group reduces bis(indole) cytotoxicity. Cell viability values of bis(indole)-treated wells were normalized to the mean of untreated wells (set as 100% cell viability). Cell viability of 1HAEo- cells was measured via MTT assay during a 48-hour incubation with the compounds. Each point represents six biological replicates within a single experiment. Three independent experiments were completed and provided similar results, data

from one experiment is shown. Error bars represent standard deviation. Data were analyzed by nonlinear regression. A sum-of-squares F test was completed to test the null hypothesis that CC_{50} values were equal for Cl02 versus Cl02 OMe (left) and Br02 versus Br02 OMe (right), P values are provided.

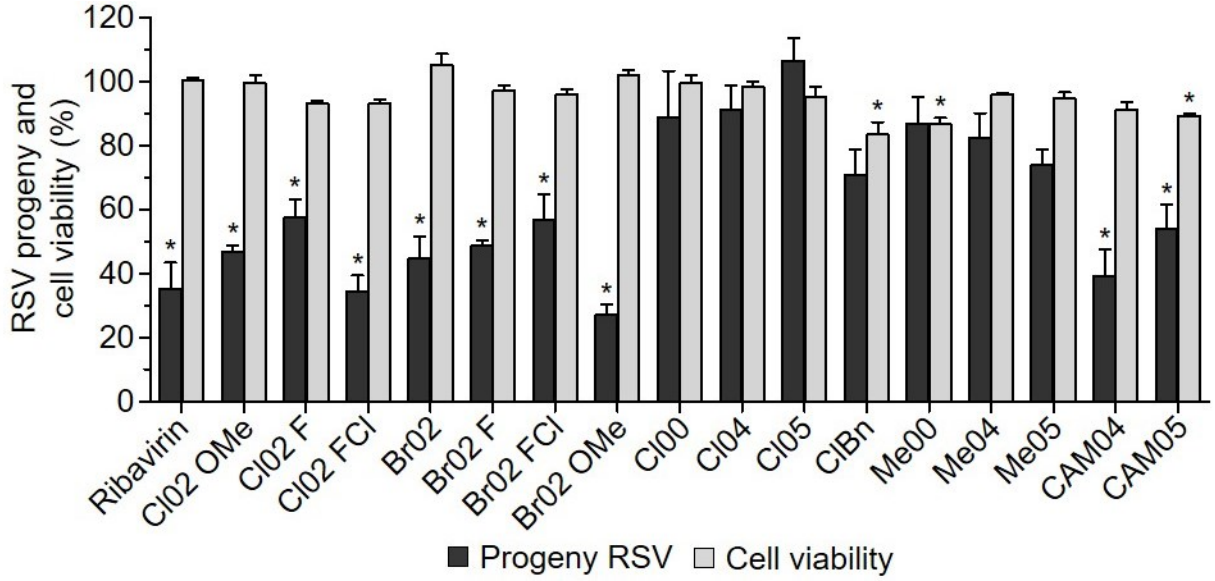

Figure 4.6. Bis(indole) compounds derived from Cl02 reduce RSV progeny production at 10 μM. RSV progeny production in bis(indole)-treated wells are presented as a percentage after normalizing to untreated wells, wherein the mean of the latter was set as 100% progeny production. Likewise, cell viability values of bis(indole)-treated wells were normalized to the mean of untreated wells (set as 100% cell viability). 1HAEo- cells were infected with RSV at an MOI of 1. At 2 hpi media was refreshed to prevent carry-over of inoculum virus. Progeny RSV was collected and transferred to HeLa cells at 48 hpi. At 24 hpi RSV-infected HeLa cells were quantified via the IF-assay. Cell viability was measured by MTT assay. Results represent three biological replicates in a single experiment and error bars represent standard deviation. Two independent experiments were completed and provided similar results, data from one of two experiments is shown. Prior to normalization results were analyzed by one way ANOVA with Bonferroni's post-test to compare treatment groups to respective untreated control groups; (*) represents $P < 0.05$.

With the exception of CAM04, compounds unrelated to Cl02 did not produce a significant reduction in RSV progeny production in the absence of cytotoxicity (**Figure 4.6**). Br02 OMe emerged as a promising compound as it provided the greatest reduction in RSV progeny production in the absence of cytotoxicity. A concentration-response experiment was completed to assay the antiviral activity and therapeutic index of Br02 OMe. In concentration-response experiments the antiviral activity of Br02 OMe was largely unchanged; an EC_{50} value of 9.0 μM was observed for Cl02 (**Figure 4.3**) and an EC_{50} value of 7.6 μM was observed for Br02 OMe (**Figure 4.7**). The CC_{50} value for Cl02 was previously observed to be 37.4 μM (**Figure 4.3**)

producing a therapeutic index of 4.1. The CC_{50} value of Br02 OMe was 93.5 µM. The improved cytotoxicity profile obtained though structural modifications to Cl02 yielding Br02 OMe resulted in an improvement of the therapeutic index from 4.1 to 12.3.

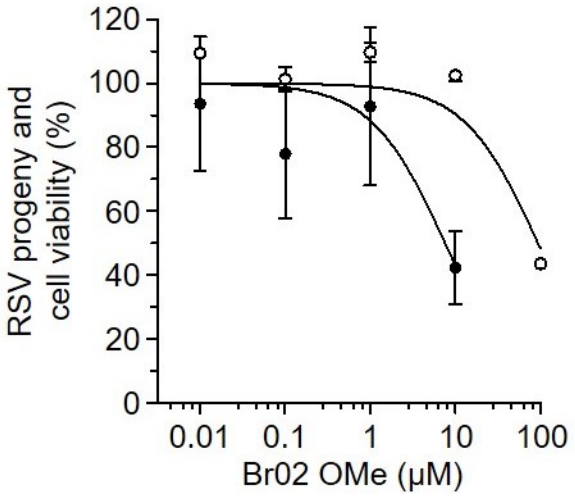

Figure 4.7. Br02 OMe reduces RSV progeny production. RSV progeny production (filled circles) in Br02 OMe-treated wells are presented as a percentage after normalizing to untreated wells, wherein the mean of the latter was set as 100% progeny production. Likewise, cell viability values (open circles) of Br02 OMe-treated wells were normalized to the mean of untreated wells (set as 100% cell viability). 1HAEo- cells were infected with RSV at an MOI of 1. At 2 hpi media was refreshed to prevent carry-over of inoculum virus and Br02 OMe was added to cell culture media. RSV progeny was collected and transferred to HeLa cells at 48 hpi. At 24 hpi RSV-infected HeLa cells were quantified using the IF-assay. Cell viability was measured by MTT assay. Data represent three biological replicates from one experiment; three independent experiments were completed and provided similar results, data from one of two experiments is shown. Error bars represent standard deviation.

A novel collection of amino acid-conjugated bis(indole) compounds, that were unrelated to Cl02, were also investigated for antiviral activity against RSV. Briefly, four amino acid-conjugated bis(indole) compounds were added to culture media over a range of concentrations from 30 nM to 100 µM. 1HAEo- cells were infected with RSV at an MOI of 1. To prevent carry over of inoculum virus into progeny RSV, fresh compound containing-media was replaced onto cells at 2 hpi. At 48 hpi progeny virus was transferred onto HeLa cells; at 24 hpi HeLa cells were fixed, immunostained, and RSV infected cells quantified via the IF-assay. Separately, 1HAEo- cells were incubated with bis(indole) compounds in parallel to monitor cytotoxicity by MTT assay. As other bis(indole) compounds had previously demonstrated antiviral activity against RSV I hypothesized that these compounds would inhibit RSV progeny production in a concentration-

dependent manner. However, the amino acid-conjugated bis(indole) compounds did not inhibit RSV replication (**Figure 4.8**). These results suggest RSV is recalcitrant to the amino acid-conjugated bis(indole) compounds. With the exception of Bis-Tryptophan, which reduced cell viability in a concentration-dependent manner, these compounds did not elicit a reduction in cell viability. Given the absence of antiviral activity amino acid-conjugated bis(indole) compounds were not explored further.

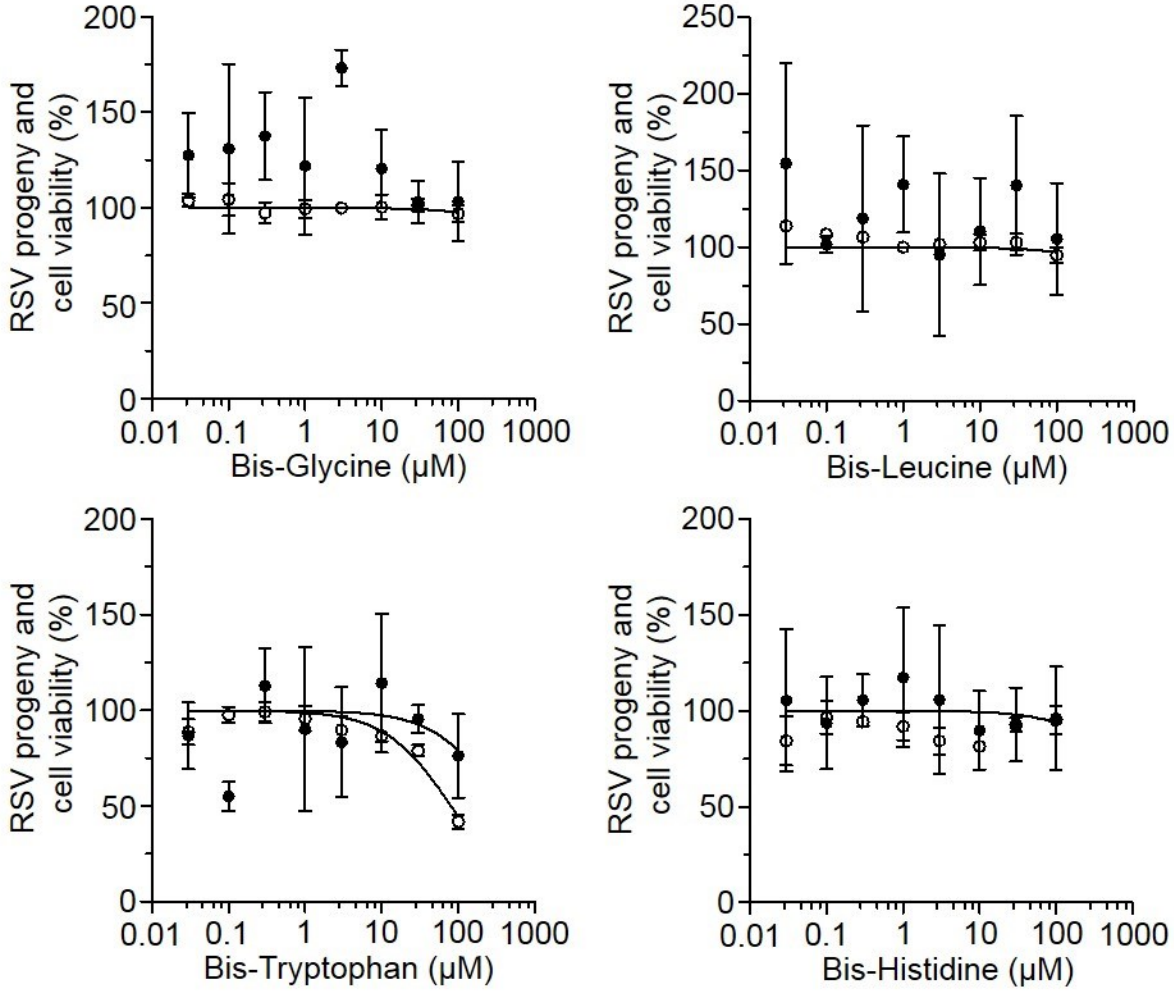

Figure 4.8. Amino acid-conjugated bis(indole) compounds do not inhibit RSV progeny production. RSV progeny production (filled circles) in compound-treated wells are presented as a percentage after normalizing to untreated wells, wherein the mean of the latter was set as 100% progeny production. Likewise, cell viability values (open circles) of compound-treated wells were normalized to the mean of untreated wells (set as 100% cell viability). 1HAEo- cells were infected with RSV at an MOI of 1. At 2 hpi media was refreshed to prevent carry-over of inoculum virus. RSV progeny was collected and transferred to HeLa cells at 48 hpi. At 24 hpi, RSV-infected HeLa cells were quantified using the IF-assay. Cell viability was measured by MTT assay. Data represent

three biological replicates from one independent experiment and error bars represent standard deviation.

These results suggest amino acid-conjugated bis(indole) compounds do not inhibit RSV replication. An important future direction will be continued structural modifications to Cl02-inspired bis(indole) compounds to improve antiviral activity against RSV. The next aim of chapter four was to characterize the antiviral mechanism of action of Cl02 and Cl02-inspired bis(indole) compounds.

4.2.2. Characterizing the mechanism of inhibition of bis(indole) compounds

Many RSV antiviral compounds inhibit viral entry through blocking fusion, including palivizumab [155], GS-5806 [205], ALX-0171 [215], MDT 637 [218], BMS-433771 [219] and TMC-353121 [220]. The remaining RSV antivirals target viral transcription. The majority of these compounds target RSV-L, the RdRp subunit responsible for catalyzing nucleotide polymerization. RSV-L targeting compounds included lumicitabine [212], BI-D [213], PC786 [196], YM-53403 [77], BCX-4430 [222], GS-5734 [221], and AZ-27 [195]. Alternatively, RSV604 inhibits RSV transcription by binding RSV-N. Collectively, RSV antivirals have been described which target a variety of processes essential to RSV replication. Theoretically, it also remains possible that novel RSV antiviral compounds will be discovered which target other essential processes in the RSV life cycle.

It is important to characterize the mechanism of action of antiviral compounds. This understanding may help predict how antiviral resistance could evolve, is necessary for clinical licensing, helps establish intellectual property rights, and is worth pursuing simply to satisfy scientific curiosity. An *in vitro* viral transcription assay was completed to help elucidate the mechanism of action of bis(indole) compounds. RSV was also serial passaged in the presence of bis(indole) compounds to develop resistant RSV escape mutants.

4.2.2.1. In vitro viral transcription assay

In the IF-protocol used to identify bis(indole) compounds with RSV-antiviral activity, Cl02 inhibited RSV progeny production in a concentration-dependent manner. The antiviral activity of Cl02 was not lost when Cl02 was added at 2 hpi (**Figure 4.5**). This result suggested that Cl02 was not a fusion inhibitor and did not inhibit RSV entry into the cell. I hypothesized that Cl02 inhibited RSV progeny production through interfering with the RSV RdRp complex. To test this hypothesis an *in vitro* viral transcription assay, described previously [195,316], was performed. Briefly, RSV-

infected HEp-2 cells were lysed and cell lysate was added to an *in vitro* transcription reaction mixture. This mixture contained actinomycin D to inhibit cellular polymerases from transcribing mRNA and contained α 32-P uridine triphosphate. During transcription incorporation of α 32-P into the phosphodiester RNA backbone radiolabeled RNA transcripts. To test the hypothesis that Cl02 targeted the RSV RdRp, Cl02 was added to the *in vitro* transcription reaction mixture. Following the reaction, viral transcripts were separated by electrophoresis on a 4% acrylamide 7 M urea gel. After separation of transcripts gels were dried for 2 hours at 80 °C and transferred into a cassette containing a phosphor screen for autoradiography imaging.

In the mock RSV infection-lysate lane no bands were observed confirming inhibition of cellular transcription by actinomycin D (**Figure 4.9a**). Bands of the expected migration pattern were observed in the untreated RSV infection-lysate lane. Band intensity was slightly reduced by increasing concentrations of Cl01. Cl02 reduced the intensity of bands in a concentration-dependent manner to a greater extent. This result was not unexpected, given the structural similarity of Cl01 and Cl02. These results suggest that both Cl01 and Cl02 interfered with RSV viral transcription (**Figure 4.9a**). A total of four experimental replicates were produced. The RSV-F and RSV-NS2 bands were quantified through densitometry as the intensity of these bands were representative of the intensity of all bands within each treatment group. The RSV-F and RSV-NS2 bands from each treatment group were then normalized to the respective RSV-F or RSV-NS2 bands in the untreated RSV-infected control lanes. These results indicated increasing Cl01 and increasing Cl02 concentrations significantly reduced the production of RSV mRNA transcripts (**Figure 4.9b**). This result supports the conclusion that bis(indole) compounds target the RSV RdRp complex. It is important to note that a limitation of this assay is that it does not reveal which component of the RSV RdRp complex is targeted. Any component of the RSV RdRp, which includes RSV-L, -P, -M2-1, and -N and cellular host proteins, may be targeted by bis(indole) compounds. As Cl02 was added to the reaction mixture after cell lysates had been collected this result also suggests that Cl02 does need to be metabolized inside of the host cell to become active.

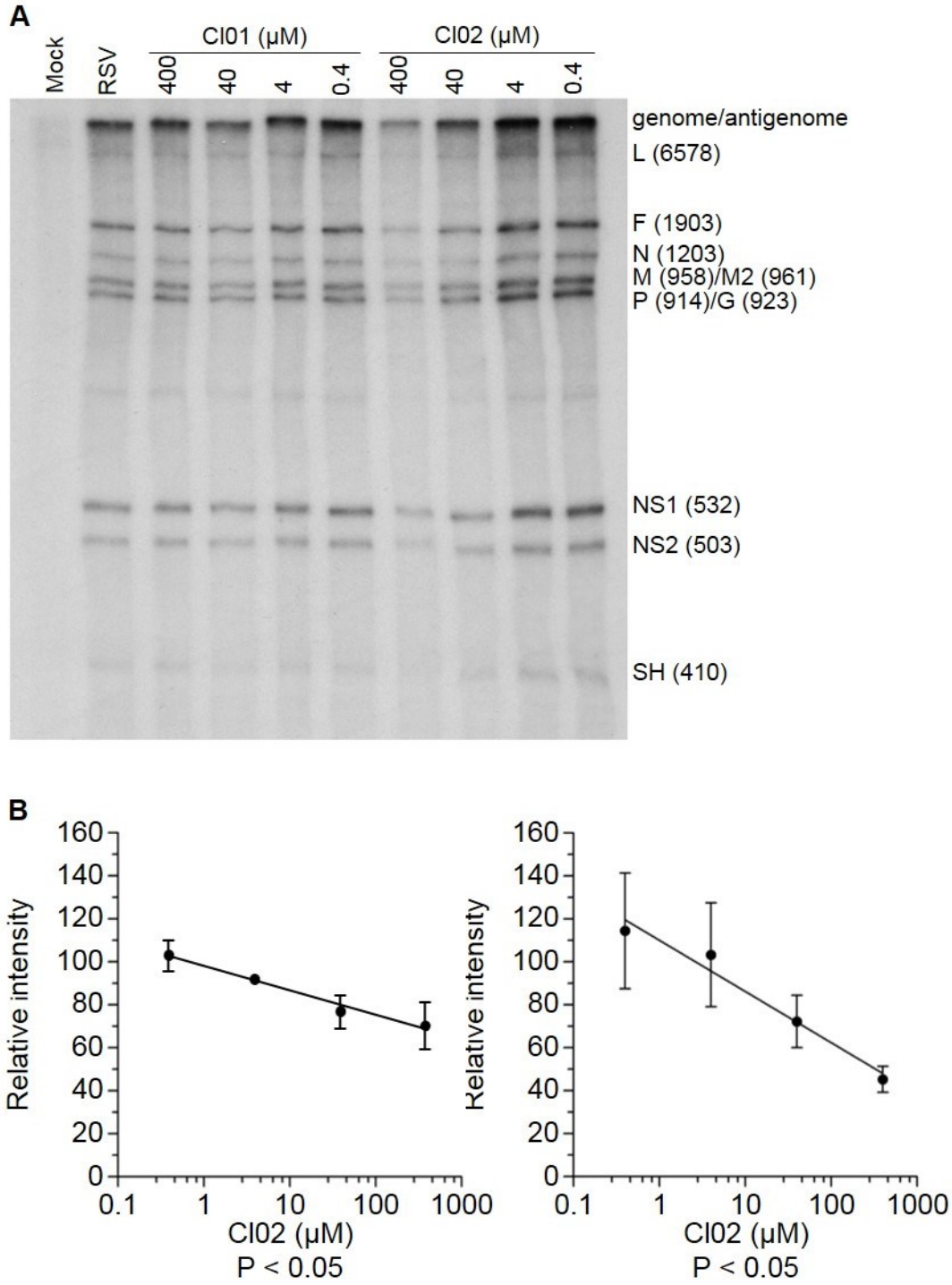

Figure 4.9. Cl02 reduces *in vitro* RSV transcription. (A) Autoradiography was used to measure the production of RSV mRNA following an *in vitro* transcription reaction. In this assay RSV-infected cell lysate was combined with Cl01 or Cl02 in a transcription reaction mixture that contained α 32-P uridine triphosphate. Predicted band sizes (in nucleoside bases) are provided. (B) Densitometry was used to quantify band intensity of RSV-F and RSV-NS2 transcripts. These values were normalized against the density of RSV-F or RSV-NS2 bands in the RSV-infected

untreated control group labelled "RSV". Four independent experiments were completed and normalized values were plotted against concentrations. Error bars represent standard deviation. The least squares method of linear regression was used to fit a line and an F-test was performed to test the null hypothesis that the slope of the line equalled zero. This null hypothesis was rejected ($P < 0.05$).

4.2.2.2. Resistant mutant escape assay

The results of the *in vitro* viral transcription assay support the conclusion that the antiviral mechanism of action for Cl02 is inhibition of the RSV RdRp complex. However, this result does not distinguish which component of this complex is targeted. RSV RdRp is primarily comprised of RSV-L, -P, and -M2-1 and these viral proteins are sufficient for *in vitro* viral transcription [62,63]. The RSV-N protein and host chaperone protein HSP90 also support RSV RdRp processivity [79]. Thus, interference with RSV transcription by Cl02 could be mediated by targeting viral or cellular components of the RdRp complex. I hypothesized that if RSV was serial passaged in the presence of bis(indole) compounds a resistant escape mutant may evolve. The presence of an RSV escape mutant would suggest bis(indole) compounds target a viral protein.

To test this hypothesis, 1HAEo- cells were infected with RSV and treated with 20 μM or 50 μM Cl02 or Br02 OMe. At 48-72 hpi media containing progeny virus was collected and transferred onto a fresh 1HAEo- cell monolayer. An untreated RSV-infected control treatment was included to ensure the initial MOI used and duration of passages were conducive to RSV replication. In untreated control wells viral titers increased during passaging, crashed, and then increased again (**Figure 4.10**). This pattern is consistent with the von Magnus effect [333-335]. This phenomenon is due to the accumulation defective interfering particles (DIPs). The structural proteins of DIPs are the same as infectious virus, however, DIPs lack viable genomes and are non-infectious as a result. DIPs propagate during coinfection with viable virus and reduce the production of viable progeny. These coinfections are frequent as viral titers increase. However, as DIPs overtake viable virus coinfection becomes less frequent resulting in a crash in progeny titers. The von Magnus effect is observed during rapid viral replication. Therefore, these results suggest that the 48 to 72-hour passaging time used in this protocol was conducive to rapid RSV replication.

In the wells that were treated with Cl02 or Br02 OMe, RSV replication was below the limit of detection for 10-11 passages (**Figure 4.10**). RSV progeny emerged at subsequent passages. The amount of progeny produced was typically greater in wells which were treated with a bis(indole) compound concentration of 20 μM versus 50 μM. While progeny virus emerged the amount of

progeny released remained substantially lower in wells treated with bis(indole) compounds than in untreated control wells. These results do not suggest a fit and highly resistant RSV strain emerged. Instead, these results suggest that it is possible for RSV to gain a slight degree of resistance to bis(indole) compounds. The emergence of weakly resistant RSV strains supports the conclusion that bis(indole) compounds target an RSV protein component of RSV RdRp. Future studies which isolate and sequence resistant escape mutants will enable the precise identification of the target of bis(indole) compounds.

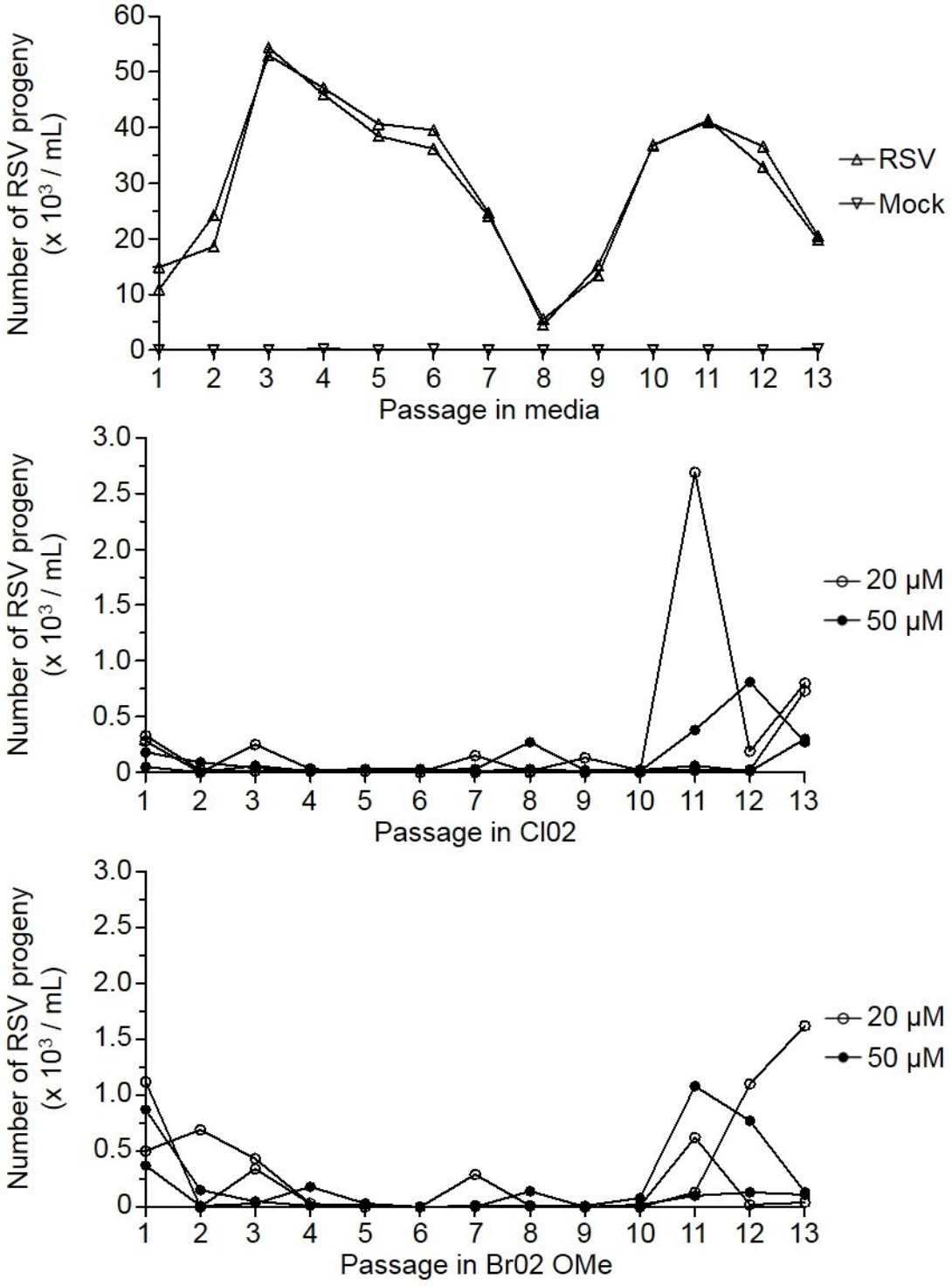

Figure 4.10. RSV replication emerges during serial passaging in Cl02 and Br02 OMe. 1HAEo- cells were infected with RSV at an MOI of 0.1 or mock infected with PBS. Progeny RSV was passaged in duplicate in the presence of Cl02 or Br02 OMe; progeny was collected and passaged at 48 to 72-hour intervals and diluted 1:5 at each passage. Progeny collected at each

passage was quantified in HeLa cells via the IF-assay. Each point represents a single biological replicate.

4.3. Discussion

Bis(indole) compounds provide an attractive target for antiviral development as they are highly amenable to structural modification through dual catalytic chemistry which produces adducts at high yield under ambient conditions [313]. These compounds were inspired by Isatisine A, the active component of antiviral herbal remedies. Modest antiviral activity of Isatisine A against HIV has been described previously [297]. The IF-protocol used to identify compounds with antiviral activity against RSV measured the production of viable progeny RSV. This assay identifies RSV inhibitors in an unbiased manner as inhibition of any component of the viral life cycle will reduce RSV progeny production. The bis(indole) compound Cl02 was found to inhibit RSV progeny production. A collection of compounds with structural similarity to Cl02 were synthesized and screened for antiviral activity against RSV. Compounds related to Cl02 consistently reduced RSV progeny production. Most notably, the Cl02-derived compound Br02 OMe had the greatest antiviral activity and lowest cytotoxicity of the Cl02-based compounds. Bis(indole) compounds other than Cl02 and Br02 OMe had RSV-antiviral activity in 10 μM screens. These compounds are worthy of future analysis. However, as Cl02 and Br02 OMe were the most active RSV-antiviral bis(indole) compounds identified, these compounds were pursued.

Elucidating the mechanism of action of antiviral bis(indole) compounds was then pursued. The antiviral effect of Cl02 persisted when compounds were added at 2 hpi leading to the hypothesis that these compounds did not inhibit viral entry and instead inhibited RSV RdRp. An *in vitro* viral transcription assay was completed to determine whether RSV RdRp was targeted by bis(indole) compounds and RSV mRNA production was reduced by increasing concentrations of Cl02. These results support the conclusion that the target of bis(indole) compounds is the RSV RdRp complex. While the RdRp complex is primarily comprised of RSV proteins [62,63], host proteins such as HSP90 also contribute to processivity [79]. To determine whether the target of bis(indole) compounds was a host or viral protein, a resistant mutant escape assay was conducted. RSV was serial passaged in the presence of Cl02 and Br02 OMe. After 10 passages a modest amount of RSV progeny release was observed in the presence of bis(indole) compounds. These results suggest weakly resistant RSV strains emerged due to the selective pressure applied by passaging in the presence of bis(indole) compounds. Collectively, these results suggest that the target of bis(indole) compounds

is an RSV protein component of the RSV RdRp complex. Therefore, bis(indole) compounds may target any viral constituents of this complex, which include RSV-L, -P, -M2-1, and -N. As RSV-L is the catalytic subunit of the RSV RdRp complex it is the most likely target, however, future work will be needed to validate this hypothesis.

Two antiviral compounds which target RSV-L have progressed to phase 2 clinical trials, lumicitabine [76] and PC786 [196]. This is the furthest RSV-L inhibitors have progressed in clinical trials to date. Unfortunately, clinical trials studying lumicitabine were recently cancelled, suggesting limited activity or toxicity concerns. Lumicitabine is a deoxycytidine nucleoside analogue containing one chlorine and one fluorine group [336]. Following entry into the host cell lumicitabine is triphosphorylated and competes with cytidine triphosphate for access to RSV RdRp; after binding near the active site chain termination occurs. The parent compound of lumicitabine also inhibits PIV-3 and VSV RdRp *in vitro*. Interestingly, slight structural modifications to lumicitabine confers activity against HCV RdRp, a positive sense ssRNA virus [76]. Serial passaging of RSV in the presence of increasing concentrations of lumicitabine yielded resistant mutants. These mutants possessed 4 amino acid substitution mutations, each mapping to the third conserved region of RSV RdRp within motif B which lies near the catalytic active site. These mutations included RSV-L M628L, A789V, L795I, and I796V.

PC786 contrasts lumicitabine as it is a nonnucleoside small molecule inhibitor of RSV-L [196]. During serial passaging of PC786 escape mutants (RSV-L Y1631H or Y1631L) emerged at passage three. As lumicitabine is not a nucleoside analogue, it is not surprising that the locations of mutations differed between lumicitabine and PC786. The RSV-L Y1631H mutation also conferred resistance to PC786 parent compounds AZ-27 and YM-53403 [77,195]. As a future direction our research group plans to isolate escape mutants resistant to bis(indole) compounds and determine the precise RSV target of bis(indole) compounds. While the mechanisms of inhibition differ, lumicitabine and PC 786 both target RSV-L. It will be interesting to learn whether Cl02 and Br02 OMe also targets RSV-L or if another component of the RdRp complex is targeted.

Assaying antiviral activity of bis(indole) compounds against RSV *in vivo* will be a key step in the development of these compounds. A variety of model systems for RSV infection are available and include mice, cotton rats, lambs, nonhuman primates, and healthy adult human volunteers [337]. The appropriateness of respective models is discussed in chapter 6.

Br02 OMe inhibited RSV replication with an EC_{50} of 7.6 μM and a CC_{50} of 93.5 μM, yielding a therapeutic index of 12.3. As the therapeutic index is greater than 10, Br02 OMe constitutes a hit. The translation of hits, discovered during antiviral screening, into lead compounds requires considerable resources. By comparison, RSV-L inhibitors in clinical trials have EC_{50} values of 0.1 nM to 50.6 nM for PC786, and 1.3 μM to 2.7 μM for lumicitabine [76,196]. These compounds provide benchmarks for the continued development with Br02 OMe. However, these values are not the only consideration. As progress is made it will be equally important to consider ADME properties [338]. In this respect bis(indole) compounds have a head start as they obey at least three of the four Lipinski medicinal chemistry criteria [332].

Chapter 5: TLR7-mediated enhancement of RSV replication by the nucleoside analogue loxoribine

5.1. Introduction

PRRs are germ line encoded receptors which are fundamental to the detection of pathogens and the initiation of the host immune response. Pathogens typically present multiple molecular entities bound by PRRs. RSV is detected by cellular receptors from the TLR, RIG-I-like Receptor (RLR), and NOD-like Receptor (NLR) families. From the TLR family putative receptor-ligand interactions include the TLR2-TLR6 heterodimer and an unknown RSV ligand at the plasma membrane [339], TLR3 and endosomal dsRNA [340,341], TLR4 and RSV-F at the plasma membrane [126], and TLR7 and endosomal ssRNA [136,223-229]. From the RLR family RIG-I binds cytosolic 5'-triphosphorylated dsRNA and MDA5 binds cytosolic dsRNA [55-57]. Finally, from the NLR family NOD2 is capable of binding cytosolic ssRNA [342]. My interest in the intersection of TLR7 signalling and RSV infection arose from the observation that stimulation of 1HAEo- human airway epithelial cells with the TLR7 agonist loxoribine resulted in an increase in RSV progeny production (**Figure 3.5**). Enhancement of RSV replication following stimulation of an innate immune receptor was unexpected, however, a similar effect has been observed previously *in vivo*. In mice treated with the TLR7/8 agonist R-848 the severity of RSV infection was enhanced [289]. Confirming TLR7-mediated enhancement of RSV replication, and characterizing the mechanism of enhancement, was the aim of this chapter.

In addition to presenting a scientifically interesting phenomenon, the possibility of TLR7-mediated enhancement of RSV replication also has important clinical implications. TLR7 agonists have been licensed as immunomodulatory therapies for over a decade [230]. More recently, TLR7 agonists have been investigated as treatments for asthma and allergic airway diseases. While asthma is a heterologous syndrome, a substantial portion of asthma is characterized by an inappropriate T_H2 immune response. Specifically, T_H2 $CD4^+$ T cells or type 2 innate lymphoid cells produce IL-4, IL-5 and IL-13 which drive eosinophilia, goblet cell hyperplasia, inflammation, airway hyperreactivity and airway remodeling [31]. Stimulation of TLR7 drives a T_H1 response characterized by the release of IFNα [225,226], and to a lesser extent the production of pro-inflammatory cytokines tumor necrosis factor α, IL-6 and IL-12 [227,232,233]. Importantly, TLR7 stimulation antagonizes the T_H2 response [290-293]. Therefore, the TLR7 agonists imiquimod and R-848 have been studied extensively in mouse and rat ovalbumin-sensitization models of airway

hyperresponse [reviewed in [343]]. Other TLR7 agonists including AZ12441970 [344,345] and 2-substituted-8-hydroxyadenine [346,347] have been investigated in a similar manner. In these small animal models of asthma, treatment with TLR7 agonists counteracted the hallmarks of asthma; TLR7 agonists induced a T_H1 immune response, reduced airway hyperresponse and reduced airway remodelling [343].

In a phase I clinical trial the TLR7 agonist GSK2245035 was explored as a therapeutic for allergic rhinitis, another airway disease characterized by an inappropriate T_H2 response, and mild asthma. GSK2245035 was well tolerated in adult volunteers, however, efficacy data is not available (NCT01480271 and NCT01607372; [294]). A phase IIa clinical trial studying the TLR7 agonist AZD8848 found that symptom severity following allergen challenge was modestly reduced [295]. These studies reflect the interest in the pharmaceutical development of TLR7 agonists to treat airway diseases. This patient population is also at risk for respiratory viral infections; RSV infection is a major cause of exacerbations in asthmatic patients. If TLR7 agonists enhance RSV replication it may heighten the severity of RSV infection in an already vulnerable population. Therefore, I decided to characterize how loxoribine enhances RSV replication.

TLR7 is expressed in a variety of immune cells including pDCs, monocytes, macrophages, B cells, T cells, mast cells, and eosinophils, and is also present in non-immune cells including neurons, glial cells and airway epithelial cells [265-269]. After cleavage, mature TLR7 is located in endosomes; upon ligand binding TLR7 signals through MyD88 to activate IRF7, NF-κB and AP-1 transcription factors [99,100,240-246]. The natural ligand of TLR7 is ssRNA [223,225,226], however, TLR7 also recognizes synthetic guanosine analogues such as imiquimod, loxoribine, R-848, and CL097 [229,232,248-252]. The function of TLR7 has primarily been characterized in pDCs where stimulation results in substantial type I IFN production via the IRF7 transcription factor [136]. RSV has evolved multiple strategies for abrogating the IFN response [53,94-97], as a result RSV replication is largely unaffected by IFN [146]. The AP-1 transcription factor is also activated by TLR7 stimulation. AP-1 is activated through the MAPK ERK. ERK phosphorylation downstream of TLR7 signalling is essential for AP-1 activation [224,240]. The TLR7 agonist loxoribine was discovered during a search for small molecule stimulants of B and NK cells [249]. Compounds related to loxoribine, such as 8-chloro-7-deazaguanosine and 7-thia-8-oxoguanosine, were investigated for antiviral activity in rats. It was noted that these compounds lacked *in vitro* antiviral activity and instead stimulated an antiviral

IFN response [250,251]. In these studies rats were infected via intraperitoneal injection with viruses including Banzi Virus, Encephalomyocarditis Virus, and Semliki Forest virus. Respiratory viral infections were not investigated. It was later discovered that TLR7 is the receptor through which loxoribine stimulated an IFN response [252].

In the following experiments, I observed that enhancement of RSV replication was not unique to loxoribine, as stimulation with the TLR7 agonist CL097 also increased RSV progeny production in a concentration-dependent manner. TLR7 was found to be present in 1HAEo- cells and TLR7 signalling was necessary for enhancement of RSV replication by loxoribine. RSV infection requires ERK activation [298], and ERK is activated following TLR7 stimulation [224]. As expected, ERK activation was increased following TLR7 stimulation; inhibition of ERK activation prevented loxoribine-mediated enhancement of RSV progeny production. These results suggest TLR7 stimulation enhances RSV replication in an ERK-dependent manner.

5.2. Results

5.2.1. Enhancement of RSV replication by TLR7 agonists in 1HAEo- cells

While screening nucleoside analogues for antiviral activity against RSV, I observed darker blue spot immunostaining in cells that had been treated with loxoribine during RSV infection. As staining is proportional to the amount of viral protein present, I inferred that treatment with loxoribine made 1HAEo- cells conducive to RSV replication. This observation was unexpected, as loxoribine is a well-defined TLR7 agonist [224,252].

Previously, loxoribine treatment had resulted in an increase in RSV progeny production (**Figure 3.5**). I hypothesized that increasing concentrations of loxoribine would result in increased RSV progeny production. To test this hypothesis human airway epithelial 1HAEo- cells were treated with different concentrations of loxoribine during a 48-hour infection. Loxoribine binds TLR7 with a dissociation constant (K_D) of 5.6 μM [229]. In the literature, loxoribine is typically used at concentrations of 100 μM – 2 mM [224,252]. Therefore, 1HAEo- cells were treated with a range of loxoribine concentrations from 0.5 μM to 500 μM. Progeny virus was collected and quantified via the IF-assay. In a concentration-dependent manner, treatment with loxoribine increased RSV progeny production. At a concentration of 500 μM loxoribine, RSV progeny production was increased by 3.4-fold (**Figure 5.1a**). These results supported the hypothesis and demonstrated that the enhancement of RSV replication by loxoribine was concentration dependent.

It was unexpected that stimulation of TLR7 would benefit RSV replication, yet outside of TLR7 stimulation loxoribine is not known to have any other biological activities. However, cellular receptors may demonstrate promiscuity with respect to ligand binding [348]. Therefore, it was essential to determine whether loxoribine altered RSV replication through stimulation of TLR7 or via a different uncharacterized mechanism of action. The first method used to approach this question was to treat 1HAEo- cells with an alternate TLR7 agonist. I hypothesized that if loxoribine enhanced RSV replication via TLR7 stimulation, then treating cells with the TLR7 agonist CL097 would also enhance RSV replication in a concentration-dependent manner. Treatment of 1HAEo- cells with CL097 during RSV infection increased the production of progeny RSV (**Figure 5.1a**). These results supported the conclusion that loxoribine enhanced RSV replication through stimulation of TLR7.

To this point, experiments demonstrating TLR7 agonist-mediated RSV enhancement were completed in immortalized 1HAEo- cells. To determine whether these observations were an artifact of working with immortalized cells I examined the affect of loxoribine on RSV replication in primary HBE cells. Access to primary HBE cells was limited, and due to the sensitivity of primary HBE cells in tissue culture, I elected to examine TLR7 agonists at concentrations not exceeding 100 μM. As I had observed concentration-dependent enhancement of RSV replication with two different TLR7 agonists in 1HAEo- cells, I hypothesized that RSV replication would be enhanced by TLR7 agonists in HBE cells. To test this hypothesis, HBE cells were isolated from donors and treated with loxoribine. In each donor I observed a non-significant trend towards increased RSV progeny production (**Figure 5.1b**). The relatively low concentration of 100 μM loxoribine used in this experiment may account for the lack of a significant increase in progeny RSV production. Due to limited access to primary HBE cells experimentation with higher concentrations of loxoribine was not completed. However, at a concentration of 100 μM loxoribine the observed trend towards increased progeny RSV production by primary HBE suggests TLR7-mediated enhancement of RSV replication is not an artifact of experimentation in immortalized 1HAEo- cells.

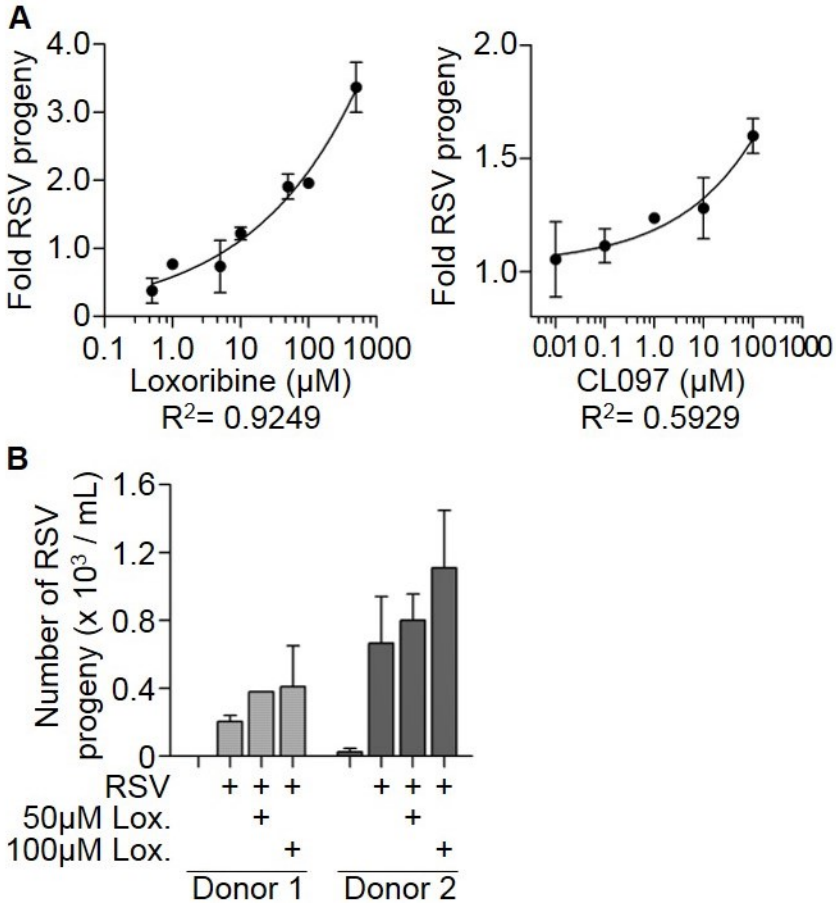

Figure 5.1. TLR7 agonists increase RSV progeny production during infection of airway epithelial cells. (A) 1HAEo- cells were infected with RSV at an MOI of 1 and treated with loxoribine or CL097. Progeny RSV was collected at 48 hpi and transferred onto HeLa cells. At 24 hpi HeLa cells were fixed, blue spot immunostained, and RSV infected cells were quantified. This data represents three biological replicates from one independent experiment and error bars represent standard deviation; two independent experiments were completed and provided similar results, data from one of two experiments is shown. The data was analyzed by nonlinear regression to create a best-fit curve. The R^2 values were determined through sum-of-squares analysis. (B) HBE cells were infected with RSV at an MOI of 0.5 and treated with 50 μM loxoribine (Lox.) or 100 μM loxoribine. At 48 hpi progeny RSV was collected and transferred to HeLa cells; at 24 hpi HeLa cells were fixed and blue spot immunostained. RSV foci of infection were quantified using the EVOS FL Auto microscope. Each bar represents two biological replicates and error bars represent standard deviation. Results were analyzed via one way ANOVA and no significant treatment effect was observed.

5.2.2. TLR7 expression and siRNA knockdown in 1HAEo- cells

As two distinct TLR7 agonists enhanced RSV replication, I hypothesized that the mechanism of enhancement was dependent on TLR7. TLR7 is known to be expressed in airway epithelial cells [266]. To confirm the presence of TLR7 in 1HAEo- cells TLR7 protein was identified via western

blot. Ramos human B lymphoma cell lysate was included as a positive control as Ramos cells are known to express full length TLR7 at approximately 140kDa. In Ramos cells full length TLR7 was detected at the expected size of 140kDa. In 1HAEo- cells TLR7 was detected at 150kDa, 100kDa and 50kDa (**Figure 5.2a**). The 150kDa band represents uncleaved TLR7; the discrepancy in size of full length TLR7 between Ramos cells and 1HAEo- cells may be due to differing post-translational modifications between the two cell types. To confirm the fidelity of the TLR7 antibody, siRNA targeting TLR7 mRNA was used to knock down TLR7. 1HAEo- cells were transfected with AllStars Cell Death siRNA in parallel to assay transfection efficiency. This proprietary blend of siRNAs rapidly induced cell death following transfection confirming a high transfection efficiency (**Figure 5.2b**). TLR7 was readily detectable in 1HAEo- cells transfected with non-targeting siRNA, however, transfection with siRNA targeting TLR7 transcripts resulted in a substantial reduction in TLR7 protein. These results suggest the antibody used in the western blot reliably detected TLR7 (**Figure 5.2a**). TLR7 cleavage by furin-like proprotein convertases is necessary for TLR7 signaling [237,239]. It is unclear why cleaved TLR7 was not detected in Ramos cells, as these cells are known to be responsive to TLR7 agonists [252]. Nonetheless, I expected to detect cleaved TLR7 in 1HAEo- cells. Cleaved TLR7 was detected at approximately 100kDa and 50kDa. TLR7 siRNA also substantially reduced the amount of cleaved TLR7 present (**Figure 5.2**). These observations suggest that 1HAEo- cells express TLR7, and that siRNA knockdown greatly reduces the amount of TLR7 protein present in 1HAEo- cells.

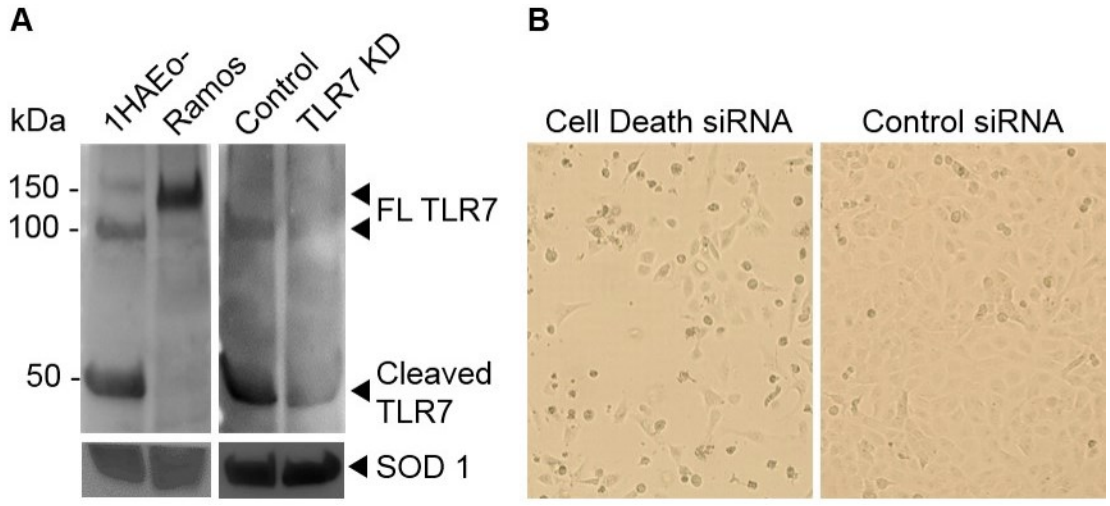

Figure 5.2. 1HAEo- cells express functional-form cleaved TLR7. (A) A western blot was performed to detect full length (FL) and cleaved TLR7 in 1HAEo- and Ramos cell lysates. Cleaved TLR7 was knocked down following a 48-hour transfection of 1HAEo- cells with TLR7 specific

siRNATLR7_6. Detection of SOD1 was used as a loading control. **(B)** In 1HAEo- cells, a high degree of cell rounding was observed for cells transfected with AllStars Cell Death siRNA. 1HAEo- cells were transfected with 20 μM siRNA for 48 hours.

5.2.3. Inhibition of TLR7 abrogates RSV replication enhancement by loxoribine

Two distinct TLR7 agonists enhanced the replication of RSV, and the presence of TLR7 was confirmed in 1HAEo- cells. Therefore, I hypothesized that enhancement of RSV replication was dependent on TLR7. To test this hypothesis two complementary approaches were taken. The first approach utilized IRS-661, a phosphorothioate-backbone oligonucleotide which antagonizes TLR7 signalling. IRS-661 has been used previously to block TLR7-ligand interactions in cell culture and *in vivo* [263]. I hypothesized that treating cells with IRS-661 would prevent enhancement of RSV replication by TLR7 agonists. To test this hypothesis 1HAEo- cells were treated with 1 mM loxoribine with or without cotreatment with IRS-661. IRS-661 was also added to cells which were not treated with loxoribine. For each of these treatments, cells were infected with RSV and progeny virus was collected at 48 hpi. In cells that were not treated with loxoribine, IRS-661 did not affect the replication of RSV (**Figure 5.3a**). Incubation with loxoribine significantly increased the production of RSV progeny virus as expected. Treatment with IRS-661 prevented the enhancement of RSV progeny production by loxoribine. These results suggest that enhancement of RSV replication by loxoribine is dependent on TLR7.

As an alternative means of testing whether TLR7 was necessary for enhancement of RSV replication by loxoribine, TLR7 expression was knocked down by siRNA transfection. Confirmation of TLR7 knockdown was confirmed previously by western blot (**Figure 5.2a**). 1HAEo- cells transfected with TLR7 siRNA or transfected with a non-specific control siRNA were treated with loxoribine and infected with RSV. Two TLR7-targeting siRNA were utilized. TLR7 knock down by both TLR7 siRNA significantly reduced the production of RSV progeny in these loxoribine-treated cells (**Figure 5.3b**). Antagonism of TLR7 by IRS-661 and siRNA knockdown of TLR7 prevented loxoribine-mediated enhancement of RSV replication. Collectively, these results support the conclusion that enhancement of RSV replication by loxoribine is mediated by TLR7.

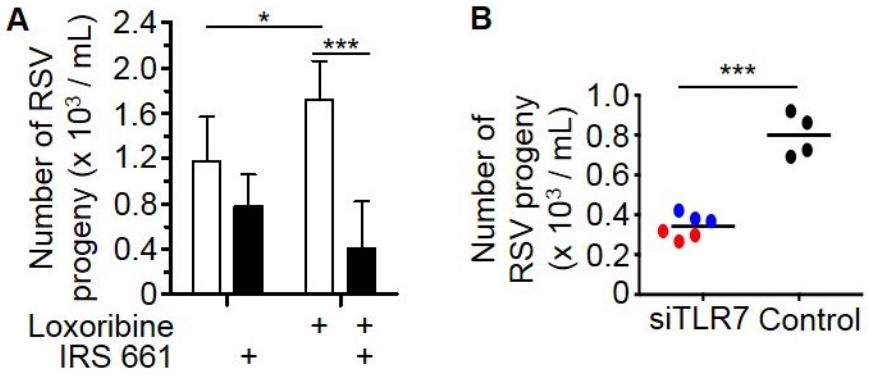

Figure 5.3. Enhancement of RSV replication by loxoribine is mediated by TLR7. (A) RSV progeny production following addition of 1000 µM loxoribine and/or 1 µM IRS-661. Following 1HAEo- cell infection with RSV at an MOI of 2, media was replaced at 2 hpi to remove inoculum virus. Progeny RSV was collected at 48 hpi and transferred to HeLa cells for quantification via the IF-assay. (*) indicates $P < 0.05$ and (***) indicates $P < 0.001$, which was determined via ANOVA with Bonferroni's post-test. Each bar represents six biological replicates from a single independent experiment; two independent experiments were completed and provided similar results, data from one of two experiments is shown. Error bars represent standard deviation. (B) 1HAEo- cells were transfected for 48 hours with 20 µM of control (nonspecific RNA) or TLR7-targeting siRNA prior to infection. Two TLR7-targeting siRNA oligonucleotides were utilized, siRNA_TLR7_6 (red) and siRNA_TLR7_12 (blue). 1HAEo- cells were then infected with RSV at an MOI of 1 and treated with 400 µM loxoribine. Progeny RSV was collected at 48 hpi and transferred onto HeLa cells for quantification via the IF-assay. (***) indicates $P < 0.001$, which was determined via t-test. Each point represents a biological replicate from one independent experiment.

5.2.4. Loxoribine enhances RSV replication after viral entry

In prior experiments, loxoribine was added to cell culture media 2 hours before infection resulting in an increase in RSV progeny production. This increase could be the result of increased entry of RSV into 1HAEo- cells following TLR7 stimulation. To test this hypothesis HBE cells were treated with TLR7 agonists loxoribine or CL097. HBE cells were then infected with RSV and the total number of RSV foci of infection were counted at 48 hpi. Treatment with loxoribine or CL097 did not increase the number of RSV foci of infection (**Figure 5.4a)**. These results failed to support the hypothesis. Therefore, stimulation of TLR7 did not appear to benefit the entry of RSV into host cells. Alternatively, TLR7 stimulation may have created a cellular environment more conducive to RSV replication. Therefore, I hypothesized that the affect of loxoribine was not produced through an increase in RSV entry. To gain insight on the stage of viral replication which benefitted from loxoribine treatment a time of addition assay was completed. 1HAEo- cells were treated with loxoribine 2 hours prior to RSV infection, at the time of infection, or at 2, 4, or 8 hpi. Progeny RSV was collected at 24 hpi to ensure progeny reflected a single viral replication cycle

[319]. A significant increase in RSV progeny production was observed when loxoribine was added 2 hours prior to infection, at the time of infection, and at 4 hpi (**Figure 5.4b**). When loxoribine was added at 8 hpi the production of RSV progeny was not affected. For all treatment groups it is essential to note that wells were washed with PBS and fresh media was replaced onto cells at 2 hpi to prevent carry over of inoculum virus into the progeny RSV which was collected at 24 hpi. This fresh media was supplemented with loxoribine for the -2, 0, and 2 hpi treatment groups. Therefore, RSV had entered cells prior to treatment with loxoribine in the 2 hpi and 4 hpi treatment groups. This supports the conclusion that loxoribine does not enhance RSV entry and is consistent with the earlier observation that loxoribine treatment does not increase the number of cells initially infected (**Figure 5.4a**). Instead, these results suggest loxoribine creates a cellular environment more conducive to RSV replication early during infection.

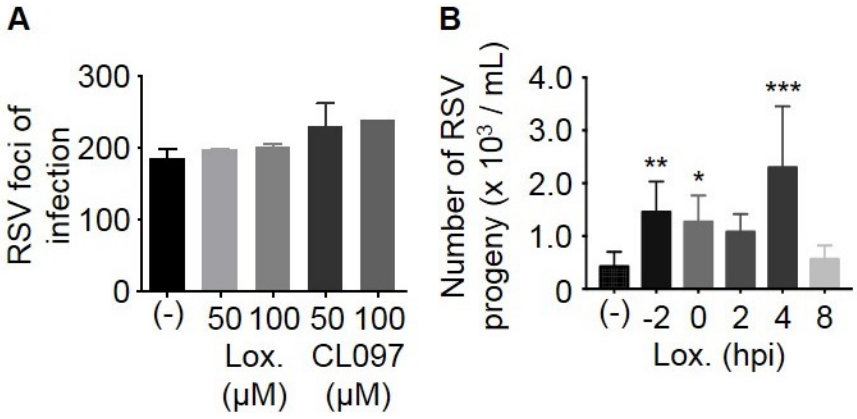

Figure 5.4. Loxoribine enhances RSV replication after viral entry. (A) Primary HBE cells were treated with loxoribine or CL097 and infected with RSV at an MOI of 0.5. At 48 hpi these cells were fixed and RSV-infected cells were identified by blue spot immunostaining. RSV foci of infection were manually quantified using the EVOS FL Auto microscope. Each bar represents two biological replicates and error bars represent standard deviation (with exception of 100 μM CL097 wherein one replicate was lost during experimentation). These results were analyzed by one way ANOVA and no significant treatment effect was observed. (B) The time of loxoribine addition determines significance of enhancement of RSV replication. 1HAEo- cells were infected with RSV at an MOI of 1. 400 μM loxoribine was added at indicated times relative to infection. At 24 hpi progeny RSV was collected and transferred to HeLa cells. At 2 hpi media on HeLa cells was refreshed to remove loxoribine. At 24 hpi HeLa cells were fixed, stained, and RSV infected cells quantified via the IF-assay. Each bar represents three biological replicates from one independent experiment; error bars represent standard deviation. Results were compared to the untreated (-) group via one ANOVA with Bonferroni's post test; (*) indicates $P < 0.05$, (**) indicates $P < 0.01$ and (***) indicates $P < 0.001$.

5.2.5. ERK phosphorylation is necessary for loxoribine-mediated enhancement of RSV replication

Following stimulation TLR7 signals through three major pathways culminating in the activation of transcription factors IRF7, NF-κB, and AP-1 [240]. Of the latter pathway, the MAPK ERK is an important regulator and TLR7 stimulation by loxoribine has previously been observed to result in ERK activation [224,240]. Phosphorylation of ERK also results immediately during RSV infection and inhibition of this signalling significantly reduces RSV replication [298]. I hypothesized that ERK activation following stimulation of TLR7 by loxoribine was responsible for enhancement of RSV replication.

Before testing this hypothesis, I confirmed that TLR7 stimulation resulted in ERK phosphorylation in 1HAEo- cells. 1HAEo- cells were treated with loxoribine and cell lysates were collected at various time points. In response to treatment with loxoribine the level of phosphorylated ERK was highly elevated at 10- and 30-minutes post treatment and remained elevated 60 minutes after treatment (**Figure 5.5a**). Given the importance of ERK phosphorylation to RSV replication observed previously [298], phosphorylation of ERK following TLR7 stimulation provided a possible mechanism by which loxoribine enhanced RSV replication.

UO126 is a potent inhibitor of ERK phosphorylation which functions by inhibiting the upstream kinases responsible for ERK phosphorylation, MEK-1 and MEK-2 [349]. As TLR7 stimulation resulted in ERK phosphorylation, and ERK phosphorylation benefits RSV replication, I hypothesized that if ERK phosphorylation was inhibited by treatment of cells with UO126 then loxoribine-mediated enhancement of RSV replication would be prevented. Before testing this hypothesis, the effect of cotreatment of loxoribine and UO126 on 1HAEo- cell viability was measured. No reduction in cell viability was observed at any of the concentrations tested (**Figure 5.5b**). Activation of ERK in 1HAEo- cells during RSV infection and inhibition of ERK phosphorylation by UO126 was also confirmed (**Figure 5.5c**; please note experiment 5.5c was conducted by L. Bilawchuk). 1HAEo- cells were then treated with 200 μM or 400 μM loxoribine with or without UO126. Treatment of 1HAEo- cells with loxoribine produced the expected increase in RSV progeny production and treatment of 1HAEo- cells with UO126 produced the expected decrease in RSV progeny production. If enhancement of RSV replication by loxoribine was mediated by ERK activation, then no enhancement of RSV progeny production would be expected during co-treatment with loxoribine and UO126. In cells co-treated with loxoribine and

UO126, inhibition of ERK activation abrogated enhancement of RSV progeny production by loxoribine (**Figure 5.5d**). These results supported the conclusion that ERK activation following TLR7 stimulation was responsible for enhancement of RSV replication.

Loxoribine-induced ERK activation may benefit RSV through many mechanisms. In particular, apoptosis may be inhibited by ERK activation during viral infection [350] and inhibition of apoptosis enhances RSV replication [91,287]. Therefore, the hypothesis that loxoribine treatment benefited RSV replication by inhibiting apoptosis was tested. To test this hypothesis 1HAEo- cells were infected with RSV and treated with loxoribine. At 2 hpi and 24 hpi cell lysates were collected and markers for apoptosis were measured via western blot. Accumulation of autoproteolytically cleaved caspase-3 occurs during late stages of apoptosis. Cleaved caspase-3 then proteolytically cleaves over 40 cellular proteins to drive apoptosis. The hallmark apoptotic process of DNA fragmentation results from DFF-45 cleavage by caspase-3 and cellular blebbing follows cleavage of α-fodrin and gelsolin by caspase-3 [351]. To determine whether loxoribine treatment inhibited apoptosis accumulation of cleaved caspase-3 was measured. ERK also influences the necroptotic cell death pathway via interaction with receptor-interacting protein 1 (RIP1) and receptor-interacting protein 3 (RIP3) [352]. RIP1 is activated by autophosphorylation resulting in dimerization and RIP1 activation is sufficient for the induction of necroptosis [353]. Following activation of RIP1, RIP1 and RIP3 phosphorylate Mixed Lineage Kinase domain-like (MLKL) protein which oligomerizes and physically disrupts cell membrane integrity [354]. Phosphorylated RIP1 and phosphorylated MLKL were measured as markers for early and late necroptosis, respectively.

At 2 hpi, RSV infection caused accumulation of phosphorylated RIP1 and treatment with loxoribine opposed this accumulation (**Figure 5.5e**; please note experiment 5.5e was conducted by L. Bilawchuk). At 24 hpi loxoribine treatment of infected cells no longer reduced phosphorylated RIP1 accumulation and a slight increase in phosphorylated MLKL was observed. At 24 hpi the most substantial effect of treating RSV-infected cells with loxoribine was an accumulation of cleaved caspase-3. These results suggest treating RSV-infected 1HAEo- cells with loxoribine may delay necroptosis at early time points, however, necroptosis and apoptosis are increased by loxoribine treatment at 24 hpi. While necroptosis may be delayed by loxoribine treatment at early time points during RSV infection, these results do not support the hypothesis that loxoribine treatment enhances RSV infection by inhibiting necroptosis or apoptosis.

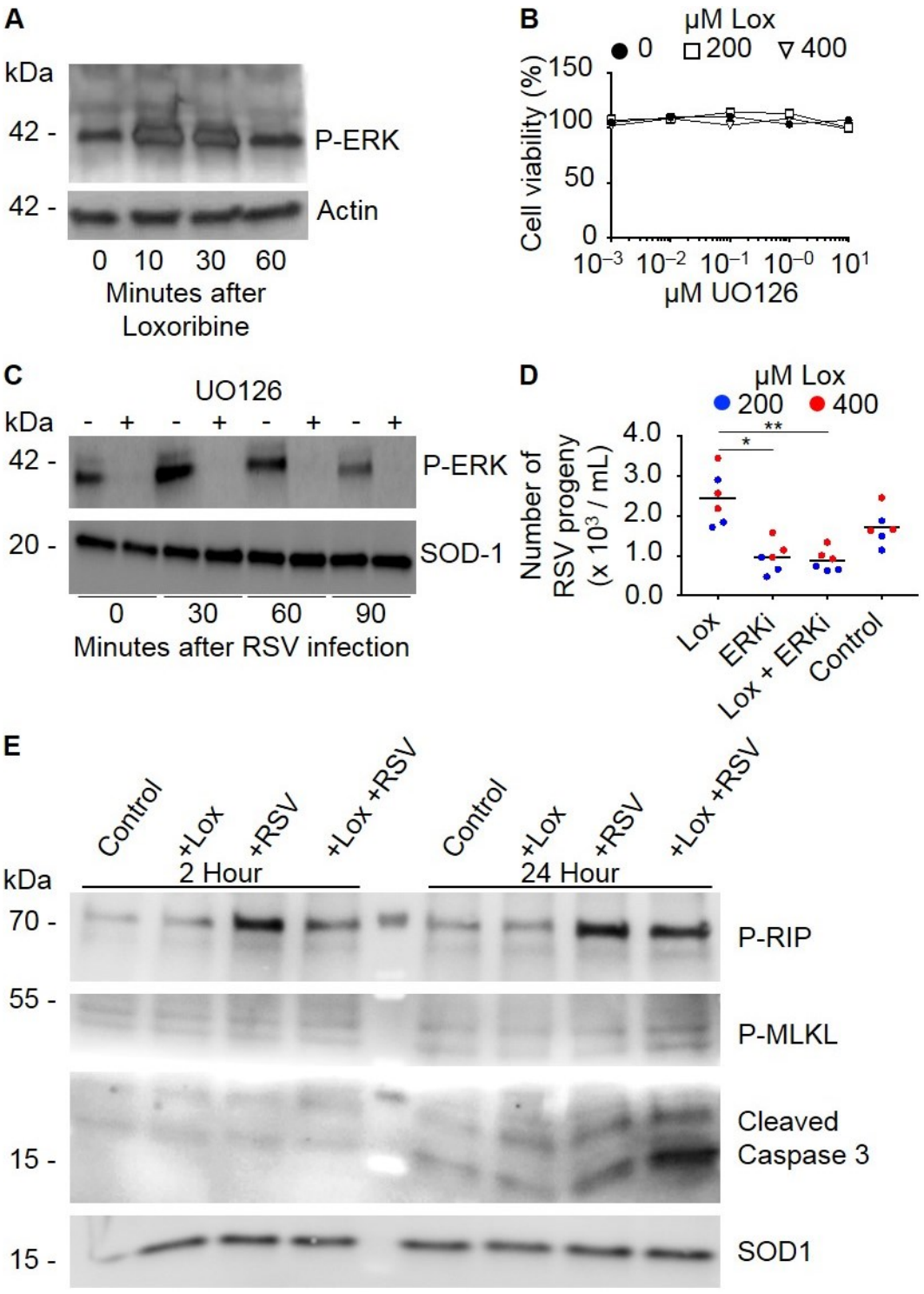

Figure 5.5. Phosphorylation of ERK is necessary for loxoribine-mediated enhancement of RSV replication. (A) Phosphorylated ERK (P-ERK) in 1HAEo- cells was measured by western blot after treatment with 100 μM loxoribine; actin was measured as a loading control. (B) Potential cytotoxic effects of the combination of loxoribine (Lox) and the MEK inhibitor UO126 were assayed in 1HAEo- cells via MTT assay. 1HAEo- cells were treated with loxoribine at 200 μM or

400 μM and were treated with UO126 at 1 μM. (C) 1HAEo- cells were infected with RSV at an MOI of 1 and treated with UO126. Cell lysates were collected and P-ERK was detected via western blot; SOD1 was measured as a loading control. (D) 1HAEo- cells were treated with loxoribine (Lox) at 200 μM (blue) or 400 μM (red) with or without 1 μM UO126, which inhibits ERK (ERKi) phosphorylation. 1HAEo- cells were then infected with RSV at an MOI of 1. At 48 hpi progeny RSV was collected and quantified. (*) indicates $P < 0.05$, (**) indicates $P < 0.01$ as determined by one way ANOVA with Bonferroni's post-test. Results represent three biological replicates from one independent experiment. Two independent experiments were completed and provided similar results, data from one of two experiments is shown. (E) 1HAEo- cells were infected with RSV at an MOI of 1. A western blot was used to detect phosphorylated RIP1 (P-RIP), phosphorylated MLKL (P-MLKL), and cleaved caspase-3 in loxoribine-treated RSV-infected 1HAEo- cells at 2 and 24 hpi. SOD1 was measured as a loading control.

5.3. Discussion

These results demonstrate that stimulation of 1HAEo- cells with the TLR7 agonist loxoribine enhances the replication of RSV in a concentration-dependent manner. In particular, the results of different experiments consistently observed an increase in RSV progeny production when cells were treated with loxoribine (**Figure 5.1; Figure 5.3; Figure 5.4; and Figure 5.5**). Increased entry by RSV was ruled out as a possible mechanism of enhancement as loxoribine treatment did not increase the number of 1HAEo- cells infected and treatment with loxoribine after RSV entry continued to enhance replication until 4 hpi. As loxoribine is a TLR7 agonist, I hypothesized that loxoribine enhanced RSV replication via stimulation of TLR7. TLR7 expression was confirmed in 1HAEo- cells and inhibition of TLR7 signalling through siRNA knockdown of TLR7, or through antagonism of TLR7 by IRS-661, prevented enhancement of RSV replication. These results support the conclusion that loxoribine enhances RSV replication in a TLR7-dependent manner.

Activation of the MAPK ERK has been observed following TLR7 stimulation and is known to be essential for RSV replication [298]. Therefore, the importance of ERK activation to TLR7-mediated enhancement of RSV replication was investigated. It was first confirmed that ERK is activated in 1HAEo- cells in response to TLR7 stimulation and RSV infection. To determine whether TLR7-mediated ERK phosphorylation benefited RSV replication, cells were treated with UO126. UO126 is a small molecule inhibitor of ERK activators MEK-1 and MEK-2. Treatment with UO126 prevented TLR7-mediated enhancement of RSV replication supporting the conclusion that this enhancement of RSV replication was mediated by ERK activation (**Figure 5.6**). These results, in

combination with the results of previous studies, suggest RSV coopts host MAPK activation to benefit viral replication.

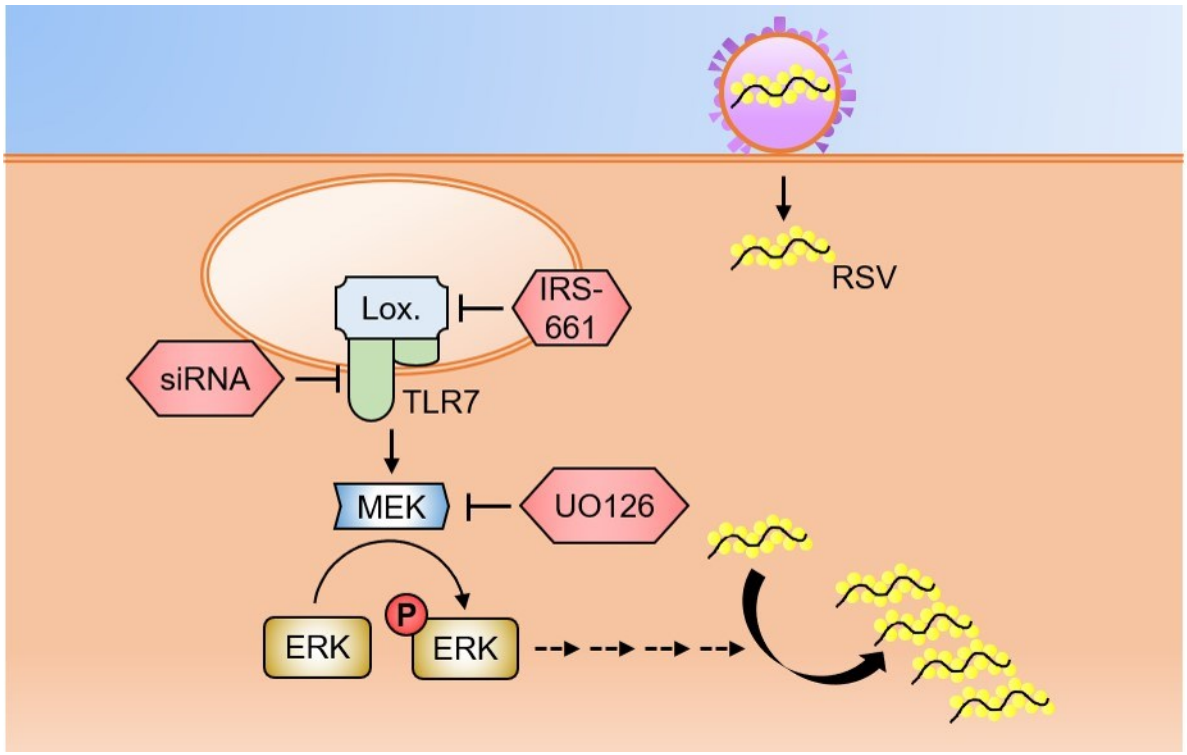

Figure 5.6. Model of TLR7-mediated enhancement of RSV replication. Following fusion with the host membrane the RSV genome is released into the cytosol. Stimulation of endosomal TLR7 with loxoribine (Lox.) results in phosphorylation of ERK by MEK. This cascade results in enhanced RSV replication. Inhibition of the TLR7-loxoribine interaction by IRS-661, siRNA knockdown of TLR7, or inhibition of ERK phosphorylation by MEK are sufficient to prevent this enhancement.

The most pressing question remaining from this body of work is the mechanism by which loxoribine-activated ERK benefits RSV replication. While the mechanism by which loxoribine-activated ERK benefits RSV replication has not been elucidated, exciting future directions remain to be studied. MAPK pathways such as the ERK pathway are highly interconnected and activation of MAPKs have pleiotropic effects on cellular processes [355]. Thus, it may be difficult to discern the mechanism by which phosphorylation of ERK benefits RSV replication. Perhaps the most promising answer to this question lies with Carbamoyl Phosphate Synthetase II (CPSII). CPSII catalyzes the rate limiting step of *de novo* pyrimidine nucleotide biosynthesis in the host cell [356]. CPSII is upregulated by ERK. This provides a rationale for the hypothesis that loxoribine-induced ERK activation may benefit RSV replication by increasing the pool of pyrimidine nucleotides

necessary for replication. Other examples of how ERK activation enhances viral replication have been described previously. HIV proteins Rev, Tat, Gag and Nef are directly phosphorylated by activated ERK resulting in HIV replication [357]. It is possible that activated ERK directly phosphorylates RSV proteins in a similar fashion that in turn benefits replication. Alternatively, the effect of ERK activation on RSV replication may be indirect. For example, ERK signalling can influence the cell death pathways apoptosis and necroptosis [350,352]. Previously, inhibition of apoptosis in neutrophils was observed to enhance RSV replication [287] and RSV deliberately inhibits apoptosis via RSV-NS-1 and RSV-NS-2 [91]. As loxoribine treatment enhanced RSV replication via ERK activation we tested the hypothesis that loxoribine treatment benefited RSV replication through inhibition of apoptosis or necroptosis-induced cell death. However, the results did not support this hypothesis and the mechanism by which ERK activation benefits RSV replication remains an open question. Complicating this question is that the understanding of response networks of cellular kinases to RSV infection is largely fragmented. Network based analyses, as pioneered by others [350], may be required for loxoribine-mediated enhancement of RSV replication to be fully understood.

Following RSV infection ERK phosphorylation is bimodal with peaks observed during entry at 10-30 minutes post infection and later during replication at 4-6 hpi [358,359]. Interestingly, in the time of addition assay loxoribine stimulation at these time points (0 and 4 hpi) significantly increased RSV progeny production, but treatment at 8 hpi did not affect RSV progeny production. While progeny production was increased at 2 hpi, this increase was not significant. These results suggest that combinatorial activation of ERK by loxoribine and RSV replication may have the greatest effect on RSV progeny production.

An essential distinction in this thesis is that the results suggest exogenous stimulation of TLR7 by agonists benefit RSV replication. These results do not speak to whether RSV benefits from TLR7 stimulation during natural infection. However, I hypothesize that this is the case. An important question to address is how the genome of RSV, located in the cytosol during infection, might gain access to endosomes where TLR7 is located. The pathway to TLR7 stimulation is apparent for viruses such as IAV and VSV that enter via endocytosis, as an error during entry positions the genome along the pathway to mature TLR7-containing endosomes. Indeed, IFN production during infection of pDC by VSV or IAV is dependent on endosomal acidification indicating these viruses

are detected by TLR7 [136]. Lund *et al* also observed that IFN production during Sendai virus infection was dependent on endosomal acidification, suggesting TLR7 is relevant to the detection of RNA viruses that enter the host cell via fusion. Hypothetically, the pathway by which cytosolic RSV RNA may access the endosome may be via autophagocytosis. This pathway captures cytosolic contents and delivers them to late endosomes (known also as multivesicular bodies) [360]. Characterization of the mechanism by which RSV RNA accesses TLR7 remains an important area for further research.

To gain further understanding of the influence of TLR7 stimulation on RSV replication it will be necessary to conduct experiments in animal models. It is reasonable to hypothesize that the antiviral affects of TLR7 stimulation will offset the enhancement of RSV replication in the context of a complete immune system. However, it is important to note that TLR7 may not be crucial in the antiviral response to RSV. The immune response to RSV in TLR7-deficient mice is altered but disease severity does not increase [288]. Evidence from studies of RSV infection in the presence of exogenous TLR7 stimulation *in vivo* also do not support the hypothesis that the beneficial effects of TLR7 will offset enhancement of replication. Johnson *et al* previously examined the potential of TLR7 agonists as adjuvants for RSV vaccination strategies. Stimulation of TLR9 successfully improved the outcome of vaccination with FI-RSV, however, stimulation with the TLR7/8 agonist R-848 failed to confer a benefit. Furthermore, treatment of primary RSV infection in mice with R-848 was detrimental and increased disease severity [289]. The authors hypothesized that this result was due to increased immunopathology following TLR7 stimulation. Based on my results, I would instead hypothesize that stimulation of TLR7 during RSV infection in mice would enhance disease severity through increased replication of RSV in the airway epithelium. It is important to note that increased immunopathology and increased viral replication are not mutually exclusive, as increased viral replication may result in increased immunopathology. Results from the Johnson *et al* study also provides preliminary support for this alternate hypothesis. Treatment with R-848 resulted in a trend towards increased viral lung titers at time points overlapping with peak weight loss [289]. This increase in viral load occurred despite increased IFN-γ production following TLR7 stimulation. Furthermore, their conclusion that immunopathology produced increased disease severity following TLR7 stimulation is undermined by a reduction in lung eosinophilia.

If TLR7 signalling enhances RSV replication *in vivo* there are important clinical implications. It would be essential to begin monitoring for RSV infections in ongoing clinical trials of TLR7 agonists. When RSV infections occur, supportive therapy may be required. While it would be possible to provide prophylactic palivizumab treatment to limit RSV infections in clinical trial participants, this would add considerable costs and may confound results. Cotreatment with TLR7 agonists and palivizumab would also not be practical on a large scale if TLR7 agonists become approved for the treatment of airway diseases. If RSV infection severity is increased in individuals receiving TLR7 agonist therapy it may offset the benefit of these therapies and preclude their use. Finally, during the study of TLR7 agonists special care should be paid to young who have not previously been infected with RSV. The failed FI-RSV vaccination campaign of the 1960s revealed the potentially tragic consequences of enhancing RSV replication in this population.

These results also beg the question, in the absence of exogenous TLR7 stimulation does RSV benefit from TLR7 signalling? Answering this question may offer interesting insight towards understanding how RSV has evolved to be best adapted to the human host. Future studies should be conducted to address this question.

It was already established that RSV is exquisitely evolved to counteract the host immune response. RSV impedes the production and response to IFN by targeting signalling pathways downstream of PRRs and the Type I IFN receptor [101]. Furthermore, if IFN is produced the effect on RSV replication is limited; exogenous addition of IFN has a limited affect on RSV replication in cell culture [146]. The mechanisms by which RSV interferes with the immune response contributes to the poor immunological protection gained following infection and the marked ability of RSV to re-infect adults throughout life [147]. The results of this research project build on this knowledge, finding that not only does RSV counteract the immune response, RSV replication may benefit from stimulation of the immune system. Stimulation of 1HAEo- cells with the TLR7 agonist loxoribine enhanced RSV replication in a TLR7-dependent and ERK activation-dependent manner. For the first time, this project described the enhancement of RSV replication in airway epithelial cells following exogenous stimulation of an innate immune PRR.

Chapter 6: Summary and Future Directions

6.1. Summary

RSV infection imposes a significant burden of disease on infants, the elderly, and immunocompromised individuals. Despite intensive efforts, no efficacious antivirals to treat RSV infection are available, nor are vaccines available to prevent infection. The discovery of compounds with antiviral activity against RSV is of paramount importance. In this thesis a total of ten nucleoside analogues, twenty-nine bis(indole) compounds, and one additional small molecule were tested for antiviral activity against RSV. Equally important is understanding factors which may increase the severity of disease associated with RSV infection. Novel discoveries in both areas are described in this thesis; this work describes the establishment of a novel strategy for RSV antiviral compound discovery, the discovery of antiviral bis(indole) compounds, and characterizes the discovery of loxoribine-mediated enhancement of RSV replication.

Chapter three describes the development of screening assays to identify RSV antivirals and screening of nucleoside analogues during this process. Ribavirin is a nucleoside analogue with well described antiviral activity against RSV in cell culture. Ribavirin was used to validate each iteration of screening protocols. Initially, the effect of ribavirin on RSV replication complex morphology was examined. As early as 6 hpi a reduction in the size of replication complexes was observed via spinning disc confocal microscopy. While this offered a rapid means of detecting antiviral activity the process of identifying replication complexes was time intensive and not conducive to high throughput screening. Subsequent screening protocols used colourimetric or fluorescent immunostaining to detect RSV infection in 1HAEo- cell monolayers. Automated detection of colourimetric staining was made possible through incorporation of the EliSpot plate reader, and the protocol was optimized to best utilize this instrument. Automated detection of fluorescent signals by the Operetta HCIS offered a more reliable means of quantification as this method was not hindered by technical limitations of colourimetric staining. The final progression in this protocol was quantifying the production of progeny RSV instead of quantifying infected cells in the initially infected cell monolayer. This yielded an unbiased means of identifying compounds that inhibited any component of the RSV replication cycle. The pursuit of a novel screening protocol and investigation of nucleoside analogues culminated with the identification of antiviral activity of cytarabine against RSV. Cytarabine is a chemotherapeutic cytosine analogue

which had a therapeutic index of 21.6 against RSV. A limitation of chapter three is that all work was completed in the 1HAEo- immortalized cell line. Measuring the antiviral activity of cytarabine in additional cell lines, in primary cells, and subsequently in animal models will be necessary to determine the clinical potential of this compound.

In chapter four bis(indole) compounds were investigated for antiviral activity against RSV using the Operetta HCIS-based high throughput screen (referred to as the IF-screen) developed in chapter three. The Isatisine-A inspired bis(indole) compounds were of great interest as they obey the Lipinski criteria for drug development. Furthermore, collaboration with a group who has expertise in the synthesis of bis(indole) compounds enabled guided synthesis of novel compounds. During screening of the second collection of bis(indole) compounds Cl02 was identified as having antiviral activity against RSV. To reduce cytotoxicity a series of Cl02 inspired compounds was synthesized and investigated in 1HAEo- cells via MTT cell viability assay. Structural modifications which reduced cytotoxicity were identified. The Cl02-inspired compounds also reduced RSV progeny production. Br02 OMe was found to have the most favourable antiviral activity to cytotoxicity ratio, with a therapeutic index of 12.3. A limitation of these results is that experimentation was limited to 1HAEo- cell lines and only one strain of RSV was included. Testing Br02 OMe against additional strains of RSV, including clinical isolates, will increase the confidence of bis(indole) compounds as RSV-antivirals.

Br02 OMe offers an exciting hit for continued synthesis campaigns towards identifying a novel class of RSV antivirals. An *in vitro* viral transcription assay was used to elucidate the mechanism of action of bis(indole) compounds. Cl02 reduced viral transcription in a concentration-dependent manner, supporting the conclusion that Cl02 inhibits the RSV RdRp. During serial passaging of RSV in the presence of bis(indole) compounds a low level of RSV replication was observed after 10 passages. This suggests the emergence of weakly resistant RSV strains. The emergence of resistant strains suggests a viral protein component of RSV RdRp, such as RSV-L, -P, -M2-1, or -N, is targeted by bis(indole) compounds.

During screening of nucleoside analogues treatment with loxoribine was observed to increase the production of RSV progeny. Loxoribine is a TLR7 agonist, therefore, this observation was unexpected. Given this unexpected observation, and interest by research groups in utilizing TLR7 agonists as immunomodulatory therapeutics of allergic airway diseases, enhancement of RSV

replication by loxoribine was further characterized. Increased RSV progeny production in loxoribine-treated 1HAEo- cells was confirmed to be concentration-dependent and this enhancement was reproduced with the distinct TLR7 agonist Cl097. A trend towards increased RSV progeny production was also observed in primary human airway epithelial cells treated with loxoribine. Antagonism of TLR7 by IRS-661 and by TLR7 knockdown prevented enhancement of RSV replication by loxoribine, supporting the conclusion that enhancement of RSV replication by loxoribine was mediated by stimulation of TLR7. Treatment with loxoribine did not enhance entry by RSV, instead this treatment enhanced replication after entry. Treatment with loxoribine as late as 4 hpi continued to significantly increase the production of RSV progeny. Treatment of 1HAEo- cells with loxoribine was observed to increase phosphorylation of ERK, which is known to benefit RSV replication. Inhibition of ERK signalling prevented loxoribine-mediated enhancement of RSV replication supporting the conclusion that this enhancement was mediated by increased ERK activation. This research suggests that caution should be employed during the investigation of TLR7 agonists for the treatment of airway diseases. Further study in appropriate *in vivo* models will be needed to determine the physiological significance of this enhancement of RSV replication.

6.2. Future Directions

Going forward it will be necessary to assay the antiviral activity of bis(indole) compounds *in vivo* in small animal models. A variety of animal models exist, with benefits and drawbacks to each. The most important consideration would be testing for antiviral activity against the appropriate virus, which would include lab-adapted and clinical human RSV strains. This consideration rules out using cognate models of RSV infection such as bovine RSV infection in cattle or PVM infection of mice [337]. Mice have been used extensively in the study of RSV, and an interesting range of susceptibility exists between different inbred strains. Stark *et al* found AKR/J to be the most permissive mouse strain tested, followed by 129P3/J, BALB/cJ, CBA/J, C3H/HeJ, DBA/J, and A/J. Finally, C57/BL6J was the least permissive to RSV infection [361]. It is important to note that in this study all mouse strains were inoculated with 10^7 plaque forming units (PFU), a relatively high amount of virus. This inoculum reflects how resistant mice are to RSV infection in general. Cotton rats are a popular small animal model of RSV infection. Infection in the upper and lower respiratory tracts can be established with an intranasal inoculation with 10^4 PFU and resultant peak viral titers are approximately 100-fold higher than in mice [217]. Therefore, cotton rats

are much more susceptible to RSV infection. A limitation of the cotton rat model is that symptoms during infection are limited [337]. This limitation is not as critical in antiviral studies as viral titers can simply be measured in lung homogenates. However, this would limit the applicability of the cotton rat model for studying enhancement of RSV infection severity. Cotton rats have been used in preclinical studies of RSV antiviral compounds including JNJ-678 [362], TMC353121 [363], MDT-637, BMS-433771, and BTA-C585 [217]. Cotton rats would provide a good small animal model for examining the antiviral effects of bis(indole) compounds against RSV *in vivo*, before moving on to larger animals or adult human volunteer challenge studies.

While cumbersome for handling due to their size, the neonatal lamb offers a robust model for RSV infection. The airways of lambs are similar to humans in size, structure, and branching patterns [364]. More importantly, neonatal lambs are much more susceptible to RSV infection than rodent models, and symptoms of infection mirror those observed in human infants. The neonatal lamb model was used to characterize JNJ-678 [362], a fusion inhibitor currently in clinical trials. Finally, human challenge experiments in healthy adult volunteers have been used extensively to test RSV antiviral candidates prior to clinical trials. The fusion inhibitor GS-5806 [206,207] and nucleoside analogue lumicitabine have been tested in this manner [212].

Gaining a better understanding of the signaling cascade downstream of TLR7 that benefits RSV replication is an important area for future research. Specifically, the signaling cascade from TLR7 to the AP-1 transcription factor via MAPKs may be important yet is poorly defined. This is in contrast to the signaling cascades leading to the IRF-7 and NF-κB transcription factors, which are well defined [240,247]. While it has been suggested that AP-1 is activated through TAK-1, experimental evidence supporting this assertion is lacking and further research in this area is required. The results of this thesis suggest the MAPK ERK is of primary importance to the enhancement of RSV replication. These results may help guide future research.

Examining TLR7-mediated enhancement of RSV replication *in vivo* will be an interesting pursuit and may answer an array of questions. In the context of a functional immune response the benefits of TLR7 stimulation are expected to be more pronounced, however, will this benefit offset the expected increase in RSV replication in the airway epithelium? Alternatively, will immune stimulation in the context of enhanced RSV replication result in exacerbated immunopathology and increased disease severity? Previously, stimulation of TLR7 in the context RSV infection in

mice was observed to result in increased weight loss [289]. This observation suggests that stimulation of TLR7 during RSV infection will not simply bolster the immune response and benefit the host. It is important to note that the purpose of the study by Johnson *et al* was not to evaluate TLR7-mediated enhancement of RSV replication [289]. Therefore, answering the aforementioned questions will require a new line of experimentation. It will be essential to monitor disease severity through a variety of parameters including weight loss, viral load in the lungs, airway hyperresponse, and airway inflammation. Selecting the appropriate animal model will be important to studying the effect of TLR7 stimulation on disease severity. Cotton rats would be more appropriate than mice, as RSV replication is highly attenuated in mice [337]. However, symptom severity is limited in cotton rats. Instead, the neonatal lamb model would be an ideal choice for studying TLR7-mediated enhancement of RSV infection. The neonatal lamb is highly susceptible to RSV infection, shares similar airway structure to humans, and infection presents with similar symptoms [337,364].

Works Cited

1 Adams, M. J., Lefkowitz, E. J., King, A. M. Q., Harrach, B., Harrison, R. L., Knowles, N. J., Kropinski, A. M., Krupovic, M., Kuhn, J. H., Mushegian, A. R., Nibert, M., Sabanadzovic, S., Sanfacon, H., Siddell, S. G., Simmonds, P., Varsani, A., Zerbini, F. M., Gorbalenya, A. E. & Davison, A. J. Changes to taxonomy and the International Code of Virus Classification and Nomenclature ratified by the International Committee on Taxonomy of Viruses (2017). *Arch Virol* **162**, 2505-2538 (2017).

2 Blount, R. E., Jr., Morris, J. A. & Savage, R. E. Recovery of cytopathogenic agent from chimpanzees with coryza. *Proc Soc Exp Biol Med* **92**, 544-549 (1956).

3 Chanock, R., Roizman, B. & Myers, R. Recovery from infants with respiratory illness of a virus related to chimpanzee coryza agent (CCA). I. Isolation, properties and characterization. *Am J Hyg* **66**, 281-290 (1957).

4 Andrew, J. D. & Gardner, P. S. Occurrence of Respiratory Syncytial Virus in Acute Respiratory Diseases in Infancy. *Br Med J* **2**, 1447-1448 (1963).

5 Morales, F., Calder, M. A., Inglis, J. M., Murdoch, P. S. & Williamson, J. A study of respiratory infections in the elderly to assess the role of respiratory syncytial virus. *J Infect* **7**, 236-247 (1983).

6 Kim, H. W., Canchola, J. G., Brandt, C. D., Pyles, G., Chanock, R. M., Jensen, K. & Parrott, R. H. Respiratory syncytial virus disease in infants despite prior administration of antigenic inactivated vaccine. *Am J Epidemiol* **89**, 422-434 (1969).

7 American Academy of Pediatrics Committee on Infectious Diseases: Use of ribavirin in the treatment of respiratory syncytial virus infection. *Pediatrics* **92**, 501-504 (1993).

8 Smith, D. W., Frankel, L. R., Mathers, L. H., Tang, A. T., Ariagno, R. L. & Prober, C. G. A controlled trial of aerosolized ribavirin in infants receiving mechanical ventilation for severe respiratory syncytial virus infection. *N Engl J Med* **325**, 24-29 (1991).

9 Ribavirin for severe RSV infection. *N Engl J Med* **325**, 1884-1886 (1991).

10 Meert, K. L., Sarnaik, A. P., Gelmini, M. J. & Lieh-Lai, M. W. Aerosolized ribavirin in mechanically ventilated children with respiratory syncytial virus lower respiratory tract disease: a prospective, double-blind, randomized trial. *Crit Care Med* **22**, 566-572 (1994).

11 Law, B. J., Wang, E. E., MacDonald, N., McDonald, J., Dobson, S., Boucher, F., Langley, J., Robinson, J., Mitchell, I. & Stephens, D. Does ribavirin impact on the hospital course of children with respiratory syncytial virus (RSV) infection? An analysis using the pediatric investigators collaborative network on infections in Canada (PICNIC) RSV database. *Pediatrics* **99**, E7 (1997).

12 Palivizumab, a humanized respiratory syncytial virus monoclonal antibody, reduces hospitalization from respiratory syncytial virus infection in high-risk infants. The IMpact-RSV Study Group. *Pediatrics* **102**, 531-537 (1998).

13 Robinson, J. L., Le Saux, N., Canadian Paediatric Society, I. D. & Immunization, C. Preventing hospitalizations for respiratory syncytial virus infection. *Paediatr Child Health* **20**, 321-333 (2015).

14 Leader, S. & Kohlhase, K. Respiratory syncytial virus-coded pediatric hospitalizations, 1997 to 1999. *Pediatr Infect Dis J* **21**, 629-632 (2002).

15 Mitchell, I., Defoy, I. & Grubb, E. Burden of Respiratory Syncytial Virus Hospitalizations in Canada. *Can Respir J* **2017**, 4521302 (2017).

16 Paes, B. A., Mitchell, I., Banerji, A., Lanctot, K. L. & Langley, J. M. A decade of respiratory syncytial virus epidemiology and prophylaxis: translating evidence into everyday clinical practice. *Can Respir J* **18**, e10-19 (2011).

17 Nair, H., Nokes, D. J., Gessner, B. D., Dherani, M., Madhi, S. A., Singleton, R. J., O'Brien, K. L., Roca, A., Wright, P. F., Bruce, N., Chandran, A., Theodoratou, E., Sutanto, A., Sedyaningsih, E. R., Ngama, M., Munywoki, P. K., Kartasasmita, C., Simoes, E. A., Rudan, I., Weber, M. W. & Campbell, H. Global burden of acute lower respiratory infections due to respiratory syncytial virus in young children: a systematic review and meta-analysis. *Lancet* **375**, 1545-1555 (2010).

18 Shi, T., McAllister, D. A., O'Brien, K. L., Simoes, E. A. F., Madhi, S. A., Gessner, B. D., Polack, F. P., Balsells, E., Acacio, S., Aguayo, C., Alassani, I., Ali, A., Antonio, M., Awasthi, S., Awori, J. O., Azziz-Baumgartner, E., Baggett, H. C., Baillie, V. L., Balmaseda, A., Barahona, A., Basnet, S., Bassat, Q., Basualdo, W., Bigogo, G., Bont, L., Breiman, R. F., Brooks, W. A., Broor, S., Bruce, N., Bruden, D., Buchy, P., Campbell, S., Carosone-Link, P., Chadha, M., Chipeta, J., Chou, M., Clara, W., Cohen, C., de Cuellar, E., Dang, D. A., Dash-Yandag, B., Deloria-Knoll, M., Dherani, M., Eap, T., Ebruke, B. E., Echavarria, M., de Freitas Lazaro Emediato, C. C., Fasce, R. A., Feikin, D. R., Feng, L., Gentile, A., Gordon, A., Goswami, D., Goyet, S., Groome, M., Halasa, N., Hirve, S., Homaira, N., Howie, S. R. C., Jara, J., Jroundi, I., Kartasasmita, C. B., Khuri-Bulos, N., Kotloff, K. L., Krishnan, A., Libster, R., Lopez, O., Lucero, M. G., Lucion, F., Lupisan, S. P., Marcone, D. N., McCracken, J. P., Mejia, M., Moisi, J. C., Montgomery, J. M., Moore, D. P., Moraleda, C., Moyes, J., Munywoki, P., Mutyara, K., Nicol, M. P., Nokes, D. J., Nymadawa, P., da Costa Oliveira, M. T., Oshitani, H., Pandey, N., Paranhos-Baccala, G., Phillips, L. N., Picot, V. S., Rahman, M., Rakoto-Andrianarivelo, M., Rasmussen, Z. A., Rath, B. A., Robinson, A., Romero, C., Russomando, G., Salimi, V., Sawatwong, P., Scheltema, N., Schweiger, B., Scott, J. A. G., Seidenberg, P., Shen, K., Singleton, R., Sotomayor, V., Strand, T. A., Sutanto, A., Sylla, M., Tapia, M. D., Thamthitiwat, S., Thomas, E. D., Tokarz, R., Turner, C., Venter, M., Waicharoen, S., Wang, J., Watthanaworawit, W., Yoshida, L. M., Yu, H., Zar, H. J., Campbell, H., Nair, H. & Network, R. S. V. G. E. Global, regional, and national disease burden estimates of acute lower respiratory infections due to respiratory syncytial virus in young children in 2015: a systematic review and modelling study. *Lancet* **390**, 946-958 (2017).

19 Hall, C. B., Weinberg, G. A., Iwane, M. K., Blumkin, A. K., Edwards, K. M., Staat, M. A., Auinger, P., Griffin, M. R., Poehling, K. A., Erdman, D., Grijalva, C. G., Zhu, Y. & Szilagyi, P. The burden of respiratory syncytial virus infection in young children. *N Engl J Med* **360**, 588-598 (2009).

20 Van de Steen, O., Miri, F., Gunjaca, M., Klepac, V., Gross, B., Notario, G. & Wegzyn, C. M. The Burden of Severe Respiratory Syncytial Virus Disease Among Children Younger than 1 Year in Central and Eastern Europe. *Infect Dis Ther* **5**, 125-137 (2016).

21 Paes, B., Steele, S., Janes, M. & Pinelli, J. Risk-Scoring Tool for respiratory syncytial virus prophylaxis in premature infants born at 33-35 completed weeks' gestational age in Canada. *Curr Med Res Opin* **25**, 1585-1591 (2009).

22 Figueras-Aloy, J., Manzoni, P., Paes, B., Simoes, E. A., Bont, L., Checchia, P. A., Fauroux, B. & Carbonell-Estrany, X. Defining the Risk and Associated Morbidity and Mortality of Severe Respiratory Syncytial Virus Infection Among Preterm Infants

Without Chronic Lung Disease or Congenital Heart Disease. *Infect Dis Ther* **5**, 417-452 (2016).
23 Paes, B., Fauroux, B., Figueras-Aloy, J., Bont, L., Checchia, P. A., Simoes, E. A., Manzoni, P. & Carbonell-Estrany, X. Defining the Risk and Associated Morbidity and Mortality of Severe Respiratory Syncytial Virus Infection Among Infants with Chronic Lung Disease. *Infect Dis Ther* **5**, 453-471 (2016).
24 Heikkinen, T., Valkonen, H., Lehtonen, L., Vainionpaa, R. & Ruuskanen, O. Hospital admission of high risk infants for respiratory syncytial virus infection: implications for palivizumab prophylaxis. *Arch Dis Child Fetal Neonatal Ed* **90**, F64-68 (2005).
25 Widmer, K., Zhu, Y., Williams, J. V., Griffin, M. R., Edwards, K. M. & Talbot, H. K. Rates of hospitalizations for respiratory syncytial virus, human metapneumovirus, and influenza virus in older adults. *J Infect Dis* **206**, 56-62 (2012).
26 Falsey, A. R., Hennessey, P. A., Formica, M. A., Cox, C. & Walsh, E. E. Respiratory syncytial virus infection in elderly and high-risk adults. *N Engl J Med* **352**, 1749-1759 (2005).
27 Lee, N., Lui, G. C., Wong, K. T., Li, T. C., Tse, E. C., Chan, J. Y., Yu, J., Wong, S. S., Choi, K. W., Wong, R. Y., Ngai, K. L., Hui, D. S. & Chan, P. K. High morbidity and mortality in adults hospitalized for respiratory syncytial virus infections. *Clin Infect Dis* **57**, 1069-1077 (2013).
28 Falsey, A. R., Cunningham, C. K., Barker, W. H., Kouides, R. W., Yuen, J. B., Menegus, M., Weiner, L. B., Bonville, C. A. & Betts, R. F. Respiratory syncytial virus and influenza A infections in the hospitalized elderly. *J Infect Dis* **172**, 389-394 (1995).
29 Lessler, J., Reich, N. G., Brookmeyer, R., Perl, T. M., Nelson, K. E. & Cummings, D. A. Incubation periods of acute respiratory viral infections: a systematic review. *Lancet Infect Dis* **9**, 291-300 (2009).
30 DeVincenzo, J. P., Wilkinson, T., Vaishnaw, A., Cehelsky, J., Meyers, R., Nochur, S., Harrison, L., Meeking, P., Mann, A., Moane, E., Oxford, J., Pareek, R., Moore, R., Walsh, E., Studholme, R., Dorsett, P., Alvarez, R. & Lambkin-Williams, R. Viral load drives disease in humans experimentally infected with respiratory syncytial virus. *Am J Respir Crit Care Med* **182**, 1305-1314 (2010).
31 Lambrecht, B. N. & Hammad, H. The immunology of asthma. *Nat Immunol* **16**, 45-56 (2015).
32 Stein, R. T., Sherrill, D., Morgan, W. J., Holberg, C. J., Halonen, M., Taussig, L. M., Wright, A. L. & Martinez, F. D. Respiratory syncytial virus in early life and risk of wheeze and allergy by age 13 years. *Lancet* **354**, 541-545 (1999).
33 Sigurs, N., Aljassim, F., Kjellman, B., Robinson, P. D., Sigurbergsson, F., Bjarnason, R. & Gustafsson, P. M. Asthma and allergy patterns over 18 years after severe RSV bronchiolitis in the first year of life. *Thorax* **65**, 1045-1052 (2010).
34 Wu, P., Dupont, W. D., Griffin, M. R., Carroll, K. N., Mitchel, E. F., Gebretsadik, T. & Hartert, T. V. Evidence of a causal role of winter virus infection during infancy in early childhood asthma. *Am J Respir Crit Care Med* **178**, 1123-1129 (2008).
35 Jackson, D. J., Gangnon, R. E., Evans, M. D., Roberg, K. A., Anderson, E. L., Pappas, T. E., Printz, M. C., Lee, W. M., Shult, P. A., Reisdorf, E., Carlson-Dakes, K. T., Salazar, L. P., DaSilva, D. F., Tisler, C. J., Gern, J. E. & Lemanske, R. F., Jr. Wheezing rhinovirus illnesses in early life predict asthma development in high-risk children. *Am J Respir Crit Care Med* **178**, 667-672 (2008).

36 Henderson, J., Hilliard, T. N., Sherriff, A., Stalker, D., Al Shammari, N. & Thomas, H. M. Hospitalization for RSV bronchiolitis before 12 months of age and subsequent asthma, atopy and wheeze: a longitudinal birth cohort study. *Pediatr Allergy Immunol* **16**, 386-392 (2005).
37 Kuehni, C. E., Spycher, B. D. & Silverman, M. Causal links between RSV infection and asthma: no clear answers to an old question. *Am J Respir Crit Care Med* **179**, 1079-1080 (2009).
38 Stein, R. T. & Martinez, F. D. Respiratory syncytial virus and asthma: still no final answer. *Thorax* **65**, 1033-1034 (2010).
39 Simoes, E. A., Groothuis, J. R., Carbonell-Estrany, X., Rieger, C. H., Mitchell, I., Fredrick, L. M., Kimpen, J. L. & Palivizumab Long-Term Respiratory Outcomes Study, G. Palivizumab prophylaxis, respiratory syncytial virus, and subsequent recurrent wheezing. *J Pediatr* **151**, 34-42, 42 e31 (2007).
40 Griffiths, C., Drews, S. J. & Marchant, D. J. Respiratory Syncytial Virus: Infection, Detection, and New Options for Prevention and Treatment. *Clin Microbiol Rev* **30**, 277-319 (2017).
41 Sloan, C., Heaton, M., Kang, S., Berrett, C., Wu, P., Gebretsadik, T., Sicignano, N., Evans, A., Lee, R. & Hartert, T. The impact of temperature and relative humidity on spatiotemporal patterns of infant bronchiolitis epidemics in the contiguous United States. *Health Place* **45**, 46-54 (2017).
42 Welliver, R. C., Sr. Temperature, humidity, and ultraviolet B radiation predict community respiratory syncytial virus activity. *Pediatr Infect Dis J* **26**, S29-35 (2007).
43 Janet, S., Broad, J. & Snape, M. D. Respiratory syncytial virus seasonality and its implications on prevention strategies. *Hum Vaccin Immunother* **14**, 234-244 (2018).
44 Collins, P. L. & Graham, B. S. Viral and host factors in human respiratory syncytial virus pathogenesis. *J Virol* **82**, 2040-2055 (2008).
45 Morawska, L. Droplet fate in indoor environments, or can we prevent the spread of infection? *Indoor Air* **16**, 335-347 (2006).
46 Firquet, S., Beaujard, S., Lobert, P. E., Sane, F., Caloone, D., Izard, D. & Hober, D. Survival of Enveloped and Non-Enveloped Viruses on Inanimate Surfaces. *Microbes Environ* **30**, 140-144 (2015).
47 Hall, C. B., Douglas, R. G., Jr. & Geiman, J. M. Possible transmission by fomites of respiratory syncytial virus. *J Infect Dis* **141**, 98-102 (1980).
48 Hall, C. B., Douglas, R. G., Jr., Schnabel, K. C. & Geiman, J. M. Infectivity of respiratory syncytial virus by various routes of inoculation. *Infect Immun* **33**, 779-783 (1981).
49 Kulkarni, H., Smith, C. M., Lee Ddo, H., Hirst, R. A., Easton, A. J. & O'Callaghan, C. Evidence of Respiratory Syncytial Virus Spread by Aerosol. Time to Revisit Infection Control Strategies? *Am J Respir Crit Care Med* **194**, 308-316 (2016).
50 Roy, C. J. & Milton, D. K. Airborne transmission of communicable infection--the elusive pathway. *N Engl J Med* **350**, 1710-1712 (2004).
51 Collins, P. L. & Melero, J. A. Progress in understanding and controlling respiratory syncytial virus: still crazy after all these years. *Virus Res* **162**, 80-99 (2011).
52 Tawar, R. G., Duquerroy, S., Vonrhein, C., Varela, P. F., Damier-Piolle, L., Castagne, N., MacLellan, K., Bedouelle, H., Bricogne, G., Bhella, D., Eleouet, J. F. & Rey, F. A.

Crystal structure of a nucleocapsid-like nucleoprotein-RNA complex of respiratory syncytial virus. *Science* **326**, 1279-1283 (2009).
53 Lifland, A. W., Jung, J., Alonas, E., Zurla, C., Crowe, J. E., Jr. & Santangelo, P. J. Human respiratory syncytial virus nucleoprotein and inclusion bodies antagonize the innate immune response mediated by MDA5 and MAVS. *J Virol* **86**, 8245-8258 (2012).
54 Mogensen, T. H. Pathogen recognition and inflammatory signaling in innate immune defenses. *Clin Microbiol Rev* **22**, 240-273, Table of Contents (2009).
55 Yoneyama, M., Kikuchi, M., Natsukawa, T., Shinobu, N., Imaizumi, T., Miyagishi, M., Taira, K., Akira, S. & Fujita, T. The RNA helicase RIG-I has an essential function in double-stranded RNA-induced innate antiviral responses. *Nat Immunol* **5**, 730-737 (2004).
56 Yoneyama, M., Kikuchi, M., Matsumoto, K., Imaizumi, T., Miyagishi, M., Taira, K., Foy, E., Loo, Y. M., Gale, M., Jr., Akira, S., Yonehara, S., Kato, A. & Fujita, T. Shared and unique functions of the DExD/H-box helicases RIG-I, MDA5, and LGP2 in antiviral innate immunity. *J Immunol* **175**, 2851-2858 (2005).
57 Hornung, V., Ellegast, J., Kim, S., Brzozka, K., Jung, A., Kato, H., Poeck, H., Akira, S., Conzelmann, K. K., Schlee, M., Endres, S. & Hartmann, G. 5'-Triphosphate RNA is the ligand for RIG-I. *Science* **314**, 994-997 (2006).
58 Clemens, M. J., Hershey, J. W., Hovanessian, A. C., Jacobs, B. C., Katze, M. G., Kaufman, R. J., Lengyel, P., Samuel, C. E., Sen, G. C. & Williams, B. R. PKR: proposed nomenclature for the RNA-dependent protein kinase induced by interferon. *J Interferon Res* **13**, 241 (1993).
59 Garcia, M. A., Gil, J., Ventoso, I., Guerra, S., Domingo, E., Rivas, C. & Esteban, M. Impact of protein kinase PKR in cell biology: from antiviral to antiproliferative action. *Microbiol Mol Biol Rev* **70**, 1032-1060 (2006).
60 Clemens, M. J. & Elia, A. The double-stranded RNA-dependent protein kinase PKR: structure and function. *J Interferon Cytokine Res* **17**, 503-524 (1997).
61 Groskreutz, D. J., Babor, E. C., Monick, M. M., Varga, S. M. & Hunninghake, G. W. Respiratory syncytial virus limits alpha subunit of eukaryotic translation initiation factor 2 (eIF2alpha) phosphorylation to maintain translation and viral replication. *J Biol Chem* **285**, 24023-24031 (2010).
62 Noton, S. L., Deflube, L. R., Tremaglio, C. Z. & Fearns, R. The respiratory syncytial virus polymerase has multiple RNA synthesis activities at the promoter. *PLoS Pathog* **8**, e1002980 (2012).
63 Fearns, R. & Collins, P. L. Role of the M2-1 transcription antitermination protein of respiratory syncytial virus in sequential transcription. *J Virol* **73**, 5852-5864 (1999).
64 Grosfeld, H., Hill, M. G. & Collins, P. L. RNA replication by respiratory syncytial virus (RSV) is directed by the N, P, and L proteins; transcription also occurs under these conditions but requires RSV superinfection for efficient synthesis of full-length mRNA. *J Virol* **69**, 5677-5686 (1995).
65 Collins, P. L., Hill, M. G., Cristina, J. & Grosfeld, H. Transcription elongation factor of respiratory syncytial virus, a nonsegmented negative-strand RNA virus. *Proc Natl Acad Sci U S A* **93**, 81-85 (1996).
66 Collins, P. L., Hill, M. G., Camargo, E., Grosfeld, H., Chanock, R. M. & Murphy, B. R. Production of infectious human respiratory syncytial virus from cloned cDNA confirms an essential role for the transcription elongation factor from the 5' proximal open reading

frame of the M2 mRNA in gene expression and provides a capability for vaccine development. *Proc Natl Acad Sci U S A* **92**, 11563-11567 (1995).
67 Poch, O., Sauvaget, I., Delarue, M. & Tordo, N. Identification of four conserved motifs among the RNA-dependent polymerase encoding elements. *EMBO J* **8**, 3867-3874 (1989).
68 Cowton, V. M., McGivern, D. R. & Fearns, R. Unravelling the complexities of respiratory syncytial virus RNA synthesis. *J Gen Virol* **87**, 1805-1821 (2006).
69 Barik, S. The structure of the 5' terminal cap of the respiratory syncytial virus mRNA. *J Gen Virol* **74 (Pt 3)**, 485-490 (1993).
70 Kingston, R. L., Hamel, D. J., Gay, L. S., Dahlquist, F. W. & Matthews, B. W. Structural basis for the attachment of a paramyxoviral polymerase to its template. *Proc Natl Acad Sci U S A* **101**, 8301-8306 (2004).
71 Dupuy, L. C., Dobson, S., Bitko, V. & Barik, S. Casein kinase 2-mediated phosphorylation of respiratory syncytial virus phosphoprotein P is essential for the transcription elongation activity of the viral polymerase; phosphorylation by casein kinase 1 occurs mainly at Ser(215) and is without effect. *J Virol* **73**, 8384-8392 (1999).
72 Asenjo, A., Calvo, E. & Villanueva, N. Phosphorylation of human respiratory syncytial virus P protein at threonine 108 controls its interaction with the M2-1 protein in the viral RNA polymerase complex. *J Gen Virol* **87**, 3637-3642 (2006).
73 Tremaglio, C. Z., Noton, S. L., Deflube, L. R. & Fearns, R. Respiratory syncytial virus polymerase can initiate transcription from position 3 of the leader promoter. *J Virol* **87**, 3196-3207 (2013).
74 Kuo, L., Grosfeld, H., Cristina, J., Hill, M. G. & Collins, P. L. Effects of mutations in the gene-start and gene-end sequence motifs on transcription of monocistronic and dicistronic minigenomes of respiratory syncytial virus. *J Virol* **70**, 6892-6901 (1996).
75 Kuo, L., Fearns, R. & Collins, P. L. Analysis of the gene start and gene end signals of human respiratory syncytial virus: quasi-templated initiation at position 1 of the encoded mRNA. *J Virol* **71**, 4944-4953 (1997).
76 Deval, J., Hong, J., Wang, G., Taylor, J., Smith, L. K., Fung, A., Stevens, S. K., Liu, H., Jin, Z., Dyatkina, N., Prhavc, M., Stoycheva, A. D., Serebryany, V., Liu, J., Smith, D. B., Tam, Y., Zhang, Q., Moore, M. L., Fearns, R., Chanda, S. M., Blatt, L. M., Symons, J. A. & Beigelman, L. Molecular Basis for the Selective Inhibition of Respiratory Syncytial Virus RNA Polymerase by 2'-Fluoro-4'-Chloromethyl-Cytidine Triphosphate. *PLoS Pathog* **11**, e1004995 (2015).
77 Sudo, K., Miyazaki, Y., Kojima, N., Kobayashi, M., Suzuki, H., Shintani, M. & Shimizu, Y. YM-53403, a unique anti-respiratory syncytial virus agent with a novel mechanism of action. *Antiviral Res* **65**, 125-131 (2005).
78 Challa, S., Scott, A. D., Yuzhakov, O., Zhou, Y., Tiong-Yip, C. L., Gao, N., Thresher, J. & Yu, Q. Mechanism of action for respiratory syncytial virus inhibitor RSV604. *Antimicrob Agents Chemother* **59**, 1080-1087 (2015).
79 Munday, D. C., Wu, W., Smith, N., Fix, J., Noton, S. L., Galloux, M., Touzelet, O., Armstrong, S. D., Dawson, J. M., Aljabr, W., Easton, A. J., Rameix-Welti, M. A., de Oliveira, A. P., Simabuco, F. M., Ventura, A. M., Hughes, D. J., Barr, J. N., Fearns, R., Digard, P., Eleouet, J. F. & Hiscox, J. A. Interactome analysis of the human respiratory syncytial virus RNA polymerase complex identifies protein chaperones as important cofactors that promote L-protein stability and RNA synthesis. *J Virol* **89**, 917-930 (2015).

80 Drake, J. W. Rates of spontaneous mutation among RNA viruses. *Proc Natl Acad Sci U S A* **90**, 4171-4175 (1993).
81 Steinhauer, D. A., Domingo, E. & Holland, J. J. Lack of evidence for proofreading mechanisms associated with an RNA virus polymerase. *Gene* **122**, 281-288 (1992).
82 Lauring, A. S. & Andino, R. Quasispecies theory and the behavior of RNA viruses. *PLoS Pathog* **6**, e1001005 (2010).
83 McLellan, J. S., Chen, M., Leung, S., Graepel, K. W., Du, X., Yang, Y., Zhou, T., Baxa, U., Yasuda, E., Beaumont, T., Kumar, A., Modjarrad, K., Zheng, Z., Zhao, M., Xia, N., Kwong, P. D. & Graham, B. S. Structure of RSV fusion glycoprotein trimer bound to a prefusion-specific neutralizing antibody. *Science* **340**, 1113-1117 (2013).
84 Tayyari, F., Marchant, D., Moraes, T. J., Duan, W., Mastrangelo, P. & Hegele, R. G. Identification of nucleolin as a cellular receptor for human respiratory syncytial virus. *Nat Med* **17**, 1132-1135 (2011).
85 Karron, R. A., Buonagurio, D. A., Georgiu, A. F., Whitehead, S. S., Adamus, J. E., Clements-Mann, M. L., Harris, D. O., Randolph, V. B., Udem, S. A., Murphy, B. R. & Sidhu, M. S. Respiratory syncytial virus (RSV) SH and G proteins are not essential for viral replication in vitro: clinical evaluation and molecular characterization of a cold-passaged, attenuated RSV subgroup B mutant. *Proc Natl Acad Sci U S A* **94**, 13961-13966 (1997).
86 Johnson, S. M., McNally, B. A., Ioannidis, I., Flano, E., Teng, M. N., Oomens, A. G., Walsh, E. E. & Peeples, M. E. Respiratory Syncytial Virus Uses CX3CR1 as a Receptor on Primary Human Airway Epithelial Cultures. *PLoS Pathog* **11**, e1005318 (2015).
87 Bukreyev, A., Whitehead, S. S., Murphy, B. R. & Collins, P. L. Recombinant respiratory syncytial virus from which the entire SH gene has been deleted grows efficiently in cell culture and exhibits site-specific attenuation in the respiratory tract of the mouse. *J Virol* **71**, 8973-8982 (1997).
88 Whitehead, S. S., Bukreyev, A., Teng, M. N., Firestone, C. Y., St Claire, M., Elkins, W. R., Collins, P. L. & Murphy, B. R. Recombinant respiratory syncytial virus bearing a deletion of either the NS2 or SH gene is attenuated in chimpanzees. *J Virol* **73**, 3438-3442 (1999).
89 Karron, R. A., Wright, P. F., Belshe, R. B., Thumar, B., Casey, R., Newman, F., Polack, F. P., Randolph, V. B., Deatly, A., Hackell, J., Gruber, W., Murphy, B. R. & Collins, P. L. Identification of a recombinant live attenuated respiratory syncytial virus vaccine candidate that is highly attenuated in infants. *J Infect Dis* **191**, 1093-1104 (2005).
90 Barik, S. Respiratory syncytial virus mechanisms to interfere with type 1 interferons. *Curr Top Microbiol Immunol* **372**, 173-191 (2013).
91 Bitko, V., Shulyayeva, O., Mazumder, B., Musiyenko, A., Ramaswamy, M., Look, D. C. & Barik, S. Nonstructural proteins of respiratory syncytial virus suppress premature apoptosis by an NF-kappaB-dependent, interferon-independent mechanism and facilitate virus growth. *J Virol* **81**, 1786-1795 (2007).
92 Wu, W., Tran, K. C., Teng, M. N., Heesom, K. J., Matthews, D. A., Barr, J. N. & Hiscox, J. A. The interactome of the human respiratory syncytial virus NS1 protein highlights multiple effects on host cell biology. *J Virol* **86**, 7777-7789 (2012).
93 Randall, R. E. & Goodbourn, S. Interferons and viruses: an interplay between induction, signalling, antiviral responses and virus countermeasures. *J Gen Virol* **89**, 1-47 (2008).

94 Ling, Z., Tran, K. C. & Teng, M. N. Human respiratory syncytial virus nonstructural protein NS2 antagonizes the activation of beta interferon transcription by interacting with RIG-I. *J Virol* **83**, 3734-3742 (2009).
95 Swedan, S., Musiyenko, A. & Barik, S. Respiratory syncytial virus nonstructural proteins decrease levels of multiple members of the cellular interferon pathways. *J Virol* **83**, 9682-9693 (2009).
96 Ren, J., Liu, T., Pang, L., Li, K., Garofalo, R. P., Casola, A. & Bao, X. A novel mechanism for the inhibition of interferon regulatory factor-3-dependent gene expression by human respiratory syncytial virus NS1 protein. *J Gen Virol* **92**, 2153-2159 (2011).
97 Goswami, R., Majumdar, T., Dhar, J., Chattopadhyay, S., Bandyopadhyay, S. K., Verbovetskaya, V., Sen, G. C. & Barik, S. Viral degradasome hijacks mitochondria to suppress innate immunity. *Cell Res* **23**, 1025-1042 (2013).
98 Dhar, J., Cuevas, R. A., Goswami, R., Zhu, J., Sarkar, S. N. & Barik, S. 2'-5'-Oligoadenylate Synthetase-Like Protein Inhibits Respiratory Syncytial Virus Replication and Is Targeted by the Viral Nonstructural Protein 1. *J Virol* **89**, 10115-10119 (2015).
99 Ning, S., Pagano, J. S. & Barber, G. N. IRF7: activation, regulation, modification and function. *Genes Immun* **12**, 399-414 (2011).
100 Honda, K., Yanai, H., Negishi, H., Asagiri, M., Sato, M., Mizutani, T., Shimada, N., Ohba, Y., Takaoka, A., Yoshida, N. & Taniguchi, T. IRF-7 is the master regulator of type-I interferon-dependent immune responses. *Nature* **434**, 772-777 (2005).
101 Taniguchi, T. & Takaoka, A. The interferon-alpha/beta system in antiviral responses: a multimodal machinery of gene regulation by the IRF family of transcription factors. *Curr Opin Immunol* **14**, 111-116 (2002).
102 Ivashkiv, L. B. & Donlin, L. T. Regulation of type I interferon responses. *Nat Rev Immunol* **14**, 36-49 (2014).
103 Fensterl, V. & Sen, G. C. Interferons and viral infections. *Biofactors* **35**, 14-20 (2009).
104 Lo, M. S., Brazas, R. M. & Holtzman, M. J. Respiratory syncytial virus nonstructural proteins NS1 and NS2 mediate inhibition of Stat2 expression and alpha/beta interferon responsiveness. *J Virol* **79**, 9315-9319 (2005).
105 Munir, S., Le Nouen, C., Luongo, C., Buchholz, U. J., Collins, P. L. & Bukreyev, A. Nonstructural proteins 1 and 2 of respiratory syncytial virus suppress maturation of human dendritic cells. *J Virol* **82**, 8780-8796 (2008).
106 de Graaff, P. M., de Jong, E. C., van Capel, T. M., van Dijk, M. E., Roholl, P. J., Boes, J., Luytjes, W., Kimpen, J. L. & van Bleek, G. M. Respiratory syncytial virus infection of monocyte-derived dendritic cells decreases their capacity to activate CD4 T cells. *J Immunol* **175**, 5904-5911 (2005).
107 Munir, S., Hillyer, P., Le Nouen, C., Buchholz, U. J., Rabin, R. L., Collins, P. L. & Bukreyev, A. Respiratory syncytial virus interferon antagonist NS1 protein suppresses and skews the human T lymphocyte response. *PLoS Pathog* **7**, e1001336 (2011).
108 Kotelkin, A., Belyakov, I. M., Yang, L., Berzofsky, J. A., Collins, P. L. & Bukreyev, A. The NS2 protein of human respiratory syncytial virus suppresses the cytotoxic T-cell response as a consequence of suppressing the type I interferon response. *J Virol* **80**, 5958-5967 (2006).
109 Kiss, G., Holl, J. M., Williams, G. M., Alonas, E., Vanover, D., Lifland, A. W., Gudheti, M., Guerrero-Ferreira, R. C., Nair, V., Yi, H., Graham, B. S., Santangelo, P. J. & Wright, E. R. Structural analysis of respiratory syncytial virus reveals the position of M2-1

between the matrix protein and the ribonucleoprotein complex. *J Virol* **88**, 7602-7617 (2014).
110 Meng, J., Stobart, C. C., Hotard, A. L. & Moore, M. L. An overview of respiratory syncytial virus. *PLoS Pathog* **10**, e1004016 (2014).
111 Anderson, L. J., Hierholzer, J. C., Tsou, C., Hendry, R. M., Fernie, B. F., Stone, Y. & McIntosh, K. Antigenic characterization of respiratory syncytial virus strains with monoclonal antibodies. *J Infect Dis* **151**, 626-633 (1985).
112 Johnson, P. R., Spriggs, M. K., Olmsted, R. A. & Collins, P. L. The G glycoprotein of human respiratory syncytial viruses of subgroups A and B: extensive sequence divergence between antigenically related proteins. *Proc Natl Acad Sci U S A* **84**, 5625-5629 (1987).
113 Vandini, S., Biagi, C. & Lanari, M. Respiratory Syncytial Virus: The Influence of Serotype and Genotype Variability on Clinical Course of Infection. *Int J Mol Sci* **18** (2017).
114 Trento, A., Casas, I., Calderon, A., Garcia-Garcia, M. L., Calvo, C., Perez-Brena, P. & Melero, J. A. Ten years of global evolution of the human respiratory syncytial virus BA genotype with a 60-nucleotide duplication in the G protein gene. *J Virol* **84**, 7500-7512 (2010).
115 Zlateva, K. T., Lemey, P., Vandamme, A. M. & Van Ranst, M. Molecular evolution and circulation patterns of human respiratory syncytial virus subgroup a: positively selected sites in the attachment g glycoprotein. *J Virol* **78**, 4675-4683 (2004).
116 Grad, Y. H., Newman, R., Zody, M., Yang, X., Murphy, R., Qu, J., Malboeuf, C. M., Levin, J. Z., Lipsitch, M. & DeVincenzo, J. Within-host whole-genome deep sequencing and diversity analysis of human respiratory syncytial virus infection reveals dynamics of genomic diversity in the absence and presence of immune pressure. *J Virol* **88**, 7286-7293 (2014).
117 Martinello, R. A., Chen, M. D., Weibel, C. & Kahn, J. S. Correlation between respiratory syncytial virus genotype and severity of illness. *J Infect Dis* **186**, 839-842 (2002).
118 Laham, F. R., Mansbach, J. M., Piedra, P. A., Hasegawa, K., Sullivan, A. F., Espinola, J. A. & Camargo, C. A., Jr. Clinical Profiles of Respiratory Syncytial Virus Subtypes A AND B Among Children Hospitalized with Bronchiolitis. *Pediatr Infect Dis J* **36**, 808-810 (2017).
119 Walsh, E. E., McConnochie, K. M., Long, C. E. & Hall, C. B. Severity of respiratory syncytial virus infection is related to virus strain. *J Infect Dis* **175**, 814-820 (1997).
120 Fodha, I., Vabret, A., Ghedira, L., Seboui, H., Chouchane, S., Dewar, J., Gueddiche, N., Trabelsi, A., Boujaafar, N. & Freymuth, F. Respiratory syncytial virus infections in hospitalized infants: association between viral load, virus subgroup, and disease severity. *J Med Virol* **79**, 1951-1958 (2007).
121 Devincenzo, J. P. Natural infection of infants with respiratory syncytial virus subgroups A and B: a study of frequency, disease severity, and viral load. *Pediatr Res* **56**, 914-917 (2004).
122 Elawar, F., Griffiths, C. D., Zhu, D., Bilawchuk, L. M., Jensen, L. D., Forss, L., Tang, J., Hazes, B., Drews, S. J. & Marchant, D. J. A Virological and Phylogenetic Analysis of the Emergence of New Clades of Respiratory Syncytial Virus. *Sci Rep* **7**, 12232 (2017).

123 Buckingham, S. C., Bush, A. J. & Devincenzo, J. P. Nasal quantity of respiratory syncytical virus correlates with disease severity in hospitalized infants. *Pediatr Infect Dis J* **19**, 113-117 (2000).
124 Kurt-Jones, E. A., Popova, L., Kwinn, L., Haynes, L. M., Jones, L. P., Tripp, R. A., Walsh, E. E., Freeman, M. W., Golenbock, D. T., Anderson, L. J. & Finberg, R. W. Pattern recognition receptors TLR4 and CD14 mediate response to respiratory syncytial virus. *Nat Immunol* **1**, 398-401 (2000).
125 Shirey, K. A., Pletneva, L. M., Puche, A. C., Keegan, A. D., Prince, G. A., Blanco, J. C. & Vogel, S. N. Control of RSV-induced lung injury by alternatively activated macrophages is IL-4R alpha-, TLR4-, and IFN-beta-dependent. *Mucosal Immunol* **3**, 291-300 (2010).
126 Marr, N., Turvey, S. E. & Grandvaux, N. Pathogen recognition receptor crosstalk in respiratory syncytial virus sensing: a host and cell type perspective. *Trends Microbiol* **21**, 568-574 (2013).
127 McNamara, P. S., Ritson, P., Selby, A., Hart, C. A. & Smyth, R. L. Bronchoalveolar lavage cellularity in infants with severe respiratory syncytial virus bronchiolitis. *Arch Dis Child* **88**, 922-926 (2003).
128 Everard, M. L., Swarbrick, A., Wrightham, M., McIntyre, J., Dunkley, C., James, P. D., Sewell, H. F. & Milner, A. D. Analysis of cells obtained by bronchial lavage of infants with respiratory syncytial virus infection. *Arch Dis Child* **71**, 428-432 (1994).
129 Johnson, J. E., Gonzales, R. A., Olson, S. J., Wright, P. F. & Graham, B. S. The histopathology of fatal untreated human respiratory syncytial virus infection. *Mod Pathol* **20**, 108-119 (2007).
130 Brand, H. K., Ferwerda, G., Preijers, F., de Groot, R., Neeleman, C., Staal, F. J., Warris, A. & Hermans, P. W. CD4+ T-cell counts and interleukin-8 and CCL-5 plasma concentrations discriminate disease severity in children with RSV infection. *Pediatr Res* **73**, 187-193 (2013).
131 Lukens, M. V., van de Pol, A. C., Coenjaerts, F. E., Jansen, N. J., Kamp, V. M., Kimpen, J. L., Rossen, J. W., Ulfman, L. H., Tacke, C. E., Viveen, M. C., Koenderman, L., Wolfs, T. F. & van Bleek, G. M. A systemic neutrophil response precedes robust CD8(+) T-cell activation during natural respiratory syncytial virus infection in infants. *J Virol* **84**, 2374-2383 (2010).
132 Russell, C. D., Unger, S. A., Walton, M. & Schwarze, J. The Human Immune Response to Respiratory Syncytial Virus Infection. *Clin Microbiol Rev* **30**, 481-502 (2017).
133 Cortjens, B., de Boer, O. J., de Jong, R., Antonis, A. F., Sabogal Pineros, Y. S., Lutter, R., van Woensel, J. B. & Bem, R. A. Neutrophil extracellular traps cause airway obstruction during respiratory syncytial virus disease. *J Pathol* **238**, 401-411 (2016).
134 Siegal, F. P., Kadowaki, N., Shodell, M., Fitzgerald-Bocarsly, P. A., Shah, K., Ho, S., Antonenko, S. & Liu, Y. J. The nature of the principal type 1 interferon-producing cells in human blood. *Science* **284**, 1835-1837 (1999).
135 Smit, J. J., Rudd, B. D. & Lukacs, N. W. Plasmacytoid dendritic cells inhibit pulmonary immunopathology and promote clearance of respiratory syncytial virus. *J Exp Med* **203**, 1153-1159 (2006).
136 Lund, J. M., Alexopoulou, L., Sato, A., Karow, M., Adams, N. C., Gale, N. W., Iwasaki, A. & Flavell, R. A. Recognition of single-stranded RNA viruses by Toll-like receptor 7. *Proc Natl Acad Sci U S A* **101**, 5598-5603 (2004).

137 Vermaelen, K. & Pauwels, R. Pulmonary dendritic cells. *Am J Respir Crit Care Med* **172**, 530-551 (2005).
138 Schlender, J., Hornung, V., Finke, S., Gunthner-Biller, M., Marozin, S., Brzozka, K., Moghim, S., Endres, S., Hartmann, G. & Conzelmann, K. K. Inhibition of toll-like receptor 7- and 9-mediated alpha/beta interferon production in human plasmacytoid dendritic cells by respiratory syncytial virus and measles virus. *J Virol* **79**, 5507-5515 (2005).
139 Delgado, M. F., Coviello, S., Monsalvo, A. C., Melendi, G. A., Hernandez, J. Z., Batalle, J. P., Diaz, L., Trento, A., Chang, H. Y., Mitzner, W., Ravetch, J., Melero, J. A., Irusta, P. M. & Polack, F. P. Lack of antibody affinity maturation due to poor Toll-like receptor stimulation leads to enhanced respiratory syncytial virus disease. *Nat Med* **15**, 34-41 (2009).
140 Mosmann, T. R. & Coffman, R. L. TH1 and TH2 cells: different patterns of lymphokine secretion lead to different functional properties. *Annu Rev Immunol* **7**, 145-173 (1989).
141 Legg, J. P., Hussain, I. R., Warner, J. A., Johnston, S. L. & Warner, J. O. Type 1 and type 2 cytokine imbalance in acute respiratory syncytial virus bronchiolitis. *Am J Respir Crit Care Med* **168**, 633-639 (2003).
142 Aberle, J. H., Aberle, S. W., Dworzak, M. N., Mandl, C. W., Rebhandl, W., Vollnhofer, G., Kundi, M. & Popow-Kraupp, T. Reduced interferon-gamma expression in peripheral blood mononuclear cells of infants with severe respiratory syncytial virus disease. *Am J Respir Crit Care Med* **160**, 1263-1268 (1999).
143 Mangodt, T. C., Van Herck, M. A., Nullens, S., Ramet, J., De Dooy, J. J., Jorens, P. G. & De Winter, B. Y. The role of Th17 and Treg responses in the pathogenesis of RSV infection. *Pediatr Res* **78**, 483-491 (2015).
144 Mukherjee, S., Lindell, D. M., Berlin, A. A., Morris, S. B., Shanley, T. P., Hershenson, M. B. & Lukacs, N. W. IL-17-induced pulmonary pathogenesis during respiratory viral infection and exacerbation of allergic disease. *Am J Pathol* **179**, 248-258 (2011).
145 Reed, G., Jewett, P. H., Thompson, J., Tollefson, S. & Wright, P. F. Epidemiology and clinical impact of parainfluenza virus infections in otherwise healthy infants and young children < 5 years old. *J Infect Dis* **175**, 807-813 (1997).
146 Atreya, P. L. & Kulkarni, S. Respiratory syncytial virus strain A2 is resistant to the antiviral effects of type I interferons and human MxA. *Virology* **261**, 227-241 (1999).
147 Hall, C. B., Walsh, E. E., Long, C. E. & Schnabel, K. C. Immunity to and frequency of reinfection with respiratory syncytial virus. *J Infect Dis* **163**, 693-698 (1991).
148 Baicus, A. History of polio vaccination. *World J Virol* **1**, 108-114 (2012).
149 Jancar, S. & Sanchez Crespo, M. Immune complex-mediated tissue injury: a multistep paradigm. *Trends Immunol* **26**, 48-55 (2005).
150 Polack, F. P., Teng, M. N., Collins, P. L., Prince, G. A., Exner, M., Regele, H., Lirman, D. D., Rabold, R., Hoffman, S. J., Karp, C. L., Kleeberger, S. R., Wills-Karp, M. & Karron, R. A. A role for immune complexes in enhanced respiratory syncytial virus disease. *J Exp Med* **196**, 859-865 (2002).
151 Smith, G., Raghunandan, R., Wu, Y., Liu, Y., Massare, M., Nathan, M., Zhou, B., Lu, H., Boddapati, S., Li, J., Flyer, D. & Glenn, G. Respiratory syncytial virus fusion glycoprotein expressed in insect cells form protein nanoparticles that induce protective immunity in cotton rats. *PLoS One* **7**, e50852 (2012).

152 Karron, R. A., Buchholz, U. J. & Collins, P. L. Live-attenuated respiratory syncytial virus vaccines. *Curr Top Microbiol Immunol* **372**, 259-284 (2013).
153 Wright, P. F., Karron, R. A., Belshe, R. B., Thompson, J., Crowe, J. E., Jr., Boyce, T. G., Halburnt, L. L., Reed, G. W., Whitehead, S. S., Anderson, E. L., Wittek, A. E., Casey, R., Eichelberger, M., Thumar, B., Randolph, V. B., Udem, S. A., Chanock, R. M. & Murphy, B. R. Evaluation of a live, cold-passaged, temperature-sensitive, respiratory syncytial virus vaccine candidate in infancy. *J Infect Dis* **182**, 1331-1342 (2000).
154 Malkin, E., Yogev, R., Abughali, N., Sliman, J., Wang, C. K., Zuo, F., Yang, C. F., Eickhoff, M., Esser, M. T., Tang, R. S. & Dubovsky, F. Safety and immunogenicity of a live attenuated RSV vaccine in healthy RSV-seronegative children 5 to 24 months of age. *PLoS One* **8**, e77104 (2013).
155 Johnson, S., Oliver, C., Prince, G. A., Hemming, V. G., Pfarr, D. S., Wang, S. C., Dormitzer, M., O'Grady, J., Koenig, S., Tamura, J. K., Woods, R., Bansal, G., Couchenour, D., Tsao, E., Hall, W. C. & Young, J. F. Development of a humanized monoclonal antibody (MEDI-493) with potent in vitro and in vivo activity against respiratory syncytial virus. *J Infect Dis* **176**, 1215-1224 (1997).
156 Feltes, T. F., Cabalka, A. K., Meissner, H. C., Piazza, F. M., Carlin, D. A., Top, F. H., Jr., Connor, E. M., Sondheimer, H. M. & Cardiac Synagis Study, G. Palivizumab prophylaxis reduces hospitalization due to respiratory syncytial virus in young children with hemodynamically significant congenital heart disease. *J Pediatr* **143**, 532-540 (2003).
157 Geskey, J. M., Thomas, N. J. & Brummel, G. L. Palivizumab: a review of its use in the protection of high risk infants against respiratory syncytial virus (RSV). *Biologics* **1**, 33-43 (2007).
158 Hampp, C., Kauf, T. L., Saidi, A. S. & Winterstein, A. G. Cost-effectiveness of respiratory syncytial virus prophylaxis in various indications. *Arch Pediatr Adolesc Med* **165**, 498-505 (2011).
159 Banerji, A., Lanctot, K. L., Paes, B. A., Masoud, S. T., Tam, D. Y., Macdonald, W. A. & Roberts, A. Comparison of the cost of hospitalization for respiratory syncytial virus disease versus palivizumab prophylaxis in Canadian Inuit infants. *Pediatr Infect Dis J* **28**, 702-706 (2009).
160 Malley, R., DeVincenzo, J., Ramilo, O., Dennehy, P. H., Meissner, H. C., Gruber, W. C., Sanchez, P. J., Jafri, H., Balsley, J., Carlin, D., Buckingham, S., Vernacchio, L. & Ambrosino, D. M. Reduction of respiratory syncytial virus (RSV) in tracheal aspirates in intubated infants by use of humanized monoclonal antibody to RSV F protein. *J Infect Dis* **178**, 1555-1561 (1998).
161 Helmink, B. J., Ragsdale, C. E., Peterson, E. J. & Merkel, K. G. Comparison of Intravenous Palivizumab and Standard of Care for Treatment of Respiratory Syncytial Virus Infection in Mechanically Ventilated Pediatric Patients. *J Pediatr Pharmacol Ther* **21**, 146-154 (2016).
162 Wu, H., Pfarr, D. S., Johnson, S., Brewah, Y. A., Woods, R. M., Patel, N. K., White, W. I., Young, J. F. & Kiener, P. A. Development of motavizumab, an ultra-potent antibody for the prevention of respiratory syncytial virus infection in the upper and lower respiratory tract. *J Mol Biol* **368**, 652-665 (2007).
163 Crowe, J. E., Firestone, C. Y., Crim, R., Beeler, J. A., Coelingh, K. L., Barbas, C. F., Burton, D. R., Chanock, R. M. & Murphy, B. R. Monoclonal antibody-resistant mutants

selected with a respiratory syncytial virus-neutralizing human antibody fab fragment (Fab 19) define a unique epitope on the fusion (F) glycoprotein. *Virology* **252**, 373-375 (1998).
164 Zhao, X., Chen, F. P. & Sullender, W. M. Respiratory syncytial virus escape mutant derived in vitro resists palivizumab prophylaxis in cotton rats. *Virology* **318**, 608-612 (2004).
165 Zhu, Q., Patel, N. K., McAuliffe, J. M., Zhu, W., Wachter, L., McCarthy, M. P. & Suzich, J. A. Natural polymorphisms and resistance-associated mutations in the fusion protein of respiratory syncytial virus (RSV): effects on RSV susceptibility to palivizumab. *J Infect Dis* **205**, 635-638 (2012).
166 Boivin, G., Caouette, G., Frenette, L., Carbonneau, J., Ouakki, M. & De Serres, G. Human respiratory syncytial virus and other viral infections in infants receiving palivizumab. *J Clin Virol* **42**, 52-57 (2008).
167 Zhu, Q., McAuliffe, J. M., Patel, N. K., Palmer-Hill, F. J., Yang, C. F., Liang, B., Su, L., Zhu, W., Wachter, L., Wilson, S., MacGill, R. S., Krishnan, S., McCarthy, M. P., Losonsky, G. A. & Suzich, J. A. Analysis of respiratory syncytial virus preclinical and clinical variants resistant to neutralization by monoclonal antibodies palivizumab and/or motavizumab. *J Infect Dis* **203**, 674-682 (2011).
168 Witkowski, J. T., Robins, R. K., Sidwell, R. W. & Simon, L. N. Design, synthesis, and broad spectrum antiviral activity of 1- -D-ribofuranosyl-1,2,4-triazole-3-carboxamide and related nucleosides. *J Med Chem* **15**, 1150-1154 (1972).
169 Kim, Y. I., Pareek, R., Murphy, R., Harrison, L., Farrell, E., Cook, R. & DeVincenzo, J. The antiviral effects of RSV fusion inhibitor, MDT-637, on clinical isolates, vs its achievable concentrations in the human respiratory tract and comparison to ribavirin. *Influenza Other Respir Viruses* **11**, 525-530 (2017).
170 Chapman, J., Abbott, E., Alber, D. G., Baxter, R. C., Bithell, S. K., Henderson, E. A., Carter, M. C., Chambers, P., Chubb, A., Cockerill, G. S., Collins, P. L., Dowdell, V. C., Keegan, S. J., Kelsey, R. D., Lockyer, M. J., Luongo, C., Najarro, P., Pickles, R. J., Simmonds, M., Taylor, D., Tyms, S., Wilson, L. J. & Powell, K. L. RSV604, a novel inhibitor of respiratory syncytial virus replication. *Antimicrob Agents Chemother* **51**, 3346-3353 (2007).
171 Hong, Z. & Cameron, C. E. Pleiotropic mechanisms of ribavirin antiviral activities. *Prog Drug Res* **59**, 41-69 (2002).
172 Sidwell, R. W., Huffman, J. H., Khare, G. P., Allen, L. B., Witkowski, J. T. & Robins, R. K. Broad-spectrum antiviral activity of Virazole: 1-beta-D-ribofuranosyl-1,2,4-triazole-3-carboxamide. *Science* **177**, 705-706 (1972).
173 Scholtissek, C. Inhibition of influenza RNA synthesis by virazole (ribavirin). *Arch Virol* **50**, 349-352 (1976).
174 Huffman, J. H., Sidwell, R. W., Khare, G. P., Witkowski, J. T., Allen, L. B. & Robins, R. K. In vitro effect of 1-beta-D-ribofuranosyl-1,2,4-triazole-3-carboxamide (virazole, ICN 1229) on deoxyribonucleic acid and ribonucleic acid viruses. *Antimicrob Agents Chemother* **3**, 235-241 (1973).
175 Hruska, J. F., Bernstein, J. M., Douglas, R. G., Jr. & Hall, C. B. Effects of ribavirin on respiratory syncytial virus in vitro. *Antimicrob Agents Chemother* **17**, 770-775 (1980).
176 Feld, J. J. & Hoofnagle, J. H. Mechanism of action of interferon and ribavirin in treatment of hepatitis C. *Nature* **436**, 967-972 (2005).
177 Houghton, M. Hepatitis C: the next 25years. *Antiviral Res* **110**, 77-78 (2014).

178 Leyssen, P., Balzarini, J., De Clercq, E. & Neyts, J. The predominant mechanism by which ribavirin exerts its antiviral activity in vitro against flaviviruses and paramyxoviruses is mediated by inhibition of IMP dehydrogenase. *J Virol* **79**, 1943-1947 (2005).
179 Parker, W. B. Metabolism and antiviral activity of ribavirin. *Virus Res* **107**, 165-171 (2005).
180 Robins, R. K., Revankar, G. R., McKernan, P. A., Murray, B. K., Kirsi, J. J. & North, J. A. The importance of IMP dehydrogenase inhibition in the broad spectrum antiviral activity of ribavirin and selenazofurin. *Adv Enzyme Regul* **24**, 29-43 (1985).
181 Vignuzzi, M., Stone, J. K. & Andino, R. Ribavirin and lethal mutagenesis of poliovirus: molecular mechanisms, resistance and biological implications. *Virus Res* **107**, 173-181 (2005).
182 Crotty, S., Maag, D., Arnold, J. J., Zhong, W., Lau, J. Y., Hong, Z., Andino, R. & Cameron, C. E. The broad-spectrum antiviral ribonucleoside ribavirin is an RNA virus mutagen. *Nat Med* **6**, 1375-1379 (2000).
183 Pfeiffer, J. K. & Kirkegaard, K. A single mutation in poliovirus RNA-dependent RNA polymerase confers resistance to mutagenic nucleotide analogs via increased fidelity. *Proc Natl Acad Sci U S A* **100**, 7289-7294 (2003).
184 Aljabr, W., Touzelet, O., Pollakis, G., Wu, W., Munday, D. C., Hughes, M., Hertz-Fowler, C., Kenny, J., Fearns, R., Barr, J. N., Matthews, D. A. & Hiscox, J. A. Investigating the Influence of Ribavirin on Human Respiratory Syncytial Virus RNA Synthesis by Using a High-Resolution Transcriptome Sequencing Approach. *J Virol* **90**, 4876-4888 (2016).
185 Tiong-Yip, C. L., Plant, H., Sharpe, P., Fan, J., Rich, K., Gorseth, E. & Yu, Q. Development of a high-throughput replicon assay for the identification of respiratory syncytial virus inhibitors. *Antiviral Res* **101**, 75-81 (2014).
186 Noah, J. W., Severson, W. E., Chung, D. H., Moore, B., Jia, F., Xu, X., Maddox, C., Rasmussen, L., Sosa, M. I., Tower, N. A., Ananthan, S., Evans, C. W., White, E. L., Jonsson, C., Matharu, D. S., Flaherty, D. P., Simpson, D. S., Golden, J. E. & Aube, J. in *Probe Reports from the NIH Molecular Libraries Program* (2010).
187 Malykhina, O., Yednak, M. A., Collins, P. L., Olivo, P. D. & Peeples, M. E. A respiratory syncytial virus replicon that is noncytotoxic and capable of long-term foreign gene expression. *J Virol* **85**, 4792-4801 (2011).
188 Gobel, J., Gartland, M., Gurley, S. H., Kadwell, S., Gillie, D., Moore, C. & Goetz, A. A Phenotypic High-Throughput Screen with RSV-Infected Primary Human Small Airway Epithelial Cells (SAECs). *J Biomol Screen* **20**, 729-738 (2015).
189 Andries, K., Moeremans, M., Gevers, T., Willebrords, R., Sommen, C., Lacrampe, J., Janssens, F. & Wyde, P. R. Substituted benzimidazoles with nanomolar activity against respiratory syncytial virus. *Antiviral Res* **60**, 209-219 (2003).
190 Gorcea, C. M., Tholouli, E., Turner, A., Saif, M., Davies, E., Battersby, E. & Dignan, F. L. Effective use of oral ribavirin for respiratory syncytial viral infections in allogeneic haematopoietic stem cell transplant recipients. *J Hosp Infect* **95**, 214-217 (2017).
191 Ghosh, S., Champlin, R. E., Englund, J., Giralt, S. A., Rolston, K., Raad, I., Jacobson, K., Neumann, J., Ippoliti, C., Mallik, S. & Whimbey, E. Respiratory syncytial virus upper respiratory tract illnesses in adult blood and marrow transplant recipients: combination

therapy with aerosolized ribavirin and intravenous immunoglobulin. *Bone Marrow Transplant* **25**, 751-755 (2000).

192 Shah, D. P., Ghantoji, S. S., Shah, J. N., El Taoum, K. K., Jiang, Y., Popat, U., Hosing, C., Rondon, G., Tarrand, J. J., Champlin, R. E. & Chemaly, R. F. Impact of aerosolized ribavirin on mortality in 280 allogeneic haematopoietic stem cell transplant recipients with respiratory syncytial virus infections. *J Antimicrob Chemother* **68**, 1872-1880 (2013).

193 Laganas, V. A., Dunn, E. F., McLaughlin, R. E., Tiong-Yip, C. L., Yuzhakov, O., Isabella, V. M., Hill, P. & Yu, Q. Characterization of novel respiratory syncytial virus inhibitors identified by high throughput screen. *Antiviral Res* **115**, 71-74 (2015).

194 Plant, H., Stacey, C., Tiong-Yip, C. L., Walsh, J., Yu, Q. & Rich, K. High-Throughput Hit Screening Cascade to Identify Respiratory Syncytial Virus (RSV) Inhibitors. *J Biomol Screen* **20**, 597-605 (2015).

195 Noton, S. L., Nagendra, K., Dunn, E. F., Mawhorter, M. E., Yu, Q. & Fearns, R. Respiratory Syncytial Virus Inhibitor AZ-27 Differentially Inhibits Different Polymerase Activities at the Promoter. *J Virol* **89**, 7786-7798 (2015).

196 Coates, M., Brookes, D., Kim, Y. I., Allen, H., Fordyce, E. A. F., Meals, E. A., Colley, T., Ciana, C. L., Parra, G. F., Sherbukhin, V., Stockwell, J. A., Thomas, J. C., Hunt, S. F., Anderson-Dring, L., Onions, S. T., Cass, L., Murray, P. J., Ito, K., Strong, P., DeVincenzo, J. P. & Rapeport, G. Preclinical Characterization of PC786, an Inhaled Small-Molecule Respiratory Syncytial Virus L Protein Polymerase Inhibitor. *Antimicrob Agents Chemother* **61** (2017).

197 Duvall, J. R., VerPlank, L., Ludeke, B., McLeod, S. M., Lee, M. D. t., Vishwanathan, K., Mulrooney, C. A., Le Quement, S., Yu, Q., Palmer, M. A., Fleming, P., Fearns, R., Foley, M. A. & Scherer, C. A. Novel diversity-oriented synthesis-derived respiratory syncytial virus inhibitors identified via a high throughput replicon-based screen. *Antiviral Res* **131**, 19-25 (2016).

198 Bonavia, A., Franti, M., Pusateri Keaney, E., Kuhen, K., Seepersaud, M., Radetich, B., Shao, J., Honda, A., Dewhurst, J., Balabanis, K., Monroe, J., Wolff, K., Osborne, C., Lanieri, L., Hoffmaster, K., Amin, J., Markovits, J., Broome, M., Skuba, E., Cornella-Taracido, I., Joberty, G., Bouwmeester, T., Hamann, L., Tallarico, J. A., Tommasi, R., Compton, T. & Bushell, S. M. Identification of broad-spectrum antiviral compounds and assessment of the druggability of their target for efficacy against respiratory syncytial virus (RSV). *Proc Natl Acad Sci U S A* **108**, 6739-6744 (2011).

199 Mason, S. W., Lawetz, C., Gaudette, Y., Do, F., Scouten, E., Lagace, L., Simoneau, B. & Liuzzi, M. Polyadenylation-dependent screening assay for respiratory syncytial virus RNA transcriptase activity and identification of an inhibitor. *Nucleic Acids Res* **32**, 4758-4767 (2004).

200 Liuzzi, M., Mason, S. W., Cartier, M., Lawetz, C., McCollum, R. S., Dansereau, N., Bolger, G., Lapeyre, N., Gaudette, Y., Lagace, L., Massariol, M. J., Do, F., Whitehead, P., Lamarre, L., Scouten, E., Bordeleau, J., Landry, S., Rancourt, J., Fazal, G. & Simoneau, B. Inhibitors of respiratory syncytial virus replication target cotranscriptional mRNA guanylylation by viral RNA-dependent RNA polymerase. *J Virol* **79**, 13105-13115 (2005).

201 Carrat, F., Vergu, E., Ferguson, N. M., Lemaitre, M., Cauchemez, S., Leach, S. & Valleron, A. J. Time lines of infection and disease in human influenza: a review of volunteer challenge studies. *Am J Epidemiol* **167**, 775-785 (2008).
202 Jefferson, T., Jones, M. A., Doshi, P., Del Mar, C. B., Hama, R., Thompson, M. J., Spencer, E. A., Onakpoya, I., Mahtani, K. R., Nunan, D., Howick, J. & Heneghan, C. J. Neuraminidase inhibitors for preventing and treating influenza in healthy adults and children. *Cochrane Database Syst Rev*, CD008965 (2014).
203 El Saleeby, C. M., Bush, A. J., Harrison, L. M., Aitken, J. A. & Devincenzo, J. P. Respiratory syncytial virus load, viral dynamics, and disease severity in previously healthy naturally infected children. *J Infect Dis* **204**, 996-1002 (2011).
204 Broadbent, L., Groves, H., Shields, M. D. & Power, U. F. Respiratory syncytial virus, an ongoing medical dilemma: an expert commentary on respiratory syncytial virus prophylactic and therapeutic pharmaceuticals currently in clinical trials. *Influenza Other Respir Viruses* **9**, 169-178 (2015).
205 Perron, M., Stray, K., Kinkade, A., Theodore, D., Lee, G., Eisenberg, E., Sangi, M., Gilbert, B. E., Jordan, R., Piedra, P. A., Toms, G. L., Mackman, R. & Cihlar, T. GS-5806 Inhibits a Broad Range of Respiratory Syncytial Virus Clinical Isolates by Blocking the Virus-Cell Fusion Process. *Antimicrob Agents Chemother* **60**, 1264-1273 (2015).
206 Mackman, R. L., Sangi, M., Sperandio, D., Parrish, J. P., Eisenberg, E., Perron, M., Hui, H., Zhang, L., Siegel, D., Yang, H., Saunders, O., Boojamra, C., Lee, G., Samuel, D., Babaoglu, K., Carey, A., Gilbert, B. E., Piedra, P. A., Strickley, R., Iwata, Q., Hayes, J., Stray, K., Kinkade, A., Theodore, D., Jordan, R., Desai, M. & Cihlar, T. Discovery of an oral respiratory syncytial virus (RSV) fusion inhibitor (GS-5806) and clinical proof of concept in a human RSV challenge study. *J Med Chem* **58**, 1630-1643 (2015).
207 DeVincenzo, J. P., Whitley, R. J., Mackman, R. L., Scaglioni-Weinlich, C., Harrison, L., Farrell, E., McBride, S., Lambkin-Williams, R., Jordan, R., Xin, Y., Ramanathan, S., O'Riordan, T., Lewis, S. A., Li, X., Toback, S. L., Lin, S. L. & Chien, J. W. Oral GS-5806 activity in a respiratory syncytial virus challenge study. *N Engl J Med* **371**, 711-722 (2014).
208 Stevens, M., Rusch, S., DeVincenzo, J., Kim, Y. I., Harrison, L., Meals, E. A., Boyers, A., Fok-Seang, J., Huntjens, D., Lounis, N., Mari, N. K., Remmerie, B., Roymans, D., Koul, A. & Verloes, R. Antiviral Activity of Oral JNJ-53718678 in Healthy Adult Volunteers Challenged with Respiratory Syncytial Virus: A Placebo-Controlled Study. *J Infect Dis* (2018).
209 Lam, J. K., Chow, M. Y., Zhang, Y. & Leung, S. W. siRNA Versus miRNA as Therapeutics for Gene Silencing. *Mol Ther Nucleic Acids* **4**, e252 (2015).
210 DeVincenzo, J., Lambkin-Williams, R., Wilkinson, T., Cehelsky, J., Nochur, S., Walsh, E., Meyers, R., Gollob, J. & Vaishnaw, A. A randomized, double-blind, placebo-controlled study of an RNAi-based therapy directed against respiratory syncytial virus. *Proc Natl Acad Sci U S A* **107**, 8800-8805 (2010).
211 Gottlieb, J., Zamora, M. R., Hodges, T., Musk, A. W., Sommerwerk, U., Dilling, D., Arcasoy, S., DeVincenzo, J., Karsten, V., Shah, S., Bettencourt, B. R., Cehelsky, J., Nochur, S., Gollob, J., Vaishnaw, A., Simon, A. R. & Glanville, A. R. ALN-RSV01 for prevention of bronchiolitis obliterans syndrome after respiratory syncytial virus infection in lung transplant recipients. *J Heart Lung Transplant* **35**, 213-221 (2016).

212 DeVincenzo, J. P., McClure, M. W., Symons, J. A., Fathi, H., Westland, C., Chanda, S., Lambkin-Williams, R., Smith, P., Zhang, Q., Beigelman, L., Blatt, L. M. & Fry, J. Activity of Oral ALS-008176 in a Respiratory Syncytial Virus Challenge Study. *N Engl J Med* **373**, 2048-2058 (2015).
213 Fearns, R. & Deval, J. New antiviral approaches for respiratory syncytial virus and other mononegaviruses: Inhibiting the RNA polymerase. *Antiviral Res* **134**, 63-76 (2016).
214 Saez-Llorens, X., Moreno, M. T., Ramilo, O., Sanchez, P. J., Top, F. H., Jr., Connor, E. M. & Group, M.-S. Safety and pharmacokinetics of palivizumab therapy in children hospitalized with respiratory syncytial virus infection. *Pediatr Infect Dis J* **23**, 707-712 (2004).
215 Detalle, L., Stohr, T., Palomo, C., Piedra, P. A., Gilbert, B. E., Mas, V., Millar, A., Power, U. F., Stortelers, C., Allosery, K., Melero, J. A. & Depla, E. Generation and Characterization of ALX-0171, a Potent Novel Therapeutic Nanobody for the Treatment of Respiratory Syncytial Virus Infection. *Antimicrob Agents Chemother* **60**, 6-13 (2016).
216 Hultberg, A., Temperton, N. J., Rosseels, V., Koenders, M., Gonzalez-Pajuelo, M., Schepens, B., Ibanez, L. I., Vanlandschoot, P., Schillemans, J., Saunders, M., Weiss, R. A., Saelens, X., Melero, J. A., Verrips, C. T., Van Gucht, S. & de Haard, H. J. Llama-derived single domain antibodies to build multivalent, superpotent and broadened neutralizing anti-viral molecules. *PLoS One* **6**, e17665 (2011).
217 Heylen, E., Neyts, J. & Jochmans, D. Drug candidates and model systems in respiratory syncytial virus antiviral drug discovery. *Biochem Pharmacol* **127**, 1-12 (2017).
218 Douglas, J. L., Panis, M. L., Ho, E., Lin, K. Y., Krawczyk, S. H., Grant, D. M., Cai, R., Swaminathan, S., Chen, X. & Cihlar, T. Small molecules VP-14637 and JNJ-2408068 inhibit respiratory syncytial virus fusion by similar mechanisms. *Antimicrob Agents Chemother* **49**, 2460-2466 (2005).
219 Cianci, C., Meanwell, N. & Krystal, M. Antiviral activity and molecular mechanism of an orally active respiratory syncytial virus fusion inhibitor. *J Antimicrob Chemother* **55**, 289-292 (2005).
220 Bonfanti, J. F., Meyer, C., Doublet, F., Fortin, J., Muller, P., Queguiner, L., Gevers, T., Janssens, P., Szel, H., Willebrords, R., Timmerman, P., Wuyts, K., van Remoortere, P., Janssens, F., Wigerinck, P. & Andries, K. Selection of a respiratory syncytial virus fusion inhibitor clinical candidate. 2. Discovery of a morpholinopropylaminobenzimidazole derivative (TMC353121). *J Med Chem* **51**, 875-896 (2008).
221 Warren, T. K., Jordan, R., Lo, M. K., Ray, A. S., Mackman, R. L., Soloveva, V., Siegel, D., Perron, M., Bannister, R., Hui, H. C., Larson, N., Strickley, R., Wells, J., Stuthman, K. S., Van Tongeren, S. A., Garza, N. L., Donnelly, G., Shurtleff, A. C., Retterer, C. J., Gharaibeh, D., Zamani, R., Kenny, T., Eaton, B. P., Grimes, E., Welch, L. S., Gomba, L., Wilhelmsen, C. L., Nichols, D. K., Nuss, J. E., Nagle, E. R., Kugelman, J. R., Palacios, G., Doerffler, E., Neville, S., Carra, E., Clarke, M. O., Zhang, L., Lew, W., Ross, B., Wang, Q., Chun, K., Wolfe, L., Babusis, D., Park, Y., Stray, K. M., Trancheva, I., Feng, J. Y., Barauskas, O., Xu, Y., Wong, P., Braun, M. R., Flint, M., McMullan, L. K., Chen, S. S., Fearns, R., Swaminathan, S., Mayers, D. L., Spiropoulou, C. F., Lee, W. A., Nichol, S. T., Cihlar, T. & Bavari, S. Therapeutic efficacy of the small molecule GS-5734 against Ebola virus in rhesus monkeys. *Nature* **531**, 381-385 (2016).
222 Warren, T. K., Wells, J., Panchal, R. G., Stuthman, K. S., Garza, N. L., Van Tongeren, S. A., Dong, L., Retterer, C. J., Eaton, B. P., Pegoraro, G., Honnold, S., Bantia, S., Kotian,

P., Chen, X., Taubenheim, B. R., Welch, L. S., Minning, D. M., Babu, Y. S., Sheridan, W. P. & Bavari, S. Protection against filovirus diseases by a novel broad-spectrum nucleoside analogue BCX4430. *Nature* **508**, 402-405 (2014).

223 Gantier, M. P., Tong, S., Behlke, M. A., Xu, D., Phipps, S., Foster, P. S. & Williams, B. R. TLR7 is involved in sequence-specific sensing of single-stranded RNAs in human macrophages. *J Immunol* **180**, 2117-2124 (2008).

224 Heil, F., Ahmad-Nejad, P., Hemmi, H., Hochrein, H., Ampenberger, F., Gellert, T., Dietrich, H., Lipford, G., Takeda, K., Akira, S., Wagner, H. & Bauer, S. The Toll-like receptor 7 (TLR7)-specific stimulus loxoribine uncovers a strong relationship within the TLR7, 8 and 9 subfamily. *Eur J Immunol* **33**, 2987-2997 (2003).

225 Diebold, S. S., Kaisho, T., Hemmi, H., Akira, S. & Reis e Sousa, C. Innate antiviral responses by means of TLR7-mediated recognition of single-stranded RNA. *Science* **303**, 1529-1531 (2004).

226 Heil, F., Hemmi, H., Hochrein, H., Ampenberger, F., Kirschning, C., Akira, S., Lipford, G., Wagner, H. & Bauer, S. Species-specific recognition of single-stranded RNA via toll-like receptor 7 and 8. *Science* **303**, 1526-1529 (2004).

227 Vollmer, J., Tluk, S., Schmitz, C., Hamm, S., Jurk, M., Forsbach, A., Akira, S., Kelly, K. M., Reeves, W. H., Bauer, S. & Krieg, A. M. Immune stimulation mediated by autoantigen binding sites within small nuclear RNAs involves Toll-like receptors 7 and 8. *J Exp Med* **202**, 1575-1585 (2005).

228 Jurk, M., Heil, F., Vollmer, J., Schetter, C., Krieg, A. M., Wagner, H., Lipford, G. & Bauer, S. Human TLR7 or TLR8 independently confer responsiveness to the antiviral compound R-848. *Nat Immunol* **3**, 499 (2002).

229 Zhang, Z., Ohto, U., Shibata, T., Krayukhina, E., Taoka, M., Yamauchi, Y., Tanji, H., Isobe, T., Uchiyama, S., Miyake, K. & Shimizu, T. Structural Analysis Reveals that Toll-like Receptor 7 Is a Dual Receptor for Guanosine and Single-Stranded RNA. *Immunity* **45**, 737-748 (2016).

230 Ahn, C. S. & Huang, W. W. Imiquimod in the treatment of cutaneous warts: an evidence-based review. *Am J Clin Dermatol* **15**, 387-399 (2014).

231 Hanna, E., Abadi, R. & Abbas, O. Imiquimod in dermatology: an overview. *Int J Dermatol* **55**, 831-844 (2016).

232 Lebold, K. M., Jacoby, D. B. & Drake, M. G. Toll-Like Receptor 7-Targeted Therapy in Respiratory Disease. *Transfus Med Hemother* **43**, 114-119 (2016).

233 Hemmi, H., Kaisho, T., Takeuchi, O., Sato, S., Sanjo, H., Hoshino, K., Horiuchi, T., Tomizawa, H., Takeda, K. & Akira, S. Small anti-viral compounds activate immune cells via the TLR7 MyD88-dependent signaling pathway. *Nat Immunol* **3**, 196-200 (2002).

234 Nishiya, T. & DeFranco, A. L. Ligand-regulated chimeric receptor approach reveals distinctive subcellular localization and signaling properties of the Toll-like receptors. *J Biol Chem* **279**, 19008-19017 (2004).

235 Kim, Y. M., Brinkmann, M. M., Paquet, M. E. & Ploegh, H. L. UNC93B1 delivers nucleotide-sensing toll-like receptors to endolysosomes. *Nature* **452**, 234-238 (2008).

236 Casrouge, A., Zhang, S. Y., Eidenschenk, C., Jouanguy, E., Puel, A., Yang, K., Alcais, A., Picard, C., Mahfoufi, N., Nicolas, N., Lorenzo, L., Plancoulaine, S., Senechal, B., Geissmann, F., Tabeta, K., Hoebe, K., Du, X., Miller, R. L., Heron, B., Mignot, C., de Villemeur, T. B., Lebon, P., Dulac, O., Rozenberg, F., Beutler, B., Tardieu, M., Abel, L.

& Casanova, J. L. Herpes simplex virus encephalitis in human UNC-93B deficiency. *Science* **314**, 308-312 (2006).
237 Kanno, A., Yamamoto, C., Onji, M., Fukui, R., Saitoh, S., Motoi, Y., Shibata, T., Matsumoto, F., Muta, T. & Miyake, K. Essential role for Toll-like receptor 7 (TLR7)-unique cysteines in an intramolecular disulfide bond, proteolytic cleavage and RNA sensing. *Int Immunol* **25**, 413-422 (2013).
238 Petes, C., Odoardi, N. & Gee, K. The Toll for Trafficking: Toll-Like Receptor 7 Delivery to the Endosome. *Front Immunol* **8**, 1075 (2017).
239 Hipp, M. M., Shepherd, D., Gileadi, U., Aichinger, M. C., Kessler, B. M., Edelmann, M. J., Essalmani, R., Seidah, N. G., Reis e Sousa, C. & Cerundolo, V. Processing of human toll-like receptor 7 by furin-like proprotein convertases is required for its accumulation and activity in endosomes. *Immunity* **39**, 711-721 (2013).
240 Kawai, T. & Akira, S. Signaling to NF-kappaB by Toll-like receptors. *Trends Mol Med* **13**, 460-469 (2007).
241 Kawai, T., Sato, S., Ishii, K. J., Coban, C., Hemmi, H., Yamamoto, M., Terai, K., Matsuda, M., Inoue, J., Uematsu, S., Takeuchi, O. & Akira, S. Interferon-alpha induction through Toll-like receptors involves a direct interaction of IRF7 with MyD88 and TRAF6. *Nat Immunol* **5**, 1061-1068 (2004).
242 Oganesyan, G., Saha, S. K., Guo, B., He, J. Q., Shahangian, A., Zarnegar, B., Perry, A. & Cheng, G. Critical role of TRAF3 in the Toll-like receptor-dependent and -independent antiviral response. *Nature* **439**, 208-211 (2006).
243 Hacker, H., Redecke, V., Blagoev, B., Kratchmarova, I., Hsu, L. C., Wang, G. G., Kamps, M. P., Raz, E., Wagner, H., Hacker, G., Mann, M. & Karin, M. Specificity in Toll-like receptor signalling through distinct effector functions of TRAF3 and TRAF6. *Nature* **439**, 204-207 (2006).
244 Uematsu, S., Sato, S., Yamamoto, M., Hirotani, T., Kato, H., Takeshita, F., Matsuda, M., Coban, C., Ishii, K. J., Kawai, T., Takeuchi, O. & Akira, S. Interleukin-1 receptor-associated kinase-1 plays an essential role for Toll-like receptor (TLR)7- and TLR9-mediated interferon-{alpha} induction. *J Exp Med* **201**, 915-923 (2005).
245 Hoshino, K., Sugiyama, T., Matsumoto, M., Tanaka, T., Saito, M., Hemmi, H., Ohara, O., Akira, S. & Kaisho, T. IkappaB kinase-alpha is critical for interferon-alpha production induced by Toll-like receptors 7 and 9. *Nature* **440**, 949-953 (2006).
246 Kawasaki, T. & Kawai, T. Toll-like receptor signaling pathways. *Front Immunol* **5**, 461 (2014).
247 Gilliet, M., Cao, W. & Liu, Y. J. Plasmacytoid dendritic cells: sensing nucleic acids in viral infection and autoimmune diseases. *Nat Rev Immunol* **8**, 594-606 (2008).
248 Chi, H., Li, C., Zhao, F. S., Zhang, L., Ng, T. B., Jin, G. & Sha, O. Anti-tumor Activity of Toll-Like Receptor 7 Agonists. *Front Pharmacol* **8**, 304 (2017).
249 Reitz, A. B., Goodman, M. G., Pope, B. L., Argentieri, D. C., Bell, S. C., Burr, L. E., Chourmouzis, E., Come, J., Goodman, J. H., Klaubert, D. H. & et al. Small-molecule immunostimulants. Synthesis and activity of 7,8-disubstituted guanosines and structurally related compounds. *J Med Chem* **37**, 3561-3578 (1994).
250 Smee, D. F., Alaghamandan, H. A., Ramasamy, K. & Revankar, G. R. Broad-spectrum activity of 8-chloro-7-deazaguanosine against RNA virus infections in mice and rats. *Antiviral Res* **26**, 203-209 (1995).

251 Smee, D. F., Alaghamandan, H. A., Cottam, H. B., Sharma, B. S., Jolley, W. B. & Robins, R. K. Broad-spectrum in vivo antiviral activity of 7-thia-8-oxoguanosine, a novel immunopotentiating agent. *Antimicrob Agents Chemother* **33**, 1487-1492 (1989).
252 Lee, J., Chuang, T. H., Redecke, V., She, L., Pitha, P. M., Carson, D. A., Raz, E. & Cottam, H. B. Molecular basis for the immunostimulatory activity of guanine nucleoside analogs: activation of Toll-like receptor 7. *Proc Natl Acad Sci U S A* **100**, 6646-6651 (2003).
253 Viriyakosol, S., Tobias, P. S., Kitchens, R. L. & Kirkland, T. N. MD-2 binds to bacterial lipopolysaccharide. *J Biol Chem* **276**, 38044-38051 (2001).
254 Krieg, A. M., Wu, T., Weeratna, R., Efler, S. M., Love-Homan, L., Yang, L., Yi, A. K., Short, D. & Davis, H. L. Sequence motifs in adenoviral DNA block immune activation by stimulatory CpG motifs. *Proc Natl Acad Sci U S A* **95**, 12631-12636 (1998).
255 Yamada, H., Gursel, I., Takeshita, F., Conover, J., Ishii, K. J., Gursel, M., Takeshita, S. & Klinman, D. M. Effect of suppressive DNA on CpG-induced immune activation. *J Immunol* **169**, 5590-5594 (2002).
256 Zhu, F. G., Reich, C. F. & Pisetsky, D. S. Inhibition of murine dendritic cell activation by synthetic phosphorothioate oligodeoxynucleotides. *J Leukoc Biol* **72**, 1154-1163 (2002).
257 Stunz, L. L., Lenert, P., Peckham, D., Yi, A. K., Haxhinasto, S., Chang, M., Krieg, A. M. & Ashman, R. F. Inhibitory oligonucleotides specifically block effects of stimulatory CpG oligonucleotides in B cells. *Eur J Immunol* **32**, 1212-1222 (2002).
258 Han, H. & Hurley, L. H. G-quadruplex DNA: a potential target for anti-cancer drug design. *Trends Pharmacol Sci* **21**, 136-142 (2000).
259 Gursel, I., Gursel, M., Yamada, H., Ishii, K. J., Takeshita, F. & Klinman, D. M. Repetitive elements in mammalian telomeres suppress bacterial DNA-induced immune activation. *J Immunol* **171**, 1393-1400 (2003).
260 Duramad, O., Fearon, K. L., Chang, B., Chan, J. H., Gregorio, J., Coffman, R. L. & Barrat, F. J. Inhibitors of TLR-9 act on multiple cell subsets in mouse and man in vitro and prevent death in vivo from systemic inflammation. *J Immunol* **174**, 5193-5200 (2005).
261 Ho, P. P., Fontoura, P., Ruiz, P. J., Steinman, L. & Garren, H. An immunomodulatory GpG oligonucleotide for the treatment of autoimmunity via the innate and adaptive immune systems. *J Immunol* **171**, 4920-4926 (2003).
262 Zeuner, R. A., Ishii, K. J., Lizak, M. J., Gursel, I., Yamada, H., Klinman, D. M. & Verthelyi, D. Reduction of CpG-induced arthritis by suppressive oligodeoxynucleotides. *Arthritis Rheum* **46**, 2219-2224 (2002).
263 Barrat, F. J., Meeker, T., Gregorio, J., Chan, J. H., Uematsu, S., Akira, S., Chang, B., Duramad, O. & Coffman, R. L. Nucleic acids of mammalian origin can act as endogenous ligands for Toll-like receptors and may promote systemic lupus erythematosus. *J Exp Med* **202**, 1131-1139 (2005).
264 Pawar, R. D., Ramanjaneyulu, A., Kulkarni, O. P., Lech, M., Segerer, S. & Anders, H. J. Inhibition of Toll-like receptor-7 (TLR-7) or TLR-7 plus TLR-9 attenuates glomerulonephritis and lung injury in experimental lupus. *J Am Soc Nephrol* **18**, 1721-1731 (2007).
265 Hornung, V., Rothenfusser, S., Britsch, S., Krug, A., Jahrsdorfer, B., Giese, T., Endres, S. & Hartmann, G. Quantitative expression of toll-like receptor 1-10 mRNA in cellular

subsets of human peripheral blood mononuclear cells and sensitivity to CpG oligodeoxynucleotides. *J Immunol* **168**, 4531-4537 (2002).

266 Shikhagaie, M. M., Andersson, C. K., Mori, M., Kortekaas Krohn, I., Bergqvist, A., Dahl, R., Ekblad, E., Hoffmann, H. J., Bjermer, L. & Erjefalt, J. S. Mapping of TLR5 and TLR7 in central and distal human airways and identification of reduced TLR expression in severe asthma. *Clin Exp Allergy* **44**, 184-196 (2014).

267 Sha, Q., Truong-Tran, A. Q., Plitt, J. R., Beck, L. A. & Schleimer, R. P. Activation of airway epithelial cells by toll-like receptor agonists. *Am J Respir Cell Mol Biol* **31**, 358-364 (2004).

268 Ioannidis, I., Ye, F., McNally, B., Willette, M. & Flano, E. Toll-like receptor expression and induction of type I and type III interferons in primary airway epithelial cells. *J Virol* **87**, 3261-3270 (2013).

269 Gorden, K. B., Gorski, K. S., Gibson, S. J., Kedl, R. M., Kieper, W. C., Qiu, X., Tomai, M. A., Alkan, S. S. & Vasilakos, J. P. Synthetic TLR agonists reveal functional differences between human TLR7 and TLR8. *J Immunol* **174**, 1259-1268 (2005).

270 Hart, O. M., Athie-Morales, V., O'Connor, G. M. & Gardiner, C. M. TLR7/8-mediated activation of human NK cells results in accessory cell-dependent IFN-gamma production. *J Immunol* **175**, 1636-1642 (2005).

271 Song, Y., Zhuang, Y., Zhai, S., Huang, D., Zhang, Y., Kang, W., Li, X., Liu, Q., Yu, Q. & Sun, Y. Increased expression of TLR7 in CD8(+) T cells leads to TLR7-mediated activation and accessory cell-dependent IFN-gamma production in HIV type 1 infection. *AIDS Res Hum Retroviruses* **25**, 1287-1295 (2009).

272 Dominguez-Villar, M., Gautron, A. S., de Marcken, M., Keller, M. J. & Hafler, D. A. TLR7 induces anergy in human CD4(+) T cells. *Nat Immunol* **16**, 118-128 (2015).

273 Drake, M. G., Scott, G. D., Proskocil, B. J., Fryer, A. D., Jacoby, D. B. & Kaufman, E. H. Toll-like receptor 7 rapidly relaxes human airways. *Am J Respir Crit Care Med* **188**, 664-672 (2013).

274 Kaufman, E. H., Fryer, A. D. & Jacoby, D. B. Toll-like receptor 7 agonists are potent and rapid bronchodilators in guinea pigs. *J Allergy Clin Immunol* **127**, 462-469 (2011).

275 Edwards, L., Ferenczy, A., Eron, L., Baker, D., Owens, M. L., Fox, T. L., Hougham, A. J. & Schmitt, K. A. Self-administered topical 5% imiquimod cream for external anogenital warts. HPV Study Group. Human PapillomaVirus. *Arch Dermatol* **134**, 25-30 (1998).

276 von Krogh, G., Lacey, C. J., Gross, G., Barrasso, R. & Schneider, A. European course on HPV associated pathology: guidelines for primary care physicians for the diagnosis and management of anogenital warts. *Sex Transm Infect* **76**, 162-168 (2000).

277 Harrison, C. J., Miller, R. L. & Bernstein, D. I. Posttherapy suppression of genital herpes simplex virus (HSV) recurrences and enhancement of HSV-specific T-cell memory by imiquimod in guinea pigs. *Antimicrob Agents Chemother* **38**, 2059-2064 (1994).

278 Chen, M., Griffith, B. P., Lucia, H. L. & Hsiung, G. D. Efficacy of S26308 against guinea pig cytomegalovirus infection. *Antimicrob Agents Chemother* **32**, 678-683 (1988).

279 Bergmann, J. F., de Bruijne, J., Hotho, D. M., de Knegt, R. J., Boonstra, A., Weegink, C. J., van Vliet, A. A., van de Wetering, J., Fletcher, S. P., Bauman, L. A., Rahimy, M., Appleman, J. R., Freddo, J. L., Janssen, H. L. & Reesink, H. W. Randomised clinical trial: anti-viral activity of ANA773, an oral inducer of endogenous interferons acting via TLR7, in chronic HCV. *Aliment Pharmacol Ther* **34**, 443-453 (2011).

280 Gane, E. J., Lim, Y. S., Gordon, S. C., Visvanathan, K., Sicard, E., Fedorak, R. N., Roberts, S., Massetto, B., Ye, Z., Pflanz, S., Garrison, K. L., Gaggar, A., Mani Subramanian, G., McHutchison, J. G., Kottilil, S., Freilich, B., Coffin, C. S., Cheng, W. & Kim, Y. J. The oral toll-like receptor-7 agonist GS-9620 in patients with chronic hepatitis B virus infection. *J Hepatol* **63**, 320-328 (2015).

281 Hammerbeck, D. M., Burleson, G. R., Schuller, C. J., Vasilakos, J. P., Tomai, M., Egging, E., Cochran, F. R., Woulfe, S. & Miller, R. L. Administration of a dual toll-like receptor 7 and toll-like receptor 8 agonist protects against influenza in rats. *Antiviral Res* **73**, 1-11 (2007).

282 Awais, M., Wang, K., Lin, X., Qian, W., Zhang, N., Wang, C., Wang, K., Zhao, L., Fu, Z. F. & Cui, M. TLR7 Deficiency Leads to TLR8 Compensative Regulation of Immune Response against JEV in Mice. *Front Immunol* **8**, 160 (2017).

283 Neighbours, L. M., Long, K., Whitmore, A. C. & Heise, M. T. Myd88-dependent toll-like receptor 7 signaling mediates protection from severe Ross River virus-induced disease in mice. *J Virol* **86**, 10675-10685 (2012).

284 Dyer, K. D., Garcia-Crespo, K. E., Glineur, S., Domachowske, J. B. & Rosenberg, H. F. The Pneumonia Virus of Mice (PVM) model of acute respiratory infection. *Viruses* **4**, 3494-3510 (2012).

285 Davidson, S., Kaiko, G., Loh, Z., Lalwani, A., Zhang, V., Spann, K., Foo, S. Y., Hansbro, N., Uematsu, S., Akira, S., Matthaei, K. I., Rosenberg, H. F., Foster, P. S. & Phipps, S. Plasmacytoid dendritic cells promote host defense against acute pneumovirus infection via the TLR7-MyD88-dependent signaling pathway. *J Immunol* **186**, 5938-5948 (2011).

286 Scagnolari, C., Midulla, F., Pierangeli, A., Moretti, C., Bonci, E., Berardi, R., De Angelis, D., Selvaggi, C., Di Marco, P., Girardi, E. & Antonelli, G. Gene expression of nucleic acid-sensing pattern recognition receptors in children hospitalized for respiratory syncytial virus-associated acute bronchiolitis. *Clin Vaccine Immunol* **16**, 816-823 (2009).

287 Lindemans, C. A., Coffer, P. J., Schellens, I. M., de Graaff, P. M., Kimpen, J. L. & Koenderman, L. Respiratory syncytial virus inhibits granulocyte apoptosis through a phosphatidylinositol 3-kinase and NF-kappaB-dependent mechanism. *J Immunol* **176**, 5529-5537 (2006).

288 Lukacs, N. W., Smit, J. J., Mukherjee, S., Morris, S. B., Nunez, G. & Lindell, D. M. Respiratory virus-induced TLR7 activation controls IL-17-associated increased mucus via IL-23 regulation. *J Immunol* **185**, 2231-2239 (2010).

289 Johnson, T. R., Rao, S., Seder, R. A., Chen, M. & Graham, B. S. TLR9 agonist, but not TLR7/8, functions as an adjuvant to diminish FI-RSV vaccine-enhanced disease, while either agonist used as therapy during primary RSV infection increases disease severity. *Vaccine* **27**, 3045-3052 (2009).

290 Van, L. P., Bardel, E., Gregoire, S., Vanoirbeek, J., Schneider, E., Dy, M. & Thieblemont, N. Treatment with the TLR7 agonist R848 induces regulatory T-cell-mediated suppression of established asthma symptoms. *Eur J Immunol* **41**, 1992-1999 (2011).

291 Xirakia, C., Koltsida, O., Stavropoulos, A., Thanassopoulou, A., Aidinis, V., Sideras, P. & Andreakos, E. Toll-like receptor 7-triggered immune response in the lung mediates acute and long-lasting suppression of experimental asthma. *Am J Respir Crit Care Med* **181**, 1207-1216 (2010).

292 Camateros, P., Tamaoka, M., Hassan, M., Marino, R., Moisan, J., Marion, D., Guiot, M. C., Martin, J. G. & Radzioch, D. Chronic asthma-induced airway remodeling is prevented by toll-like receptor-7/8 ligand S28463. *Am J Respir Crit Care Med* **175**, 1241-1249 (2007).
293 Moisan, J., Camateros, P., Thuraisingam, T., Marion, D., Koohsari, H., Martin, P., Boghdady, M. L., Ding, A., Gaestel, M., Guiot, M. C., Martin, J. G. & Radzioch, D. TLR7 ligand prevents allergen-induced airway hyperresponsiveness and eosinophilia in allergic asthma by a MYD88-dependent and MK2-independent pathway. *Am J Physiol Lung Cell Mol Physiol* **290**, L987-995 (2006).
294 Tsitoura, D., Ambery, C., Price, M., Powley, W., Garthside, S., Biggadike, K. & Quint, D. Early clinical evaluation of the intranasal TLR7 agonist GSK2245035: Use of translational biomarkers to guide dosing and confirm target engagement. *Clin Pharmacol Ther* **98**, 369-380 (2015).
295 Greiff, L., Ahlstrom-Emanuelsson, C., Alenas, M., Almqvist, G., Andersson, M., Cervin, A., Dolata, J., Lindgren, S., Martensson, A., Young, B. & Widegren, H. Biological effects and clinical efficacy of a topical Toll-like receptor 7 agonist in seasonal allergic rhinitis: a parallel group controlled phase IIa study. *Inflamm Res* **64**, 903-915 (2015).
296 Das, A., Heesters, B. A., Bialas, A., O'Flynn, J., Rifkin, I. R., Ochando, J., Mittereder, N., Carlesso, G., Herbst, R. & Carroll, M. C. Follicular Dendritic Cell Activation by TLR Ligands Promotes Autoreactive B Cell Responses. *Immunity* **46**, 106-119 (2017).
297 Liu, J. F., Jiang, Z. Y., Wang, R. R., Zheng, Y. T., Chen, J. J., Zhang, X. M. & Ma, Y. B. Isatisine A, a novel alkaloid with an unprecedented skeleton from leaves of Isatis indigotica. *Org Lett* **9**, 4127-4129 (2007).
298 Kong, X., San Juan, H., Behera, A., Peeples, M. E., Wu, J., Lockey, R. F. & Mohapatra, S. S. ERK-1/2 activity is required for efficient RSV infection. *FEBS Lett* **559**, 33-38 (2004).
299 Cozens, A. L., Yezzi, M. J., Yamaya, M., Steiger, D., Wagner, J. A., Garber, S. S., Chin, L., Simon, E. M., Cutting, G. R., Gardner, P. & et al. A transformed human epithelial cell line that retains tight junctions post crisis. *In Vitro Cell Dev Biol* **28A**, 735-744 (1992).
300 DuBridge, R. B., Tang, P., Hsia, H. C., Leong, P. M., Miller, J. H. & Calos, M. P. Analysis of mutation in human cells by using an Epstein-Barr virus shuttle system. *Mol Cell Biol* **7**, 379-387 (1987).
301 Giard, D. J., Aaronson, S. A., Todaro, G. J., Arnstein, P., Kersey, J. H., Dosik, H. & Parks, W. P. In vitro cultivation of human tumors: establishment of cell lines derived from a series of solid tumors. *J Natl Cancer Inst* **51**, 1417-1423 (1973).
302 Zaheer, R. S., Wiehler, S., Hudy, M. H., Traves, S. L., Pelikan, J. B., Leigh, R. & Proud, D. Human rhinovirus-induced ISG15 selectively modulates epithelial antiviral immunity. *Mucosal Immunol* **7**, 1127-1138 (2014).
303 Gey, G. O., Coffman, W. D. & Kubicek, M. T. Tissue Culture Studies of the Proliferative Capacity of Cervical Carcinoma and Normal Epithelium. *Cancer Research* **12**, 264-265 (1952).
304 Lacroix, M. Persistent use of "false" cell lines. *Int J Cancer* **122**, 1-4 (2008).
305 Chen, T. R. Re-evaluation of HeLa, HeLa S3, and HEp-2 karyotypes. *Cytogenet Cell Genet* **48**, 19-24 (1988).
306 Klein, G., Giovanella, B., Westman, A., Stehlin, J. S. & Mumford, D. An EBV-genome-negative cell line established from an American Burkitt lymphoma; receptor

characteristics. EBV infectibility and permanent conversion into EBV-positive sublines by in vitro infection. *Intervirology* **5**, 319-334 (1975).
307 Ammerman, N. C., Beier-Sexton, M. & Azad, A. F. Growth and maintenance of Vero cell lines. *Curr Protoc Microbiol* **Appendix 4**, Appendix 4E (2008).
308 Churchill, L., Chilton, F. H., Resau, J. H., Bascom, R., Hubbard, W. C. & Proud, D. Cyclooxygenase metabolism of endogenous arachidonic acid by cultured human tracheal epithelial cells. *Am Rev Respir Dis* **140**, 449-459 (1989).
309 Hallak, L. K., Spillmann, D., Collins, P. L. & Peeples, M. E. Glycosaminoglycan sulfation requirements for respiratory syncytial virus infection. *J Virol* **74**, 10508-10513 (2000).
310 Bilawchuk, L. M., Griffiths, C. D., Jensen, L. D., Elawar, F. & Marchant, D. J. The Susceptibilities of Respiratory Syncytial Virus to Nucleolin Receptor Blocking and Antibody Neutralization are Dependent upon the Method of Virus Purification. *Viruses* **9** (2017).
311 Mosmann, T. Rapid colorimetric assay for cellular growth and survival: application to proliferation and cytotoxicity assays. *J Immunol Methods* **65**, 55-63 (1983).
312 Colpitts, C. C., Ustinov, A. V., Epand, R. F., Epand, R. M., Korshun, V. A. & Schang, L. M. 5-(Perylen-3-yl)ethynyl-arabino-uridine (aUY11), an arabino-based rigid amphipathic fusion inhibitor, targets virion envelope lipids to inhibit fusion of influenza virus, hepatitis C virus, and other enveloped viruses. *J Virol* **87**, 3640-3654 (2013).
313 Atienza, B. J. P., Jensen, L. D., Noton, S. L., Ansalem, A. K. V., Hobman, T., Fearns, R., Marchant, D. J. & West, F. G. Dual Catalytic Synthesis of Antiviral Compounds Based on Metallocarbene-Azide Cascade Chemistry. *J Org Chem* (2018).
314 Buss, N. & Cammack, N. Measuring the effectiveness of antiretroviral agents. *Antivir Ther* **6**, 1-7 (2001).
315 Marchant, D., Neil, S. J., Aubin, K., Schmitz, C. & McKnight, A. An envelope-determined, pH-independent endocytic route of viral entry determines the susceptibility of human immunodeficiency virus type 1 (HIV-1) and HIV-2 to Lv2 restriction. *J Virol* **79**, 9410-9418 (2005).
316 Canter, D. M., Jackson, R. L. & Perrault, J. Faithful and efficient in vitro reconstitution of vesicular stomatitis virus transcription using plasmid-encoded L and P proteins. *Virology* **194**, 518-529 (1993).
317 De Clercq, E. & Li, G. Approved Antiviral Drugs over the Past 50 Years. *Clin Microbiol Rev* **29**, 695-747 (2016).
318 Lichtman, M. A. A historical perspective on the development of the cytarabine (7days) and daunorubicin (3days) treatment regimen for acute myelogenous leukemia: 2013 the 40th anniversary of 7+3. *Blood Cells Mol Dis* **50**, 119-130 (2013).
319 Knipe, D. M. & Howley, P. M. *Fields virology*. 6th edn, (Wolters Kluwer/Lippincott Williams & Wilkins Health, 2013).
320 McDonald, T. P., Pitt, A. R., Brown, G., Rixon, H. W. & Sugrue, R. J. Evidence that the respiratory syncytial virus polymerase complex associates with lipid rafts in virus-infected cells: a proteomic analysis. *Virology* **330**, 147-157 (2004).
321 Arakawa, H., Maeda, M. & Tsuji, A. Chemiluminescent Assay of Various Enzymes Using Indoxyl Derivatives as Substrate and Its Applications to Enzyme-Immunoassay and DNA Probe Assay. *Anal Biochem* **199**, 238-242 (1991).

322 Shigeta, S., Hinuma, Y., Suto, T. & Ishida, N. The cell to cell infection of respiratory syncytial virus in HEp-2 monolayer cultures. *J Gen Virol* **3**, 129-131 (1968).
323 Berridge, M. V. & Tan, A. S. Characterization of the cellular reduction of 3-(4,5-dimethylthiazol-2-yl)-2,5-diphenyltetrazolium bromide (MTT): subcellular localization, substrate dependence, and involvement of mitochondrial electron transport in MTT reduction. *Arch Biochem Biophys* **303**, 474-482 (1993).
324 Huet, O., Petit, J. M., Ratinaud, M. H. & Julien, R. NADH-dependent dehydrogenase activity estimation by flow cytometric analysis of 3-(4,5-dimethylthiazolyl-2-yl)-2,5-diphenyltetrazolium bromide (MTT) reduction. *Cytometry* **13**, 532-539 (1992).
325 Hadaczek, P., Ozawa, T., Soroceanu, L., Yoshida, Y., Matlaf, L., Singer, E., Fiallos, E., James, C. D. & Cobbs, C. S. Cidofovir: a novel antitumor agent for glioblastoma. *Clin Cancer Res* **19**, 6473-6483 (2013).
326 Soma, M. A. & Albert, D. M. Cidofovir: to use or not to use? *Curr Opin Otolaryngol Head Neck Surg* **16**, 86-90 (2008).
327 Calista, D. Topical 1% cidofovir for the treatment of basal cell carcinoma. *Eur J Dermatol* **12**, 562-564 (2002).
328 Dyawanapelly, S., Kumar, A. & Chourasia, M. K. Lessons Learned from Gemcitabine: Impact of Therapeutic Carrier Systems and Gemcitabine's Drug Conjugates on Cancer Therapy. *Crit Rev Ther Drug Carrier Syst* **34**, 63-96 (2017).
329 Cai, J., Damaraju, V. L., Groulx, N., Mowles, D., Peng, Y., Robins, M. J., Cass, C. E. & Gros, P. Two distinct molecular mechanisms underlying cytarabine resistance in human leukemic cells. *Cancer Res* **68**, 2349-2357 (2008).
330 Tchesnokov, E. P., Raeisimakiani, P., Ngure, M., Marchant, D. & Gotte, M. Recombinant RNA-Dependent RNA Polymerase Complex of Ebola Virus. *Sci Rep* **8**, 3970 (2018).
331 Lowenberg, B., Pabst, T., Vellenga, E., van Putten, W., Schouten, H. C., Graux, C., Ferrant, A., Sonneveld, P., Biemond, B. J., Gratwohl, A., de Greef, G. E., Verdonck, L. F., Schaafsma, M. R., Gregor, M., Theobald, M., Schanz, U., Maertens, J., Ossenkoppele, G. J., Dutch-Belgian Cooperative Trial Group for, H.-O. & Swiss Group for Clinical Cancer Research Collaborative, G. Cytarabine dose for acute myeloid leukemia. *N Engl J Med* **364**, 1027-1036 (2011).
332 Lipinski, C. A., Lombardo, F., Dominy, B. W. & Feeney, P. J. Experimental and computational approaches to estimate solubility and permeability in drug discovery and development settings. *Adv Drug Deliv Rev* **46**, 3-26 (2001).
333 Henle, W. & Henle, G. Interference of Inactive Virus with the Propagation of Virus of Influenza. *Science* **98**, 87-89 (1943).
334 Von Magnus, P. Incomplete forms of influenza virus. *Adv Virus Res* **2**, 59-79 (1954).
335 Frensing, T. Defective interfering viruses and their impact on vaccines and viral vectors. *Biotechnol J* **10**, 681-689 (2015).
336 Wang, G., Deval, J., Hong, J., Dyatkina, N., Prhavc, M., Taylor, J., Fung, A., Jin, Z., Stevens, S. K., Serebryany, V., Liu, J., Zhang, Q., Tam, Y., Chanda, S. M., Smith, D. B., Symons, J. A., Blatt, L. M. & Beigelman, L. Discovery of 4'-chloromethyl-2'-deoxy-3',5'-di-O-isobutyryl-2'-fluorocytidine (ALS-8176), a first-in-class RSV polymerase inhibitor for treatment of human respiratory syncytial virus infection. *J Med Chem* **58**, 1862-1878 (2015).

337 Bem, R. A., Domachowske, J. B. & Rosenberg, H. F. Animal models of human respiratory syncytial virus disease. *Am J Physiol Lung Cell Mol Physiol* **301**, L148-156 (2011).
338 Tang, Y. T. & Marshall, G. R. Virtual screening for lead discovery. *Methods Mol Biol* **716**, 1-22 (2011).
339 Murawski, M. R., Bowen, G. N., Cerny, A. M., Anderson, L. J., Haynes, L. M., Tripp, R. A., Kurt-Jones, E. A. & Finberg, R. W. Respiratory syncytial virus activates innate immunity through Toll-like receptor 2. *J Virol* **83**, 1492-1500 (2009).
340 Liu, P., Jamaluddin, M., Li, K., Garofalo, R. P., Casola, A. & Brasier, A. R. Retinoic acid-inducible gene I mediates early antiviral response and Toll-like receptor 3 expression in respiratory syncytial virus-infected airway epithelial cells. *J Virol* **81**, 1401-1411 (2007).
341 Rudd, B. D., Burstein, E., Duckett, C. S., Li, X. & Lukacs, N. W. Differential role for TLR3 in respiratory syncytial virus-induced chemokine expression. *J Virol* **79**, 3350-3357 (2005).
342 Sabbah, A., Chang, T. H., Harnack, R., Frohlich, V., Tominaga, K., Dube, P. H., Xiang, Y. & Bose, S. Activation of innate immune antiviral responses by Nod2. *Nat Immunol* **10**, 1073-1080 (2009).
343 Drake, M. G., Kaufman, E. H., Fryer, A. D. & Jacoby, D. B. The therapeutic potential of Toll-like receptor 7 stimulation in asthma. *Inflamm Allergy Drug Targets* **11**, 484-491 (2012).
344 Matsui, H., Tomizawa, H., Eiho, K., Kashiwazaki, Y., Edwards, S., Biffen, M., Bell, J. P., Bahl, A., Leishman, A. J., Murray, C. M., Takaku, H. & Ueda, Y. Mechanism of action of inhibition of allergic immune responses by a novel antedrug TLR7 agonist. *J Immunol* **189**, 5194-5205 (2012).
345 Biffen, M., Matsui, H., Edwards, S., Leishman, A. J., Eiho, K., Holness, E., Satterthwaite, G., Doyle, I., Wada, H., Fraser, N. J., Hawkins, S. L., Aoki, M., Tomizawa, H., Benjamin, A. D., Takaku, H., McInally, T. & Murray, C. M. Biological characterization of a novel class of toll-like receptor 7 agonists designed to have reduced systemic activity. *Br J Pharmacol* **166**, 573-586 (2012).
346 Vultaggio, A., Nencini, F., Fitch, P. M., Fili, L., Maggi, L., Fanti, P., deVries, A., Beccastrini, E., Palandri, F., Manuelli, C., Bani, D., Giudizi, M. G., Guarna, A., Annunziato, F., Romagnani, S., Maggi, E., Howie, S. E. & Parronchi, P. Modified adenine (9-benzyl-2-butoxy-8-hydroxyadenine) redirects Th2-mediated murine lung inflammation by triggering TLR7. *J Immunol* **182**, 880-889 (2009).
347 Vultaggio, A., Nencini, F., Pratesi, S., Maggi, L., Guarna, A., Annunziato, F., Romagnani, S., Parronchi, P. & Maggi, E. The TLR7 ligand 9-benzyl-2-butoxy-8-hydroxy adenine inhibits IL-17 response by eliciting IL-10 and IL-10-inducing cytokines. *J Immunol* **186**, 4707-4715 (2011).
348 Anderson, C. A., Solari, R. & Pease, J. E. Biased agonism at chemokine receptors: obstacles or opportunities for drug discovery? *J Leukoc Biol* **99**, 901-909 (2016).
349 Favata, M. F., Horiuchi, K. Y., Manos, E. J., Daulerio, A. J., Stradley, D. A., Feeser, W. S., Van Dyk, D. E., Pitts, W. J., Earl, R. A., Hobbs, F., Copeland, R. A., Magolda, R. L., Scherle, P. A. & Trzaskos, J. M. Identification of a novel inhibitor of mitogen-activated protein kinase kinase. *J Biol Chem* **273**, 18623-18632 (1998).

350 Jensen, K. J., Garmaroudi, F. S., Zhang, J., Lin, J., Boroomand, S., Zhang, M., Luo, Z., Yang, D., Luo, H., McManus, B. M. & Janes, K. A. An ERK-p38 subnetwork coordinates host cell apoptosis and necrosis during coxsackievirus B3 infection. *Cell Host Microbe* **13**, 67-76 (2013).
351 Porter, A. G. & Janicke, R. U. Emerging roles of caspase-3 in apoptosis. *Cell Death Differ* **6**, 99-104 (1999).
352 Najjar, M., Saleh, D., Zelic, M., Nogusa, S., Shah, S., Tai, A., Finger, J. N., Polykratis, A., Gough, P. J., Bertin, J., Whalen, M., Pasparakis, M., Balachandran, S., Kelliher, M., Poltorak, A. & Degterev, A. RIPK1 and RIPK3 Kinases Promote Cell-Death-Independent Inflammation by Toll-like Receptor 4. *Immunity* **45**, 46-59 (2016).
353 Christofferson, D. E. & Yuan, J. Necroptosis as an alternative form of programmed cell death. *Curr Opin Cell Biol* **22**, 263-268 (2010).
354 Wang, H., Sun, L., Su, L., Rizo, J., Liu, L., Wang, L. F., Wang, F. S. & Wang, X. Mixed lineage kinase domain-like protein MLKL causes necrotic membrane disruption upon phosphorylation by RIP3. *Mol Cell* **54**, 133-146 (2014).
355 Robinson, M. J. & Cobb, M. H. Mitogen-activated protein kinase pathways. *Curr Opin Cell Biol* **9**, 180-186 (1997).
356 Graves, L. M., Guy, H. I., Kozlowski, P., Huang, M., Lazarowski, E., Pope, R. M., Collins, M. A., Dahlstrand, E. N., Earp, H. S., 3rd & Evans, D. R. Regulation of carbamoyl phosphate synthetase by MAP kinase. *Nature* **403**, 328-332 (2000).
357 Jacque, J. M., Mann, A., Enslen, H., Sharova, N., Brichacek, B., Davis, R. J. & Stevenson, M. Modulation of HIV-1 infectivity by MAPK, a virion-associated kinase. *EMBO J* **17**, 2607-2618 (1998).
358 Monick, M., Staber, J., Thomas, K. & Hunninghake, G. Respiratory syncytial virus infection results in activation of multiple protein kinase C isoforms leading to activation of mitogen-activated protein kinase. *J Immunol* **166**, 2681-2687 (2001).
359 Dickey, L. L., Duncan, J. K., Hanley, T. M. & Fearns, R. Decapping protein 1 phosphorylation modulates IL-8 expression during respiratory syncytial virus infection. *Virology* **481**, 199-209 (2015).
360 Tooze, S. A., Abada, A. & Elazar, Z. Endocytosis and autophagy: exploitation or cooperation? *Cold Spring Harb Perspect Biol* **6**, a018358 (2014).
361 Stark, J. M., McDowell, S. A., Koenigsknecht, V., Prows, D. R., Leikauf, J. E., Le Vine, A. M. & Leikauf, G. D. Genetic susceptibility to respiratory syncytial virus infection in inbred mice. *J Med Virol* **67**, 92-100 (2002).
362 Roymans, D., Alnajjar, S. S., Battles, M. B., Sitthicharoenchai, P., Furmanova-Hollenstein, P., Rigaux, P., Berg, J. V. D., Kwanten, L., Ginderen, M. V., Verheyen, N., Vranckx, L., Jaensch, S., Arnoult, E., Voorzaat, R., Gallup, J. M., Larios-Mora, A., Crabbe, M., Huntjens, D., Raboisson, P., Langedijk, J. P., Ackermann, M. R., McLellan, J. S., Vendeville, S. & Koul, A. Therapeutic efficacy of a respiratory syncytial virus fusion inhibitor. *Nat Commun* **8**, 167 (2017).
363 Rouan, M. C., Gevers, T., Roymans, D., de Zwart, L., Nauwelaers, D., De Meulder, M., van Remoortere, P., Vanstockem, M., Koul, A., Simmen, K. & Andries, K. Pharmacokinetics-pharmacodynamics of a respiratory syncytial virus fusion inhibitor in the cotton rat model. *Antimicrob Agents Chemother* **54**, 4534-4539 (2010).
364 Derscheid, R. J. & Ackermann, M. R. Perinatal lamb model of respiratory syncytial virus (RSV) infection. *Viruses* **4**, 2359-2378 (2012).